

# Analysis of toxic effects and nutrient stress in aquatic ecosystems

Daniel Bontje





**Analysis of toxic effects and nutrient  
stress in aquatic ecosystems**

**Daniel Bontje**



*Acknowledgements* - The research in this thesis has been supported by the MODELKEY project and was carried out at the Department of Theoretical Biology, Vrije Universiteit Amsterdam, the Netherlands. The MODELKEY acronym stands for Models for Assessing and Forecasting the Impact of Environmental Key Pollutants on Marine and Freshwater Ecosystems and Biodiversity. The MODELKEY project is funded by the EC 6th Framework programme in 'Sustainable Development, Global Change and Ecosystems' under Contract-No. 511237 GOCE. There was close collaboration with ECT, Oekotoxikologie GmbH, Flörsheim/Main.

*Cover picture* - Canal Lage Vaart, photo taken in September 2009 in the Netherlands in Flevoland near Ketelhaven at coordinates  $+52^{\circ} 34' 32.25''$ ,  $+5^{\circ} 45' 7.45''$ .

*PDF* - An electronic version of this document can be obtained from the website of the Vrije Universiteit Libaray, <http://www.ubvu.vu.nl> or from the Department of Theoretical Biology, <http://www.bio.vu.nl/thb/research/bib>.

*Printed by* - Gildeprint Drukkerijen - [www.gildeprint.nl](http://www.gildeprint.nl)

VRIJE UNIVERSITEIT

ANALYSIS OF TOXIC EFFECTS AND NUTRIENT  
STRESS IN AQUATIC ECOSYSTEMS

ACADEMISCH PROEFSCHRIFT

ter verkrijging van de graad Doctor aan  
de Vrije Universiteit Amsterdam,  
op gezag van de rector magnificus  
prof.dr. L.M. Bouter,  
in het openbaar te verdedigen  
ten overstaan van de promotiecommissie  
van de faculteit der Aard- en Levenswetenschappen  
op dinsdag 29 juni 2010 om 11.45 uur  
in de aula van de universiteit,  
De Boelelaan 1105

door

Daniel Maarten Bontje

geboren te Zoetermeer

promotor: prof.dr. S.A.L.M. Kooijman  
copromotor: dr.ir. B.W. Kooi

When I wake up in the morning, love  
and the sun light hurts my eyes  
And something without warning, love  
bears heavy on my mind

Then I look at you  
and the world's alright with me  
Just one look at you  
and I know it's gonna be –

A lovely day - lovely day

*Bill Withers – A Lovely Day*



# Contents

<b>1</b>	<b>General introduction</b>	<b>1</b>
1.1	Introduction . . . . .	1
1.2	Example of model construction and analysis . . . . .	3
1.2.1	From conceptual framework to model construction . . . . .	3
1.2.2	Example of mathematical model construction from conceptual framework . . . . .	5
1.2.3	Model analysis using bifurcation theory . . . . .	8
1.2.4	Incorporation of toxicant effect with DEBtox module . . . . .	12
1.2.5	Bifurcation analysis of exposed ecosystem . . . . .	13
1.2.6	2D-bifurcation analysis of exposed ecosystem . . . . .	14
1.2.7	Bifurcation analyses as input for hazard and risk assessment . . . . .	16
	References . . . . .	17
<b>2</b>	<b>Modelling long-term ecotoxicological effects on an algal population under dynamic nutrient stress</b>	<b>21</b>
2.1	Introduction . . . . .	22
2.2	Material and Methods . . . . .	23
2.2.1	Experimental data of system with nitrogen, <i>Cryptomonas sp.</i> and toxicant . . . . .	23
2.2.2	Formulation of the model . . . . .	23
2.2.3	Toxicant concentration-effect relationships . . . . .	27
2.2.4	Equilibrium density and the PET . . . . .	28
2.2.5	Data fitting method . . . . .	29
2.3	Results . . . . .	29
2.3.1	Data fitting results . . . . .	29
2.3.2	Algal population extinction threshold . . . . .	30
2.4	Discussion . . . . .	33
2.4.1	Comparing results with literature . . . . .	33
2.4.2	Assumption justification . . . . .	34
2.5	Conclusions . . . . .	35

2.6	Appendix . . . . .	36
	References . . . . .	37
<b>3</b>	<b>Feeding threshold for predators stabilises predator-prey systems</b>	<b>43</b>
3.1	Introduction . . . . .	44
3.2	Formulation of the model . . . . .	45
3.3	Analysis of the models . . . . .	49
3.3.1	The Rosenzweig-MacArthur model . . . . .	49
3.3.2	The mass-balance model . . . . .	51
3.4	Applying the MB model on experimental data . . . . .	54
3.4.1	Experimental setup and data description . . . . .	54
3.4.2	Fitting method . . . . .	54
3.4.3	Fitting results . . . . .	55
3.5	Discussion and conclusions . . . . .	58
3.6	Appendix . . . . .	60
	References . . . . .	61
<b>4</b>	<b>Modelling direct and indirect ecotoxicological effects on an algalivorous ciliate population under dynamic nutrient stress</b>	<b>65</b>
4.1	Introduction . . . . .	66
4.2	Material and Methods . . . . .	67
4.2.1	Data description . . . . .	67
4.2.2	Formulation of the model . . . . .	68
4.2.3	Data fitting method . . . . .	75
4.3	Results . . . . .	75
4.4	Discussion and conclusions . . . . .	80
4.5	Appendix . . . . .	82
	References . . . . .	85
<b>5</b>	<b>Sublethal toxic effects in a simple aquatic food chain</b>	<b>87</b>
5.1	Introduction . . . . .	88
5.2	Model formulations and analysis . . . . .	91
5.3	Model for nutrient-prey system . . . . .	92
5.3.1	Unstressed nutrient-population system . . . . .	94
5.3.2	Stressed nutrient-population system . . . . .	94
5.4	Analysis of the nutrient-prey system . . . . .	97
5.4.1	Unstressed nutrient-prey system . . . . .	99
5.4.2	Stressed nutrient-prey-toxicant system . . . . .	101
5.5	Model for nutrient-prey-predator system . . . . .	105
5.5.1	Stressed system: both populations affected by toxicant . . . . .	105
5.5.2	Stressed system: predator unaffected by toxicant . . . . .	110

---

5.6	Analysis of nutrient-prey-predator system . . . . .	110
5.6.1	Unstressed nutrient-prey-predator system . . . . .	110
5.6.2	Stressed system: both populations affected by toxicant . . . . .	113
5.6.3	Stressed system: predator unaffected by toxicant . . . . .	113
5.7	Discussion . . . . .	117
5.8	Conclusions . . . . .	120
	References . . . . .	122
<b>6</b>	<b>Sublethal toxicological effects</b>	
	<b>in a generic aquatic ecosystem</b>	<b>127</b>
6.1	Introduction . . . . .	128
6.2	Formulation of the ecological model . . . . .	132
6.3	Analysis of the unexposed aquatic system . . . . .	136
6.3.1	Results for the unexposed aquatic system . . . . .	137
6.4	Formulation of the ecotoxicological model . . . . .	139
6.4.1	Model for the fate of the toxicant . . . . .	139
6.4.2	Simplified bioaccumulation model . . . . .	145
6.4.3	The effect module . . . . .	146
6.5	Analysis of the exposed generic aquatic system . . . . .	147
6.5.1	Analysis of the exposed R-system . . . . .	147
6.5.2	Results for the exposed aquatic system . . . . .	152
6.6	Discussion . . . . .	153
6.7	Conclusions . . . . .	157
6.8	Appendix A . . . . .	159
6.9	Appendix B . . . . .	162
	References . . . . .	165
<b>7</b>	<b>Discussion</b>	<b>171</b>
<b>8</b>	<b>English summary</b>	<b>177</b>
	References . . . . .	183
	<b>Nederlandse samenvatting</b>	<b>185</b>
	<b>List of publications</b>	<b>189</b>
	<b>Dankwoord</b>	<b>191</b>
	<b>Acknowledgements – Project Modelkey</b>	<b>194</b>



# Chapter 1

## General introduction

### 1.1 Introduction

Aquatic ecosystems are complex systems consisting of nutrients, biotic pelagic and benthic communities, pools of detritus and the bulk of both water and sediment. Anthropogenic activities can lead to multiple types of stresses including emissions of toxicants and nutrients into the environment. These toxicants affect species in the aquatic ecosystems and nutrients can cause eutrophication. Our aim is to describe the long-term effects of a toxicant in low concentrations on an aquatic ecosystem given various nutrient levels. To that end we formulate a mathematical model which can be used to run simulations and make predictions. This mathematical model describes the relevant biological, chemical and physical processes acting in the aquatic ecosystem. Eventually, these predictions can be used as input for risk assessment.

It has been recognized for many years that in risk assessment the extrapolation of toxicity bioassay results to potential toxicant effects on ecosystems is complicated [8, 9, 10]. The use of population or even ecosystem data is relatively scarce in ecotoxicological risk assessment as data on these scales is scarce. In practice, mostly a reductionist approach is taken. Experiments are performed at lower levels of biological organization, the individual or population (for microorganisms) level, and then these results are extrapolated to predict effects on the higher levels: populations and ecosystems [28]. Detailed models for populations in aquatic ecosystems have been formulated and analysed [1, 2, 14, 23]. By simulating various toxic loading levels the time-evolution of both the populations and toxicant concentrations are calculated. Although this gives insight into the short-term effects on populations, it is cumbersome to draw clear conclusions in a risk assessment for the long-term sublethal effects on ecosystem functioning and structure.

Emissions of toxicants lead to accumulation in the environmental compart-

ments of water and the complex matrix that forms the sediment. Simultaneously, the toxicants bioaccumulation into organic material such as biota and detritus. Various toxicokinetic models describe these type of accumulations [4, 5, 11, 17, 19, 25, 27]. The models proposed in these papers are in many cases based on the *ecosystem equilibrium assumption* and on the *equilibrium partitioning principle* for the chemicals [5]. This allows for a strictly independent modelling of the ecological and toxicological processes, whereby classical models from both disciplines are used: ecosystem models and toxicokinetic models. Bioconcentration factors, BCF, BAF and BSAF, are parameters in toxicokinetic models and a fixed dietary preference matrix based on some data entries is in most cases the only information about the ecological status used for the calculation of the distribution of the toxicant over the different compartments.

By independently modelling the ecology and toxicology processes there is no interaction between the two and non-linear feedback loops between the two are per definition excluded. We claim that an exposed ecosystem is a perturbation of the non-exposed system or reference system. Also we think toxicants should be modelled to work on the level of the individual. Therefore the assumptions on which the toxicant effect model are based should be in agreement with the assumptions on which the reference model is based. When they are in agreement we expect that non-linear feedback loops will emerge from the formulated ecosystem model.

We will study a process-based and generic aquatic model whereby no equilibrium assumptions are made *a priori*. This means that nutrient loading, species densities and toxicant concentrations vary over time. Toxicants affect the individual behaviour while consequences on the ecosystem level are asked for. Therefore in our integrated, holistic modelling approach, the model combines descriptions of chemical (toxicant fate including individual uptake) and biological processes (feeding, predation, competition). Models of these processes at the individual level are lifted up to the population level and finally ecosystem level whereby besides interactions between populations also interactions with the environment are taken into account. Indirect effects arise as emergent property of the system due to the use of coupled ordinary differential equations. The complexity of the resulting models ranges from one trophic level in an Erlenmeyer to multi-trophic systems which resemble a riverine system with sediment. The least complex models were calibrated on experimental data and the model for the riverine system was based on our own previous results and literature values.

This process based mathematical modelling approach is combined with bifurcation analysis to assess the direct and indirect effects of both toxicological and ecological stress on the functioning and structure of generic aquatic ecosystems. The bifurcation analysis yields the dependency of ecosystem structures

(species presence) and ecosystem dynamics (cyclic or constant densities) on combinations of nutrient and toxicant stress.

## 1.2 Example of model construction and analysis

For readers less familiar with modelling and bifurcation analysis Sections 1.2.1–1.2.7 provide a short introduction into the methods used in this Thesis. This includes the construction of a computer model from a conceptual framework via a mathematical model.

### 1.2.1 From conceptual framework to model construction

#### The conceptual framework and extrapolation

Extrapolation is stating "what if" questions. These questions can only be answered when we understand the system. Understanding comes from previous work, literature and a bit of intuition. This understanding is internally consistent and usable to construct hypotheses which can be tested against (new) experimental data and (new) literature. From this understanding we can build conceptual frameworks from which we can derive mathematical equations. These equations then can be used to make computer codes from which we can build a computer model. Then this computer model can be used to answer the "what if" questions, or alternatively named *scenarios*, by calculating endpoint values. With endpoints being for example species densities or the degree of inhibition of a physiological process such as photosynthesis.

We stress that the ability to do an extrapolation is but just one of the results of a conceptual framework. More importantly, the conceptual framework is a simple picture of reality, it will always be incomplete by definition. The challenge is to find the minimal number of relevant processes in the studied problem which together still explain most of the observed behaviour of the system.

It is a success when the conceptual framework generates a quantifiable model which has the proper dynamics of the system behaviour and predicts species densities in the right order of magnitude.

Also, complex ecosystem models are high dimensional and non-linear, meaning they can only be investigated with the aid of a computer. Therefore the conceptual framework must be presented in the form of a computer model. Later in this introduction, the usefulness of bifurcation analysis will be shown for analysing the behaviour of an exposed multi-trophic ecosystem.

The quantifiable models that are build are not the research goals but the research tools that can be used for testing the realism of a conceptual framework

and to analyse the behaviour of the ecological model based on that conceptual framework.

Below, the steps that lead to the formation of a conceptual framework up to model validation are discussed. After these paragraphs Section 1.2.3 and further explain the bifurcation theory which we use to analyse models for multi-trophic ecosystems and to analyse the effect of toxicants on these systems.

### **Conceptual framework leads to mathematical model**

The conceptual framework should summarize reality with a minimal number of relevant processes and still be able to explain most of the observed behaviour of the exposed ecosystem. Thereby the framework consist of an idea of who eats what and how, how will the individuals grow, reproduce and die, what happens to dead biomass, where does the nutrient for the phototrophs come from and are there one or more growth limiting factors, etcetera. This framework can be sketchy or very detailed, but eventually it should look like a flow chart of species interactions and species-environment dependencies.

However, this conceptual framework says nothing on the value of densities and fluxes within this framework. Additional assumptions need to be made on how the interactions can be approximated with equations, leading to a mathematical model. The equations in the mathematical model describe the change of the variables over time and simultaneously the size of the fluxes at given time points depending on chosen parameter values.

For spatially homogenous ecosystem models, one can use ordinary differential equations (ODEs). These ODEs consist of variables and parameters. Parameters are always constant in value and often describe a species property such as death rate or maximum feeding rate, while variables vary over time and often denote biomass densities or environmental factors such as temperature or light intensity. Variables are for example prey and predator densities, and fluxes are for example the total number of prey eaten by all predators together. Fluxes are often expressed in numbers or mass per time, densities often in numbers or mass per area or volume.

### **Mathematical model leads to computer model and simulations**

Now we can transform the mathematical model into computer code and make a *computer model*. By using experimental values, literature values and common sense, values can be assigned to parameters and the initial values of the variables can be chosen. Combining these values with the computer model makes it possible to run simulations. These simulations are a direct consequence of the conceptual framework mentioned earlier. Changing the framework means

repeating all steps leading to the computer model.

### **Parameter estimation**

Values for the parameters used in the computer model can also be obtained by fitting the model to data. Then the units of the model output should match the units in which the data is measured, conversion factors might be needed. Preferably, there are endpoint measurements that quantify the fluxes and there are endpoint measurements that quantify the variables. This would give the most certainty that the computer model can be parametrized on the data set. If for example a conceptual framework for an ecosystem in a contaminated lake was made and used to produce a computer model, then this computer model could now be fitted on measurements from that lake and parameter values are obtained.

### **Extrapolation with the computer model**

Different scenarios can now be executed and evaluated as parameter values are known. For example, testing the consequence of changing the toxicant influx into the lake of the earlier example can now be simulated with the computer model. The resulting extrapolations will include non-linear responses as an indirect result of the constructed ODEs in the mathematical model that underlies the computer model.

### **Validation**

Assumptions were made to formulate the conceptual framework: these might be wrong. By using different scenarios as falsifiable hypotheses one can test the underlying assumptions of the conceptual framework. This requires that first the predictions are made and are then tested against experimental data. Validation is rarely done with complex ecosystem models. Often all available data was already used to estimate parameter values. The production or collection of new experimental data for validation can easily become extremely expensive. The activities leading to the validation of an ecosystem model can take longer than the careers of the scientists involved.

#### **1.2.2 Example of mathematical model construction from conceptual framework**

The previous sections emphasized the importance of the conceptual framework. This section will show how different ‘building blocks’ in a conceptual framework can be combined to obtain a mathematical model for a small artificial ecosystem in a confined volume, e.g. an ecosystem in an Erlenmeyer flask.

Then this ecosystem will be analysed using bifurcation theory to illustrate the application of this theory.

### Mass balance model

Let us assume this flask contains one limiting nutrient for an algal species, one algal species and one algivorous organism such as a ciliate and optionally one toxicant either a herbicide that only affects the algae or an insecticide which we model to only affect the ciliates. This will allow us to study the reference system and the effect of each toxicant on that system. This setup is very similar to what is used in Chapter 2 and 4.

Algae need mass and energy to produce new biomass and to maintain their current biomass. Let us assume that in this laboratory setup the amount of light is in surplus, thus we do not need to model the light. Let us also assume that all nutrients, including micro-nutrients such as vitamins, needed by the algae are in surplus except for one nutrient: nitrogen. This nitrogen can be available in the form of salts, detritus or small organic compounds. We also assume the limiting nutrient is not bio-transformed into a volatile compound as evaporation would complicate the calculation of a mass balance.

Let us measure the algal density in amount of nitrogen incorporated into its biomass, mol N/L and the amount of N available in the medium also in mol N/L. The *variable* denoting the algal biomass we take to be  $P(t)$  (P for producer) and  $N(t)$  for the density of the nutrient.  $Z(t)$  is the variable that denotes the density of the predator, a ciliate species, also in mol N/L. All variables are functions of time,  $t$ . The variable  $N_T(t)$  denotes the total amount of nitrogen in the closed system and is given by the equation below

$$N_T(t) = N(t) + P(t) + Z(t) .$$

As the system is closed for nitrogen, the total amount of nitrogen in the flask is constant and given by its value at the start of the experiment ( $t = 0$ ):

$$N_T = N(0) + P(0) + Z(0) . \tag{1.1}$$

The first equation has no number while the second does. It is customary to either number all equations or only the ones which are referred to in the text. We use the latter style.

### Algal growth and death model

As stated, algae need mass to produce new biomass. Let us assume the algae need a certain time to process a unit of  $N$ , known as the nutrient handling time  $h_N$ . This leads to a maximum feeding rate of  $P$  on  $N$  as the amount of time

is limited per day. Also, the rate at which a new unit of  $N$  is encountered depends on intensity of searching for  $N$  by  $P$ , the searching rate  $v_N$ . The above set of  $h_N$  and  $v_N$  together form a Holling type-II functional response [13, 22] as denoted by  $f(N)$ .

$$f(N) = \frac{v_N N}{1 + v_N h_N N}$$

The maintenance and mortality rates add to a single loss term, denoted by the *per capita* death rate  $d_P$ . This combination of a Holling type-II functional response and a constant death rate for the algae is known as a Marr-Pirt model formulation [16, 20, 24].

### Predator growth and death model

We use the same Marr-Pirt formulation for the ciliate population  $Z$ . Therefore the ciliates die with the constant death rate  $d_Z$  and  $f(P)$  denotes the feeding of the predator  $Z$  on the algae  $P$ . Also, we take the predator to be less than 100 percent efficient in converting algal biomass into ciliate biomass, denoted by the yield coefficient  $y_{PZ}$ .

### Detritus and nutrient recycling model

Per unit of time, there are three fluxes of dead biomass produced, namely  $d_P P$  and  $d_Z Z$  and a flux related to inefficient feeding of  $Z$  on  $P$ , namely  $Z(1 - y_{PZ})f(P)$ . If we assume that unidentified and uncharacterized bacteria feed on this dead biomass (detritus) and turn it into small nitrogen-containing compounds then a closed nutrient loop is formed. Therefore, we obtained a *nutrient cycle*.

If we assume that the growth, death and detritus degradation rates of the bacteria are much higher then the rate at which detritus is produced then the bacteria are always in a steady-state with the detritus density. Due to the assumed high detritus degradation rate and slow detritus production rates both the bacteria and detritus densities will be low. This means there are negligible amounts of nitrogen in the detritus pool and bacterial population. Therefore we can ignore the detritus and bacteria in the mass-balancing of the model formulation. Therefore, albeit indirectly, we assume the detritus is instantaneously converted into nitrogen-containing compounds. This type of reasoning with fast and slow rates is known as making a *quasi steady-state* assumption.

### Coupled ODEs for this ecosystem

The above variables and mass fluxes together form the set of ordinary differential equations (ODEs) shown below,

$$\begin{aligned}\frac{dN}{dt} &= -P \frac{v_N N}{1 + v_N h_N N} + (1 - y_{PZ}) Z \frac{v_P P}{1 + v_P h_P P} + d_P P + d_Z Z, \\ \frac{dP}{dt} &= P \left( \frac{v_N N}{1 + v_N h_N N} - d_P \right) - Z \frac{v_P P}{1 + v_P h_P P}, \\ \frac{dZ}{dt} &= Z \left( y_{PZ} \frac{v_P P}{1 + v_P h_P P} - d_Z \right).\end{aligned}$$

In order to obtain the more familiar notation of the Holling Type-II functional response parameters with a maximum ingestion rate and a nutrient half-saturation constant we take  $I_{NP} = 1/h_N$  and  $K_{NP} = 1/(v_N h_N)$ , similar for  $I_{PZ}$  and  $K_P$ . This results in

$$\begin{aligned}\frac{dN}{dt} &= -P I_{NP} \frac{N}{K_N + N} + (1 - y_{PZ}) Z I_{PZ} \frac{P}{K_P + P} + d_P P + d_Z Z, \\ \frac{dP}{dt} &= P \left( I_{NP} \frac{N}{K_N + N} - d_P \right) - Z I_{PZ} \frac{P}{K_P + P}, \\ \frac{dZ}{dt} &= Z \left( y_{PZ} I_{PZ} \frac{P}{K_P + P} - d_Z \right).\end{aligned}$$

Using Eq. (1.1) and mass-conservation gives an ODE-set reduced with one less dimension

$$\begin{aligned}\frac{dP}{dt} &= P \left( I_{NP} \frac{N_T - P - Z}{K_N + N_T - P - Z} - d_P \right) - Z I_{PZ} \frac{P}{K_P + P}, \\ \frac{dZ}{dt} &= Z \left( y_{PZ} I_{PZ} \frac{P}{K_P + P} - d_Z \right).\end{aligned}$$

For later use in Eq. 1.3 it is convenient to write the system as below

$$\frac{dP}{dt} = f_1(P, Z) = P \left( I_{NP} \frac{(N_T - P - Z)}{K_N + (N_T - P - Z)} - d_P \right) - Z I_{PZ} \frac{P}{K_P + P}, \quad (1.2a)$$

$$\frac{dZ}{dt} = f_2(P, Z) = Z \left( y_{PZ} I_{PZ} \frac{P}{K_P + P} - d_Z \right). \quad (1.2b)$$

### 1.2.3 Model analysis using bifurcation theory

#### Model analysis

By coding the above ODE-system into software using a programming environment we can run simulations, for this we used Matlab [21]. These *simulations*

require initial values for the variables  $P$  and  $Z$  and values for the biological parameters such as the death rates, maximum feeding rates and nutrient half-saturation constants and feeding efficiency. We can perform short-term simulations and long-term simulations, plot the results and then describe the behaviour of the system. This *numerical* approach is informative but not very precise.

The long-term behaviour of the system at each equilibrium can also be analysed *analytically*. First one solves  $\frac{dP}{dt} = 0$  and  $\frac{dZ}{dt} = 0$ , either by hand or with special software such as Maple [18]. Then the resulting expressions can be used to calculate the equilibria. Finally, the stability of the equilibria can be determined and the behaviour of the system at that specific equilibrium can be determined. This approach fails with many higher dimensional systems.

The *Jacobian* matrix  $\mathbf{J}$  contains information on the local behaviour of the system given a specific equilibrium  $E_i$ . The Jacobian matrix consist of the partial derivatives of the ODE-system evaluated at  $E_i$  as exemplified below

$$\mathbf{J} = \begin{bmatrix} \frac{\partial f_1}{\partial P} & \frac{\partial f_1}{\partial Z} \\ \frac{\partial f_2}{\partial P} & \frac{\partial f_2}{\partial Z} \end{bmatrix} \quad (1.3)$$

The so called *eigenvectors*  $v$  and *eigenvalues*  $\lambda$  are solutions of the equation set  $\mathbf{J}v = v\lambda$ . In the two dimensional case, the eigenvalues are conjugated complex numbers and the solutions of a quadratic formula  $\det(\mathbf{J} - \lambda\mathbf{I}) = 0$ , where  $\mathbf{I}$  is the unit matrix. For three and higher dimensional systems the Routh-Hurwitz criteria can be applied [7].

The calculated eigenvalues are either real or complex, meaning having real and imaginary parts. This results in the following equilibrium characteristics: (1) When the real parts are negative, the equilibrium is *stable*. (2) When at least one real part is positive, the equilibrium is *unstable*.

Bifurcation analysis deals with the study of the dependencies of the long-term dynamics on a parameter. From the classification of the stability given above, we conclude that by varying the parameter, the stability of the equilibrium changes when one real eigenvalue or the real parts of a pair of complex conjugated eigenvalues equals zero. The parameter value where this occurs is called a *bifurcation point*, given all other parameters remain constant.

For two dimensional systems there are three important types of bifurcation points. When both eigenvalues are real, for parameter values close to the bifurcation point, we distinguish two types namely the *tangent* bifurcation and the *transcritical* bifurcation.

When the eigenvalues are complex (and the equilibrium is close to the bifurcation point), a *Hopf* bifurcation occurs when the real parts of the pair of conjugated eigenvalues are zero.

There are also other special cases. One option is that not just one, but both eigenvalues are zero. Such a point is known as a bifurcation point of

*higher codimension*. We do not consider these points here. The special case where both eigenvalues are zero, that is a Hopf and a tangent bifurcation occur simultaneously, this point is called Bogdanov-Takens point.

Bifurcation points can be followed by changing one or more parameters simultaneously. Software that has been specifically designed to do this is e.g. AUTO [6]. When after simulation an equilibrium is found (usually a positive and stable one), this equilibrium can be followed as a function of one parameter by means of *continuation* rather than simulation, by making use of a corrector-predictor method that estimates how the equilibrium changes as function of a change in the parameter used. Special test functions are implemented in AUTO that indicate when a bifurcation point is encountered while following this equilibrium, and what type of bifurcation it is (a Hopf or otherwise). Also, the software has utilities to further track this equilibrium as a function of two parameters, that allows us to determine if there are regions in the two-parameter space where for instance the Hopf-bifurcation does exist. When changing two parameters a collection of similar bifurcation points form a 2D bifurcation curve

In the following examples we will show how the ODE-system for  $P$  and  $Z$  will respond to increasing values of  $N_T$ . We will follow both changes in biomass densities and long-term dynamics. Three possible equilibria are possible: no species present, only producer present, both producer and predator are present.

For very low nutrient values both producer and predator can not exist. Increasing  $N_T$  above a threshold value allows for the existence of  $P$ . This threshold value is a bifurcation point, namely a transcritical bifurcation point where an eigenvalue is. Let us denote this threshold value of  $N_T$  with  $P_{inv}$ . In other words, if  $N_T \geq P_{inv}$  then an algae population can exist stably in this system.

Given  $N_T \geq P_{inv}$  ‘no algae present’ is an unstable equilibrium and ‘algae present’ is a stable equilibrium. From this we learn that if  $N_T < P_{inv}$  there is only one non-negative solution and for  $N_T \geq P_{inv}$  there are two non-negative solutions. Generally, given the same parameter values but different initial conditions, a system can have multiple solutions and thus multiple equilibria.

In mathematical terms, by increasing  $N_T$  from below to above  $P_{inv}$  the system goes from having one non-negative stable point to having one non-negative stable point *and* one non-negative unstable point. At the exact value  $N_T = P_{inv}$  the eigenvalue of the equilibrium is zero and the one equilibrium splits in two. Thus a zero eigenvalue means in a biological sense species invasion and is known as a transcritical bifurcation.

By further increasing the value of  $N_T$  the density of  $P$  increases until  $Z$  can invade into the system at  $Z_{inv}$ ; this is also a transcritical bifurcation point.

At even higher values of  $N_T$  the prey-predator system shows cyclic be-

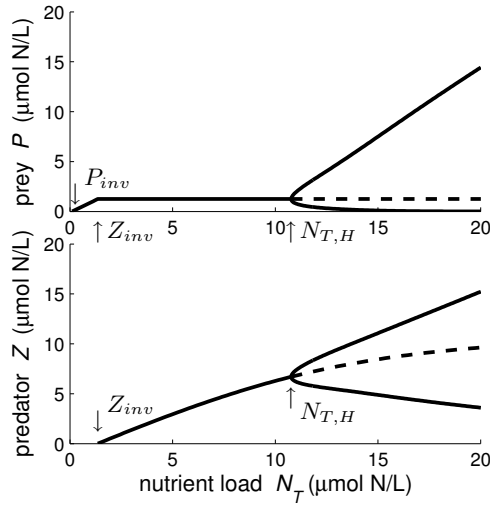


Figure 1.1: The biomasses of  $P$  (top) and  $Z$  (bottom) depend on the total nutrient load  $N_T$ . The algal invasion occurs at  $N_T = P_{inv} > 0$  and the predator invasion at  $N_T = Z_{inv}$ . Before the Hopf at  $N_T = N_{T,H}$ , the solid line denotes the stable equilibrium values, after the Hopf, the minima and maxima are denoted by the solid line and the unstable equilibrium values by the dotted line.

behaviour, in this case stable limit cycles. Let us denote this value of  $N_T$  with  $N_{T,H}$ . The transition of a non-cyclic stable equilibrium to an unstable equilibrium with a stable limit cycle occurs when the eigenvalues of the equilibrium gain a complex part and the real parts are zero. This transition point is known as a *Hopf-bifurcation*. For  $N_T > N_{T,H}$ , increasing  $N_T$  will cause the amplitudes of the oscillations to increase. Eventually the minima of an oscillation will approach a low value. As a result the prey population can become very low and extinction due to stochastic fluctuations becomes likely. This phenomena of unexpected species extinction when an increase of biomass was expected after nutrient enrichment is called the *paradox of enrichment*.

To illustrate the use of bifurcation theory Fig. 1.1 was constructed with AUTO. The horizontal axis denotes the nutrient loading of the system ( $N_T$ ), the vertical axes either represents algal biomass  $P$  or the predator biomass  $Z$ . The algae can invade at  $N_T = P_{inv}$ , then their biomass increases with increasing values of  $N_T$ . When  $N_T = Z_{inv}$ , the ciliates can invade. Increasing  $N_T$  will no longer increase  $P$  but  $Z$ . This continues until  $N_T = N_{T,H}$ , at that nutrient loading the Hopf is located. Right of the Hopf the system shows cyclic behaviour with increasing amplitudes of the oscillations when increasing  $N_T$ . Note that the very low densities of  $P$  further after the Hopf might lead to extinction via stochastic events.

In the next section we will incorporate a module to include the effects of a toxicant on the reference system. Then the model analysis will continue.

### 1.2.4 Incorporation of toxicant effect with DEBtox module

Bedaux and Kooijman developed an approach to quantify the effect of a toxicant on the biological rates used in Dynamic Energy Budget (DEB) modelling [3, 15]. With this approach, named DEBtox, two parameters are needed per affected rate that is related to a biological process. One of the toxicity parameters is the no-effect concentration (NEC). Below this threshold the toxicant has no effect on the rate and thus no effect on a biological process and thus no effect on an individual. The other is the tolerance concentration (TC) which represents the strength of the toxic effect. Together these parameters describe the response of a process to a low internal toxicant concentration, for example, the value of the parameter that stands for the rate of photosynthesis becomes a function of the internal toxicant concentration.

The output of the ecosystem model depends on the parameter values used, the effect of a toxicant on the level of physiological processes is elevated to the level of a complete system via the affected parameter. Thus the effect of the toxicant on a process over time is integrated via the ODEs which model the affected organisms and its interaction with its environment and other species.

To include the effect of a herbicide on the growth rate of the algae, the model of Eq. (1.2) is extended with the NEC and TC parameters. See [15] for an application of this threshold method on algal growth inhibition. It is assumed that the internal toxicant concentration in unicellulars is in equilibrium with the constant external concentration, i.e., the internal toxicant concentration is proportional to the toxicant concentration in the medium, see also [26, 12, 11]. The large surface-area-to-volume ratio of unicellulars justifies this assumption.

Under unexposed situations the maximum growth rate has a constant value denoted by  $I_{NP}(0)$ . When the medium toxicant concentration ( $c$ ) is below the threshold value the toxicant does not affect the growth rate and thus  $I_{NP}(c) = I_{NP}(0)$ . This threshold value is called the no-effect concentration (NEC); denoted by  $c_{0,I_{NP}}$  for the producers growth rate. Increasing the toxicant concentration from the NEC-value with the value of the tolerance concentration ( $c_T$ ) results in a halving of the maximum growth rate. The tolerance concentration for the maximum growth rate is denoted with  $c_{T,I_{NP}}$ .

The expressions below describe the effect of the herbicide on the producers growth rate:

$$I_{NP}(c) = I_{NP}(0) \left( 1 + \frac{\max(0, (c - c_{0,I_{NP}}))}{c_{T,I_{NP}}} \right)^{-1} \quad (1.4)$$

If we want to model the effect of an insecticide on the death rate of the predator we use the same approach. The effect of the insecticide on the death rate ( $d_Z$ ) is described in a similar manner as for the effect on the death rate with a tolerance concentration ( $c_{T,d_Z}$ ) and NEC ( $c_{0,d_Z}$ ). The expressions below describe the effect of an insecticide on the death rate of the predator:

$$d_{Z(c)} = d_Z(0) \left( 1 + \frac{\max(0, (c - c_{0,d_Z}))}{c_{T,d_Z}} \right) \quad (1.5)$$

### 1.2.5 Bifurcation analysis of exposed ecosystem

The effect of changing the nutrient load of the system on the biomass of the producer and predator was illustrated with Fig. 1.1. In that figure the continuation parameter was  $N_T$ . In Figure 1.2 the continuation parameter is  $c_W$ , the water concentration of the toxicant. As only  $c_W$  is continued the other parameters are constant.

The left panel of Figure 1.2 illustrates the effect of only a herbicide on the biomass density of the producer and predator. The herbicide does not affect  $Z$  but only the producers growth rate. Below the no-effect concentration of  $5 \mu\text{g/L}$  both biomass densities are constant and equal to the reference state. Without the predator present the producer density would have been higher, but the ‘surplus’ biomass is used to sustain the predator.

While the toxicant affects the producer directly it is the predator which suffers as first the consequences. As primary production of the producers goes down, the producers make less new biomass and thus less new prey for the predator, leading to the extinction of  $Z$ . Around a herbicide concentration of  $13.5 \mu\text{g/L}$  the predator goes extinct ( $Z_{ext}$ ) as the producer generates no longer ‘surplus’ biomass. Then with the predator being extinct the effect of high toxicant concentrations on the producer becomes visible. Slowly the  $P$  reduces in density until it goes extinct ( $P_{ext}$ ).

Although the toxicant is a herbicide the first observable effect is on the predator biomass, followed by a decline in producer biomass and finally at a high toxicant concentration extinction of the producer follows.

The right panel of Fig. 1.2 illustrates the effect of the insecticide on the biomass density of the producer and predator.  $P$  is insensitive to the insecticide. The insecticide increases the death rate of the predator, this causes the predator biomass to become lower until at toxicant concentrations  $Z_{ext}$  the predator goes extinct. Lower densities of  $Z$  reduce the predation pressure on  $P$ , therefore  $P$  increases in density until it reaches the maximum attainable density given this specific nutrient load. Thus the increase of the producer densities is an indirect effect of the toxicant.

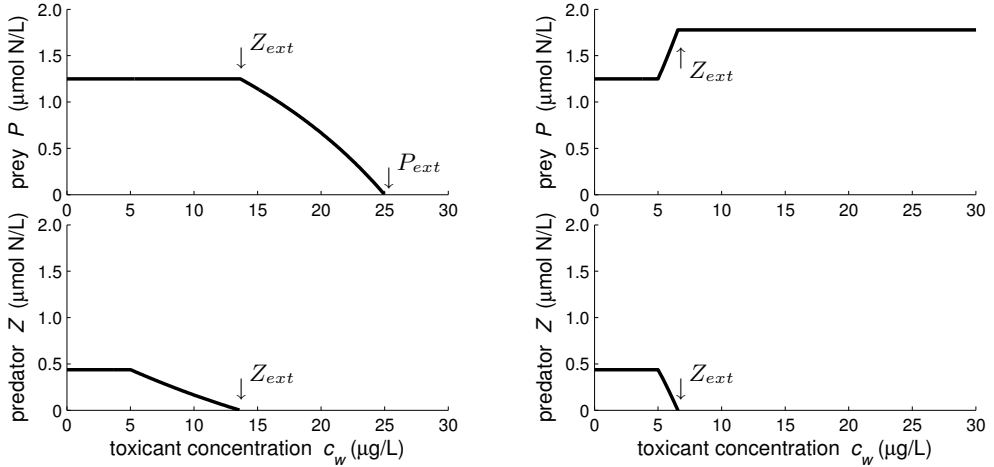


Figure 1.2: Left panel: the biomasses of  $P$  and  $Z$  depend on a constant total nutrient load  $N_T$  and an increasing concentration of a herbicide with a no-effect concentration of  $5 \mu\text{g/L}$ . Right panel: the biomasses of  $P$  and  $Z$  depend on a constant total nutrient load  $N_T$  and an increasing concentration of an insecticide with a no-effect concentration of  $5 \mu\text{g/L}$ .

### 1.2.6 2D-bifurcation analysis of exposed ecosystem

The effect of continuation parameter  $N_T$  on the biomass densities of the producer and predator was shown in Fig. 1.1. Similarly, the effect on the biomass densities of continuing parameter  $c_W$  was shown in Fig. 1.2. In both analyses the species composition of the ecosystem was: no species present, only producer present or producer and predator present. Possible ecosystem behaviour was stable equilibria and cyclic. It is also possible to continue two parameters at the same time, as illustrated with Fig. 1.3. Now, not biomasses are shown but the species composition of the ecosystem and the behaviour of the system given the combination nutrient loading and toxicant concentration. We devised a method to find areas in the parameter-space where the ecosystem is quantitatively not affected. These areas we defined to be no-effect regions (in analogy to the no-effect concentration). These areas are formed by combinations of values for nutrient loading and toxicant loading where the biomass densities are not affected. The bifurcation analysis also resulted in areas where the quantities are changed but not the ecosystem structure. Finally we determined where quantitative changes in biomasses occurred and simultaneously the behaviour of the ecosystem was changed. Thus in this system toxicant stress is just one stress beside nutrient stress.

In the left panel of Fig. 1.3 the producer invasion threshold curve, or transcritical bifurcation (TC) curve, is perpendicular to the horizontal axis when the toxicant concentration is below the NEC. At higher toxicant concentra-

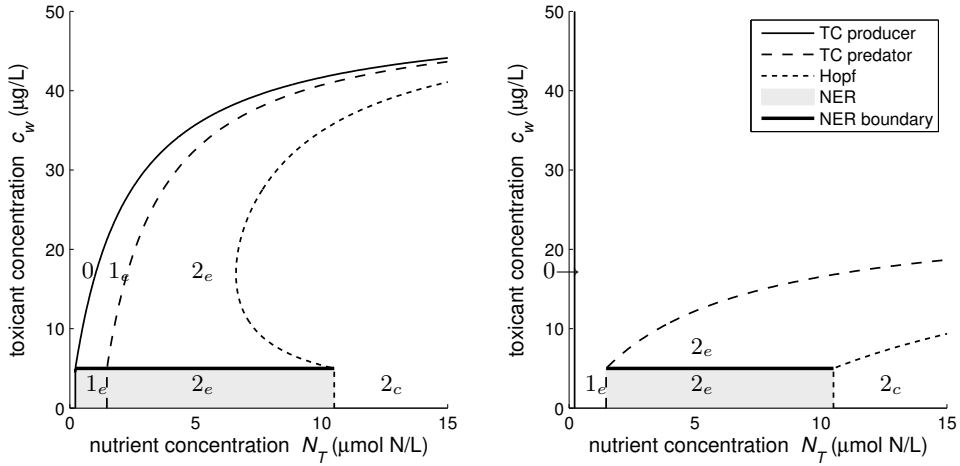


Figure 1.3: Left panel: 2D-bifurcation diagram with continuation parameters the nutrient load  $N_T$  and the herbicide concentration  $c_W$ . Right panel: 2D-bifurcation diagram with continuation parameters the nutrient load  $N_T$  and the insecticide concentration  $c_W$ . The legend applies for both panels. 1 stands for only producer present. 2 stands for both producer and predator present. Areas with stable equilibria are denoted with subscripted  $e$  and areas with cyclic behaviour are denoted with  $c$ . The grey area is the no-effect region (NER).

tions the TC curve moves to the right as higher nutrient loadings are needed to compensate for the toxicant presence. The predators TC curve is first also perpendicular to the horizontal axis and follows the producers TC. The Hopf-curve is also affected by the presence of the toxicant above the NEC. Gray denotes the no-effect region (NER) where presence of the toxicant has no effect on the quantitative behaviour of the system. When the toxicant has effect, the NER boundary (solid black line) is crossed.

It can be observed that the area where both species can occur simultaneously is limited, even at the reference state. This area is only reduced with increasing toxicant concentrations.

In the right panel of Fig. 1.3 the effect of different nutrient loadings and an insecticide on the species composition of the system is shown. The producer invasion threshold (TC) remains parallel to the toxicant axis as the producer is unaffected by the toxicant. The predator invasion threshold is shifted to higher nutrient loadings if the toxicant concentration increases. The Hopf-curve is shifted similarly. The area where both species occur together and provide the highest species diversity possible in this system is confined by the predator TC, the Hopf and part of the horizontal axis. This illustrates how the ecosystem composition depends on both nutrient load and insecticide presence.

### 1.2.7 Bifurcation analyses as input for hazard and risk assessment

So far we analysed the effects of one toxicant at a time on a deterministic ecosystem. Given a set of parameter values for the ecology, species properties and toxicant concentration we can calculate the long-term behaviour and composition of the ecosystem. For example, the right panel of Fig. 1.2 can be used to determine the densities of prey and predator at  $N_T = 2$  depending on the insecticide concentration  $c_W$ . Therefore we can assess for each possible  $c_W$  the negative consequence or hazard to the ecological system, for example the extinction of the predator.

If we take  $c_W$  to be normally distributed with a known mean and variance instead of being deterministic then the resulting biomass densities become uncertain, including the presence or absence of the predator. We can calculate the chance of predator extinction if the distribution of  $c_W$  is well characterized as we know at which deterministic  $c_W$  the predator goes extinct. Thus we can read from Fig. 1.4 that  $Z$  has a 88.5 percent chance of not going extinct for the presented distribution of  $c_W$ .

However, if the type of distribution of  $c_W$  and the values of its characterizing parameters are unknown then an extinction chance can not be calculated. If we do know an upper confidence value as a worst case scenario of the toxicant concentration then we can do the following. If we want a high likelihood that  $Z$  will persist and we know the 95% upper boundary of  $c_W$ , then the right panel of Fig. 1.4 shows that for  $N_T = 2.1$  there is this a 95% certainty that  $c_W$  will have that value or lower and therefore  $Z$  can be near its extinction threshold but not over it.

The above result is a specific example of an approach which can be generalized for more complex ecosystems with more species as described below.

Bifurcation analysis makes it possible to determine areas of species composition and behaviour of the ecosystem given deterministic nutrient and toxicant loading. The bifurcation curves in these analyses are deterministic. If the continued parameter on the 2D bifurcation has a stochastic distribution then the locations of the bifurcation curves become uncertain, leading to uncertain boundaries of areas with certain species composition. Thus the precise locations of invasion, extinction or occurrence of cyclic behaviour become lost.

There where the upper boundary of the uncertainty area ends, one can read with a degree of certainty the species composition of the ecosystem and determine persistence or extinction of the species of interest. Therefore the upper boundary forms a collection of worst case scenarios for the continued parameter and sets the ecological 'safe' parameter ranges under which the toxicant may occur without species loss compared to the reference state.

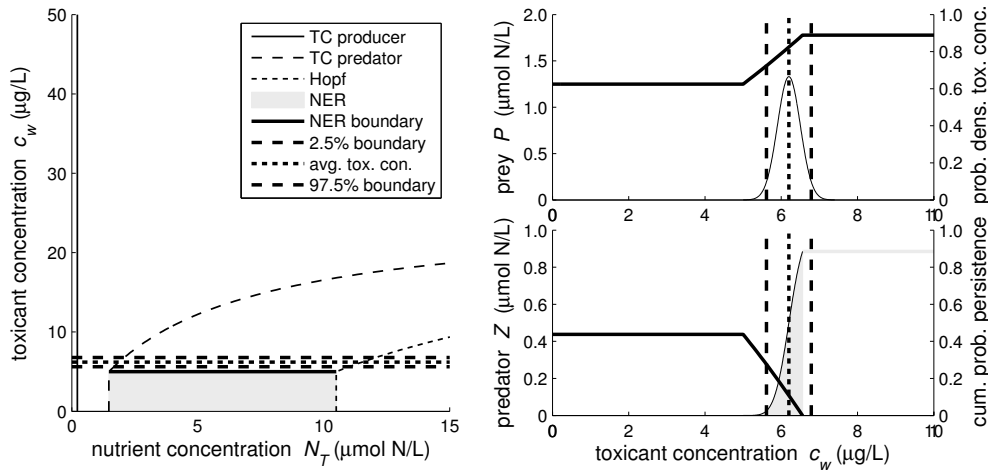


Figure 1.4: The left panel is identical to the right panel of Fig. 1.3 but now the uncertainty in the toxicant concentration is depicted by the horizontal 95%-confidence interval. There where the uncertainty interval overlaps a deterministic extinction threshold there is a risk of extinction. At higher nutrient levels there is no overlap and the the predator is unlikely to go extinct given the toxicant distribution. The right panel is a vertical cross-section of the left panel at  $N_T = 2$  and identical to the right panel of Fig. 1.2 when zooming on the lower toxicant concentrations. Added to this close-up in the upper panel is the distribution of the toxicant concentration and its mean and 95%-confidence interval. The second upper y-axis denotes the toxicant concentration probability density function. In the lower left the likelihood of the persistence of  $Z$  can be read on the second y-axis. Given the distribution for  $c_w$  there is an 88.5 percent change that the predator will persist, albeit at lowered densities.

# References

- [1] J. A. Arnot and F. A. P. C. Gobas. A food web bioaccumulation model for organic chemicals in aquatic ecosystems. *Environmental Toxicology and Chemistry*, 23(4):2343–2355, 2004.
- [2] S. M. Bartell, G. Lefebvre, G. Kaminski, M. Carreau, and K. R. Campbell. An ecosystem model for assessing ecological risks in Quebec rivers, lakes, and reservoirs. *Ecological Modelling*, 124(1):43–67, 1999.
- [3] J. J. M. Bedaux and S. A. L. M. Kooijman. Statistical analysis of bioassays based on hazard modelling. *Environmental and Ecological Statistics*, 1:303–314, 1994.
- [4] J. Campfens and D. MacKay. Fugacity-based model of PCB bioaccumulation in complex aquatic food webs. *Environmental Science Technology*, 31:577–583, 1997.
- [5] D. M. Di Toro, S. C. Zarb, D. J. Hansen, R. C. Swartz, C. E. Cowan, S. P. Pavlou, H. E. Allen, N. A. Thomas, and P. R. Paquin. Technical basis for establishing sediment quality criteria for nonionic organic chemicals using equilibrium partitioning. *Environmental Toxicology and Chemistry*, 10:1541–1583., 1991.
- [6] E. J. Doedel and B. Oldeman. Auto 07p: Continuation and bifurcation software for ordinary differential equations. Technical report, Concordia University, Montreal, Canada, 2009.
- [7] L. Edelstein-Keshet. *Mathematical Models in Biology*. Birkhäuser Mathematics Series. The Random House, New York, 1st edition, 1988.
- [8] S. Ferson, L. R. Ginzburg, and R. A. Goldstein. Inferring ecological risk from toxicity bioassays. *Water, Air, & Soil Pollution*, 90(1/2):71–82, 1996.
- [9] V. Forbes and P. Calow. Population growth rate as a basis for ecological risk assessment of toxic chemicals. *Philosophical Transactions of the Royal Society London – B series*, 357:1299–1306, 2002.

- 
- [10] V. Forbes, P. Calow, and R. M. Silby. The extrapolation problem and how population modeling can help. *Environmental Toxicology and Chemistry*, 27(10):1987–1994, 2008.
- [11] F. A. P. C. Gobas. A model for predicting the bioaccumulation of hydrophobic organic chemicals in aquatic food-webs: application to Lake Ontario. *Ecological Modelling*, 69:1–17, 1993.
- [12] F. A. P. C. Gobas, E. J. McNeil, L. Lovett-Doust, and G. D. Haffner. Bioconcentration of chlorinated aromatic hydrocarbons in aquatic macrophytes (*Myriophyllum spicatum*). *Environmental Science and Technology*, 25:924–929, 1991.
- [13] C. S. Holling. Some characteristics of simple types of predation and parasitism. *The Canadian Entomologist*, 91(7):385–398, 1959.
- [14] A. A. Koelmans, A. Van der Heijde, L. M. Knijff, and R. H. Aalderink. Integrated modelling of eutrophication and organic contaminant fate & effects in aquatic ecosystems. A review. *Water Research*, 35(15):3517–3536, 2001.
- [15] S. A. L. M. Kooijman, A. O. Hanstveit, and N. Nyholm. No-effect concentrations in algal growth inhibition tests. *Water Research*, 30(7):1625–1632, July 1996.
- [16] S. A. L. M. Kooijman. *Dynamic Energy Budget theory for metabolic organisation*. Cambridge University Press, Great Britain, Cambridge, 2010.
- [17] P. F. Landrum, H. Lee, and M. J. Lydy. Toxicokinetics in aquatic systems: model comparisons and use in hazard assessment. *Environmental Toxicology and Chemistry*, 11:1709–1725, 1992.
- [18] Maplesoft. *Maple*. Maplesoft, Waterloo, Ontario, Canada, 2003.
- [19] R. D. Markwell, D. W. Connell, and A. J. Gabric. Bioaccumulation of lipophilic compounds from sediments by oligochaetes. *Water Research*, 23:1443–1450, 1989.
- [20] A. G. Marr, E. H. Nilson, and D. J. Clark. The maintenance requirement of *Escherichia coli*. *Annals of the New York Academy of Sciences*, 102:536548, 1962.
- [21] Matlab. *Matlab package*. The MathWorks, Natick, Massachusetts, USA, 2008.

- 
- [22] R. V. O'Neill, D. L. DeAngelis, J. J. Pastor, B. J. Jackson, and W. M. Post. Multiple nutrient limitations in ecological models. *Ecological Modelling*, 46:147–163, 1989.
- [23] R. A. Park, J. S. Clough, and M. C. Wellman. Aquatox: Modeling environmental fate and ecological effects in aquatic ecosystems. *Ecological Modelling*, 213:1–15, 2008.
- [24] S. J. Pirt. The maintenance energy of bacteria in growing cultures. *Proceedings of the Royal Society of London B (Biological Sciences)*, 163:224231, 1965.
- [25] S. Sharpe and D. Mackay. A framework for evaluating bioaccumulation in food webs. *Environmental Science Technology*, 34:1203–1213, 2000.
- [26] D. T. Sijm, K. W. Broersen, D. F. De Roode, and P. Mayer. Bioconcentration kinetics of hydrophobic chemicals in different densities of *chlorella pyrenoidosa*. *Environmental Toxicology and Chemistry*, 17(9):1695–1704, 1998.
- [27] R. V. Thomann, J. Connolly, and T. F. Parkerton. An equilibrium model of organic chemical accumulation in aquatic food webs with sediment interaction. *Environmental Toxicology and Chemistry*, 11:615–629, 1992.
- [28] D. J. Versteeg, S. E. Belanger, and G. J. Carr. Understanding single-species and model ecosystem sensitivity: data-based comparison. *Environmental Toxicology and Chemistry*, 18:13291346, 1999.

## Chapter 2

# Modelling long-term ecotoxicological effects on an algal population under dynamic nutrient stress

D. Bontje, B.W. Kooi, M. Liebig and S.A.L.M. Kooijman  
*Water Research*, 43:3292–3300, 2009.

We study the effects of toxicants on the functioning of a phototrophic unicellular organism (an algae) in a simple aquatic microcosm by applying a parameter-sparse model. The model allows us to study the interaction between ecological and toxicological effects. Nutrient stress and toxicant stress, together or alone, can cause extinction of the algal population. The modelled algae consume dissolved inorganic nitrogen (DIN) under surplus light and use it for growth and maintenance. Dead algal biomass is mineralized by bacterial activity, leading to nutrient recycling. The ecological model is coupled with a toxicity-module that describes the dependency of the algal growth and death rate on the toxicant concentration. Model parameter fitting is performed on experimental data from Liebig et al. [27]. These experiments were especially designed to include nutrient limitation, nutrient recycling and long-term exposure to toxicants. The flagellate species *Cryptomonas sp.* was exposed to the herbicide prometryn and insecticide methyl parathion in semi-closed Erlenmeyers. Given the total limiting amount of nitrogen in the system, the estimated toxicant concentration at which a long-term steady population of algae goes extinct will be derived. We intend to use the results of this study to

investigate the effects of ecological (environmental) and toxicological stresses on more realistic ecosystem structure and functioning.

## 2.1 Introduction

When assessing the ecological status of a river, the effects of both toxicant and environmental stresses on multiple species have to be accounted for [6]. Laboratory toxicity tests, on the other hand, generally concern a single stress and a single species. The use of population models for extrapolation from single species ecotoxicological observations to the relevant effects on an ecosystem is discussed in Forbes et al. [11] and in Forbes and Callow [12]. Here for modelling purposes, an aquatic ecosystem contains a limiting nutrient and functional groups: producers, predators and decomposers to ensure nutrient recycling.

In order to study direct and indirect effects of toxicants, the bottom trophic levels of this system have been exposed and studied by Liebig et al. [27]. In these Erlenmeyer experiments the flagellate *Cryptomonas sp.* represents the producers, the ciliate *U. furcata* represents the predators and undetermined bacteria are the decomposers. The system is exposed to either a herbicide or a pesticide for 14 days. The nutrient level is maximum at the onset and is reduced by the algae. Therefore, the nutrient concentration declines dynamically during the batch experiments and becomes limiting after the first days. In Liebig et al. [27], the data sets were analysed using the traditional toxicity test procedures [33]. These procedures may only be applied under exponential growth conditions, which holds true for the first days of the algal data sets when nutrients are abundant and thus no interactive effects of nutrient limitation and toxic stress occur.

In this paper, we perform an analysis of the limiting nutrient-*Cryptomonas sp.* subsystem using the full duration of the experiment. Consequently, the analysis is extended outside the exponential growth phase and includes nutrient limitation. To perform this extended analysis, we apply a process-based ecotoxicological model in which the growth and death of the species is simulated using a deterministic Marr-Pirt model [23, 19]. Dead algal biomass is mineralized by bacterial activity. The model considers recycling of the limiting nutrient. To incorporate the toxicant effect the DEBtox approach [4, 24] is applied where two parameters are needed per affected process such as growth or mortality. One of the toxicity parameters is the no-effect concentration (NEC). Below this threshold the toxicant has no effect on an individual. The other is the tolerance concentration (TC) which represents the strength of the toxic effect. Parameter values, standard deviations and their covariance are estimated by fitting the resulting model on the experimental data from Liebig

et al. [27] with a least-sum-of-squares method. This provides simultaneously the toxicological parameters, NEC and TC, and the biological parameters, such as growth rate, hazard rate and nutrient half-saturation constant.

The algal growth dynamics, including steady-state biomass, depend on these biological parameters. Toxicants affect biological processes and thus the dynamics. Dynamic behaviour is also affected by nutrient availability. Hence, the effects of a toxicant and a nutrient on the dynamics, which are difficult to separate in nature, are taken into account in the model formulation simultaneously.

Hallam et al. [17] introduced the population extinction threshold (PET) being defined as the highest ambient chemical concentration at which the population could persist during long-term exposure. Extinction of a population can be caused by a too low nutrient availability (starvation) but also because of toxic effects causing increased death rate or reduced growth efficiency. From the deterministic model the expressions for the PET are derived. In the Appendix, the stochastic formulation of the PET which respects covariance between parameters is given. The estimated toxicological and biological parameters are used to study the dependence of both extinction and persistence of the algae on toxicant concentration and nutrient load.

## 2.2 Material and Methods

### 2.2.1 Experimental data of system with nitrogen, *Cryptomonas sp.* and toxicant

Liebig et al. [27] performed in Erlenmeyers 14-day exposure experiments with the flagellated algae *Cryptomonas sp.* and the herbicide prometryn (CAS 7287-19-6), which inhibits photosystem II, and the insecticide methyl parathion (CAS 298-00-0) which is an acetylcholinesterase inhibitor. In these experiments chemical stress and nutrient limitation occur simultaneously. Figure 2.1 [27, Fig 1A therein] shows the growth curves for cell numbers affected by each toxicant. The measured number of cells ( $V(t)$ ) is converted into algal biomass ( $A$ ) expressed in mol N L<sup>-1</sup> by using a fitted constant amount of nitrogen per cell ( $N_{cell}$ ). Chemical analysis indicated a recovery of close to 100% of the nominal concentrations of the toxicants [27].

### 2.2.2 Formulation of the model

Algae harvest energy from sunlight which they store in carbohydrates. Carbohydrates provide both energy and mass which are combined with other assimilated nutrients from the medium, such as dissolved inorganic nitrogen (DIN), which includes ammonium and nitrite, to synthesize algal biomass [5].

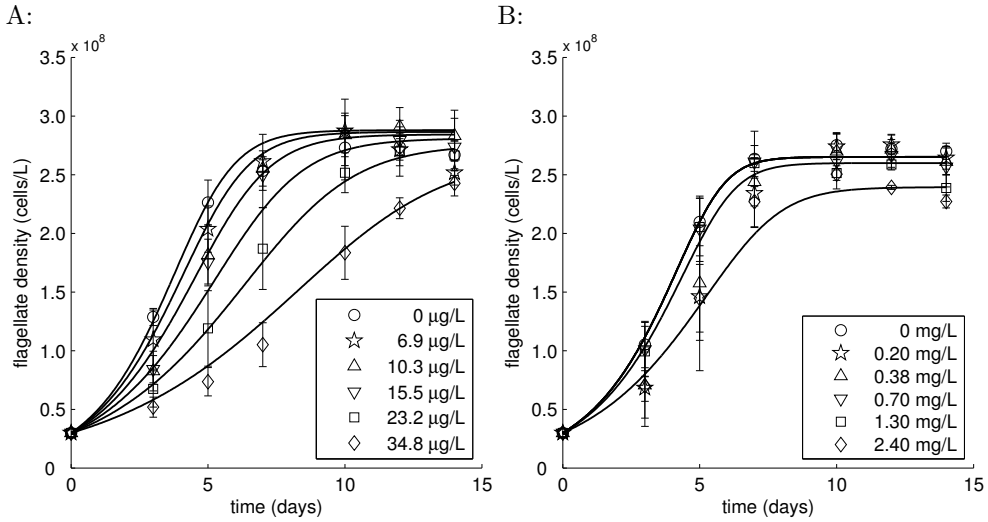


Figure 2.1: Calculated and measured algal densities are affected by prometryn and methyl parathion. See Table 2.2 for parameter values of the fit for each dataset. Averages and variances are based on four replicates. A: Prometryn was modelled to affect the growth rate. B: Methyl parathion was modelled to affect the hazard rate. The NEC is above the first three exposure concentrations. Therefore only the simulations with the highest two exposure concentrations differ from the control.

This new biomass is used by the algae for growth while energy is used for maintenance (including basal respiration and turn-over of macro-molecules). Products of the maintenance process, such as ammonium and carbon dioxide, are excreted into the environment [47]. The ammonium is utilized again by the phytoplankton [26].

Bacteria feed on dead algal biomass and dead bacteria. Bacteria have to maintain themselves and thus excrete metabolic products such as ammonium and carbon dioxide, similar for metabolic products of the growth process. Excrements that contain the element nitrogen are considered nutrients for the algae. This closes the recycling circle of the limiting nutrient to algae, to bacteria and back to the limiting nutrient.

In the following model, the growth-limiting nutrient for the algae is dissolved inorganic nitrogen (DIN). DIN includes all nitrogen containing simple compounds such as the salts dissolved in the medium e.g.  $\text{NaNO}_3$ . Carbon dioxide can enter and leave the Erlenmeyer, allowing the algae to fix carbon. Carbon is assumed to be present in non-limiting amounts as the algae are aerated. All nutrients except DIN, are assumed to be present in abundance and are not modelled. DIN is converted into algal biomass, dead algal biomass results in detritus which is re-mineralized.

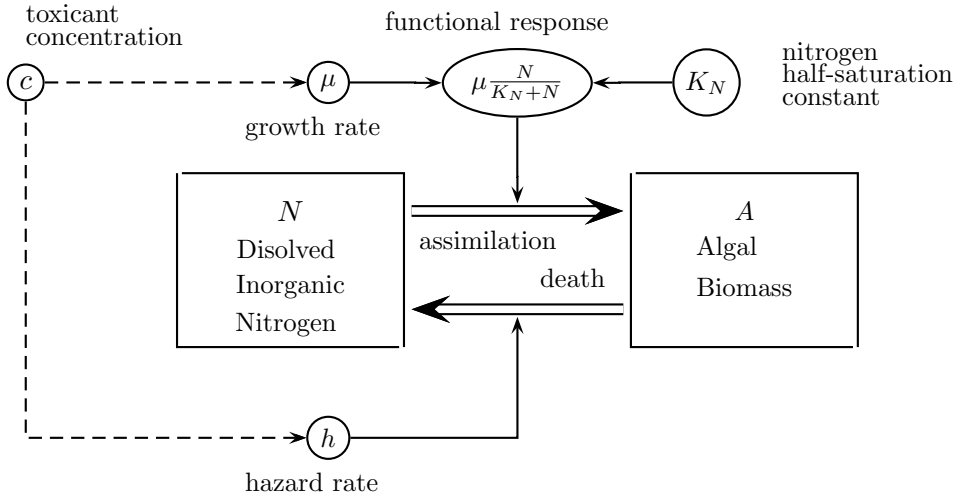


Figure 2.2: The scheme shows how the nitrogen cycles through the semi-closed system turning from nutrient into algal biomass, and eventually into to small compounds that together form the nutrients for the algae. Light enters and heat leaves, while the limiting nutrient (nitrogen) remains inside. Toxicants can affect the growth rate or hazard rate or both.

Table 2.1: List of Variables, Parameters and Constants

Symbol	Name	Units
$A(t)$	Amount of nitrogen present in the biomass of the producer	$\text{mol N L}^{-1}$
$c$	Concentration of the toxicant in the medium	$\text{gram L}^{-1}$
$c_0$	No-effect concentration (NEC) of the toxicant in the medium	$\text{gram L}^{-1}$
$c_T$	Measure of tolerance of organism to toxicant	$\text{gram L}^{-1}$
$D$	Amount of nitrogen present in detritus	$\text{mol N L}^{-1}$
$d_A$	Intrinsic death rate of the producer	$\text{day}^{-1}$
$h$	Hazard rate of the producer	$\text{day}^{-1}$
$k_D$	Detritus degradation rate	$\text{day}^{-1}$
$k_M$	Maintenance rate for producer	$\text{day}^{-1}$
$k_{N_m}$	Maximum nitrogen uptake rate	$\text{day}^{-1}$
$K_N$	Half-saturation constant for nitrogen assimilation	$\text{mol N L}^{-1}$
$\mu$	Algal growth rate	$\text{day}^{-1}$
$N(t)$	Nitrogen concentration in medium	$\text{mol N L}^{-1}$
$N_{cell}$	Amount of nitrogen per algal cell	$\text{mol N cell}^{-1}$
$N_T$	Total bioavailable amount of nitrogen in the system	$\text{mol N L}^{-1}$
$t$	Time	days
$V(t)$	Measured cell density	$\# \text{ cells L}^{-1}$

A mass balance model formulation leads to a set of ordinary differential equations (ODEs) which describes the change over time of dissolved inorganic nitrogen DIN ( $N$ ), total algal biomass ( $A$ ) and detritus density ( $D$ ) in the medium. The three state variables  $N$ ,  $A$ , and  $D$  are expressed in mol nitrogen per litre. Modelling population growth with ODEs is appropriate for dividing algae [22]. Table 2.1 gives the symbol and units of each used variables, parameters and constants.

$$f_N(N) = \frac{N}{K_N + N} \quad (2.1a)$$

$$\frac{dN}{dt} = k_D D + A(k_M + (1 - y_{NA})k_{N_m}f_N(N) - k_{N_m}f_N(N)) \quad (2.1b)$$

$$\frac{dA}{dt} = A(y_{NA}k_{N_m}f_N(N) - k_M - d_A) \quad (2.1c)$$

$$\frac{dD}{dt} = d_A A - k_D D \quad (2.1d)$$

Nutrient assimilation  $f_N(N)$  is modelled with a Holling type II functional response, where the maximum nutrient uptake rate is  $k_{N_m}$ ,  $K_N$  is the nutrient half-saturation constant. The yield of algal biomass on DIN is denoted by  $y_{NA}$ .  $k_M$  denotes the maintenance rate of the algae. The first two terms in Eq. (2.1b) between the brackets model the labile (maintenance and assimilation) products excreted by the algae. The term  $Ak_{N_m}(1 - y_{NA})f_N(N)$  describes the flux of DIN which is not synthesized into algal biomass. Abundant bacterial activity degrades all nitrogen containing compounds into a form that can be assimilated by the algae.  $d_A$  is the intrinsic death rate of the algae, dead algae become detritus. The degradation rate of detritus by bacteria is denoted by  $k_D$ .

The effective nutrient uptake and assimilation rate are identical to the maximum growth rate  $\mu$ , with  $\mu = y_{NA}k_{N_m}$  which is substituted into the above set of equations.

Bacteria have relatively high growth rates and thus high assimilation rates and therefore high substrate degradation rates compared to algal growth. Algae have relatively low death rates and therefore  $k_D \gg d_A$ . This allows for the assumption that the rate of change of the detritus biomass is much faster than the rate of change of the nutrient in the medium and algal biomass, i.e.  $dD/dt = 0$ . From Eq. (2.1d) the quasi-steady-state equilibrium value of the detritus  $D^* = Ad_A/k_D$  is found.

As a last step, taking  $h = k_M + d_A$  yields what we call a hazard rate. Above substitutions result in:

$$\frac{dN}{dt} = A\left(h - \mu \frac{N}{K_N + N}\right) \quad (2.2a)$$

$$\frac{dA}{dt} = A\left(\mu \frac{N}{K_N + N} - h\right) \quad (2.2b)$$

In Figure 2.2 the mass fluxes of this system are shown. This formulation shows that nitrogen is recycled between nutrient ( $N$ ) and algae ( $A$ ). Consequently, the total amount of nitrogen in the system ( $N_T$ ) is constant, yielding:

$$N_T = N(t) + A(t) = N(0) + A(0) \quad (2.3)$$

Eliminating variable  $N$  from system Eq. (2.2) using Eq. (2.3) gives the following algal growth equation:

$$\frac{dA}{dt} = A\left(\frac{\mu}{\frac{K_N}{N_T - A} + 1} - h\right) \quad (2.4)$$

The equilibrium density of the algae  $A^*$  can be found by solving  $dA/dt = 0$ , this yields:

$$A^* = N_T - K_N \frac{h}{\mu - h} \quad (2.5)$$

Thus the equilibrium density depends on the total amount of limiting nutrient in the system ( $N_T$ ). Furthermore, it depends on the species specific growth rate ( $\mu$ ), hazard rate ( $h$ ) and the nutrient half-saturation constant ( $K_N$ ).

### 2.2.3 Toxicant concentration-effect relationships

To include the effect of toxicants on the growth and death of the algae, the model of Eq. (2.4) is extended with a threshold method developed by Bedaux and Kooijman [4]. See Kooijman et al. [24] for an application of this threshold method to algal growth inhibition tests.

It is assumed that the internal toxicant concentration in a unicellular is in equilibrium with the constant external concentration, i.e., the internal toxicant concentration is proportional to the toxicant concentration in the medium, see also [43, 16, 15]. The large surface-area-to-volume ratio of unicellulars justifies this assumption.

Under unexposed situations the hazard rate has a constant value denoted by  $h(0)$ . When the medium toxicant concentration ( $c$ ) is below the threshold

value the toxicant does not affect the hazard rate and thus  $h(c) = h(0)$ . This threshold value is called the no-effect concentration (NEC); denoted by  $c_{0,h}$  for the hazard rate. Increasing the toxicant concentration from the NEC-value with the value of the tolerance concentration ( $c_T$ ) results in a doubling of the hazard rate. The tolerance concentration for the hazard rate is denoted with  $c_{T,h}$

The expressions below describe the effect of the toxicant on the hazard rate and the growth rate:

$$h(c) = h(0) \left( 1 + \frac{\max(0, (c - c_{0,h}))}{c_{T,h}} \right) \quad (2.6a)$$

$$\mu(c) = \mu(0) \left( 1 + \frac{\max(0, (c - c_{0,\mu}))}{c_{T,\mu}} \right)^{-1} \quad (2.6b)$$

The effect of a toxicant on the growth rate ( $\mu$ ) is described in similar manner as for the effect on the hazard rate with a tolerance concentration ( $c_{T,\mu}$ ) and NEC ( $c_{0,\mu}$ ).

## 2.2.4 Equilibrium density and the PET

For each combination of nutrient load ( $N_T$ ) and toxicant concentration ( $c$ ), the expected long-term final cell density, or equilibrium density ( $A^*$ ), can be calculated. For each fixed nutrient load, there is one toxicant concentration, denoted by  $c_x$ , above which the algal density is zero; that is algal extinction.  $c_x$  can be derived by substitution of  $A^* = 0$  into Eq. (2.5) and Eq. (2.6b), leading to:

$$c_x = c_{0,\mu} + c_{T,\mu} \left( \frac{\mu(0)}{h} \left( \frac{N_T}{K_N + N_T} \right) - 1 \right) \quad (2.7)$$

The value of  $c_x$  depends on the values of the parameters  $c_{0,\mu}$ ,  $c_{T,\mu}$ ,  $\mu$ ,  $h$  and  $K_N$ .

If these values are deterministic variables, then  $c_x$  has no standard deviation. In this paper, however, the parameters are treated as estimated values fitted from experimental data. Due to measurements errors, differences in initial conditions, bio-variability, etc., data points are random. Therefore, these parameters are treated as stochastic variables and consequently  $c_x$  is also a stochastic variable with a mean and standard deviation. See the Appendix for a detailed derivation of  $c_x$ . Together, all extinction concentrations with their corresponding nutrient load form a population extinction threshold, or PET.

### 2.2.5 Data fitting method

A weighted least-sum-of-squares method with weights equal to the inverse of the variance in the measurements was used. A low sum-of-squares indicates a good fit. The data points values are assumed to be normally distributed. This makes this method identical to a maximum-likelihood method [31]. The additional assumption that the number of data points is large leads to the conclusion that the fitted parameters are multi-nominal distributed. The sum-of-squares (SSQ) is minimized with a Nelder Mead's simplex method. The mean and covariance matrix (inverse of the Hessian matrix of the SSQ with respect to the parameters) of the estimated parameters are evaluated at the minimum SSQ-point [39].

## 2.3 Results

### 2.3.1 Data fitting results

The model curve fits together with the experimental measurements are shown in Figure 2.1. Each experiment had a control case and five toxicant concentrations. For toxicant concentrations less than the NEC value, the curves coincide with the control curve. In Table 2.2, the estimated parameter values and standard deviations are listed.

The effect of the toxicant is modelled assuming that the compound affects the growth rate, the hazard rate or both. Three different scenarios were fitted:

- Scenario I: the toxicant only affects the growth rate.
- Scenario II: the toxicant only affects the hazard rate.
- Scenario III: the toxicant affects both rates.

The sum-of-squares (SSQ) was used to assess the goodness of fit for each scenario. The scenario with the lowest SSQ is assumed to give the modelled mode of action of the toxicant.

Prometryn: Scenarios I, II and III respectively fitted with a SSQ of 37.8, 53.0 and 37.6. This means that scenarios I and III fit nearly equally well. The toxicity parameters (NEC and tolerance concentration) that describe the influence of prometryn on the hazard rate have a very large standard deviation in scenario III. Also the tolerance concentration for the hazard rate was very high. This means that the effect of prometryn on the hazard rate is negligible. Furthermore, scenario I in which prometryn influences the rate of synthesis of new biomass via the growth rate has two parameters less than scenario III. Thus, prometryn scenario I is most likely. This is in agreement with the fact that the herbicide prometryn is known to influence photosystem II and

this reduces carbohydrate production and thus reduces the energy and mass available to incorporate nitrogen into new biomass.

Methyl parathion: Scenarios I, II and III respectively fitted with a SSQ of 40.7, 29.1 and 29.1. This means that for methyl parathion scenarios II and III fit equally well. The toxicity parameters (NEC and tolerance concentration) that describe the influence of methyl parathion on the assimilation and incorporation of nitrogen via the growth rate have a very large standard deviation in scenario III. Also the tolerance concentration for the growth rate was very high. This means that the effect of the pesticide methyl parathion on the growth rate is almost negligible. Furthermore, scenario II in which methyl parathion influences the hazard rate uses two parameters less than scenario III. Hence, methyl parathion affects the growth rate only slightly and scenario II is most likely.

### 2.3.2 Algal population extinction threshold

Using Eq. (2.5) and Eq. (2.6b) and the mean values from Table 2.2, we calculated the deterministic equilibrium cell densities depending on nutrient load and prometryn concentration, see Figure 2.3. The grey area represents equilibrium cell densities. When no toxicant is present, the algal biomass ( $A^*$ ) is proportional to the nutrient load ( $N_T$ ). At low nutrient concentrations the algae can not persist. On the other hand, there is a maximum toxicant concentration at which the algae can not persist even when there is a very high nutrient load (not shown in this graph). Between these extremes the algae suffer from nutrient stress and toxicant stress simultaneously. A line is formed where the grey surface of the algal densities crosses the bottom plane. This curve is the PET. It separates regions in the bottom plane where the algae can persist from where they go extinct.

Figure 2.4 shows the dependency of the extinction probability of the algae on the prometryn concentration at nutrient load of  $200 \mu\text{mol N L}^{-1}$ . The parameter values and standard deviations from Table 2.2 were used to construct the estimated extinction concentration from Eq. (2.7) and its variance using a Taylor series expansion as explained in the Appendix. For the sake of simplicity, we assumed a normal distribution of  $c_x$ .

Figure 2.5 shows how the extinction concentration is influenced by nutrient stress. As each nutrient concentration has its corresponding extinction concentration with attached uncertainty, the total set of extinction concentrations together forms the population extinction threshold. The grey area indicates the uncertainty of the PET. Below the grey area, the algae are likely to survive. The open circles indicate the measured combination of toxicant concentrations and nutrient concentration in which the algae persisted [27].

Table 2.2: Estimated parameter values based on exposure experiments to prometryn and methyl parathion as shown in Figure 2.1A and B, respectively.

prometryn (CAS 7287-19-6)			methyl parathion (CAS 298-00-0)		
Affected parameter: $\mu$			Affected parameter: $h$		
Parameter	Value	SD	Value	SD	units
$V(0)$	$3.00 \cdot 10^7$	$3.83 \cdot 10^5$	$2.99 \cdot 10^7$	$3.39 \cdot 10^5$	#cells L <sup>-1</sup>
$N_{cell}$	$7.26 \cdot 10^{-1}$	$1.32 \cdot 10^{-1}$	$8.05 \cdot 10^{-1}$	$2.75 \cdot 10^{-1}$	pmol N cell <sup>-1</sup>
$N(0)$	$2.01 \cdot 10^{-4}$	0	$2.01 \cdot 10^{-4}$	0	mol N L <sup>-1</sup>
$\mu$	$1.27 \cdot 10^0$	$1.59 \cdot 10^{-1}$	$8.05 \cdot 10^{-1}$	$3.24 \cdot 10^{-1}$	day <sup>-1</sup>
$h$	$7.20 \cdot 10^{-2}$	$5.19 \cdot 10^{-2}$	$8.97 \cdot 10^{-2}$	$1.81 \cdot 10^{-1}$	day <sup>-1</sup>
$K_N$	$2.27 \cdot 10^{-4}$	$2.19 \cdot 10^{-4}$	$9.12 \cdot 10^{-5}$	$2.90 \cdot 10^{-4}$	mol N L <sup>-1</sup>
$c_{0,\mu}$	$4.57 \cdot 10^0$	$1.68 \cdot 10^0$	> 0	-	$\mu\text{g L}^{-1}$
$c_{T,\mu}$	$3.16 \cdot 10^1$	$8.71 \cdot 10^0$	$\infty$	-	$\mu\text{g L}^{-1}$
$c_{0,h}$	> 0	-	$9.66 \cdot 10^{-1}$	$3.76 \cdot 10^{-1}$	mg L <sup>-1</sup>
$c_{T,h}$	$\infty$	-	$1.07 \cdot 10^0$	$4.11 \cdot 10^0$	mg L <sup>-1</sup>

If the standard deviation (SD) of a parameter is zero, then the value was not estimated but fixed. Note,  $A(t) = N_{cell}V(t)$ .

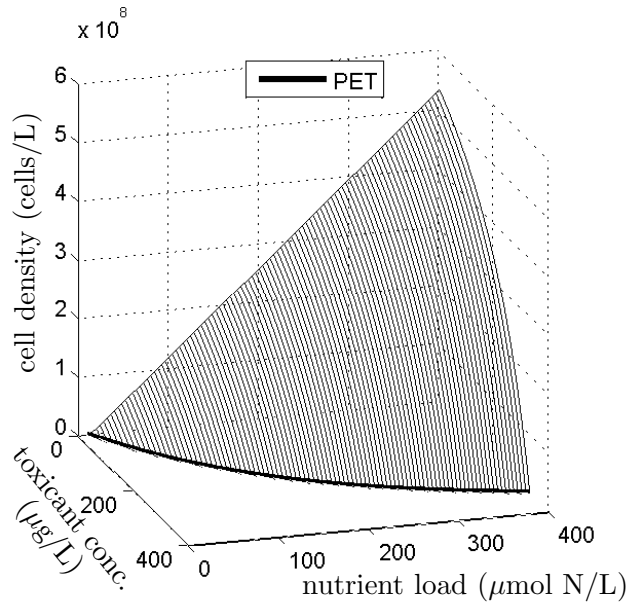


Figure 2.3: Algal densities depending on the total limiting nutrient and prometryn concentration which affect the growth rate. The bold line in the bottom plane is the Population Extinction Threshold, or PET.

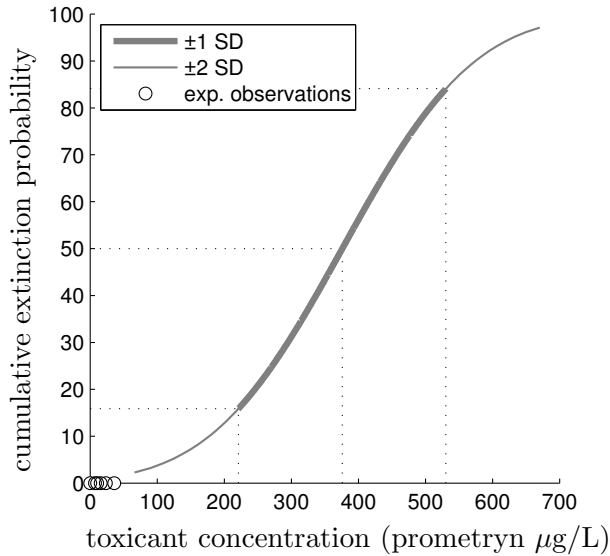


Figure 2.4: Extinction risk of algae as function of prometryn concentration at a nutrient load of  $200 \mu\text{mol N L}^{-1}$ . The open circles denote experimental algal densities that persist at the lower toxicant concentrations.

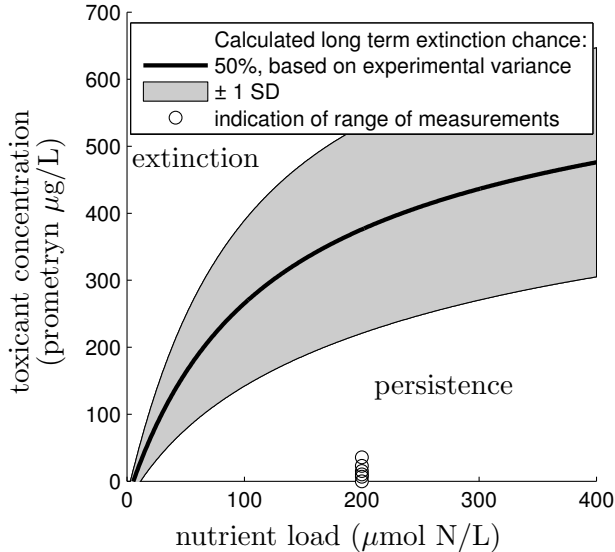


Figure 2.5: Extinction concentrations for algae populations under different nutrient conditions while exposed to prometryn. The results are summarized by showing the 50% extinction chance (solid line) and  $\pm$  one standard deviation (grey). The algae do not persist at low nutrient load even without the additional stress from prometryn. The open circles denote experimental algal densities that persist at the lower toxicant concentrations.

## 2.4 Discussion

### 2.4.1 Comparing results with literature

Freshwater and marine unicellular algal growth rates range from 0.3 to 8 day<sup>-1</sup> with clustering around a growth rate of 1 day<sup>-1</sup> [32]. In [25] growth rates of six species of phytoplankton ranged from 0.5 to 1.3 day<sup>-1</sup>. For the ‘exponential’ growth phase in the experimental control group, we estimate a growth rate ( $\mu - h$ ) of 0.7 and 1.2 day<sup>-1</sup> for the freshwater flagellated algae *Cryptomonas sp.*, see Table 2.2.

The hazard rate of light-starved salt water mixotrophic *Ochromonas sp.* is 0.66 day<sup>-1</sup> [2]. The flagellated growth form of the marine *Phaeocystis globosa* has a hazard rate of 0.07 day<sup>-1</sup> and the non-flagellated growth form 0.52 day<sup>-1</sup> [37]. In [49] structural decay rates of 0.43 to 8.93 day<sup>-1</sup> were measured. Using dissolved esterase activity as a tracer of phytoplankton lysis, lysis rates ranging from 0.026 day<sup>-1</sup> to 1.9 day<sup>-1</sup> were found [1]. An averaged dark respiration rate ranging from 0.01 to 0.4 day<sup>-1</sup> was found for microalgae [14]. In a nitrogen starvation batch experiment with the marine diatom *Ditylum brightwellii*, the algal death rate of the diatom reduced from 0.1 to 0.04 day<sup>-1</sup> when bacteria were added, likely due to remineralization of biomass [7]. We fitted from our data sets a hazard rate equal to maintenance rate plus the intrinsic death rate ( $h = k_M + d_A$ ) of 0.07 to 0.09 day<sup>-1</sup> for the freshwater algae *Cryptomonas sp.* with undetermined bacteria present, see Table 2.2.

A lumped half-saturation concentration of 0.2-15  $\mu\text{mol NO}_3^- \text{L}^{-1}$  was reported for an uncharacterized population of lake algae [38]. Berman et al. [5] reports for freshwater algae half-saturation concentrations for ammonium ranging from 0.004  $\mu\text{mol L}^{-1}$  to 0.51  $\mu\text{mol L}^{-1}$  and half-saturation concentrations for nitrate ranging from 0.007  $\mu\text{mol L}^{-1}$  to 11  $\mu\text{mol L}^{-1}$ . We found values for the nitrogen half-saturation concentration ( $K_N$ ) of 227 ( $\pm 219$ ) and 91 ( $\pm 290$ )  $\mu\text{mol N L}^{-1}$  range, see Table 2.2.

DeBiase et al. [9] found 0.06 pmol N cell<sup>-1</sup> under various nutrient conditions for *Cryptomonas sp.* In our prometryn and methyl parathion experiments with *Cryptomonas sp.* the measured average cellular content ranged from 0.21 to 0.39 pmol N cell<sup>-1</sup> [27]. We estimated for respectively the prometryn and methyl parathion experiments 0.73 ( $\pm 0.13$ ) and 0.81 ( $\pm 0.28$ ) pmol N cell<sup>-1</sup>. These values are in the same order of magnitude.

We conclude that the estimated growth rate ( $\mu - h$ ), hazard rate ( $k_M + d_A$ ), saturation constant ( $K_N$ ) and nitrogen per cell ( $N_{cell}$ ) are in the same range as reported in the literature.

By applying classical statistics to the same data set of algae exposed to prometryn, Liebig et al. [27] found a 50% growth inhibition at day 7 (EC<sub>50,7d</sub>) of 39.3  $\mu\text{g L}^{-1}$ . Further, the no-observed effect concentration (NOEC) at day

7 is  $23.2 \mu\text{g L}^{-1}$ . These effect concentrations are in close accordance with literature values for other green algae like the  $\text{EC}_{50}$  of  $12 \mu\text{g L}^{-1}$  determined for *Selenastrum cornutum* [35], the  $\text{EC}_{50,96h}$  of  $21 \mu\text{g L}^{-1}$  for *S. cornutum* and the  $\text{EC}_{50,96h}$  of  $53 \mu\text{g L}^{-1}$  for *Dunaliella tertiolecta* [13].

The algal growth inhibition test with methyl parathion using *Cryptomonas sp.* resulted in growth rate based NOEC values of  $0.73 \text{ mg L}^{-1}$  at day 14 and  $\text{EC}_{50,14d}$  of  $77.7 \text{ mg L}^{-1}$  [27]. These results are in close accordance with the NOEC values determined for the green algae *Chlamydomonas reinhardi* of 0.22 to  $1.45 \text{ mg L}^{-1}$  and a  $\text{EC}_{50,10d}$  of  $5.2 \text{ mg L}^{-1}$  [42].

Using our process-based model, we derived a time-independent no-effect concentration (NEC) for prometryn of  $4.6 \mu\text{g L}^{-1}$  and tolerance concentration ( $c_T$ ) of  $31.6 \mu\text{g L}^{-1}$ , and for methyl parathion a NEC of  $1.0 \text{ mg L}^{-1}$  and a tolerance concentration of  $1.1 \text{ mg L}^{-1}$ .

Classical effect concentrations, NOEC and  $\text{EC}_{50}$ , are time-dependent which can not be compared directly with the time-independent NEC [18]. See Kooijman et al. [24] for a discussion on NOEC and NEC.

The data fit results show that prometryn inhibits growth. This result was obtained without making prior assumptions on the simulated mode of action. In fact, it is known from molecular/physiological studies [34, 10, 40] that triazines, like prometryn, inhibit photosynthesis and thus inhibits the generation of energy available for biomass production, i.e. growth. The second compound, methyl parathion, is a cholinesterase-inhibiting organophosphorous compound. As algae lack cholinesterase, there is no specific site of action identifiable although at high concentrations methyl parathion affects photosynthesis [41]. In general, organophosphorous insecticides can reduce membrane integrity, cause leakage of cellular metabolites [29, 30] and can affect mitochondrial ATPases [44, 3]. Our model captured the effects of methyl parathion by increasing the hazard rate.

### 2.4.2 Assumption justification

To derive our parameter-sparse model, we made various assumptions. One is that the amount of biologically available nitrogen in the system remains constant, i.e.  $N_T(t) = N_T(0)$ . From day 10 until day 14, there is a constant algal density for the control and low toxicant concentrations, see Figure 2.1. This indicates a steady-state in which dead algae and maintenance products are re-mineralized, see also [7]. Remineralization during the whole experiment implies no substantial loss of nitrogen.

Another assumption was that bacterial degradation of detritus was not affected by the toxicants. No aquatic bacteria without a photosystem were found to be sensitive for prometryn [46]. Terrestrial micro-algae and cyanobacteria can even potentially benefit from organophosphates like methyl parathion by

hydrolysing the compound and liberating the phosphate [28]. From this we conclude that it is justified to make this assumption.

We also assumed that the toxicant concentration was constant; that is the organisms do not affect the toxicant concentration via degradation or accumulation. Based on an algal single cell bio-volume of  $280 \mu\text{m}^3$  [48],  $3.5 \cdot 10^5$  cells (Figure 2.1A) occupy a volume of  $1 \cdot 10^8 \mu\text{m}^3$  while 100 ml medium has a volume of  $1 \cdot 10^{14} \mu\text{m}^3$ . Therefore, even with high BCF values, the influence of the algae on medium toxicant concentrations would be negligible. This is in accordance with a recovery close to 100% [27]. The estimated TC and NEC values are based on external toxicant concentrations. If measured concentrations or predictions from a toxicant-fate model are available then these (time-varying) concentrations can be used instead of (constant) nominal values.

## 2.5 Conclusions

In our process-based modelling approach, the ecological status is affected by both nutrient stress and toxicant stress. Thus the interactive effects of a toxicant and nutrient load on the status, which are difficult to separate in nature, are taken into account. Beside estimations of the average and standard deviation of the parameters, our model yields the covariance matrix, which includes the covariances between the toxicity parameters and biological parameters. These covariances are neglected when the analysis is based on separate ecological and toxicological single species data sets.

Our final goal is to predict the effects of toxicants on the behaviour and functioning of ecosystems [21], for this we need parameters which describe the biology of the species involved, toxicity parameters for effect modelling, and a model for the environment.

Without prior assumptions we found that the herbicide prometryn inhibits algal growth, in accordance with it being a photosynthesis inhibitor. The insecticide methyl parathion was found to increase the hazard rate, which can be explained by the fact that this insecticide is known to reduce membrane integrity and causes leakage of cellular metabolites.

Liebig et al. [27] present exposure experiments with algae and ciliates: the ciliates themselves are insensitive to the herbicide prometryn, however their growth is reduced when prometryn affects the ciliates' prey. We will use the estimated algal parameter values in an extended model with predatory ciliates to study this indirect effect. This is a first step towards understanding sub-lethal toxic effects in simple aquatic food chains and eventually more complex ecosystems, see for instance [45, 20, 21, 36, 8].

## 2.6 Appendix

### Derivation of $c_x$ and approximation of its average and variance

The algae population persists when  $0 < A^* < N_T$ , (see Eq. (2.5)). This provides the persistence criterion for the chemical unstressed algae:  $N_T > K_N h / (\mu - h)$ . To include a chemical stress that affects nutrient assimilation indirectly via the growth rate ( $\mu$ ), take  $\mu$  to depend on the toxicant concentration ( $c$ ) in the environment as in Eq. (2.6b). This yields a toxicant dependent equilibrium density for the algae ( $A(c)^*$ ), see Eq. (2.5):

$$A(c)^* = N_T - \frac{K_N h}{\mu(c) - h} = N_T - K_N \left( \frac{\mu(0)}{h \left( 1 + \frac{\max(0, (c - c_{0, \mu}))}{c_{T, \mu}} \right)} - 1 \right)^{-1} \quad (2.8)$$

Let  $c_x$  be the toxicant concentration at which the algae population goes extinct, then  $A(c_x)^* = 0$ . Given that the toxicant has effect, we have  $\max(0, (c_x - c_{0, \mu})) = c_x - c_{0, \mu}$ . This yields after some algebraic manipulation Eq. (2.7). The equation below is identical to Eq. (2.7) for the calculation of the extinction concentration. The results of the SSQ fit for the parameter estimates and covariance matrix are used to estimate the expected value of  $c_x$  and its variance.

$$c_x(N_T) = g(c_0, c_T, \mu, h, K_N, N_T) \quad (2.9)$$

$$g(X_1, X_2, X_3, X_4, X_5, N_T) = X_1 + X_2 \left( \frac{X_3}{X_4} \left( \frac{N_T}{X_5 + N_T} \right) - 1 \right) \quad (2.10)$$

where  $X_i$ , with  $i \in \{1, 2, 3, 4, 5\}$ , are the stochastic variables with mean,  $\mu_{X_i}$ , and variance,  $(\text{var}[X_i])$ . Using a second order Taylor series expansion [31, p181] to approximated  $g$  around  $\mu_{X_i}$  gives:

$$g(X_1, X_2, X_3, X_4, X_5, N_T) \approx g(\mu_{X_1}, \mu_{X_2}, \mu_{X_3}, \mu_{X_4}, \mu_{X_5}, N_T) + \sum_{i=1}^{n=5} \left( \frac{\partial g}{\partial X_i} \Big|_{\mu_{X_i}} (X_i - \mu_{X_i}) \right) + \frac{1}{2} \sum_{i=1}^{n=5} \sum_{j=1}^{n=5} \left( \frac{\partial^2 g}{\partial X_i \partial X_j} \Big|_{\mu_{X_i}} (X_i - \mu_{X_i})(X_j - \mu_{X_j}) \right) \quad (2.11)$$

with  $\mathcal{E}[(X_i - \mu_{X_i})] = 0$ , the expected value around  $\mu_{X_i}$  of  $g(X_1, X_2, X_3, X_4, X_5, N_T)$  is:

$$\mathcal{E}[g(X_1, X_2, X_3, X_4, X_5, N_T)] \approx \quad (2.12)$$

$$\mu_{X_1} + \frac{\mu_{X_2} \mu_{X_3} N_T}{\mu_{X_4} (\mu_{X_5} + N_T)} - \mu_{X_2} + \frac{1}{2} \sum_{i=1}^{n=5} \sum_{j=1}^{n=5} \left( \frac{\partial^2 g}{\partial X_i \partial X_j} \Big|_{\mu_{X_i}} \text{cov}[X_i, X_j] \right)$$

The variance of  $g$  is:

$$\text{var}[g(X_1, X_2, X_3, X_4, X_5, N_T)] \approx \sum_{i=1}^{n=5} \sum_{j=1}^{n=5} \left( \frac{\partial g}{\partial X_i} \Big|_{\mu_{X_i}} \frac{\partial g}{\partial X_j} \Big|_{\mu_{X_i}} \text{cov}[X_i, X_j] \right) \quad (2.13)$$

# References

- [1] S. Agusti, M. P. Satta, M. P. Mura, and E. Benavent. Dissolved esterase activity as a tracer of phytoplankton lysis: Evidence of high phytoplankton lysis rates in the northwestern mediterranean. *Limnology and Oceanography*, 43(8):1836–1849, 1998.
- [2] A. Andersson, S. Falk, G. Samuelsson, and A. Hagstrom. Nutritional characteristics of a mixotrophic nanoflagellate, *Ochromonas sp.* . *Microbial Ecology*, 17:251–262, 1989.
- [3] M. Barbier, P. Prevot, and M. O. Soyer-Gobillard. Esterases in marine dinoflagellates and resistance to the organophosphate insecticide parathion. *International Microbiology*, 3:117–123, 2000.
- [4] J. J. M. Bedaux and S. A. L. M. Kooijman. Statistical analysis of bioassays based on hazard modelling. *Environmental and Ecological Statistics*, 1:303–314, 1994.
- [5] T. Berman, B. F. Sherr, E. Sherr, D. Wynne, and J. J McCarthy. The characteristics of ammonium and nitrate uptake by phytoplankton in lake Kinneret. *Limnology and Oceanography*, 29(2):287–297, 1984.
- [6] W. Brack, J. Bakker, E. de Deckere, C Deerenberg, J. van Gils, M Hein, P Jurajda, S. Kooijman, M. Lamoree, S. Lek, M.-J. López de Alda, A. Marcomini, I. Muñoz, S. Rattei, H. Segner, K. Thomas, P. von der Ohe, B. Westrich, D. de Zwart, and M. Schmitt-Jansen. Models for assessing and forecasting the impact of environmental key pollutants on freshwater and marine ecosystems and biodiversity. *Environmental Science & Pollution Research*, 12(5):252–256, 2005.
- [7] C. P. D. Brussaard and R. Riegman. Influence of bacteria on phytoplankton mortality with phosphorus or nitrogen as algal-growth-limiting nutrient. *Aquatic Microbial Ecology*, 14:271–280, 1998.

- [8] F. De Laender, K. A. C. De Schamphelaere, P. A. Vanrolleghem, and C. R. Janssen. Validation of an ecosystem modelling approach as a tool for ecological effect assessments. *Chemosphere*, 71:529–545, 2008.
- [9] A. E. DeBiase, R. W. Sanders, and K. G. Porter. Relative nutritional value of ciliate protozoa and algae as food for daphnia. *Microbial Ecology*, 19:199–210, 1990.
- [10] M. Faust, R. Altenburger, T. Backhaus, H. Blanck, W. Boedeker, P. Gramatica, V. Hamer, M. Scholze, M. Vighi, and L. H. Grimme. Predicting the joint algal toxicity of multi-component s-triazine mixtures at low-effect concentrations of individual toxicants. *Aquatic Toxicology*, 56:13–32, 2001.
- [11] V. E. Forbes and P. Calow. Extrapolation in ecological risk assessment: Balancing pragmatism and precaution in chemical controls legislation. *BioScience*, 52(3):249–257, 2002.
- [12] V. E. Forbes, P. Calow, and R. M. Sibly. The extrapolation problem and how population modeling can help. *Environmental Toxicology and Chemistry*, 27(10):1987–1994, 2008.
- [13] C. Gaggi, G. Sbrilli, A. M. H. El Naby, M. Bucci, M. Duccini, and E. Bacci. Toxicity and hazard ranking of s-triazine herbicides using Microtox<sup>R</sup>, two green algal species and a marine crustacean. *Environmental Toxicology and Chemistry*, 14:1065–1069, 1995.
- [14] R. J. Geider and B. A. Osborne. Respiration and microalgal growth: a review of the quantitative relationship between dark respiration and growth. *New Phytologist*, 112(3):327–341, 1989.
- [15] F. A. P. C. Gobas. A model for predicting the bioaccumulation of hydrophobic organic chemicals in aquatic food-webs: application to lake ontario. *Ecological Modelling*, 69:1–17, 1993.
- [16] F. A. P. C. Gobas, E. J. McNeil, L. Lovett-Doust, and G. D. Haffner. Bioconcentration of chlorinated aromatic hydrocarbons in aquatic macrophytes (*Myriophyllum spicatum*). *Environmental Science and Technology*, 25:924–929, 1991.
- [17] T. G. Hallam, G. A. Canziani, and R. R. Lassiter. Sublethal narcosis and population persistence: a modeling study on growth effects. *Environmental Toxicology and Chemistry*, 12:947–954, 1993.

- [18] T. Jager, E. H. W. Heugens, and S. A. L. M. Kooijman. Making sense of ecotoxicological test results: towards application of process-based models. *Ecotoxicology*, 15:305–314, 2006.
- [19] B. W. Kooi. Numerical bifurcation analysis of ecosystems in a spatially homogeneous environment. *Acta Biotheoretica*, 51:189–222, 2003.
- [20] B. W. Kooi, D. Bontje, and M. Liebig. Model analysis of simple aquatic ecosystems with sublethal toxic effects. *Mathematical Biosciences and Engineering*, 5(4):771–787, 2008.
- [21] B. W. Kooi, D. Bontje, G. A. K. van Voorn, and S. A. L. M. Kooijman. Sublethal toxic effects in a simple aquatic food chain. *Ecological Modelling*, 112:304–318, 2008.
- [22] B. W. Kooi and S. A. L. M. Kooijman. Existence and stability of microbial prey-predator systems. *Journal of Theoretical Biology*, 170:75–85, 1994.
- [23] S. A. L. M. Kooijman. *Dynamic Energy Budgets in biological systems, 2nd edn.* Cambridge University Press, Cambridge, 2000.
- [24] S. A. L. M. Kooijman, A. O. Hanstveit, and N. Nyholm. No-effect concentrations in algal growth inhibition tests. *Water Research*, 30(7):1625–1632, 1996.
- [25] S. Körner and A. Nicklisch. Allelopathic growth inhibition of selected phytoplankton species by submerged macrophytes. *Journal of Phycology*, 38:862–871, 2002.
- [26] O. Köster and F. Jüttner.  $\text{NH}_4^+$  utilization and regeneration rates in freshwater lakes determined by GCMS of derivatised dihydroindophenol. *Journal of Microbiological Methods*, 37:65–76, 1999.
- [27] M. Liebig, G. Schmidt, D. Bontje, B. W. Kooi, G. Streck, W. Traunspurger, and T. Knacker. Direct and indirect effects of pollutants on algae and algivorous ciliates in an aquatic indoor microcosm. *Aquatic Toxicology*, 88:102–110, 2008.
- [28] M. Megharaj, D. R. Madhavi, C. Sreenivasulu, A. Umamaheswari, and K. Venkateswarlu. Biodegradation of methyl parathion by soil isolates of microalgae and cyanobacteria. *Bulletin of Environmental Contamination and Toxicology*, 53(2):292–297, 1994.
- [29] P. K. Mohapatra and U. Schiewer. Effect of dimethoate and chlorfenvinphos on plasma membrane integrity of *Synechocystis sp.* PCC 6803. *Ecotoxicology and Environmental Safety*, 41:269–274, 1998.

- [30] P. K. Mohapatra, H. Schubert, and U. Schiewer. Effect of dimethoate on photosynthesis and pigment fluorescence of *Synechocystis* sp. PCC 6803. *Ecotoxicology and Environmental Safety*, 36(3):231–237, 1997.
- [31] A. M. Mood, F. A. Graybill, and D. C. Boes. *Introduction to the Theory of Statistics*. McGraw-Hill, Inc., 3<sup>th</sup> edition, 1974.
- [32] S. L. Nielsen. Size-dependent growth rates in eukaryotic and prokaryotic algae exemplified by green algae and cyanobacteria: comparisons between unicells and colonial growth forms. *Journal of Plankton Research*, 28(5):489–498, 2006.
- [33] OECD. OECD guideline for testing of chemicals - 201 Freshwater alga and cyanobacteria, growth inhibition test. <http://www.oecd.org>, March 23:1–25, 2006.
- [34] W. Oettmeier. Herbicide resistance and supersensitivity in photosystem II. *Cellular and Molecular Life Sciences*, 55:1255–1277, 1999.
- [35] Office of Pesticide Programs. Pesticide ecotoxicity database. *Environmental Fate and Effects Division, U.S. Environmental Protection Agency, Washington, D.C. Cited at: ECOTOX:Ecotoxicology Database: ([http://www.epa.gov/cgi-bin/ecotox\\_quick\\_search](http://www.epa.gov/cgi-bin/ecotox_quick_search)), accessed: Apr 19, 2005*, 2000.
- [36] R. A. Park, J. S. Clough, and M. C. Wellman. Aquatox: Modeling environmental fate and ecological effects in aquatic ecosystems. *Ecological Modelling*, 213:1–15, 2008.
- [37] L. Peperzak, R. N. M. Duin, F. Colijn, and W. W. C. Gieskes. Growth and mortality of flagellates and non-flagellate cells of *Phaeocystis globosa* (*Prymnesiophyceae*). *Journal of Plankton Research*, 22(1):107–119, 2000.
- [38] S. Présing, S. A. Herodek, T. Preston, and L. Vörös. Nitrogen uptake and the importance of internal nitrogen loading in lake Balaton. *Freshwater Biology*, 46:125–139, 2001.
- [39] H. W. Press, S. A. Teukolsky, W. T. Vetterling, and B. P. Flannery. *Numerical Recipes in C*. Cambridge University Press, 2nd edition, 1992.
- [40] C. Rioboo, O. González, C. Herrero, and A. Cid. Physiological response of freshwater microalga (*Chlorella vulgaris*) to triazine and phenylurea herbicides. *Aquatic Toxicology*, 59:225–235, 2002.
- [41] G. Saroja and S. Bose. Correlation between inhibition of photosynthesis and growth of chlorella treated with methyl parathion. *Journal of Biosciences*, 5(1):71–77, 1983.

- [42] H. Schäfer, H. Hettler, U. Fritsche, G. Pitzén, G. Röderer, and A. Wenzel. Biotests using unicellular algae and ciliates for predicting long-term effects of toxicants. *Ecotoxicology and Environmental Safety*, 27:64–81, 1994.
- [43] D. T. Sijm, K. W. Broersen, D. F. De Roode, and P. Mayer. Bioconcentration kinetics of hydrophobic chemicals in different densities of *chlorella pyrenoidosa*. *Environmental Toxicology and Chemistry*, 17(9):1695–1704, 1998.
- [44] R. Srinivas, G. S. Shamsundar, S. K. Jayalakshmi, and K. Sreeramulu. Effect of insecticides and inhibitors on P-glycoprotein ATPase (M-type) activity of resistant pest *Helicoverpa armigera*. *Current Science*, 88(9):1449–1452, 2005.
- [45] T. P. Traas, J. H. Janse, P. J. Van den Brink, T. C. M. Brock, and T. Aldenberg. A freshwater food web model for the combined effects of nutrients and insecticide stress and subsequent recovery. *Environmental Toxicology and Chemistry*, 23:521–529, 2004.
- [46] U.S. EPA. ECOTOX User Guide: Ecotoxicology Database System. version 4.0. available: <http://www.epa.gov/ecotox/>, 2006. Accessed: Aug 23, 2007.
- [47] K. Van den Meersche, J. J. Middelburg, K. Soetaert, P. Van Rijswijk, H. T. S. Boschker, and C. H. R. Heip. Carbon-nitrogen coupling and algal-bacterial interactions during an experimental bloom: Modeling a  $^{13}\text{C}$  tracer experiment. *Limnology and Oceanography*, 49(3):862–878, 2004.
- [48] T. Weisse and B. Kirchhoff. Feeding of the heterotrophic freshwater dinoflagellate peridiniopsis berolinense on cryptophytes: analysis by flow cytometry and electronic particle counting. *Aquatic Microbial Ecology*, 12:153–164, 1997.
- [49] Y. H. Wen, A. Vézina, and R. H. Peters. Allometric scaling of compartmental fluxes of phosphorus in freshwater algae. *Limnology and Oceanography*, 42(1):45–56, 1997.



## Chapter 3

# Feeding threshold for predators stabilises predator-prey systems

D. Bontje, B.W. Kooi, G.A.K. van Voorn and S.A.L.M. Kooijman  
*Math. Model. Nat. Phenom.*, 4(6):91–108, 2009.

Since Rosenzweig showed the destabilisation of exploited ecosystems, the so called *Paradox of enrichment*, several mechanisms have been proposed to resolve this paradox. In this paper we will show that a feeding threshold in the functional response for predators feeding on a prey population stabilizes the system and that there exists a minimum threshold value above which the predator-prey system is unconditionally stable with respect to enrichment. Two models are analysed, the first being the classical Rosenzweig-MacArthur (RM) model with an adapted Holling type-II functional response to include a feeding threshold. This mathematical model can be studied using analytical tools, which gives insight into the mathematical properties of the two dimensional ordinary differential equation (ODE) system and reveals underlying stabilisation mechanisms. The second model is a mass-balance (MB) model for a predator-prey-nutrient system with complete recycling of the nutrient in a closed environment. In this model a feeding threshold is also taken into account for the predator-prey trophic interaction. Numerical bifurcation analysis is performed on both models. Analysis results are compared between models and are discussed in relation to the analytical analysis of the classical RM model. Experimental data from the literature of a closed system with ciliates, algae and a limiting nutrient are used to estimate parameters for the

MB model. This microbial system forms the bottom trophic level of aquatic ecosystems and therefore a complete overview of its dynamics is essential for understanding aquatic ecosystem dynamics.

### 3.1 Introduction

In the classical Rosenzweig-MacArthur (RM) model a bifurcation occurs when the carrying capacity of the prey reaches high values [27]. Then the steady-state becomes unstable and a stable periodic solution originates. This transition is the Hopf bifurcation point. For carrying capacity values above the Hopf bifurcation point, the amplitude of the oscillatory dynamics increases. As a result the minimum value for the prey population becomes very low and extinction due to stochastic fluctuations becomes likely. This phenomenon is called the “paradox of enrichment”.

Kirk [12] suggested that the solution to the paradox of enrichment lies in the fact that many biological models show a lack of biological detail. Indeed, many biological models that include more detail than the RM model seem to resolve the paradox by preventing destabilisation under nutrient enrichment. Among the underlying mechanisms are the division of the prey-population into two subpopulations: one accessible, vulnerable or edible and one inaccessible, invulnerable or inedible [15, 2], self-limitation of the prey [12], predator-induced defence mechanisms in the prey population [32], dormancy of the predators [16] and spatial heterogeneity [11, 29, 25]. Whether these mechanisms do cause stability depends on model specifics, as for example, adaptive defence of the prey can be both stabilizing [32] and destabilizing [1].

The stability of ecological systems is extremely sensitive to the exact form of the functional response that models the trophic interactions [10]. In [31] it is shown that the paradox of enrichment can indeed be avoided by using the functional response proposed by Beddington [3] and DeAngelis et al. [8] that takes intraspecific interference between predators into account.

In this paper we evaluate the effects of a feeding threshold on ecosystem stability and/or persistence. In light of the comments made in [9], we define stability in the mathematical sense as the stability of steady states with respect to small perturbations. We use the definitions for stability as provided in [31], where *weak* stability is defined as the delayed occurrence of a Hopf bifurcation and *strong* stability as the disappearance of the Hopf bifurcation for all states of enrichment.

Here the Holling type-II functional response is adapted by the introduction of a fixed threshold for the prey population below which all prey individuals are not at risk of predation, e.g. at low food densities the predator stops searching [22, 28] or the prey hides in spatial separated areas called refuges.

Different types and causes of refuges are discussed in [4]. This type of functional response is used in aquatic ecosystem modelling, for instance in the AQUATOX program that predicts the fate of various pollutants, such as nutrients and organic chemicals, and their effects on the ecosystem, including fish, invertebrates, and aquatic plants [23, 24].

The main goal of this paper is to study how the inclusion of a feeding threshold in the Holling type-II functional response for predator-prey interaction affects the behaviour of two different models which each simulate a nutrient-algae-ciliate microbial ecosystem in a spatial homogeneous and closed environment. One model is based on a mass-balance (MB) formulation which is derived from first principles and includes complete nutrient recycling [7, 14] and the Holling type-II functional responses are used for the nutrient-algae interaction and the algae-ciliate interaction, only the latter includes a feeding threshold. The other model is the classical RM model [27] which only implicitly includes a nutrient and does not include a mass-balance.

Before starting the analysis of the effect of a feeding threshold on stability in our MB model, we first study the simpler RM model [27] as symbolic algebra programs allow for a complete analysis of the model. Then we continue with a numerical bifurcation analysis of the MB model. For both models we study the effect of the feeding threshold on the paradox of enrichment by bifurcating both the threshold value and the nutrient load of the system. Important is the minimal nutrient load of the system at which the algae can invade the system, then a transcritical bifurcation (TC) occurs. The second TC bifurcation occurs when the nutrient load is high enough to support a producer population that is sufficiently dense enough to allow predator invasion. This last TC marks the region where the prey and predator can coexist. At even higher nutrient loads a Hopf bifurcation marks regions where the system shows oscillatory dynamics [13]. We will show that the long-term dynamic behaviour of the RM and MB systems appear to be similar and are qualitatively even the same.

To illustrate the existence of a feeding threshold, we apply the MB model on experimental data consisting of dynamic growth curves of prey and predator from [33]. During batch experiments the flagellated algal species *Cryptomonas sp.* was preyed upon by one of three ciliate species, either *Balanion planctonicum*, *Urotricha furcata* or *Urotricha farcta*. All species are fresh water micro-organisms.

## 3.2 Formulation of the model

We study a spatial homogeneous and closed system with a predator,  $Z$  and a prey population,  $P$ , consuming a limiting nutrient,  $N$ . Other nutrients, including sunlight, are not limiting. The mortality rate of each population is

denoted by  $d_P$  for the prey and  $d_Z$  for the predator. Table 3.1 lists all used variables and parameters together with a short description and units.

The interactions between the trophic levels are modelled with a Holling type-II functional response. Parameters for the prey-nutrient interaction are the searching rate  $v_N$  and the nutrient handling time  $h_N$  and similar for the predator-prey interaction are the searching rate  $v_P$  and the prey handling time  $h_P$ . We implement a numerical feeding threshold,  $\tau$ , by using a maximum-function denoted with  $(P - \tau)_+ = \max(P - \tau, 0)$ , which either yields zero or a positive value when  $P > \tau$ .

The predator population digests its prey only partly. The conversion efficiency of prey biomass into predator biomass is denoted by the yield factor  $y_{PZ}$ . The unusable part of the food is ejected into the environment as faeces. This excreted material together with dead material forms detritus and is decomposed instantaneously and this gives complete recycling of the nutrient. The above leads to the following ODE system

$$\frac{dN}{dt} = -P \frac{v_N N}{1 + v_N h_N N} + (1 - y_{PZ}) Z \frac{v_P (P - \tau)_+}{1 + v_P h_P (P - \tau)_+} + d_P P + d_Z Z . \quad (3.1a)$$

$$\frac{dP}{dt} = P \left( \frac{v_N N}{1 + v_N h_N N} - d_P \right) - Z \frac{v_P (P - \tau)_+}{1 + v_P h_P (P - \tau)_+} , \quad (3.1b)$$

$$\frac{dZ}{dt} = Z \left( y_{PZ} \frac{v_P (P - \tau)_+}{1 + v_P h_P (P - \tau)_+} - d_Z \right) \quad (3.1c)$$

$$I_{NP} = 1/h_N ; \quad K_{NP} = 1/(v_N h_N) ; \quad I_{PZ} = 1/h_P ; \quad K_{PZ} = 1/(v_P h_P) .$$

The Michaelis-Menten parameters, being the maximum ingestion rates ( $I_{NP}$  and  $I_{PZ}$ ) and the nutrient half-saturation concentrations ( $K_{NP}$  and  $K_{PZ}$ ), are compound parameters of the searching rate  $v$  and the handling time  $h$ . The last three terms of Eq. (3.1a) are the terms for instantaneous and complete degradation of faeces and dead organisms. In the Appendix we show how a system of limiting nutrient, producer, predator, bacteria and detritus can be reduced to the system above while obeying mass-conservation.

Because of this recycling and mass-conservation, we can reduce the three dimensional system to an equivalent two dimensional system. Let  $N_T$  denote the nutrient load or more precise the total amount of limiting nutrient in the closed system formed by the biota  $P$ ,  $Z$  and the abiotic environment  $N$  defined as

$$N_T = N(t) + P(t) + Z(t) . \quad (3.2)$$

Adding the three equations of Eq. (3.1) shows that

$$\frac{dN_T}{dt} = 0 \quad \text{and} \quad N_T = N(0) + P(0) + Z(0),$$

that is,  $N_T$  is a constant. The resulting two dimensional system becomes

$$\begin{aligned} \frac{dP}{dt} &= P(f(N) - d_P) - Zf(P), \\ \frac{dZ}{dt} &= Z(y_{PZ}f(P) - d_Z), \\ f(N) &= \frac{v_N(N_T - P - Z)}{1 + v_N h_N(N_T - P - Z)} \quad ; \quad f(P) = I_{PZ} \frac{(P - \tau)_+}{K_{PZ} + (P - \tau)_+}. \end{aligned}$$

To have a mathematically well-posed problem we require for the initial value conditions that  $N(0) = N_T - P(0) - Z(0) > 0$ .

When taking  $h_N = 0$ ,  $f(N)$  becomes a linear functional response, this yields:

$$\frac{dP}{dt} = rP \left( 1 - \frac{P + \alpha Z}{K} \right) - Zf(P), \quad (3.3a)$$

$$\frac{dZ}{dt} = Z \left( y_{PZ}f(P) - d_Z \right), \quad (3.3b)$$

where

$$K = N_T - \frac{d_P}{v_N} \quad ; \quad r = v_N K = v_N N_T - d_P \quad ; \quad \alpha \in \{0, 1\}. \quad (3.3c)$$

In absence of the predator the prey population grows logistically. Note that the intrinsic growth rate  $r$  and carrying capacity  $K$  are both expressed as a function of  $N_T$  using parameters from Eq. (3.1).

With  $\alpha = 1$  in Eq. (3.3a) we obtain a mass-balance model for both  $P$  and  $Z$ . Posteriorly the nutrient density  $N(t)$  can be calculated using Eq. (3.2). The above ODE system with  $\alpha = 0$  is identical to the RM model, which in its usual form has  $r$  and  $K$  as independent constants. Due to our formulation,  $r \propto K$ . As will be shown in the next section, for  $\tau = 0$  the paradox of enrichment can still occur. When  $\alpha = 0$ , then the term  $Z/K$  is removed from Eq. (3.3a), leading to an ODE-system without mass-conservation. Consequently, Eq. (3.2) for  $N_T$  no longer holds and the value for variable  $N$  can not be calculated.

We briefly repeat the main differences between the RM and MB model: the first has a nutrient handling time of zero and no mass-conservation, the latter has a non-zero nutrient handling time and respects mass-conservation. By setting  $\alpha = 0$  and  $h_N = 0$  one obtains the RM model from the MB model.

Table 3.1: List of Symbols

Symbol	Description	Units
$\alpha$	Eq. (3.3) with $\alpha = 0$ forms the RM model. With $\alpha = 1$ a model with a correct mass-balance would be formed	-/-
$C$	ciliate (predator) density	#cells L <sup>-1</sup>
$d_P$	death rate prey	d <sup>-1</sup>
$d_Z$	death rate predator	d <sup>-1</sup>
$F$	flagellate (prey) density	#cells L <sup>-1</sup>
$f(P)$	Holling type-II functional response of $Z$ on $P$	d <sup>-1</sup>
$F_0(0)$	initial flagellate density without ciliates present	#cells L <sup>-1</sup>
$F_C(0)$	initial flagellate density with ciliates present	#cells L <sup>-1</sup>
$g(P)$	prey zero-growth isocline for RM model	mol N L <sup>-1</sup>
$h_N$	nutrient handling time	d
$h(P)$	prey zero-growth isocline for MB model	mol N L <sup>-1</sup>
$h_P$	prey handling time	d
$I_{FC}$	maximum specific ingestion rate of prey biomass	prey predator <sup>-1</sup> h <sup>-1</sup>
$I_{PZ}$	maximum specific ingestion rate of prey biomass	mol N mol N <sup>-1</sup> d <sup>-1</sup>
$I_{NP}$	maximum specific ingestion rate of limiting nutrient	mol N mol N <sup>-1</sup> d <sup>-1</sup>
$K$	prey's carrying capacity	mol N L <sup>-1</sup>
$K_{NP}$	nutrient half-saturation concentration for $P$ on $N$	mol N L <sup>-1</sup>
$K_{PZ}$	nutrient half-saturation concentration for $Z$ on $P$	mol N L <sup>-1</sup>
$N$	limiting nutrient concentration	mol N L <sup>-1</sup>
$n_C$	predator limiting nutrient content	pmol N /cell
$n_F$	prey limiting nutrient content	pmol N /cell
$N_T$	total amount of limiting nutrient in the system (nutrient load)	mol N L <sup>-1</sup>
$P$	prey biomass density	mol N L <sup>-1</sup>
$r$	prey <i>percapita</i> growth rate	d <sup>-1</sup>
$\tau$	feeding threshold in units of prey biomass	mol N L <sup>-1</sup>
$\tau_F$	feeding threshold expressed in flagellate density	#cells L <sup>-1</sup>
$\tau_H^*$	lower threshold limit where a Hopf bifurcation will never occur	mol N L <sup>-1</sup>
$V_C$	ciliate (predator) biovolume	$\mu\text{m}^3$
$V_F$	flagellate (prey) biovolume	$\mu\text{m}^3$
$v_N$	nutrient searching rate	mol N L <sup>-1</sup> d <sup>-1</sup>
$v_P$	prey searching rate	mol N L <sup>-1</sup> d <sup>-1</sup>
$y_{PZ}$	yield of predator biomass on prey biomass, with $0 \leq y_{PZ} \leq 1$	mol N mol N <sup>-1</sup>
$Z$	predator biomass density	mol N L <sup>-1</sup>

### 3.3 Analysis of the models

The two dimensional systems can be analysed with a stability analysis and by studying the zero-growth isoclines. The stability properties of the resulting equilibria are derived using nonlinear dynamic system theory. When  $\mathbf{J}$  denotes the Jacobian matrix evaluated at the equilibrium, its stability is directly determined by the sign of the eigenvalue of the real parts. For systems with two variables, the transcritical bifurcation,  $\tau_{TC}(N_T)$ , and the Hopf bifurcation curve,  $\tau_H(N_T)$ , are determined by  $\det \mathbf{J} = 0$  and  $\text{trace } \mathbf{J} = 0$ , respectively.

#### 3.3.1 The Rosenzweig-MacArthur model

For the RM model Eqs. (3.3) and depending on the parameter values, there is one equilibrium with no species, denoted by  $E_0$ , one with only the producer,  $E_1$ , and one with coexistence of the producer and predator,  $E_2$ . Using symbolic calculation software, such as Maple [18], we obtain algebraic expressions for the isoclines, the transcritical bifurcations and Hopf bifurcation codim-1 curves. These lengthy expressions are not given here. However, the curves are shown in the left panels of Figure 3.1.

These panels show the long-term dynamic behaviour of the two populations without and with a feeding threshold, respectively  $\tau = 0$  and  $\tau = 0.1$ . For low values of  $N_T$  only the prey population exists. For larger  $N_T$  both populations coexist stably. The transition is at the transcritical bifurcation point. Increasing  $N_T$  further, the steady-state becomes unstable and a stable periodic solution originates. This transition is at the Hopf bifurcation point. For  $N_T$  values above the Hopf bifurcation point, the amplitude of the oscillatory dynamics increases. As a result the minimum value for the prey population becomes very low and extinction due to stochastic fluctuations becomes likely. This phenomenon is called the ‘‘paradox of enrichment’’.

The results in Figure 3.1 show that the Hopf bifurcation occurs at higher  $N_T$  levels for higher threshold levels  $\tau_H$ . This suggests a stabilising effect of the feeding threshold. In order to study this effect further we calculated the two-parameter diagram where besides  $N_T$  also  $\tau$  varies. In the left panel of Figure 3.2 this diagram is shown. Note the logarithmic scale of the horizontal axis, which was needed to illustrate the asymptotic approach of the Hopf-curve towards a single threshold value at high nutrient loading. There appears to be an upper limit for the  $\tau_H$  values when  $\lim N_T \rightarrow \infty$ . The simple expression for this limiting threshold with abundant enrichment, reads

$$\tau_H^* = \lim_{N_T \rightarrow \infty} \tau_H = K_{PZ} \left( \frac{y_{PZ} I_{PZ}}{d_Z} - 1 \right)^{-2}. \quad (3.4)$$

Observe that the value of  $\tau_H^*$  solely depends on predator parameters. From Eq. (3.4) it can be observed that there is a lower threshold limit where a Hopf bifurcation will never occur for any nutrient enrichment. Therefore, the feeding threshold has a strong stabilising effect on nutrient enrichment, as defined in [31].

In order to get more insight into the disappearance of the Hopf bifurcation with feeding threshold values above  $\tau_H^*$ , we perform a phase-plane analysis of  $Z$  vs.  $P$ . We zoom in on the Hopf bifurcation diagram of the RM model in Figure 3.1, this yields the left panel of Figure 3.3 in which the two-parameter bifurcation diagram is partially repeated. Next to this panel for two points on the Hopf-curve the prey and predator zero-growth isoclines are drawn in the  $Z$  vs.  $P$  phase-space.

Taking  $dP/dt = 0$  in Eq. (3.3a) with  $\alpha = 0$  and solving  $Z$  and substituting  $Z = g(P)$ , we obtain  $g(P)$  as the function for the prey zero-growth isocline ( $P$ -isocline) given  $P > 0$

$$Z = g(P) = \frac{rP(1 - \frac{P}{K})}{f(P)}. \quad (3.5)$$

To study the stability of the equilibrium ( $E_2$ ) formed at the intersection of the prey and predator isocline we derive the Jacobian and its trace and determinant. We obtain  $\mathbf{J}_{11} = f(P)dg/dt$  and  $\mathbf{J}_{22} = 0$ , from which we derive the eigenvalues  $\lambda_{1,2}$

$$\text{Re } \lambda_{1,2} = \frac{1}{2}f(P)\frac{dg}{dP}.$$

Hence for a Hopf bifurcation we require  $dg/dP$  evaluated at the equilibrium equals to zero. Furthermore we have a stable equilibrium point when  $dg/dP < 0$  and an unstable equilibrium when  $dg/dP > 0$ .

With  $\tau = 0$ , we have the classical RM model, then the  $P$ -isocline is a parabola and the  $Z$ -isocline is a vertical line through the equilibrium value of prey population biomass. When  $dg/dP = 0$ , then a Hopf-bifurcation occurs. This specific equilibrium is denoted by point I in Figure 3.3. Decreasing  $N_T$  shifts the  $g$ -graph to the left and we have a new, stable equilibrium as  $dg/dP < 0$ . An increase in  $N_T$  shifts the  $g$ -graph to the right where  $dg/dP > 0$  and the equilibrium becomes unstable. Observe that the place of the vertical  $Z$ -isocline does not depend on  $N_T$ .

For  $\tau > 0$  the shape of the  $P$ -isocline is not a parabola. Then  $g$  has an asymptote at  $P = \tau$  and crosses the  $P$ -axis at  $P = N_T - d_P/v_N$ . For the range of  $\tau < P < N_T - d_P/v_N$  the slope of  $g$  is (mostly) negative. For points II, III and IV on the Hopf bifurcation curve we have three different positive  $\tau$ -values and we also have  $dg/dP = 0$ . For low  $\tau$ -values the equilibrium at the

Hopf bifurcation point is on a maximum of the  $P$ -isocline function (Point II), but when increasing  $\tau$  it becomes an inflection point (Point III) and then a minimum of the  $P$ -isocline function (Point IV). When the  $\tau$ -value approaches  $\tau_H^*$  (see Eq. (3.4)) the minimum of function  $g$  disappears via an inflection point, then  $dg/dP$  is always negative. Thus for  $\tau > \tau_H^*$ , the equilibrium formed by the intersection of the vertical  $Z$ -isocline and the monotonously decreasing  $P$ -isocline is stable. This explains the occurrence of strong stability.

### 3.3.2 The mass-balance model

We performed a numerical bifurcation analyses of the mass-balance model Eq. (3.1). The results are shown in the right panels of Figure 3.1. Since the parameters have the same biological meaning in both the RM and MB model, we can directly compare the results for both models.

Figure 3.1 shows how the size of the limit cycles around the Hopf depends on the total nutrient load,  $N_T$ . In both models the feeding threshold delays the occurrence of the Hopf. Large amplitudes, occurring for  $\tau = 0.1$ , mean potentially very low densities with an higher associated risk of extinction.

In Figure 3.2 the bifurcation diagrams of  $\tau$  vs  $N_T$  can be seen for both models, which contain: the invasion threshold of the algae, which is independent of  $\tau$ ; the ciliate invasion threshold which is linearly proportional to  $N_T$ ; and the Hopf-curve. These two-parameter diagrams show that there is an upper limit for the threshold for the occurrence of the Hopf bifurcation when  $N_T$  is varied. We found for the MB model the same expression for  $\tau_H^*$  as for the RM model, as given by Eq. (3.4).

In the previous section we defined  $g$  from Eq. (3.5) as being the  $P$ -isocline of the RM model, here we define similarly  $h$  as the  $P$ -isocline of the MB model (for  $P > 0$ ). For the following reasons we conclude that the behaviour of  $h$  and  $g$  is very similar. For  $\tau = 0$ , both functions first increase and then decrease and cross the  $P$ -axis at the maximal attainable prey density in absence of predator. For  $\tau > 0$ , both functions have an asymptote at  $P = \tau$  and cross the  $P$ -axis at the same location as when  $\tau = 0$ . As with the RM model, when  $\tau > \tau_H^*$  the  $P$ -isocline is monotonously decreasing, which combined with the vertical  $Z$ -isocline causes strong stability.

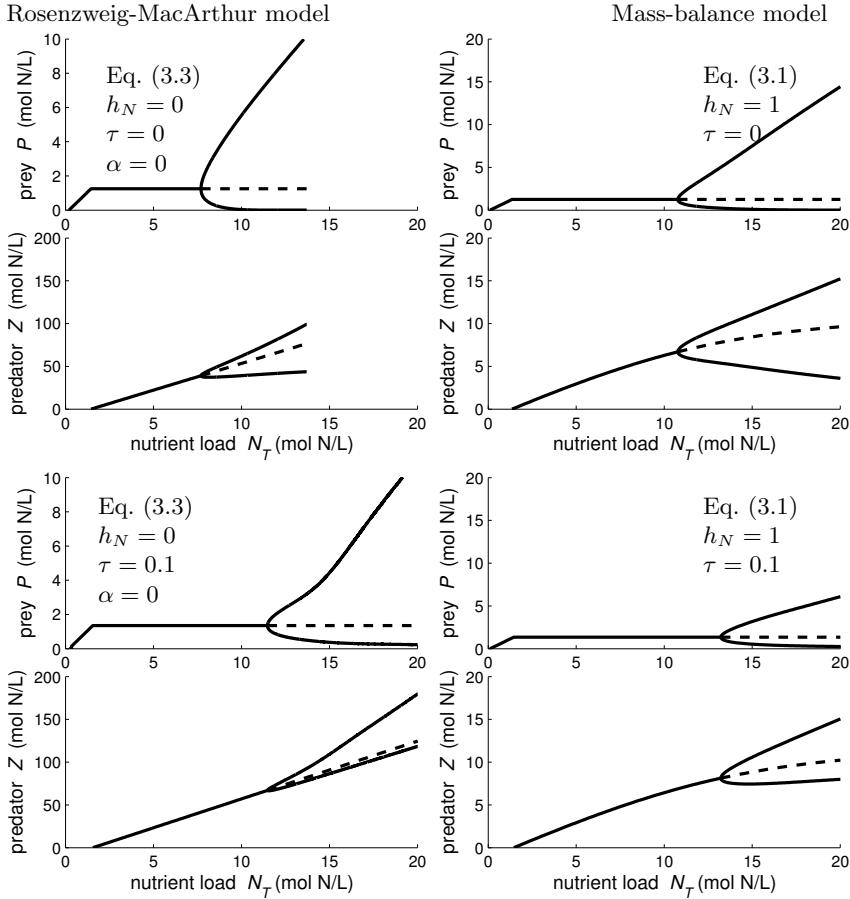


Figure 3.1: The biomasses of  $P$  and  $Z$  depend on the total nutrient load and the model used. Before the Hopf, the solid line denotes the equilibrium values, after the Hopf, the minima and maxima are denoted by the solid line and the equilibrium values by the dotted line. For the RM model, in the left hand panels, equilibrium densities were calculated with Eq. (3.3) with  $\alpha$  set to zero. The simulations in the top-left panel are not continued due to very low densities of  $P$  after  $N_T = 13.7$ . For the mass-balance model, in the right side panels, equilibrium densities were based on Eq. (3.1) with a non-zero algal nutrient handling time. Note that the two models differ in scaling of the  $Z$ -axis. For both models the following parameters values were used:  $d_Z = 0.05$ ,  $K_{PZ} = 5.00$ ,  $I_{PZ} = 0.50$ ,  $y_{PZ} = 0.50$ ,  $d_P = 0.10$ ,  $v_N = 0.50$ .

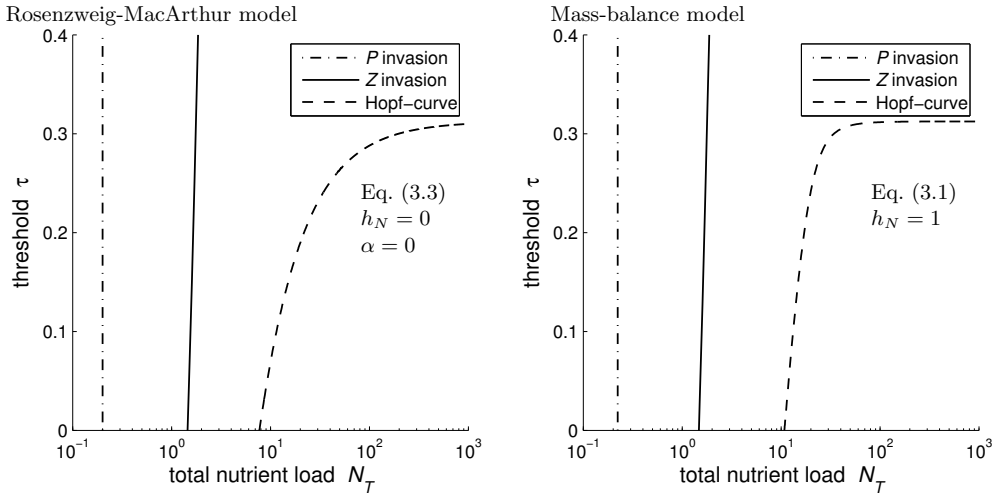


Figure 3.2: For each model the bifurcation diagram of  $\tau$  vs.  $N_T$  is shown. Each diagram contains the algal invasion threshold ( $P$ ), ciliate invasion threshold ( $Z$ ) and a Hopf-curve. For both models the following parameters values were used:  $d_Z = 0.05$ ,  $K_{PZ} = 5.00$ ,  $I_{PZ} = 0.50$ ,  $y_{PZ} = 0.50$ ,  $d_P = 0.10$ ,  $v_N = 0.50$ .

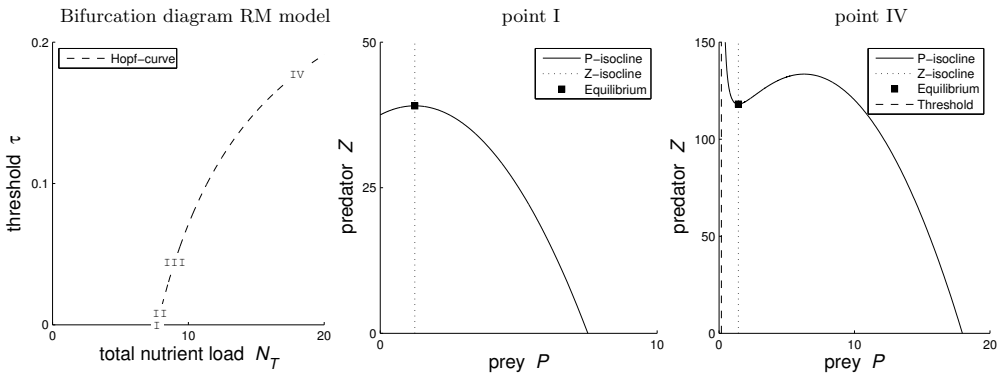


Figure 3.3: Different parameter values for nutrient load,  $N_T$ , and feeding threshold,  $\tau$ , affect the shape and location of the isoclines of the RM model (Eq. (3.3),  $\alpha = 0$ ,  $h_N = 0$ ). The left panel shows where in the bifurcation diagram the points I till IV are located on the Hopf-curve in respect to the values of  $N_T$  and  $\tau$ . Point II and III are discussed in the text. Used parameter values:  $K_{PZ} = 5.00$ ,  $I_{PZ} = 0.50$ ,  $y_{PZ} = 0.50$ ,  $d_P = 0.10$ ,  $v_N = 0.50$ ,  $d_Z = 0.05$ .  $P$ -isoclines for  $P = 0$  are omitted.

## 3.4 Applying the MB model on experimental data

To illustrate the existence of a feeding threshold, we apply the MB model on experimental data consisting of dynamic growth curves of prey and predators from [33].

### 3.4.1 Experimental setup and data description

Prior to the feeding experiments, the predatory ciliate species *Balanion planctonicum*, *Urotricha furcata* and *Urotricha farcta* were maintained on the prey species *Cryptomonas sp.*, a flagellated algae. All species are fresh water microorganisms. The body-volumes of the predators are approximately 7 to 12 times larger than their prey. In each batch experiment the algal species is preyed upon by one ciliate species. In these closed systems, there is only gas-exchange while the medium is not refreshed.

The left panels of Figure 3.4, show the experimental data and the simulated growth curves (solid lines). The top-left panel shows *B. planctonicum* feeding on *Cryptomonas sp.* and the centre-left panel shows *U. furcata*, also feeding on *Cryptomonas sp.* (vertical lines denote standard deviations, of which some are hidden by data markers.) In the control experiments, the algae were allowed to grow in 250 ml culture flasks until they reach a steady-state density. Thereafter density measurements were performed over time. In duplicates of the controls a single predatory ciliate species was added. This resulted directly in a decline of the algal population and in an increase of the predator population. Consequently, in these experiments the algae were reduced in density or went (nearly) extinct. A difference in feeding behaviour between *B. planctonicum* and *U. furcata* can be seen. The first predator exploits its resource completely, then it dies, while the latter predator does not totally consume the prey population and settles for several months into a stable equilibrium (data not shown) [33]. The bottom-left panel shows *U. farcta* feeding on *Cryptomonas sp.* No data is available for the control algal growth experiment. After 19 days the prey and predator seem to reach a stable equilibrium density.

Weisse et al. [33] used additional separate feeding experiments (semi-continuous cultures) in order to obtain the parameters for the Holling type-II functional response. Only for *U. furcata* the maximum ingestion rate, nutrient half-saturation constant and feeding threshold could be determined significantly.

### 3.4.2 Fitting method

A weighted least-sum-of-squares method with weights equal to the inverse of the variance in the measurements was used. The sum of squares (SSQ) of prey

and predator are summed into a dimensionless total SSQ, which is allowed as each measurement is weighted by its reciprocal standard deviation. A low sum-of-squares indicates a good fit. The data point values are assumed to be normally distributed. This makes this method identical to a maximum-likelihood method [20]. The SSQ is minimized with a Nelder-Mead's simplex method. The mean and covariance matrix (inverse of the Hessian matrix of the SSQ with respect to the parameters) of the estimated parameters are evaluated at the minimum SSQ-point [26]. Model fitting was done simultaneously on three data sets. Therefore, prey parameter values are identical for each data set.

### 3.4.3 Fitting results

The left panels of Figure 3.4 show the time evolution of the prey and predator populations. The right panels show the  $Z$  vs.  $P$  phase-space diagrams. In each panel experimental data is shown with its associated standard deviations and the solid line represents the fitted trajectory. The upper-right panel shows that the equilibrium for *B. planctionicum* is unstable as the trajectory of prey and predator converges to a periodic solution. The trajectory runs close to the  $Z$  and  $P$ -axis, this indicates a risk of extinction for *B. planctionicum*. In the centre-right and lower-right panels, for the two *Urotricha* species there exist a stable equilibrium to which the long-term trajectory converges.

Table 3.2 presents for each modelled species the estimated parameter-values and their uncertainties. Parameters included are initial densities, half-saturation constants, maximum feeding rates, feeding thresholds, yield factors and death rates.

We derived for *U. furcata* a feeding threshold value with  $\tau_F = 10\,500 \pm 923$  cells/ml. Furthermore, we found that the feeding threshold for *U. farcta* is a factor three lower compared to *U. furcata*. *B. planctionicum* was not found to have a feeding threshold.

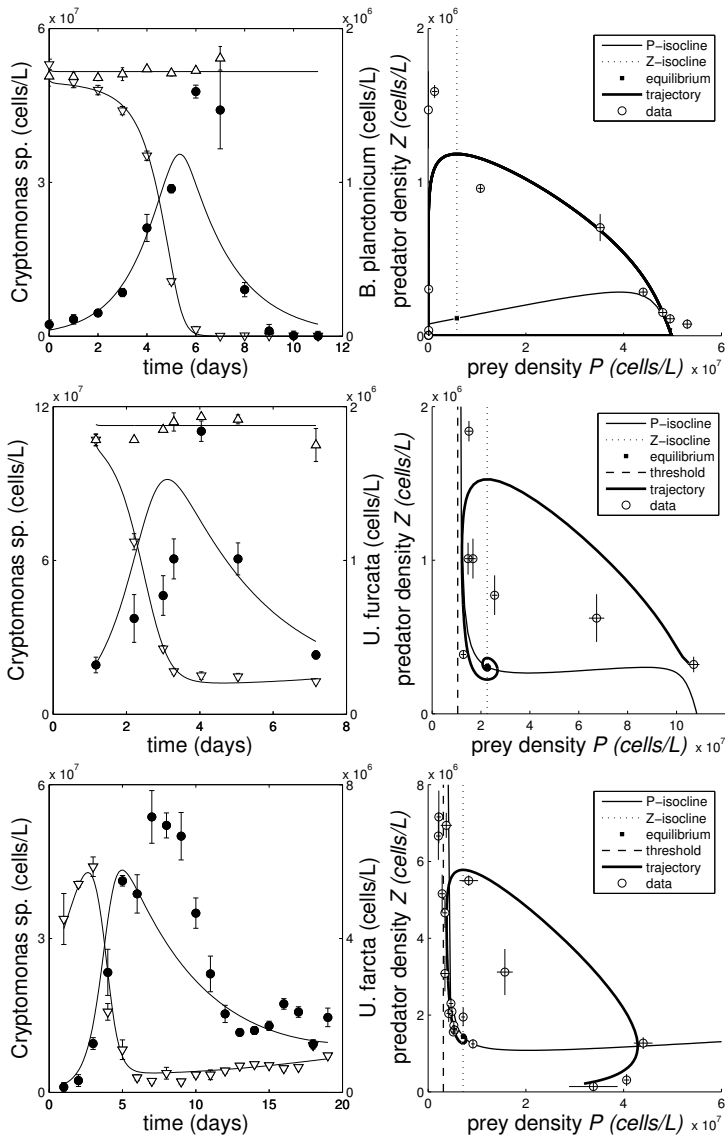


Figure 3.4: The mass-balance model based on Eq. (3.1) was fitted to experimental data from [33]. Each left panel shows a different predatory ciliate species feeding on the algal prey.  $\Delta$  denotes cell densities of the prey species *Cryptomonas sp.* without predators present,  $\nabla$  represents preyed *Cryptomonas sp.*,  $\bullet$  denotes cell densities of each ciliate species. Parameter values from Table 3.2 were used to construct simulated trajectories (solid lines in all panels) and the  $P$  and  $Z$ -isoclines in the phase-spaces of  $Z$  vs.  $P$  (right panels).  $P$ -isoclines for  $P = 0$  are omitted. Prey-predator data-point combinations in the phase-space diagrams are represented by open circles with associated standard deviations represented by the extending lines.

Table 3.2: Mass-balance model (Eq. 3.1) fitted to data from Weisse et al. [33]. Fitted parameter values

Prey species <i>Cryptomonas sp.</i>							
Symbol	Value	SD*	Units				
$I_{NP}$	$4.38 \cdot 10^{-1}$ ¶	$3.90 \cdot 10^{-2}$	day <sup>-1</sup>				
$d_P$	$1.00 \cdot 10^{-1}$	0	day <sup>-1</sup>				
$K_{NP}$	$1.00 \cdot 10^{-6}$	0	mol N L <sup>-1</sup>				
Constants and conversion factors							
$V_F$	280 £ <sub>1</sub>	0	$\mu\text{m}^3$				
$n_F$	$7.50 \cdot 10^{-1}$ £ <sub>2</sub>	0	pmol N cell <sup>-1</sup>				
Ciliate model parameters							
Predator	<i>B. planctonicum</i>		<i>U. furcata</i>		<i>U. farcta</i>		Units
Symbol	Value	SD	Value	SD	Value	SD	Units
$y_{PZ}$	$2.18 \cdot 10^{-1}$	$1.40 \cdot 10^{-2}$	$1.82 \cdot 10^{-1}$	$1.51 \cdot 10^{-2}$	$2.00 \cdot 10^{-1}$	0	-
$I_{PZ}$	$6.98 \cdot 10^0$ †	$7.89 \cdot 10^{-1}$	$1.56 \cdot 10^1$ ‡	$4.78 \cdot 10^0$	$2.26 \cdot 10^1$ §	$1.05 \cdot 10^1$	d <sup>-1</sup>
$d_Z$	$5.12 \cdot 10^{-1}$	$2.94 \cdot 10^{-2}$	$3.93 \cdot 10^{-1}$	$2.53 \cdot 10^{-2}$	$1.85 \cdot 10^{-1}$	$4.74 \cdot 10^{-3}$	d <sup>-1</sup>
$K_{FC}$	$1.16 \cdot 10^7$	$4.30 \cdot 10^6$	$7.49 \cdot 10^7$	$3.76 \cdot 10^7$	$9.46 \cdot 10^7$	$5.47 \cdot 10^7$	#cells L <sup>-1</sup>
$\tau_F$	0	0	$1.05 \cdot 10^7$	$9.23 \cdot 10^5$	$3.12 \cdot 10^6$	$2.29 \cdot 10^5$	#cells L <sup>-1</sup>
Constants and conversion factors**							
$V_C$	2015 £ <sub>3</sub>	0	3150 £ <sub>3</sub>	0	3350 £ <sub>3</sub>	0	$\mu\text{m}^3$
$n_C$	$5.40 \cdot 10^0$	0	$8.44 \cdot 10^0$	0	$1.37 \cdot 10^0$	$1.01 \cdot 10^{-1}$	pmol N cell <sup>-1</sup>
Initial conditions							
$N(0)$	0	0	0	0	$1.00 \cdot 10^{-3}$	0	mol N L <sup>-1</sup>
$F_0(0)$	$5.20 \cdot 10^7$	$2.27 \cdot 10^5$	$1.13 \cdot 10^8$	$2.76 \cdot 10^5$	n.a.	n.a.	#cells L <sup>-1</sup>
$F_C(0)$	$4.99 \cdot 10^7$	$5.10 \cdot 10^5$	$1.05 \cdot 10^8$	$2.31 \cdot 10^6$	$3.19 \cdot 10^7$	$1.15 \cdot 10^6$	#cells L <sup>-1</sup>
$C(0)$	$3.95 \cdot 10^4$	$6.78 \cdot 10^3$	$3.29 \cdot 10^5$	$4.98 \cdot 10^4$	$2.13 \cdot 10^5$	$4.76 \cdot 10^4$	#cells L <sup>-1</sup>
Compound parameter values							
$\mu_{PZ} = y_{PZ}I_{PZ} - d_Z$							
$\mu_{PZ}$	$1.01 \cdot 10^0$	-	$2.45 \cdot 10^0$	-	$4.34 \cdot 10^0$	-	d <sup>-1</sup>

\*: A standard deviation (SD) of 0 means the variable or constant has an assumed nominal value. A dash means the value is based on the fitted parameter values. \*\*: For conversion from cells/L to biomass N/L take  $P(0) = n_F F(0)$ ,  $Z(0) = n_C C(0)$ ,  $K_{PZ} = n_F K_{FC}$  and  $\tau = n_F \tau_F$ . We assumed  $n_C = n_F V_C / V_F$ , i.e. an identical amount of fmol N  $\mu\text{m}^{-3}$  for both prey and predator. This relation was not used for *U. farcta*. ¶: Corresponds to 13.4 fmol N per cell per hour. £<sub>1</sub>: Based on [34]. £<sub>2</sub>: Based on [17]. £<sub>3</sub>: Based on [33]. †: Corresponds to  $I_{FC} = 2.09 \cdot 10^0 \pm 2.37 \cdot 10^{-1}$  prey/ predator/ h. ‡: Corresponds to  $I_{FC} = 7.31 \cdot 10^0 \pm 2.24 \cdot 10^0$  prey/ predator/ h. §: Corresponds to  $I_{FC} = 1.72 \cdot 10^0 \pm 8.13 \cdot 10^{-1}$  prey/ predator/ h (propagation of errors included).

### 3.5 Discussion and conclusions

A property of the RM model is logistic growth of the prey in absence of the predator. To obtain the same property in the MB model we had to assume perfect and instantaneous nutrient recycling. We think this is warranted as Weisse et al. [33] maintained for several months *U. furcata* cultures with *Cryptomonas sp.* even without exchanging the medium.

Aquatic ecosystem modelling with a feeding threshold for the trophic interactions is controversial. For instance in [30], the indiscriminate use of (constant) threshold values in models is criticized. In [19] it is claimed that their results suggest that any such thresholds should vary with prey quality. Nevertheless, in (some) ecotoxicological effect models feeding thresholds are taken into account, including AQUATOX [23, 24].

As part of the EU MODELKEY-project for assessing impact of pollutants on ecosystems [6], we designed a closed system with a single producer in order to measure the simultaneous effects of toxicant exposure and nutrient stress. A description of the experimental setup and obtained data can be found in [17]. We analysed these data successfully using a mass-balance model in [5]. The same experimental setup was used to investigate chemical stress and nutrient stress on a community with a producer and predator, respectively *Cryptomonas sp.* and *U. furcata*, with resulting data also presented in [17]. To analysing these results, we used a model with a Holling type-II functional response for predator-prey interaction. Without the inclusion of a feeding threshold the model would not fit the data and the prey population will incorrectly be driven to extinction.

The aim of the research presented in this article was twofold. Firstly to find out whether a feeding threshold for *U. furcata* (or a similar ciliate species) can be found in other data sets than [17] and secondly what its effect would be on the long term behaviour of these modelled systems.

The absence of a feeding threshold for both *B. planctonicum* and *S. lacustris* and the presence of a threshold for *Histiobalantium bodamicum* was reported in [21]. Using batch experiment data and the MB model, we found non-zero feeding thresholds for *U. furcata* and *U. farcta* but an absence of a feeding threshold for *B. planctonicum*. More specifically for *U. furcata*, we found a maximum ingestion rate of  $I_{FC} = 7.3 \pm 2.2$  cells/cell/h, a nutrient half-saturation constant of  $K_{FC} = 74\,900 \pm 37\,600$  cells/ml and a feeding threshold of  $\tau_F = 10\,500 \pm 923$  cells/ml. Weisse et al. [33] obtained from additional separate feeding experiments the Holling type-II functional response parameters for *U. furcata*, namely a maximum ingestion rate of  $I_{FC} = 5.3 \pm 0.7$  cells/cell/h, a nutrient half-saturation constant of  $K_{FC} = 28\,200 \pm 8740$  cells/ml and a feeding threshold of  $\tau_F = 13\,350 \pm 740$  cells/ml.

In the centre-left and bottom-left panels of Figure 3.4, the maximum de-

crease of the measured prey densities does not occur at the same moment in time as the maximum increase of the measured predator densities, i.e. for *U. furcata* and *U. farcta*, respectively. The MB model and the RM model both effectively have two variables,  $P$  and  $Z$ , with  $dZ/dt$  and  $-dP/dt$  being mostly determined by the trophic interaction. Therefore, the simulated maximum decrease of the prey-curve is at the same time moment as the simulated maximum increase of the predator-curve. Thus, both models will never fit exactly on experimental data in which the maximum decline of the prey and the maximum increase of the predator do not coincide in time. This explains why the MB model does not capture the peaks of the ciliate densities at either the right moment or at the right density perfectly. Nevertheless, the fit is reasonable and justifies the use of a feeding threshold. We used the MB model as it contains as few parameters and variables as possible while the biological meaning of the used parameters is retained.

We analysed the effect of a feeding threshold and enrichment on the stability of the MB and RM model. Both models are two dimensional systems in which the sole prey population suffers from intraspecific competition and a fixed part of that prey population is invulnerable to predation. The properties of the RM model have been analysed earlier, mostly with the carrying capacity,  $K$ , as bifurcation parameter where increasing  $K$  means enrichment. Here we analysed how stability depends on the two bifurcation parameters  $N_T$  and  $\tau$ . Continuing  $N_T$  affects both  $r$  and  $K$  indirectly, see Eq. (3.3c), while normally  $r$  and  $K$  are treated as separate bifurcation parameters.

Previous studies of alternative models for the RM model implicate many potential mechanisms that can give stabilisation. These include predator-induced defence mechanisms, spatial heterogeneity and dormancy of the predators. The first two stabilizing effects work via predation-free prey populations that donate individuals to preyed populations which subsequently sustain the predators, this is classified as “donor-controlled” dynamics [2]. Dormancy is an adaptive response by the predator to a harsh environment, e.g. low prey density [16]. For copepods a feeding threshold was already known [22]. There the existence of a threshold was explained by assuming that the energy gained from captured food is too little compared to the energy spend on searching and capturing food. Therefore, not searching and not feeding is energetically more advantageous when food is limited.

When plotting  $f(P)$  vs.  $P$ , the threshold shifts the intersection of the predator-prey functional response and the  $P$ -axis to the right of the origin. The center-right and bottom-right panels of Figure 3.4 show how this shift in  $f(P)$  cause the existence of an asymptote for the  $P$ -isocline in the phase-space of  $Z$  vs.  $P$ . The presence of an asymptote makes the  $P$ -isocline a (mostly) decreasing function, with a decreasing function being an requirement for stability given a vertical  $Z$ -isocline. This sets the circumstances in which strong

stability can occur when the threshold value becomes high enough.

Eq. (2.4b) always yields a vertical isocline for the predator for both the RM and MB model, with and without a feeding threshold. For both models the prey-isocline is a function of  $P$ ,  $g(P)$  and  $h(P)$  respectively, forming a curve in the positive quadrant of the  $PZ$ -phase-space where for  $P > \tau$  there is an unique  $Z$ . Therefore, the  $P$ -isocline will always intersect the  $Z$ -isocline only once. Consequently, in our MB model and the RM model formulation, a stable equilibrium is the global stable equilibrium.

We conclude that the bifurcation diagram for the RM and MB models with the same parameter values, are qualitatively identical, even when the feeding threshold was included, but they differ quantitatively. The feeding threshold has a strong stabilising effect in both model formulations.

The dynamics of low trophic levels will affect the dynamics of higher trophic levels and consequently a complete ecosystem. Therefore the inclusion (or exclusion) of feeding thresholds in models for the lowest trophic levels should carefully be contemplated.

*Acknowledgements* - We acknowledge financial support granted by the European Commission (Contract No 511237-GOCE). The authors would like to thank Peter Abrams and one anonymous reviewer for useful comments and Markus Liebig for valuable discussions.

## 3.6 Appendix

Assume a closed ecosystem contains one species of producers,  $P$ , which capture energy from light but is effectively only limited in its growth by one type of nutrient,  $N$ , in the medium, e.g. phosphor or nitrogen containing compounds. These producers are preyed upon by predators,  $Z$ , via Holling type-II trophic interaction. The conversion of prey biomass into predator biomass is not 100% efficient, thus faeces and organic waste are produced and form together a pool of detritus,  $M$ . Biomass from deceased producers, predators and bacteria also add to this detritus. The bacteria,  $B$ , grow on detritus via Holling type-II with handling time  $h_M$  and search rate  $v_M$ . Metabolic activities of the bacteria convert detritus into new bacterial biomass and freely available nutrients for the producers. This closes the nutrient loop. Detritus is converted with efficiency  $y_{MB}$ . The bacteria die with rate  $d_B$ , remaining parameters are explained in

the text near Eq. (3.1). The above leads to the following ODE-system

$$\begin{aligned}\frac{dN}{dt} &= -P \frac{v_N N}{1 + v_N h_N N} + (1 - y_{BM}) B \frac{v_M M}{1 + v_M h_M M}, \\ \frac{dP}{dt} &= P \left( \frac{v_N N}{1 + v_N h_N N} - d_P \right) - Z \frac{v_P P}{1 + v_P h_P P}, \\ \frac{dZ}{dt} &= Z \left( y_{PZ} \frac{v_P P}{1 + v_P h_P P} - d_Z \right), \\ \frac{dB}{dt} &= B \left( y_{BM} \frac{v_M M}{1 + v_M h_M M} - d_B \right), \\ \frac{dM}{dt} &= (1 - y_{PZ}) Z \frac{v_P P}{1 + v_P h_P P} + d_P P + d_Z Z + d_B B - B \frac{v_M M}{1 + v_M h_M M}.\end{aligned}$$

Adding the masses of the degrading organisms and the dead organic material gives

$$\begin{aligned}\frac{dN}{dt} &= -P \frac{v_N N}{1 + v_N h_N N} + (1 - y_{BM}) B \frac{v_M M}{1 + v_M h_M M}, \\ \frac{dP}{dt} &= P \left( \frac{v_N N}{1 + v_N h_N N} - d_P \right) - Z \frac{v_P P}{1 + v_P h_P P}, \\ \frac{dZ}{dt} &= Z \left( y_{PZ} \frac{v_P P}{1 + v_P h_P P} - d_Z \right), \\ \frac{d(B + M)}{dt} &= (1 - y_{PZ}) Z \frac{v_P P}{1 + v_P h_P P} + d_P P + d_Z Z \\ &\quad - (1 - y_{BM}) B \frac{v_M M}{1 + v_M h_M M}.\end{aligned}$$

The rate of change of  $d(B + M)/dt$  depends on the biological rates related to feeding and death. Lets assume these rates are fast. This then allows for a quasi-steady state assumption with  $d(B + M)/dt = 0$ , that yields Eq. (3.1).

# References

- [1] P. A. Abrams and H. Matsuda. Prey adaptation as a cause of predator-prey cycles. *Evolution*, 51:1742–1750, 1997.
- [2] P. A. Abrams and C. J. Walters. Invulnerable prey and the paradox of enrichment. *Ecology*, 77:1125–1133, 1996.
- [3] J. R. Beddington. Mutual interference between parasites or predators and its effect on searching efficiency. *Journal of Animal Ecology*, 44:331–340, 1975.
- [4] A. A. Berryman and B. A. Hawkins. The refuge as an integrating concept in ecology and evolution. *Oikos*, 115(1):192–196, 2006.
- [5] D. Bontje, B. W. Kooi, M. Liebig, and S. A. L. M. Kooijman. Modelling long-term ecotoxicological effects on an algal population under dynamic nutrient stress. *Water Research*, 43:3292–3300, 2009.
- [6] W. Brack, J. Bakker, E. de Deckere, C. Deerenberg, J. van Gils, M. Hein, P. Jurajda, S. Kooijman, M. Lamoree, S. Lek, M.-J. López de Alda, A. Marcomini, I. Muñoz, S. Rattei, H. Segner, K. Thomas, P. von der Ohe, B. Westrich, D. de Zwart, and M. Schmitt-Jansen. Models for assessing and forecasting the impact of environmental key pollutants on freshwater and marine ecosystems and biodiversity. *Environmental Science & Pollution Research*, 12(5):252–256, 2005.
- [7] D. L. DeAngelis. *Dynamics of Nutrient Cycling and Food Webs*. Number 9 in Population and Community Biology series. Chapman & Hall, London, 1992.
- [8] D. L. DeAngelis, R. A. Goldstein, and R. V. O’Neill. A model for trophic interaction. *Ecology*, 56:881–892, 1975.
- [9] V. Grimm and C. Wissel. Babel, or the ecological stability discussions: an inventory and analysis of terminology and a guide for avoiding confusion. *Oecologia*, 109:323–334, 1997.

- [10] T. Gross, W. Ebenhöf, and U. Feudel. Enrichment and foodchain stability: the impact of different forms of predator-prey interaction. *Journal of Theoretical Biology*, 227:349–358, 2004.
- [11] V. A. A. Jansen. Regulation of predator-prey systems through spatial interactions: a possible solution to the paradox of enrichment. *Oikos*, 74:384–390, 1995.
- [12] K. L. Kirk. Enrichment can stabilize population dynamics: autotoxins and density dependence. *Ecology*, 79:2456–2462, 1998.
- [13] B. W. Kooi. Numerical bifurcation analysis of ecosystems in a spatially homogeneous environment. *Acta Biotheoretica*, 51(3):189–222, 2003.
- [14] B. W. Kooi, J. C. Poggiale, P. Auger, and S. A. L. M. Kooijman. Aggregation methods in food chains with nutrient recycling. *Ecological Modelling*, 157(1):69–86, 2002.
- [15] M. Kretzschmar, R. M. Nisbet, and E. McCauley. A predator-prey model for zooplankton grazing on competing algal populations. *Theoretical Population Biology*, 44:32–66, 1993.
- [16] M. Kuwamura, T. Nakazawa, and T. Ogawa. A minimum model of prey-predator system with dormancy of predators and the paradox of enrichment. *Journal of Mathematical Biology*, 58(3):459–479, 2009.
- [17] M. Liebig, G. Schmidt, D. Bontje, B. W. Kooi, G. Streck, W. Traunspurger, and T. Knacker. Direct and indirect effects of pollutants on algae and algivorous ciliates in an aquatic indoor microcosm. *Aquatic Toxicology*, 88:102–110, 2008.
- [18] Maplesoft. *Maple*. Maplesoft, Waterloo, Ontario, Canada, 2003.
- [19] A. Mitra and K. J. Flynn. Importance of interactions between food quality, quantity, and gut transit time on consumer feeding, growth, and trophic dynamics. *The American Naturalist*, 169(5):632–646, 2007.
- [20] A. M. Mood, F. A. Graybill, and D. C. Boes. *Introduction to the Theory of Statistics*. McGraw-Hill, Inc., 3<sup>th</sup> edition, 1974.
- [21] H. Müller and A. Schlegel. Responses of three freshwater planktonic ciliates with different feeding modes to cryptophyte and diatom prey. *Aquatic Microbial Ecology*, 17:49–60, 1999.
- [22] M. M. Mullin, E. F. Stewart, and F. J. Fuglister. Ingestion by planktonic grazers as a function of concentration of food. *Limnology and Oceanography*, 20:259–262, 1975.

- [23] R. A. Park and J. S. Clough. Aquatox for windows: A modular fate and effects model for aquatic ecosystems. Technical Report 2, EPA, 2004.
- [24] R.A. Park, J. S. Clough, and M. C. Wellman. Aquatox: Modeling environmental fate and ecological effects in aquatic ecosystems. *Ecological Modelling*, 213:1–15, 2008.
- [25] S. Petrovskii, B–L Li, and H. Malchow. Transition to spatiotemporal chaos can resolve the paradox of enrichment. *Ecological Complexity*, 1:37–47, 2004.
- [26] H. W. Press, S. A. Teukolsky, W. T. Vetterling, and B. P. Flannery. *Numerical Recipes in C*. Cambridge University Press, 2nd edition, 1992.
- [27] M. L. Rosenzweig and R. H. MacArthur. Graphical representation and stability conditions of predator-prey interactions. *The American Naturalist*, 97:209–223, 1963.
- [28] A. Saage, O. Vadstein, and U. Sommer. Feeding behaviour of adult *Centropages hamatus* (Copepoda, Calanoida): Functional response and selective feeding experiments. *Journal of Sea Research*, 62:16–21, 2009.
- [29] M. Scheffer and R. J. De Boer. Implications of spatial heterogeneity for the paradox of enrichment. *Ecology*, 76:2270–2277, 1995.
- [30] S. L. Strom, C. B. Miller, and B. W. Frost. What sets lower limits to phytoplankton stocks in high-nitrate, low-chlorophyll regions of the open ocean? *Marine Ecology Progress Series*, 193:19–31, 2000.
- [31] G. A. K. Van Voorn, D. Stiefs, T. Gross, B. W. Kooi, U. Feudel, and S. A. L. M. Kooijman. Stabilization due to predator interference: comparison of different analysis approaches. *Mathematical Biosciences and Engineering*, 5(3):567–583, 2008.
- [32] M. Vos, B. W. Kooi, D. L. DeAngelis, and W. M. Mooij. Inducible defences and the paradox of enrichment. *Oikos*, 105:471–480, 2004.
- [33] T. Weisse, N. Karstens, V.C.L. Meyer, L. Janke, S. Lettner, and K. Teichgräber. Niche separation in common prostome freshwater ciliates: the effect of food and temperature. *Aquatic Microbial Ecology*, 26:167–179, 2001.
- [34] T. Weisse and B Kirchhoff. Feeding of the heterotrophic freshwater dinoflagellate *Peridiniopsis berolinense* on cryptophytes: analysis by flow cytometry and electronic particle counting. *Aquatic Microbial Ecology*, 12:153–164, 1997.

## Chapter 4

# Modelling direct and indirect ecotoxicological effects on an algivorous ciliate population under dynamic nutrient stress

D. Bontje, B.W. Kooi, M. Liebig and S.A.L.M. Kooijman

In Chapter 2 we studied the effects of toxicants on the functioning of phototrophic unicellulars (algae) in a simple aquatic microcosm with a parameter-sparse model. Now we extend this model to include algivorous ciliates. The modelled algae consume dissolved inorganic nitrogen (DIN) under surplus light and use it for growth and maintenance. The ciliates feed on the algae for growth and maintenance. Dead bacteria, feeding waste-products and dead ciliates add to a detritus pool. Detritus is mineralized by bacterial activity, leading to nutrient recycling. The ecological model is coupled with a toxicity-module that describes the dependency of each species biological rates on the toxicant concentration. Model parameter fitting is performed on experimental data from Liebig et al. [9]. The flagellated algal species *Cryptomonas sp.* was exposed to the herbicide prometryn and insecticide methyl parathion in semi-closed Erlenmeyers while being preyed upon by either the ciliate *Urotricha furcata* or *Coleps spetai* with the autotrophic endosymbiont *Chlorella sp.* The effects of methyl parathion on *Urotricha furcata* are directly as an increased death rate and indirectly via a reduced prey availability as algal growth was reduced. *Coleps sp.* with its endosymbiont with chlorophyll was found to be insensitive to prometryn and only suffered from food shortage.

## 4.1 Introduction

Direct and indirect effects of contaminants in experimentally altered aquatic ecosystems have been investigated, an overview is provided by Fleeger et al. [6]. It is possible to model these ecosystems using logistic growth equations while also incorporating trophic interactions such as predation. In these models, toxicants can change the parameter values being used in the equations. An example of this type of modelling can be found in Traas et al. [15] who simulated the dynamics of the biomass of multiple functional groups in a freshwater microcosm. Adding nutrients and chlorpyrifos (insecticide) resulted in both direct and indirect effects. The effects found were non-permanent; when the toxicant concentration was reduced the total biomass of the affected organisms recovered and consequently the next trophic level regained biomass. Preston and Snell [13] derived parameter values from studies with the same compounds and organisms and then performed a simulation study in which effects of a toxicant on both the prey-predator interaction and the carrying capacity were studied. When the toxicant decreased the growth rate of a species this affected populations densities and indirectly species interactions. For example, a reduced reproductive efficiency of the predator decreases the predator density and indirectly lowers the predation pressure and consequently increases the prey density.

Organisms can suffer from multiple stresses such as nutrient shortage, toxicity and predation. All of these stresses can act simultaneously. We aim to describe and predict the effect of one or multiple toxicants on a small ecosystem that includes the following three features: primary production, predation and nutrient recycling via degradation. These attributes are all properties which are also present in complex ecosystems or communities. Our modelled community consists of bacteria, algae and algae eating ciliates. This minimal community has all the properties mentioned for a complex ecosystem and hence we name it a canonical community. By describing and predicting the events in this canonical community we will gain knowledge that can be used for setting a few steps closer to describing and predicting the effects of toxicants on more complex (natural) ecosystems.

Therefore, we need to test our models against data and against existing models. One existing model is called the Marr-Pirt model for describing growth and death of a population of organisms. We found that this model is not adequate in all situations for the ciliate's behaviour, therefore we used DEB theory to construct a more adequate model for the growth of these algal eating ciliates. Although the DEB model is more flexible in behaviour, it has a higher data demand. In a more complex situation with a toxicant-predator-prey system the Marr-Pirt model does not suffice and the DEB model does. We therefore conclude that to be able to predict the behaviour of a system

with algae, bacteria and algae eating ciliates with multiple stresses included we need a DEB modelling based approach, but only for the predator. This implies that for ecosystem modelling at least the predators should be modelled using the DEB theory.

## 4.2 Material and Methods

Section 4.2.2 presents the ordinary differential equation ODE-system that governs the growth of the algae and the ciliates feeding on them. The resulting ODE for algal growth is similar as used in Chapter 2 [3] and identical as used in Chapter 3 [4]. The growth model for the ciliates is a 1-reserve DEB model from [7] with shrinkage added from [5]. The effect of toxicants is included via a DEBtox-module [1]. Section 4.5 shows how the 1-reserve DEB model can be simplified into the model formulation as used in Chapter 3. First we will introduce the experimental data used in this Chapter, which originates from Liebig et al. [9].

### 4.2.1 Data description

Liebig et al. [9] present the effect of prometryn on an algae-ciliate system in an Erlenmeyer. The species of algae is *Cryptomonas sp.*, the species of ciliate is *Coleps spetai*. *Coleps spetai* contains an autotrophic endosymbiont (*Chlorella sp.*), which helps *Coleps spetai* in collecting energy via photosynthesis. It was observed that *Coleps spetai* is not able to sustain itself in absence of prey which indicates that the endosymbiont does not cover all metabolic requirements of its host. The measurements of the time evolution of the species densities are shown in Fig. 4.2. Panel A shows how algae with predators absent grew from a low density to a 'carrying capacity' after a few days. This level is maintained for 12 days, then the density decreases indicating a less than perfect recycling of dead algae into nutrients available for uptake. Panel B contains the growth curves of the algae while being preyed upon by the ciliates. After 4 days most of the prey is eaten while the ciliates reach their peak density at day 8. Indicating that they collect nutrient much faster then they can convert the stored nutrient into offspring. From day 8 till day 10 the ciliates decay slowly in density, after day 10 this decline increases. Observe that the algae did not go extinct completely. In panel C and D the species are exposed to 20 and 40  $\mu\text{g}$  per litre of the herbicide prometryn. In both panels the algal peak density decreases, as does the peak density of the predator. Day 8 remains the day of maximum height. In panel B and C the standard deviation of the predator densities are larger than in D.

A similar exposure experiment was done with *Urotricha furcata* feeding on *Cryptomonas sp.* while both species are exposed to the insecticide methyl

parathion in concentration of 0.00, 0.40, 1.26 and 4.00 mg per litre. Measured cell densities are shown in Fig. 4.3. In panel A the algal density increases at day 3 till 5 after which it reduced and increases again after day 8. Also after day 8 the ciliate density decreases but might reach a long-term simultaneous existence with its prey. In all panels during the first few days ciliate densities are low while the algal densities first increase slightly and then decrease sharply. This indicates a high maximum feeding rate for the ciliates. However, at the highest predator density the algal population is not depleted. With increasing toxicant concentration the maximum of the ciliate density decreased and also becomes uncertain due to increasing standard deviation. Co-existence of prey and predator seems to exist although at decreasing densities with increasing toxicant concentration. With increasing toxicant concentrations the fluctuations in densities of prey and predator dampen.

In both experiments the species were grown on standard medium but with reduced amounts of nitrogen containing salts, making nitrogen the limiting nutrient.

#### 4.2.2 Formulation of the model

Algae harvest energy from sunlight and store it as carbohydrates. For biomass synthesis, algae combine carbohydrates with other assimilated nutrients, such as dissolved inorganic nitrogen (DIN) which includes ammonium and nitrite, [2]. This new biomass is used for growth while energy from the carbohydrates is used for maintenance which includes basal respiration and turn-over of macromolecules. Products of the maintenance process, such as ammonium and carbon dioxide, are excreted into the environment [16]. The ammonium is re-utilized again by the phytoplankton [8].

Organotrophic bacteria feed on dead biomass, in our experimental setup this material is derived from perished algal, ciliates and bacteria. Bacteria have to maintain themselves and consequently excrete metabolic products which include ammonium and carbon dioxide. Similarly, the growth process leads to metabolic products. Excrements containing the element nitrogen are considered nutrients for the algae. In our experimental setup the limiting nutrient is nitrogen from dissolved compounds. The limiting nutrient cycles from algae to bacteria via detritus and back to the nitrogen containing dissolved compounds leading to a recycling circle.

In the following model formulation, DIN is the growth limiting nutrient for the algae. DIN includes all simple compounds containing nitrogen, such as the salts dissolved in the medium, e.g.  $\text{NaNO}_3$ . Non-limiting nutrients are assumed to be present in abundance and are not modelled. Algae convert DIN into biomass, which eventually becomes detritus. A mass balance model formulation leads to a set of ordinary differential equations (ODEs)

for describing the change over time of dissolved inorganic nitrogen DIN ( $N$ ), total algal biomass ( $A$ ) and detritus density ( $D$ ) in the medium. The three state variables  $N$ ,  $A$ , and  $D$  are expressed in mol nitrogen per litre. Bacterial degradation activity of converting detritus into DIN is considered to be a non-limiting factor and is not modelled. Table 4.1 provides a list of used symbols, variables, parameters, constants and units.

### Nutrient, Algae and Detritus

A Marr-Pirt like model is used for nutrient consumption, algal growth and death with the variable  $A$  denoting algal biomass (mol N/L) and  $N$  denotes the limiting nutrient concentration (mol N/L). Parameters used are  $k_A$  for algal growth rate,  $K_N$  for algal nutrient half saturation constant, and  $h_A$  for algal hazard rate. Nutrient assimilation is modelled with a Holling type-II functional response. The maximum algal growth rate has units of  $\text{time}^{-1}$ . This results in the below ODE for the change of algal biomass density over time:

$$\frac{dA}{dt} = A(k_A f(N) - h_A) \quad ; \quad f(N) = \frac{N}{K_N + N} \quad (4.1)$$

To compare simulated algal biomass ( $A$ ) with measured algal cell densities ( $F$ ) the relation of  $F = A/n_A$  is used with  $n_A$  denoting the amount of nitrogen per algal cell.

The amount of nitrogen collected from the environment by the algae on population scale is  $Ak_A f(N)$  and is denoted with  $J_{A_N,A}$ . The nitrogen lost from the population through death is  $Ah_A$  and is denoted by  $J_{A_A,h}$ . Dead biomass becomes detritus  $D$ , like  $A$  the density of detritus is expressed in mol N/L. Therefore, the flux of newly generated detritus from algal death ( $J_{A_D,h}$ ) is identical to the algal loss flux  $J_{A_A,h}$ . Bacterial density is assumed to be in steady-state with the detritus density. Taking detritus degradation to be density dependent on both the bacteria and detritus leads to a constant detritus degradation rate  $r_B$ . The flux of degraded detritus is denoted by  $J_{B_D,M}$ . The degradation of detritus produces a flux of freely available limiting nutrient ( $J_{B_N,M}$ ). This yields the below ODE system for nutrient ( $N$ ), algal biomass ( $A$ ) and detritus ( $D$ ):

$$J_{A_N,A} = J_{A_A,G} = k_A f(N)A \quad ; \quad f(N) = \frac{N}{K_N + N} \quad (4.2a)$$

$$J_{A_A,h} = J_{A_D,h} = h_A A \quad ; \quad J_{B_D,M} = J_{B_N,M} = r_B D \quad (4.2b)$$

$$\frac{dN}{dt} = J_{B_D,M} - J_{A_N,A} \quad (4.2c)$$

$$\frac{dA}{dt} = J_{A_N,G} - J_{A_A,h} \quad (4.2d)$$

$$\frac{dD}{dt} = J_{A_D,h} - J_{B_D,M} \quad (4.2e)$$

### 1-reserve model with shrinkage for ciliate growth

The ciliates consist of structure and reserve, which are described in Kooijman [7]. Reserve consists of different and unspecified chemical compounds, these compounds form an energy and mass containing pool. This pool is taken to have a constant stoichiometry, thus elemental ratios such as the C:N ratio in this pool are constant. Reserve is converted into structure which, like reserve, consists of a pool of unspecified chemical compounds with a constant elemental ratio. Thus the stoichiometry of reserve is constant but differs from the constant stoichiometry of structure. Therefore, an organism with a high reserve density has a different total elemental composition than an organism with a low reserve density. As structure has a fixed ratio of elemental nitrogen (N), elemental phosphate (P) and other elements per mole of elemental carbon (C) the amount of structure can be expressed in C-moles with a C-mole being one mole of carbon with its associated moles of other elements. The same can be done for reserve.

A Holling type-II functional response models the feeding of ciliates on the algae. Caught algae are collected ( $J_{C_A,A}$ ) and split into material targeted for assimilation into the reserves ( $J_{C_E,A}$ ) and material not assimilated and discarded as detritus ( $J_{C_D,A}$ ). Reserve is mobilised for catabolic work ( $J_{C_E,C}$ ) such as growth ( $J_{C_E,G}$ ) and maintenance ( $J_{C_E,M}$ ). Growth results in newly synthesised structure ( $J_{C_V,G}$ ) and mineralized products ( $J_{C_M,G}$ ). The maintenance process results only in mineralized products ( $J_{C_E,M}$ ). When there is not enough reserve to pay maintenance costs, structure is metabolised for its energy and material to compensate for the reserve shortage, consequently resulting in both a mineral flux ( $J_{C_V,M}$ ) and shrinkage of the organism. Eventually, the mineral fluxes  $J_{C_M,M}$  and  $J_{C_M,G}$  are targeted for excretion ( $J_{C_M,X}$ ).

The ciliate population dies with a constant rate, which translates into a *per capita* death rate  $d_C$ , resulting in fluxes of dead material ( $J_{C_E,d}$  and  $J_{C_V,d}$ ) from reserve and structure. Both fluxes together form a flux of newly formed detritus ( $J_{C_D,d}$ ). Due to this death rate, populations with relatively high specific reserve density have a constant decline of structural biomass, which can be compensated by synthesising new biomass from reserve. Populations under severe nutrient stress have a low specific reserve density, they have to pay their maintenance from both reserve and structure. Consequently, the constant decline of structural biomass can not be compensated for by synthesising fresh biomass as maintenance takes precedence of growth. See Figure 4.1 for an overview of all mass fluxes.

### Assimilation associated mass fluxes

The effective rate of algal assimilation per ciliate is  $k_C f(A)$  in units of algae per ciliate per time. This must be translated into acquired limiting nutrient per mol structure of ciliate per time via the amount of nutrient per algae and the amount of structure per ciliate ( $n_A/n_{VC}$ ) and  $c_{EA}$ .  $c_{EA}$  denotes the efficiency of transferring the limiting nutrient in algal biomass into reserve, with  $0 < c_{EA} < 1$ .  $y_{EA}$  denotes the yield of reserve on algal biomass, with  $y_{EA} = c_{EA}n_A/n_{NE}$  and  $0 < y_{EA} < \infty$ .

$$J_{C_A,A} = f(A)k_C \frac{M_V}{n_{VC}} \quad ; \quad f(A) = \frac{(F - th_A)_+}{K_A + (F - th_A)_+} \quad (4.3a)$$

$$J_{C_E,A} = y_{EA}J_{C_A,A} \quad ; \quad J_{C_A,D} = (1 - c_{EA})J_{C_A,A} \quad (4.3b)$$

with  $th_A$  being a feeding threshold expressed in algal cell density ( $F$ ) not in total algal biomass ( $A$ ). The value of  $(F - th_A)_+$  is either zero or positive which is denoted by the  $_+$  notation. This means the ciliate effectively perceives a lower prey density than there actually is. No matter how high the predation pressure a minimal density is not available for consumption resulting in a persistent minimal algal population. This might be due to refuge, too small a size, or it is more work to find and catch the prey compared to the yield in energy and mass.

### Growth and maintenance of the ciliate

Reserve is used to pay for growth and maintenance. The specific ciliate reserve density is  $m_E = M_E/M_V$ .  $n_{NV}$  is the amount of element N build in a unit of structure.  $n_{NE}$  is the amount of element N in a unit of reserve. The yield of structure on reserve is  $y_{VE}$ , with  $y_{VE} = c_{VE}n_{NE}/n_{NV}$ .  $c_{VE}$  denotes the efficiency of converting reserve into structure, the fraction  $1 - c_{VE}$  is lost during the conversion. The specific ciliate growth rate is denoted by  $r$ . Each reserve unit has the same chance to be mobilized per day. This results in a flux of mobilized reserves,  $j_{E,C}$ . When the organism changes its amount of structure,  $r \neq 0$ , this changes the specific reserve density and consequently the intensity of the mobilized reserve flux.

$j_{E,M}$  is the required amount of reserve to be spend per unit of structure on maintenance.  $j_E^M$  is the available amount of reserve which can be spend per unit of structure on maintenance. When there is not enough reserve to pay for maintenance, then structure is used to compensate for the reserve shortage.

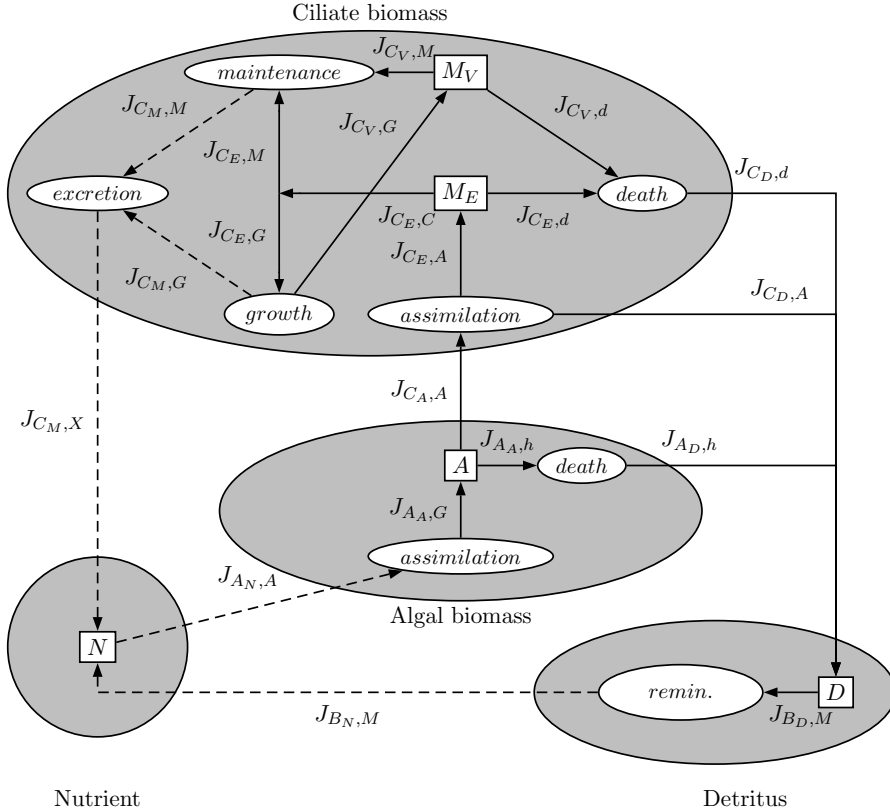


Figure 4.1: Schematic representation of the multi-species model. The limiting nutrient cycles through the system, as mineral the nutrient is assimilated into the algae, which is preyed upon by the ciliates which turns the assimilated biomass into reserve. The reserve is used for the synthesis of new biomass and for maintenance. The maintenance process yields minerals which are excreted into the medium. Eventually, biomass dies and becomes detritus. Detritus degrades into freely available minerals. Dashed lines indicate mineral fluxes, solid lines indicate biomass fluxes. Table 4.1 explains the notation for each flux.

When  $j_E^M \leq j_{E,M}$ , then structure is sacrificed to pay for maintenance to compensate for the discrepancy between  $j_E^M$  and  $j_{E,M}$ .  $j_{V,M}$  is the amount of structure per unit of structure that must be mineralized to pay for all maintenance requirements, i.e, when  $j_E^M = 0$ .  $j_V^M$  is the amount of structure mineralized per unit of structure when  $0 < j_E^M \leq j_{E,M}$  with  $j_V^M = j_{V,M}(1 - j_E^M/j_{E,M})$ . When the specific catabolic flux  $m_E k_e$  is larger than the specific maintenance flux  $j_{E,M}$ , then the organism will grow and there will be no usage of structure for maintenance. See Eq. (4.4) for the derivation of the growth rate ( $r$ ) and the growth related fluxes of reserves and structure.  $r$  is a hyperbolic function of  $m_E$  with an asymptotic maximum value of  $k_E$ . Therefore the maximum doubling time of the ciliates is  $\ln(2)/k_E$ .

Table 4.1: Mass fluxes in the system as presented in Fig. 4.1.

Flux	Organism	Type of mass	Process
$J_{i,j,k}$	$i$ =organism	$j$ =mass	$k$ =process
$J_{A_N,A}$	algae	nutrient	assimilations
$J_{A_A,h}$	algae	biomass	death
$J_{A_D,h}$	algae	detritus	death
$J_{C_A,A}$	ciliate	alga	assimilation
$J_{C_E,A}$	ciliate	reserve	storage
$J_{C_D,A}$	ciliate	detritus	assimilation
$J_{C_E,M}$	ciliate	reserve	maintenance
$J_{C_V,M}$	ciliate	structure	maintenance
$J_{C_M,M}$	ciliate	mineralized reserves and structure	maintenance
$J_{C_E,G}$	ciliate	reserve	growth
$J_{C_V,G}$	ciliate	structure	growth
$J_{C_M,G}$	ciliate	mineralized reserves	growth
$J_{C_M,X}$	ciliate	mineralized reserves and structure	excretion
$J_{C_V,d}$	ciliate	structure	death
$J_{C_E,d}$	ciliate	reserve	death
$J_{C_D,d}$	ciliate	detritus	death
$J_{B_D,M}$	bacteria	detritus	rem mineralization
$J_{B_N,M}$	bacteria	nutrient	rem mineralization

$$\left. \begin{aligned} j_{E,C} &= m_E (k_E - r) \\ r &= y_{VE} (j_{E,C} - j_{E,M}) \end{aligned} \right\} r = \frac{m_E k_E - j_{E,M}}{m_E + \frac{1}{y_{VE}}} \quad (4.4)$$

$$j_E^M = j_{E,M} \quad , \quad j_V^M = 0 \quad , \quad j_{V,G} = r$$

When the specific catabolic flux  $m_E k_e$  is less than the maintenance requirements  $j_{E,M}$ , then the organism will starve and loose structure. The conversion of structure into reserve occurs with efficiency  $c_{EV}$ .  $c_{EV}$  leads to the yield factor  $y_{EV}$ , with  $y_{EV} = c_{EV} n_{NV} / n_{NE}$ . The back conversion of structure into reserve is less efficient than the conversion of reserve into structure, therefore  $y_{EV} \leq n_{EV} \leq 1/y_{VE}$  when following a limiting element:

$$\left. \begin{aligned}
 j_{E,C} &= m_E (k_E - r) \\
 j_{E,C} &= j_E^M \\
 j_V^M &= j_{V,M} \left( 1 - \frac{j_E^M}{j_{E,M}} \right) \\
 j_V^M &= j_{V,M} \left( 1 - \frac{m_E (k_E - r)}{j_{E,M}} \right) \\
 r &= y_{VE} (j_{E,C} - j_E^M) - j_V^M = -j_V^M
 \end{aligned} \right\} \begin{aligned}
 r &= -j_{V,M} \left( 1 - \frac{m_E (k_E - r)}{j_{E,M}} \right) \\
 r &= -\frac{j_{V,M} (j_{E,M} - m_E k_E)}{j_{E,M} + j_{V,M} m_E}
 \end{aligned} \quad (4.5)$$

$$j_E^M = m_E (k_E - r) \quad , \quad j_V^M = -r \quad , \quad j_{V,G} = 0$$

If  $j_{E,C}$  exactly matches the maintenance requirements, i.e.  $j_{E,C} = j_E^M = j_{E,M}$ , then Eq. (4.5) collapses into  $r = -j_V^M = j_{V,G} = 0$

### Bookkeeping of mass fluxes leads to ODE-system

The specific fluxes denoted with the small letter  $j$  are converted into population scale fluxes denoted with the capital  $J$ . Some bookkeeping of the fluxes of the metabolites yields the mineral excretion flux ( $J_{C_M,X}$ ):

$$J_{C_V,M} = M_V j_V^M \quad ; \quad J_{C_E,M} = M_V j_E^M \quad (4.6a)$$

$$J_{C_V,G} = M_V j_{V,G} \quad ; \quad J_{C_E,G} = \frac{J_{C_V,G}}{y_{VE}} \quad (4.6b)$$

$$J_{C_E,C} = M_V j_{E,C} \quad (4.6c)$$

$$J_{C_M,G} = n_{NE} J_{C_E,G} - n_{NV} J_{C_V,G} \quad (4.6d)$$

$$J_{C_M,M} = n_{NE} J_{C_E,M} + n_{NV} J_{C_V,M} \quad (4.6e)$$

$$J_{C_M,X} = J_{C_M,G} + J_{C_M,M} \quad (4.6f)$$

The ciliates die with a constant death rate  $d_C$ , resulting in loss of both structure and the reserves contained therein. The total amount of limiting nutrient added to the pool of detritus is  $J_{C_D,d}$ . Degradation of structure and reserve is assumed to occur only after addition to the detritus pool.

$$J_{C_E,d} = d_C M_E \quad ; \quad J_{C_V,d} = d_C M_V \quad (4.7a)$$

$$J_{C_D,d} = n_{NE} J_{C_E,d} + n_{NV} J_{C_V,d} \quad (4.7b)$$

For the above described system with nutrient, algae, ciliates and detritus the following ODE-system is used. See Figure 4.1 for an overview of all fluxes.

$$\frac{dN}{dt} = J_{B_D,M} + J_{C_M,X} - J_{A_N,A} \quad (4.8a)$$

$$\frac{dA}{dt} = J_{A_N,A} - J_{A_A,h} - J_{C_A,A} \quad (4.8b)$$

$$\frac{dM_E}{dt} = J_{C_E,A} - J_{C_E,C} - J_{C_E,d} \quad (4.8c)$$

$$\frac{dM_V}{dt} = J_{C_V,G} - J_{C_V,M} - J_{C_V,d} \quad (4.8d)$$

$$\frac{dD}{dt} = J_{A_D,h} + J_{C_D,A} + J_{C_D,d} - J_{B_D,M} \quad (4.8e)$$

### 4.2.3 Data fitting method

A weighted least-sum-of-squares method with weights equal to the inverse of the variance in the measurements was used. The sum of squares (SSQ) of prey and predator are summed into a dimensionless total SSQ, which is allowed as each measurement is weighted by its reciprocal standard deviation. A low sum-of-squares indicates a good fit. The data points are assumed to be normally distributed. This makes this method identical to a maximum-likelihood method [10]. The SSQ is minimized with a Nelder-Mead's simplex method. The mean and covariance matrix (inverse of the Hessian matrix of the SSQ with respect to the parameters) of the estimated parameters are evaluated at the minimum SSQ-point [12]. Model fitting was done to the experimental data from [9] with each experiment being treated as a separate dataset.

As will be noted where relevant, some values for species properties do not result from fits on the data presented in this Chapter and are measured values from [9, 17] or are fitted values from [3, 4] which are Chapter 2 and 3.

## 4.3 Results

The model of ODE-system (4.8) was fitted on the experimental data resulting in parameter values presented in Table 4.3. During the fitting procedure the initial reserve densities of the ciliates were set at a value corresponding with half of their maximal attainable density and the initial densities of both algae and ciliates were set to the value of the measured densities at the start of each experiment. Detritus recycling was taken to be instantaneous and perfect. Based on the fitted values trajectories of the densities of the prey and predator were calculated as presented in Fig. 4.2 and Fig. 4.3.

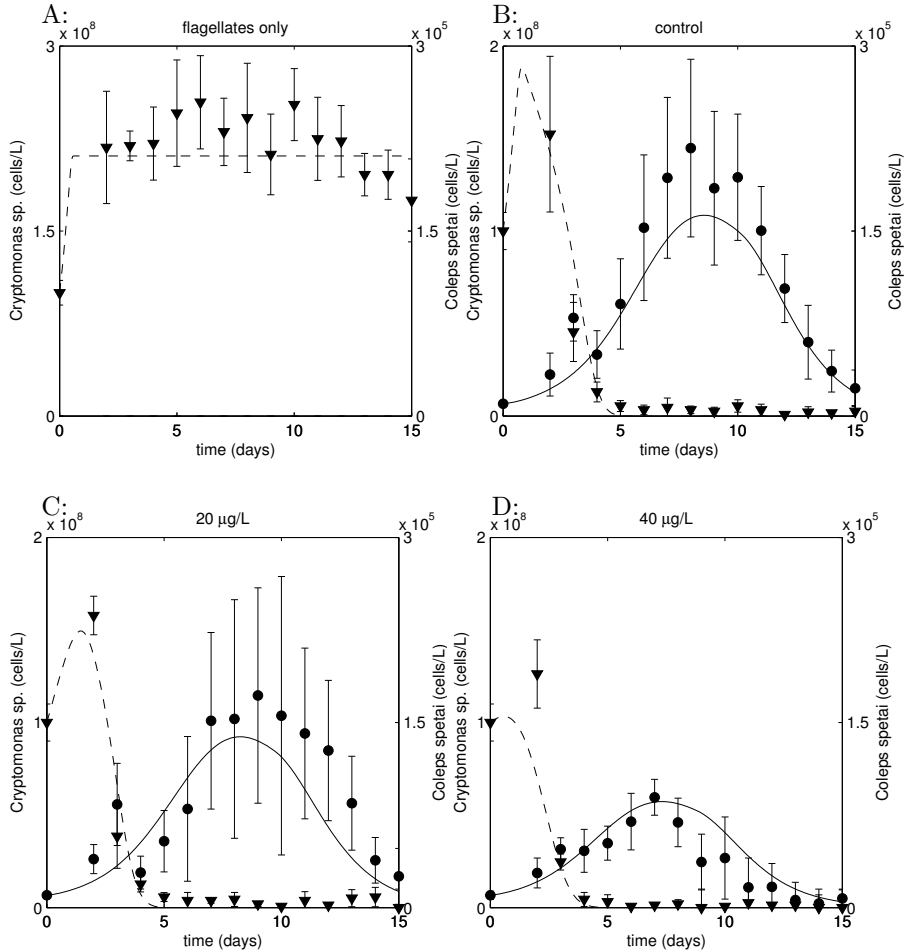


Figure 4.2: Measured time evolutions of the densities of the flagellated algal species *Cryptomonas sp.* ( $\nabla$ ) and the ciliate *Coleps spetai* ( $\bullet$ ) with PSII inhibitor prometryn present. In panel A *Cryptomonas sp.* is not preyed upon by the ciliate *Coleps spetai* and reaches a constant level after a few days. The scale for the algal density in panel A differs from panels B, C and D. The dashed lines are simulated trajectories for the prey and the solid lines are for the predator based on the fitted parameter values presented in Table 4.3.

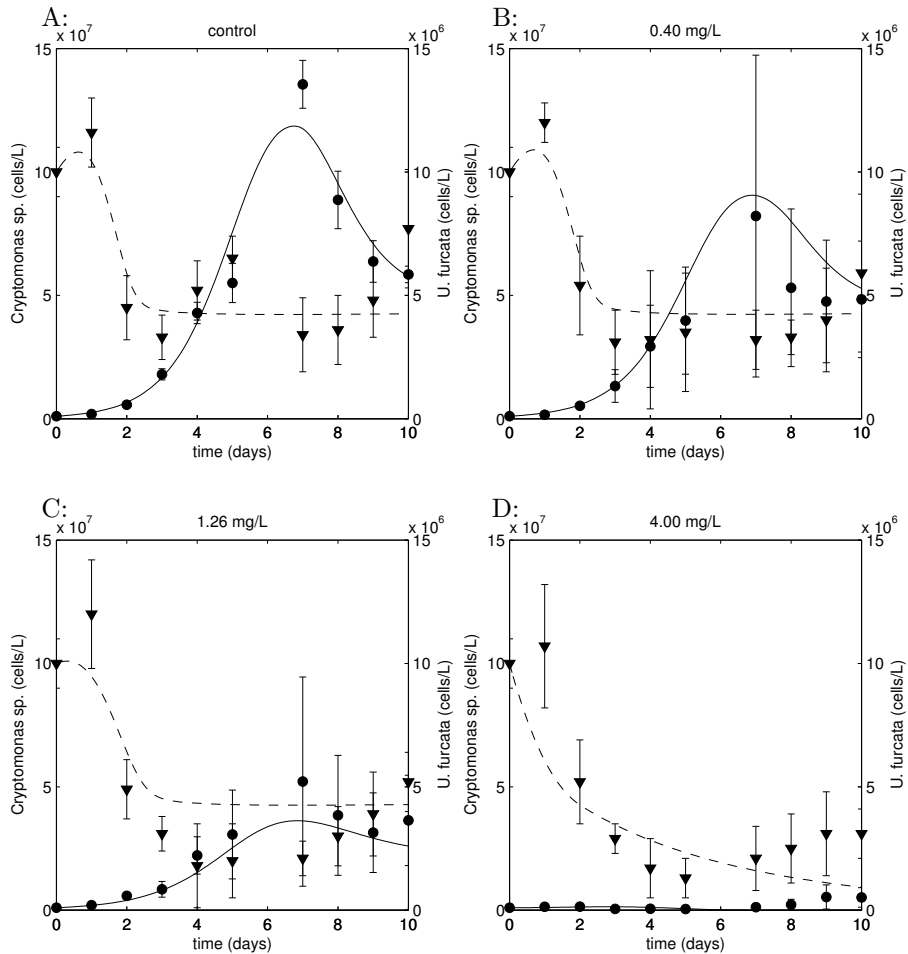


Figure 4.3: Measured time evolutions of the densities of the flagellate *Cryptomonas sp.* ( $\nabla$ ) and the ciliate *Urotricha furcata* ( $\bullet$ ) with methyl parathion present. The dashed lines are simulated trajectories for the prey and the solid lines are for the predator based on the fitted parameter values presented in Table 4.3.

Table 4.2: Description of model parameters and variables

Sym.	Description	Units
$c_{EA}$	conversion eff. of algal biomass into reserve	-/-
$c_{EV}$	conversion efficiency of structure into reserve	-/-
$c_{VE}$	conversion efficiency of reserve into structure	-/-
$d_C$	death rate ciliates	1/d
$h_C$	hazard rate ciliates	1/d
$h_A$	hazard rate algae	1/d
$j_{E,M}$	spec. maintenance requirement in mol res.	mol res./mol struc./d
$j_E^M$	actual paid spec. maintenance in mol res.	mol res./mol struc./d
$j_{V,M}$	spec. maintenance requirement in mol struc.	1/d
$j_V^M$	actual paid specific maintenance in mol struc.	1/d
$k_A$	max. growth rate algae	1/d
$k_C$	max. specific assim. rate of algae for ciliates	# algae/cil/d
$k_E$	reserve mobilization rate	1/d
$K_A$	prey half saturation constant	cells/L
$K_N$	nutrient half saturation constant	mol N/L
$n_{NE}$	mol limiting nutrient in one mol reserve	mol N/mol res.
$n_{NV}$	mol limiting nutrient in one mol structure	mol N/mol struc.
$n_{VC}$	mol structure per ciliate cell	mol struc./cell
$N_A$	mol N per <i>Cryptomonas sp.</i> cell	mol N/cell
$N_C$	mol N per ciliate cell	mol N/cell
$N_{Cc}$	mol N per <i>Coleps spetai</i> cell	mol N/cell
$N_{Cu}$	mol N per <i>Urotricha furcata</i> cell	mol N/cell
$NEC_i$	no-effect concentration for process $i$ $i \in (k_A, h_A, k_C, d_C, j_{E,M}, k_E)$	$\mu\text{gr/L}$ or $\text{mg/L}$
$v_A$	biovolume <i>Cryptomonas sp.</i>	$(\mu\text{m})^3$
$v_C$	biovolume of predatory ciliate	$(\mu\text{m})^3$
$v_{Cc}$	biovolume <i>Coleps spetai</i>	$(\mu\text{m})^3$
$v_{Cu}$	biovolume <i>Urotricha furcata</i>	$(\mu\text{m})^3$
$y_{EA}$	yield of reserve on algal biomass	mol res./mol N
$y_{EV}$	yield of reserve on structure	mol res./mol struc.
$y_{VE}$	yield of structure on reserve	mol struc./mol res.
$r_B$	degradation rate detritus	1/d
$s_f$	biovol. nitrogen content stoichiometry factor $\text{DIM}[s_f] = \text{DIM}[(N_C/v_C)/(N_A/v_A)]$	-/-
$th_A$	feeding threshold of ciliates on flagellates	cell/L
$TC_i$	tolerance concentration for process $i$ $i \in (k_A, h_A, k_C, d_C, j_{E,M}, k_E)$	$\mu\text{gr/L}$ or $\text{mg/L}$
$A$	algal density expressed in limiting nutrient	mol N/L
$N$	limiting nutrient concentration	mol N/L
$D$	detritus density expressed in limiting nutrient	mol N/L
$m_E$	specific reserve density	mol res./mol struc.
$M_E$	reserve density	mol res./L
$M_V$	structure density	mol struc./L

Table 4.3: Fitted parameter values used for time evolutions in Fig. 4.2 and 4.3

Prey	<i>Cryptomonas sp.</i>		<i>Cryptomonas sp.</i>		
Predator	<i>Urotricha furcata</i>		<i>Coleps spetai</i>		
Compound	methyl parathion		prometryn		
Figure	4.3		4.2		
Parameter	(fitted) value	#	(fitted) value	#	units
$v_A$	$2.80 \cdot 10^2$	[18]	$2.80 \cdot 10^2$	[18]	$\mu\text{m}^3$
$N_A$	$7.26 \cdot 10^{-13}$	[3]	$1.80 \cdot 10^{-12}$	1	mol N/cell
$k_A$	$1.27 \cdot 10^0$	[3]	$1.71 \cdot 10^0$	1	1/d
$K_N$	$2.38 \cdot 10^{-4}$	1	$9.69 \cdot 10^{-4}$	1	mol N/L
$h_A$	$7.20 \cdot 10^{-2}$	[3]	$7.20 \cdot 10^{-2}$	[3]	1/d
$v_C$	$3.15 \cdot 10^3$	[17]	$2.00 \cdot 10^4$	[17]	$\mu\text{m}^3$
$n_{NE}$	1	0	1	0	mol N/mol E
$n_{NV}$	1	0	1	0	mol N/mol V
$s_f$	$1.89 \cdot 10^{-1}$	1	$2.80 \cdot 10^0$	1	-/-
$k_C$	$6.30 \cdot 10^2$	1	$2.03 \cdot 10^4$	1	algae/cil./d
$K_A$	$7.49 \cdot 10^7$	[4]	$2.43 \cdot 10^8$	1	flag/L
$th_A$	$4 \times 1.05 \cdot 10^7$	[4]	0	0	alg. cells/L
$c_{EA}$	$2.63 \cdot 10^{-1}$	1	$3.15 \cdot 10^{-1}$	1	-/-
$c_{VE}$	$7.35 \cdot 10^{-1}$	1	$1.96 \cdot 10^{-1}$	1	-/-
$c_{EV}$	$4.77 \cdot 10^{-1}$	1	$9.50 \cdot 10^{-1}$	0	-/-
$k_E$	$1.04 \cdot 10^0$	1	$6.40 \cdot 10^{-1}$	1	mol E/mol E/d
$j_{EM}$	$1.02 \cdot 10^0$	1	$4.88 \cdot 10^{-1}$	1	mol E/mol V/d
$d_C$	$4.67 \cdot 10^{-2}$	1	$1.08 \cdot 10^{-1}$	1	1/d
$NEC_{k_A}$	-	0	$4.57 \cdot 10^0$	[3]	$\mu\text{gr/L}$ or $\text{mgr/L}$
$TC_{k_A}$	-	0	$3.16 \cdot 10^1$	[3]	$\mu\text{gr/L}$ or $\text{mgr/L}$
$NEC_{h_A}$	$4.88 \cdot 10^{-1}$	1	-	0	$\mu\text{gr/L}$ or $\text{mgr/L}$
$TC_{h_A}$	$3.25 \cdot 10^{-1}$	1	-	0	$\mu\text{gr/L}$ or $\text{mgr/L}$
$NEC_{k_C}$	-	0	-	0	$\mu\text{gr/L}$ or $\text{mgr/L}$
$TC_{k_C}$	-	0	-	0	$\mu\text{gr/L}$ or $\text{mgr/L}$
$NEC_{d_C}$	0	0	-	0	$\mu\text{gr/L}$ or $\text{mgr/L}$
$TC_{d_C}$	$2.55 \cdot 10^{-1}$	1	-	0	$\mu\text{gr/L}$ or $\text{mgr/L}$
$NEC_{j_{E,M}}$	-	0	-	0	$\mu\text{gr/L}$ or $\text{mgr/L}$
$TC_{j_{E,M}}$	-	0	-	0	$\mu\text{gr/L}$ or $\text{mgr/L}$
$NEC_{k_E}$	-	0	-	0	$\mu\text{gr/L}$ or $\text{mgr/L}$
$TC_{k_E}$	-	0	-	0	$\mu\text{gr/L}$ or $\text{mgr/L}$
$r_B$	$\infty$	0	$\infty$	0	1/d
Compound parameters					
$y_{EA}$	$1.91 \cdot 10^{-13}$	2	$5.68 \cdot 10^{-13}$	2	mol E/algal cell
$y_{VE}$	$7.35 \cdot 10^{-1}$	2	$1.96 \cdot 10^{-1}$	2	mol V/mol E
$y_{EV}$	$4.77 \cdot 10^{-1}$	2	$9.50 \cdot 10^{-1}$	2	mol E/mol V
$j_{VM}$	$2.14 \cdot 10^0$	2	$5.13 \cdot 10^{-1}$	2	1/d
$n_{VC}$	$7.35 \cdot 10^{-13}$	2	$1.22 \cdot 10^{-10}$	2	mol V/cil. cell
$N_C$	$1.54 \cdot 10^{-12}$	2	$3.61 \cdot 10^{-10}$	2	mol N/cil. cell
$m_{E_{r=d_C}}$	$1.10 \cdot 10^0$	2	$1.95 \cdot 10^0$	2	mol E/mol V
$y_{VA}$	$1.40 \cdot 10^{-13}$	2	$1.12 \cdot 10^{-13}$	2	mol V/algal cell

# : 0 parameter not fitted; 1 parameter fitted; 2 compound parameter;  
[i] reference to the source of the parameter value.

In Fig. 4.2 *Coleps spetai* feeds on *Cryptomonas spetai* while both species are exposed to prometryn. Prometryn marginally affected the parameter values of *Coleps spetai*, therefore we chose to let prometryn not affect the ciliate at all. This indirectly can mean that the autotrophic endosymbiont (*Chlorella sp.*) within this ciliate species is not affected adversely in its photosynthesis capacity. As only the flagellates are affected the effect of prometryn on the ciliate population is an indirect effect via reduced food availability. The dynamics in the experimental data is reproduced in the trajectories based on the data fit, including the extinction of the prey and slow decline of the predator population.

In Fig. 4.3 *Urotricha furcata* feeds on *Cryptomonas spetai* while both species are exposed to methyl parathion. In the shown data fit, methyl parathion affects the flagellates hazard rate and the ciliates death rate directly. An affected flagellate population causes reduced food availability for the ciliates, therefore methyl parathion causes an indirect effect besides its direct effects. There is seemingly a recovery of the flagellates after day 6 at the highest concentration or this is the same type of density increase as found in the control. In the control data around day 5 there is a peak in the flagellate population density which is not reproduced with the model. Long-term simulations (not shown) predict that the predator and the prey both do not go extinct, except at the highest toxicant concentration. This does not disagree with 10 days of experimental observations.

## 4.4 Discussion and conclusions

Originally, we first fitted to the data a model similar to what was used in Chapter 3. However that model formulation, also known as a Marr-Pirt model, failed to capture the dynamics present in both of the data sets presented in this Chapter. In both cases, this is due to the late peak of the ciliates compared to the period of decline of the flagellates. In the Marr-Pirt model, the biomass of flagellates would have been instantaneously converted into ciliate biomass and thus instantly increase ciliates cell densities. Due to the 1-reserve model with shrinkage it was possible to capture the delay of the increase of the ciliate populations.

As mentioned we chose to let prometryn not affect *Coleps spetai* at all as its adverse effect was marginal. However allowing prometryn to affect the ciliate would mean there are more parameters to be fitted leading to an increase in the degrees of freedom for the fitting procedure. This again would make it likely that a different local optimum could be found resulting in different parameter values. Reversely, excluding a simulated mode of action means that the degrees of freedom are reduced, meaning that some local minima become

unreachable.

The ODE-system of (4.8) is parameter rich, if all parameter values are fitted then the number of degrees of freedom is high during the fitting procedure. Then the amount of information in the experimental data must be high to fix all parameters. Therefore we used literature data of similar experiments to set values to some parameters thereby forcing the fitting procedure to work with less degrees of freedom. A lowered degree of freedom increases the ratio of data points per free parameter, making it easier for the fitting routine to converge to a local minimum. To find multiple local minima the fitting procedure must be repeated with different initial estimates for the parameter values and even if a global minimum is found one does not know that for certain.

The value for the feeding threshold for *Urotricha furcata* feeding on *Cryptomonas sp.* could not be retrieved from the data in Fig. 4.3 as the feeding rate and nutrient half-saturation concentration co-varied to a large degree. We found in Chapter 3 a feeding threshold of  $1.05 \cdot 10^7$  flagellates per litre, for the fitting exercise in this Chapter we used a fourfold of that value.

The literature is not conclusive on biovolumes of *Coleps spetai*,  $5.0 \cdot 10^4 \pm 1.0 \cdot 10^4$  in [11] and detailed measurements show a biovolume of  $2.0 \cdot 10^4$  in [14] with the latter value being used during the fitting procedure. The average cell volume of *Cryptomonas sp.* was measured to be around  $180 \mu\text{m}^3$  [19], while a value of  $280 \mu\text{m}^3$  is reported in [18]. We used this latter value as we also used it in Chapter 3. Using different biovolume values would result in different parameter values.

As the number of fitted parameter values compared to the amount of data points is high when using the DEB reserve model for the ciliates and the biovolumes of both the ciliates and flagellates differ per article it was not deemed appropriate to calculate standard deviations as using different biovolume values will change the estimated value of the fitted parameters. Providing standard deviations would imply an unjustifiable certainty as many parameters strongly co-vary.

Despite the above discussed uncertainties, we conclude that our mass-balanced ODE based model for a multi-trophic ecosystem in an Erlenmeyer with toxicants present works. The advantage of having such a model *and* having the values for the parameter lies in the fact that it is now possible to run short-term simulations and to a certain extend long-term simulations in order to interpolate between concentrations, predict effects of different exposure regimes or to predict the effect of both toxicants simultaneously present.

*Acknowledgements* - We gratefully acknowledge the financial support granted by the European Commission (Contract No 511237-GOCE).

## 4.5 Appendix

### Equilibrium density of reserve

When  $V$  is a stable density then  $dM_V/dt = 0$  and  $M_V = M_V^*$ .

$$\frac{dM_V}{dt} = J_{C_V,G} - J_{C_V,M} - J_{C_V,d} = 0 \quad (4.9a)$$

$$J_{C_V,G} > 0 | J_{C_V,M} = 0 \quad ; \quad J_{C_V,G} = J_{C_V,d} \quad (4.9b)$$

$$J_{C_V,G} = rM_V \quad ; \quad J_{C_V,d} = d_C M_V \quad ; \quad r = d_C \quad (4.9c)$$

$$J_{C_V,G} = 0 | J_{C_V,M} > 0 \quad ; \quad -J_{C_V,M} = J_{C_V,d} \quad (4.9d)$$

$$J_{C_V,M} = j_V^M M_V \quad ; \quad J_{C_V,d} = d_C M_V \quad ; \quad -j_V^M = d_C \quad (4.9e)$$

To have a non-zero solution for  $M_V^*$  then  $J_{C_V,G} = J_{C_V,d}$  and thus  $r = d_C$ . To calculate the specific reserve density when  $r = d_C$  and  $dM_V/dt = 0$ :

$$\left. \begin{array}{l} j_{E,C} = m_E(k_E - r) \\ r = y_{VE}(j_{E,C} - j_{E,M}) \end{array} \right\} r = \frac{m_E k_E - j_{E,M}}{m_E + \frac{1}{y_{VE}}}$$

$$\left. \begin{array}{l} r = d_C \\ r = \frac{m_E k_E - j_{E,M}}{m_E + \frac{1}{y_{VE}}} \end{array} \right\} m_E = \frac{j_{E,M} + \frac{d_C}{y_{VE}}}{k_E - d_C} \quad (4.10)$$

$$j_E^M = j_{E,M} \quad , \quad j_V^M = 0 \quad , \quad j_{V,G} = r = d_C$$

Given  $r = d_C$ , then  $m_E = (j_{E,M} + d_C/y_{VE})/(k_E - d_C)$ .

### Dilution by growth

$$\frac{dM_E}{dt} = J_{E,A} - J_{E,d} - J_{E,C} \quad (4.11a)$$

$$\frac{dm_E}{dt} = \left[ \frac{M_E}{M_V} \right]' = \frac{dM_E}{dt} \frac{1}{M_V} - \frac{M_E}{M_V^2} \frac{dM_V}{dt} = \frac{dM_E}{dt} \frac{1}{M_V} - \frac{M_E}{M_V} \frac{dM_V}{dt} \quad (4.11b)$$

$$\frac{dm_E}{dt} = \frac{dM_E}{dt} \frac{1}{M_V} - m_E \dot{r} = j_{E,A} - j_{E,C} - m_E \dot{r} \quad (4.11c)$$

$$\frac{dm_E}{dt} = j_{E,A} - m_E(\dot{k}_e - \dot{r}) - m_E \dot{r} = j_{E,A} - m_E \dot{k}_e \quad (4.11d)$$

Observation: by defining  $j_{E,C}$  as  $m_E(\dot{k}_e - \dot{r})$  the mobilization of reserves is linear dependent on both  $k_E$  and  $m_E$ .

### Amount of structure per ciliate

When for the ciliates growth and death are in balance,  $r = d_C$ , then the reserve density ( $m_E$ ) is in equilibrium. As the amount of structure per single ciliate is taken to be constant then the amount of nitrogen in the reserve plus the amount of nitrogen in the structure is constant at equilibrium. Thus at equilibrium the nitrogen content per ciliate is constant. From this the relative contribution of structure to the total nitrogen content of ciliate at equilibrium can be derived. As the nitrogen per unit of structure is constant ( $n_{NV}$ ) and the amount of structure per ciliate ( $n_{VC}$ ) is always constant then the values for  $n_{NV}$  and  $n_{VC}$  can be used outside equilibrium conditions when the reserve density fluctuates.

$$C = \frac{V n_{NV}}{N_C} = \text{DIM}\left(\frac{\text{mol } V/L \text{ mol } N/ \text{mol } V}{\text{mol } N / \text{cell}}\right) = \text{DIM}(\text{cells} / L) \quad (4.12a)$$

$$N_C = \frac{V}{C}(n_{NV} + m_E n_{NE}) \quad (4.12b)$$

$$\text{DIM}(N_C) = \text{DIM}\left(\frac{\text{mol } V/L}{\text{cells}/L} [( \text{mol } N/\text{mol } V) + (\text{mol } E/\text{mol } V)(\text{mol } N/\text{mol } E)]\right) \quad (4.12c)$$

$$\text{DIM}(N_C) = \text{DIM}(\text{mol } N/\text{cell}) \quad (4.12d)$$

$$m_E|_{r=d_C} = \frac{j_{E,M} + \frac{d_C}{y_{VE}}}{k_E - d_C} \quad (4.12e)$$

$$N_C|_{r=d_C} = \frac{V}{C} \left( n_{NV} + n_{NE} \frac{j_{E,M} + \frac{d_C}{y_{VE}}}{k_E - d_C} \right) \quad (4.12f)$$

$$N_C|_{r=d_C} \approx \frac{v_C}{v_A} N_A s_f \quad (4.12g)$$

$$n_{VC} = \frac{V}{C} \approx s_f N_A \frac{v_C}{v_A} \left( n_{NV} + n_{NE} \frac{j_{E,M} + \frac{d_C}{y_{VE}}}{k_E - d_C} \right)^{-1} \quad (4.12h)$$

$V$  and  $m_E$  are time dependent variables, thus  $N_C$  is variable.

## Simplifying the 1-reserve model into a Marr-Pirt model

By taking the reserve mobilisation rate ( $k_E$ ) very high compared to all other biological rates of the ciliate, the 1-reserve model for ciliate growth can be simplified into a model without reserve. A high  $k_E$  value means, results that all reserve is directly converted into structure or maintenance products. Conceptually, this can be seen as if the reserve is filled normally from feeding, then directly the reserve is emptied and spend first on maintenance and if there is surplus it is spend on growth. By setting  $k_E \rightarrow \infty$ , simplifies the equation of Eq. (4.4) for  $r$  into:

$$r_+ = y_{VE} \left( \frac{y_{EA}}{n_{NE}} k_C f(A) - j_{E,M} \right) \quad (4.13)$$

If the collected amount of nutrition is not enough to pay for all maintenance, then growth stops and part of the maintenance is paid from with structure as in Eq. (4.5):

$$r_- = -j_{V,M} \left( 1 - \frac{\frac{y_{EA}}{n_{NE}} k_C f(A)}{j_{E,M}} \right) \quad (4.14)$$

When maintenance is always paid from structure, then  $r_- = -j_{V,M}$  and  $r_+ = k_C f(A) y_{VE} y_{EA} / n_{NE}$  which leads to the the equation below:

$$r = r_+ + r_- = y_{VE} \frac{y_{EA}}{n_{NE}} k_C f(A) - j_{V,M} \quad (4.15a)$$

$$\frac{dM_V}{dt} = M_V \left( y_{VE} \frac{y_{EA}}{n_{NE}} k_C f(A) - j_{V,M} - d_C \right) \quad (4.15b)$$

The Marr-Pirt model for growth was as used in Chapter 3 for modelling both the ciliates and algae. The above ODE equation can be rewritten into the Marr-Pirt model formulation below, by taking  $h_c = j_{V,M} + d_C$  and  $y_{VA} = y_{VE} y_{EA} / n_{NE}$ . Then  $y_{VA}$  denotes the yield of ciliate biomass on algal biomass and  $h_c$  is the ciliate hazard rate.

$$\frac{dM_V}{dt} = M_V \left( y_{VA} k_C f(A) - h_c \right) \quad ; \quad y_{VA} = \frac{y_{VE} y_{EA}}{n_{NE}} \quad (4.16a)$$

$$h_c = d_C + j_{V,M} \quad ; \quad f(A) = \frac{\left( \frac{A}{N_A} - th_A \right)_+}{K_A + \left( \frac{A}{N_A} - th_A \right)_+} \quad (4.16b)$$

In equations (4.13), (4.14), (4.15a), and (4.16), the used parameters are the same as for the reserve model described in section 4.2.2.

# References

- [1] J. J. M. Bedaux and S. A. L. M. Kooijman. Statistical analysis of bioassays based on hazard modelling. *Environ. and Ecol. Stat.*, 1:303–314, 1994.
- [2] T. Berman, B. F. Sherr, E. Sherr, D. Wynne, and J. J. McCarthy. The characteristics of ammonium and nitrate uptake by phytoplankton in lake Kinneret. *Limnol. Oceanogr.*, 29(2):287–297, 1984.
- [3] D. Bontje, B. W. Kooi, M. Liebig, and S. A. L. M. Kooijman. Modelling long-term ecotoxicological effects on an algal population under dynamic nutrient stress. *Water Res.*, 43:3292–3300, 2009.
- [4] D. Bontje, B. W. Kooi, G. A. K van Voorn, and S. A. L. M. Kooijman. Feeding threshold for predators stabilises predator-prey systems. *Math. Model. Nat. Phenom.*, 4(6):91–108, 2009.
- [5] M. Eichinger, S. A. L. M. Kooijman, R. Sempéré, and J. -C. Poggiale. Consumption and release of dissolved organic carbon by marine bacteria in pulsed-substrate environment: from experiments to modelling. *Aquat. Microb. Ecol.*, 56:41–54, 2009.
- [6] J. W. Fleeger, K. R. Carman, and R. M. Nisbet. Indirect effects of contaminants in aquatic ecosystems. *Sci. Total Environ.*, 317:207–233, 2003.
- [7] S. A. L. M. Kooijman. *Dynamic Energy Budgets in biological systems, 2nd edn.* Cambridge University Press, Cambridge, 2000.
- [8] O. Köster and F. Jüttner.  $\text{NH}_4^+$  utilization and regeneration rates in freshwater lakes determined by GCMS of derivatised dihydroindophenol. *J. Microbiol. Meth.*, 37:65–76, 1999.
- [9] M. Liebig, G. Schmidt, D. Bontje, B. W. Kooi, G. Streck, W. Traunspurger, and T. Knacker. Direct and indirect effects of pollutants on algae

- and algivorous ciliates in an aquatic indoor microcosm. *Aquat. Toxicol.*, 88(2):102–110, 2008.
- [10] A. M. Mood, F. A. Graybill, and D. C. Boes. *Introduction to the Theory of Statistics*. McGraw-Hill, Inc., 3<sup>th</sup> edition, 1974.
- [11] G. Pfister, T. Sonntag, and T. Posch. Comparison of a direct live count and an improved quantitative protargol stain (qps) in determining abundance and cell volumes of pelagic freshwater protozoa. *Aquat. Microb. Ecol.*, 18:95–103, 1999.
- [12] H. W. Press, S. A. Teukolsky, W. T. Vetterling, and B. P. Flannery. *Numerical Recipes in C*. Cambridge University Press, 2nd edition, 1992.
- [13] B.L. Preston and T. W. Snell. Direct and indirect effects of sublethal toxicant exposure on population dynamics of freshwater rotifers: a modeling approach. *Aquat. Toxicol.*, 52:87–99, 2001.
- [14] T. Stabell, T. Andersen and D. Klaveness. Ecological significance of endosymbionts in a mixotrophic ciliatean experimental test of a simple model of growth coordination between host and symbiont. *J. Plankton Res.*, 24(9):889–899, 2002.
- [15] T. P. Traas, J. H. Janse, P. J. Van den Brink, T. C. M. Brock, and T. Aldenberg. A freshwater food web model for the combined effects of nutrients and insecticide stress and subsequent recovery. *Environ. Toxicol. Chem.*, 23:521–529, 2004.
- [16] K. Van den Meersche, J. J. Middelburg, K. Soetaert, P. Van Rijswijk, H. T. S. Boschker, and C. H. R. Heip. Carbon-nitrogen coupling and algal-bacterial interactions during an experimental bloom: Modeling a <sup>13</sup>C tracer experiment. *Limnol. Oceanogr.*, 49(3):862–878, 2004.
- [17] T. Weisse, N. Karstens, V.C.L. Meyer, L. Janke, S. Lettner, and K. Teichgräber. Niche separation in common prostome freshwater ciliates: the effect of food and temperature. *Aquat. Microb. Ecol.*, 26:167–179, 2001.
- [18] T. Weisse and B. Kirchoff. Feeding of the heterotrophic freshwater dinoflagellate *Peridiniopsis berolinense* on cryptophytes: analysis by flow cytometry and electronic particle counting. *Aquat. Microb. Ecol.*, 12:153–164, 1997.
- [19] T. Weisse and P. Stadler. Effect of pH on growth, cell volume, and production of freshwater ciliates, and implications for their distribution. *Limnol. Oceanogr.*, 51(4):1708–1715, 2006.

## Chapter 5

# Sublethal toxic effects in a simple aquatic food chain

B.W. Kooi, D. Bontje, G.A.K. van Voorn and S.A.L.M. Kooijman  
*Ecological Modelling*, 212:304–318, 2008.

In this Chapter we study the sublethal effect of toxicants on the functioning (biomass production, nutrient recycling) and structure (species composition and complexity) of a simple aquatic ecosystem in a well-mixed environment (chemostat system). The modelled ecosystem consists of a nutrient consumed by a prey (e.g. bacteria, alga) which, in turn, is consumed by a predator (e.g. ciliates, *Daphnia*) population. The dynamic behaviour of this ecosystem is described by a set of ordinary differential equations (ODEs): one for the nutrient and one for each population. The system is stressed by a toxicant dissolved in the in-flowing water. The transport of the toxicant is modelled using a mass balance formulation leading to an ODE. Bio-accumulation in the prey and predator populations is via uptake from the water phase, in case of the predator also via consumption of contaminated prey. Mathematically this process is described by a one-compartment model for the kinetics of the toxicant: uptake (from water and food) and elimination. The toxicant affects the development of individuals which make up populations. In the model the physiological parameters depend on the internal concentration of the toxicant in individuals. Examples of physiological parameters are cost for growth, assimilation efficiency and maintenance rate. In this Chapter we use bifurcation theory. In this way the parameter space is divided into regions with qualitatively different asymptotic dynamic behaviour of the system. A logical choice for bifurcation parameters are the strength of the forcing on the system determined by the input rate of nutrient and toxicant. Our analysis reveals that the

relationship between the population biomass and the amount of toxicant in the system is of paramount importance. The dynamic behaviour of the stressed ecosystem can be much more complicated than that of the unstressed system. For instance the nutrient-prey-contaminant system can show bi-stability and oscillatory dynamics. Due to the toxic effects a total collapse of the nutrient-prey-predator-contaminant system can occur after invasion of a predator, in which case both prey and predator population go extinct.

## 5.1 Introduction

With the theoretical assessment of consequences of toxicants on the functioning of aquatic ecosystems, five steps can be distinguished (Calow et al., 1997):

1. *Ecological theory*: Modelling of the biological functioning of the system. For an ecosystem we need
  - a model for individual life-cycle
  - a model of each population using a model of individual behaviour
  - a model for the ecosystem using models of populations, including their mutual interactions and interactions with the physical environment, such as transport of nutrients.
2. *Environmental chemical theory*: Modelling of the environmental chemistry and geochemistry to describe the fate of the toxicant in terms of transport, distribution and exposure of toxicants.
3. *Toxicological theory*: Modelling the relationship between exposure to a toxicant, toxicokinetics and behaviour of an individual.
4. *Ecotoxicological theory*: Modelling the effect of toxic stress on the individual, population and ecosystem level via bio-concentration (exclusively from water), bio-magnification (exclusively via food), and bio-accumulation (from water and food).
5. *Risk assessment*: Using the ecosystem, exposure and effect models to assess community/ecosystem consequences, *e.g.*, extinction of one or more populations.

In this Chapter we focus on point (4), where we use existing models for a simple ecosystem (1), for the fate of the toxicant (2), and an exposure model (3). It is also briefly discussed how the obtained results can be used for risk assessment (5).

The dynamical behaviour of small-scale microbial food chains or aquatic ecosystems, such as a system of nutrient, detritus, phytoplankton, zooplankton

and fish, have been studied intensively in the literature (for instance DeAngelis, 1992). Generally each population is modelled by one or a few ODE's. Two ingredients of these systems are *state variables*, such as nutrient, detritus, biomass or energy content, and *parameters*, such as maximum ingestion rate, assimilation efficiency, immigration or emigration rates, reproduction rate, searching rate for food, handling time of prey, maintenance rate and mortality rate. For the long-term dynamics important features of the ecosystem are persistence of the structural composition of the ecosystem, and the dynamical behaviour of the ecosystem, *i.e.*, the occurrence of steady states, oscillations, or chaos.

In an elementary ecological setting these parameters are species-specific constants or, in the case of diurnal or seasonal forcing (for instance, light intensity), also depending explicitly on time. In a stressed system these parameters may, in turn, depend on external parameters, such as pH, temperature, or rainfall. In the case of toxic stress, the subject of this Chapter, the population parameters depend on the concentration of a toxicant in the water, which is a state variable.

Toxicants are emitted and distributed into the ambient water. The transport of the toxicant is modelled by mass-balanced ODEs. Exposure of the organisms is by absorption from the water or via consumption of contaminated food. The kinetics of the toxicant in the organism is modelled with a first order one-compartment model where two processes are involved, namely uptake (from water and/or food) and elimination. The rates of these processes depend on the internal and water concentration of the toxicant or contaminated food availability (Kooijman and Bedaux, 1996). For each species-toxicant combination a concentration-effect relationship describes how the toxicant changes the population parameters that determine the rate of physiological processes. These parameter changes in turn affect the functioning of the ecosystem (extinction of a population, or system destabilisation).

In this Chapter we analyse the lowest level of an aquatic ecosystem. The model for the populations (*e.g.*, bacteria or algae consumed by ciliates) that compose the ecosystem is a simplified version of the DEB model (Kooijman, 2000). The toxic effects on the population level are described by the DEBtox approach for uni-cellular organisms with a simple life-history, namely propagation by binary fission (Kooijman and Bedaux, 1996). The effect module is not based on parameters estimated from descriptive models, but on process-based models where physiological parameters depend on the internal toxicant concentration. The possibly affected physiological processes (modes of action) are assimilation, maintenance, growth and mortality, *i.e.*, these processes can be the targets of the toxicant. Here we describe the consequences on the ecosystem behaviour, where nutrients and toxicant are supplied and removed at a constant rate in a spatially homogeneous chemostat (Smith and Waltman,

1994).

Bio-accumulation in food webs has also been studied by other authors (Thomann and Connolly, 1984; Thomann and Mueller, 1987; Thomann, 1989; Clark et al. 1990; Gobas, 1993; Calow et al. 1997; Traas et al. 2004a; Traas et al. 2004b). In these papers the transfer of the toxicant through the ecosystem is decoupled from dynamics of the ecosystem, by assuming the ecosystem to be in an equilibrium. For the populations, the internal concentration is assumed to be in equilibrium with the ambient concentration, that is, the concentration ratio is constant. For the prey, where uptake is only from the ambient water, this ratio is called the *Bio-Concentration Factor* (BCF). For the predator, where intake of the toxicant is also via contaminated prey, it is named *Bio-Accumulation Factor* (BAF; Thomann, 1989). Hence, for each trophic level there is an expression that links the two concentrations algebraically, and no extra ODE for the internal toxicant concentration is needed, while the two exchange rates are replaced by a single BCF parameter. This simplifies the analysis considerably. Besides the BCF, BMF and BAF values, additional information is needed on the dietary preference matrix, that fixes the feeding relationships between the prey and predator populations in the ecosystem. In this way, ecosystem dynamics and the fate of the toxicant are modelled separately.

This Chapter is organised as follows. In Section 5.2, the modelling and analysis approaches are introduced. Here we use an approach where ecological processes and the fate of the toxicant, as well as their interactions, are modelled integrately (Koelmans et al., 2001). The model for the nutrient-prey system in the chemostat is formulated in Section 5.3. The model for the unstressed system predicts simple dynamical behaviour, which is a stable equilibrium under sufficient nutrient supply. In Section 5.4 we show, that under toxic stress, the model predicts bi-stability under certain environmental conditions. In Section 5.5 the model for the nutrient-prey-predator system is formulated. Expressions for the BCF, BMF and BAF are derived. Two situations are analysed in Section 5.6. In the first case, both the prey (via water) and the predator (via water and food) population are affected by the toxicant, for instance when the toxicant is a pesticide. In the second case only the prey population is affected, for example when the toxicant is a bactericide (antibiotic) or algicide (herbicide). In the latter case, the model predicts that, after inoculation of the predator in the nutrient-prey system, a complete system collapse is possible, whereby both predator and prey species go extinct. In Section 5.7 we conclude that, due to the dynamics of the toxicant, there is an extra removal mechanism from the system. Presence of the toxicant influences the growth of the populations, which in turn changes the uptake rate of the toxicant by these populations. This feedback mechanism appears to be crucial for the occurrence of more complex dynamics in stressed as compared

Table 5.1: State variables and control parameter set for nutrient–prey–predator chemostat model. The environmental parameters, which can be experimentally manipulated, are  $D \in (0, 0.5) \text{ h}^{-1}$ ,  $N_r \in (0, 150) \text{ mg dm}^{-3}$  and  $c_r \in (0, 9) \text{ } \mu\text{g dm}^{-3}$ :  $m$  mass of toxicant,  $t$  time,  $v$  is dimension of the volume of the system and  $V$  biovolume or biomass of organism.

Var.	Description	Dimension
$N$	Nutrient mass density	$V v^{-1}$
$R$	Prey biomass density	$V v^{-1}$
$P$	Predator biomass density	$V v^{-1}$
$c_W$	Toxicant concentration in the water	$m v^{-1}$
$c_R$	Prey internal toxicant concentration	$m V^{-1}$
$c_P$	Predator internal toxicant concentration	$m V^{-1}$
Par.	Description	Dimension
$D$	Dilution rate	$t^{-1}$
$N_r$	Nutrient mass density	$V v^{-1}$
$c_r$	Toxicant concentration in influent	$m v^{-1}$

to unstressed ecosystems. Finally, in Section 5.8 a short summary is given of the results in this Chapter.

## 5.2 Model formulations and analysis

Here, we consider a simple food chain model, consisting of a nutrient consumed by a prey population, which in turn is consumed by a predator population. This two-trophic level ecosystem exists in a chemostat. The resulting model can also describe a simple ecosystem in a section of a river that is kept at constant volume. Water with nutrients flows into the system at a given rate, while water carrying organisms and nutrients flow out at the same rate. The system is stressed by a toxicant that enters the system besides the nutrient. We use the simplest possible formulation, where the state of each population is described by its biomass only. The Marr-Pirt model (Pirt, 1965) is used, which is appropriate for uni-cellular micro-organisms that propagate by binary fission. A fixed portion of the ingested food is assimilated and the assimilates are used for maintenance and growth. In this model the temporal changes of these variables are mathematically given as a system of ODEs.

One can get insight into the dynamics of a system and subsequently the sublethal effects (*e.g.*, extinction of a population or system destabilising) by

running simulations. The initial value problem is solved with various initial conditions or parameter settings. Plotting the time-courses for the population biomasses is possible, but also trajectories in the state-space where one population biomass is plotted against another. This yields direct insight into the long-term dynamics. Especially when there are multiple stable equilibria this method is, however, cumbersome and time-consuming.

When the environmental conditions are constant or periodic in time, we can apply a different and more sophisticated analysis method, namely bifurcation analysis. Based on principles from non-linear dynamic system theory, bifurcation analysis focuses on the dependency of the long-term dynamical behaviour on model parameters (Wiggins, 1990; Guckenheimer and Holmes, 1985; Kuznetsov, 2004). At least three different kinds of asymptotic behaviour can occur: constant (equilibrium), periodic (limit cycle) and chaotic (sensitivity to initial conditions).

The results of a bifurcation diagram are generally presented in bifurcation diagrams. In bifurcation diagrams the parameter space is divided into regions with the same long-term dynamical behaviour. The chosen parameters are called free or bifurcation parameters. In our case especially the chemostat control parameters, the nutrient and toxicant input and dilution rate, are appropriate. In each point in the parameter space the same species composition is considered, and only the interaction with the ambient water is changed. Also toxicological parameters can be used as bifurcation parameters in order to assess their consequences.

There is a class of bifurcations, called global bifurcations, that cannot be deduced from local information (*e.g.*, eigenvalues of the Jacobian matrix) around the stationary solution. Examples are homoclinic and heterocline point-to-point, point-to-cycle or cycle-to-cycle connections. We found homoclinic point-to-point bifurcation points for the toxic stressed nutrient-prey system, and heteroclinic point-to-point bifurcation points in the nutrient-prey-predator system.

Table 5.1 shows a list of the state variables and the control parameters. In Table 5.2, we give the parameter values used in this study. The physiological parameters are those for a bacterium-ciliate system and were also used for various food web studies, see Kooi (2003) and reference therein.

### 5.3 Model for nutrient-prey system

In this Section we discuss the nutrient-prey chemostat model with and without a toxicant.

Table 5.2: Parameter set for bacterium-ciliate model. Ecological parameters after Cunningham and Nisbet (1983):  $m$  mass of toxicant,  $t$  time,  $v$  is dimension of the volume of the system and  $V$  biovolume or biomass of organism.

Nutrient-Prey			
$\mu_{NR}$	Max. growth rate	$t^{-1}$	$0.5 \text{ h}^{-1}$
$I_{NR}$	Max. ingestion rate	$t^{-1}$	$1.25 \text{ h}^{-1}$
$k_{NR}$	Saturation constant	$V v^{-1}$	$8.0 \text{ mg dm}^{-3}$
$k_{Ru}$	Uptake rate	$v m^{-1} t^{-1}$	—
$k_{Ra}$	Elimination rate	$t^{-1}$	—
$m_{R0}$	Maintenance rate coefficient	$t^{-1}$	$0.025 \text{ h}^{-1}$
$c_{RM0}$	NoEffect Concentration (NEC)	$m V^{-1}$	$0.1 \mu \text{ g mg}^{-1}$
$c_{RM}$	Tolerance concentration ( $EC_{50} - \text{NEC}$ )	$m V^{-1}$	$0.5 \mu \text{ g mg}^{-1}$
$BCF_{WR}$	Bio-Concentration Factor	$v V^{-1}$	$1.0 \text{ dm}^3 \text{ mg}^{-1}$
Prey-Predator			
$\mu_{RP}$	Max. growth rate	$t^{-1}$	$0.2 \text{ h}^{-1}$
$I_{RP}$	Max. ingestion rate	$t^{-1}$	$0.333 \text{ h}^{-1}$
$k_{RP}$	Saturation constant	$V v^{-1}$	$9.0 \text{ mg dm}^{-3}$
$k_{Pu}$	Uptake rate	$v V^{-1} t^{-1}$	$10 \text{ dm}^3 \text{ mg}^{-1} \text{ h}^{-1}$
$k_{Pa}$	Elimination rate	$t^{-1}$	$10 \text{ dm}^3 \text{ mg}^{-1} \text{ h}^{-1}$
$m_{P0}$	Maintenance rate coefficient	$t^{-1}$	$0.01 \text{ h}^{-1}$
$c_{PM0}$	No-Effect Concentration (NEC)	$m V^{-1}$	$0.1 \mu \text{ g mg}^{-1}$
$c_{PM}$	Tolerance concentration ( $EC_{50} - \text{NEC}$ )	$m V^{-1}$	$0.5 \mu \text{ g mg}^{-1}$
$BCF_{WP}$	Bio-Concentration Factor	$v V^{-1}$	$1.0 \text{ dm}^3 \text{ mg}^{-1}$
$BAF_{WP}$	Bio-Accumulation Factor	$v V^{-1}$	—

### 5.3.1 Unstressed nutrient-population system

Let  $N(t)$  be the nutrient density and  $R(t)$  the biomass density of the population. Then the governing equations for the simple ecosystem are

$$\frac{dN}{dt} = (N_r - N)D - I_{NR} \frac{N}{k_{NR} + N} R, \quad (5.1a)$$

$$\frac{dR}{dt} = \left( \mu_{NR} \frac{N}{k_{NR} + N} - D - m_{R0} \right) R, \quad (5.1b)$$

identical to Kooi (2003). The two control parameters that can be experimentally manipulated are the dilution (flow-through) rate  $D$ , the fraction of the volume replaced per unit of time, and the nutrient density  $N_r$  in the inflow. The influx of nutrient,  $DN_r$ , the outflow of nutrient,  $DN$ , and the outflow of the population,  $DR$ , are the terms that model the interaction of the population with the environment.

The consumption of the nutrient by the population is modelled with a Holling type II functional response (Holling, 1959), that includes the maximum ingestion rate  $I_{NR}$ , the maximum growth rate  $\mu_{NR}$  (the ratio of the growth rate and ingestion rate is called the assimilation efficiency in ecology or yield in microbiology), and the saturation constant  $k_{NR}$ . These three parameters are fixed for a specific prey-nutrient combination, indicated by the double subscript of the variables. The parameter  $m_{R0}$  is the maintenance rate and models a reduction of the growth rate due to overhead costs, related to keeping the organism alive. These costs are assumed to be proportional to the biomass density of the prey  $R$ .

### 5.3.2 Stressed nutrient-population system

Let  $c_W(t)$  be the ambient water concentration of the toxicant in the system, and  $c_r$  the constant concentration of the toxicant in the inflow. The dynamics of the toxicant are described by the following mass-balance equation

$$\frac{d(c_W + c_R R)}{dt} = (c_r - (c_W + c_R R))D, \quad (5.2)$$

where we make the reasonable assumption that the volume of the system is constant. The toxicant enters the system via the inlet with a concentration  $c_r$ , in a similar way as the nutrients (the term  $N_r D$  in (5.1a)). The internal concentration of the toxicant is denoted by  $c_R$  (concentration with respect to the biomass  $R$ ). The rate at which the toxicant leaves the system consists of two terms, namely transport of the dissolved toxicant in the system,  $c_W D$ , and the toxicant absorbed by the population,  $c_R R D$ .

The one-compartment model for the internal toxicant concentration reads

$$\frac{dc_R}{dt} = k_{Ru}c_W - k_{Ra}c_R - \left( (I_{NR} - \mu_{NR}) \frac{N}{k_{NR} + N} + D + m_R(c_R) + \frac{1}{R} \frac{dR}{dt} \right) c_R, \quad (5.3)$$

where the last term is due to dilution by growth.

Equivalently, the dynamics of the exchange of the toxicant between the prey and its ambient water are described by a mass balance model for the total toxicant content in the population as the product of internal concentration  $c_R$ , and the biomass density  $R$ . Using the product rule we obtain

$$\frac{dc_R R}{dt} = (k_{Ru}c_W - k_{Ra}c_R)R - \left( (I_{NR} - \mu_{NR}) \frac{N}{k_{NR} + N} + D + m_R(c_R) \right) c_R R, \quad (5.4)$$

where the first term on the right-hand side is the exchange between the water and the organisms, and the second term is the flux of the toxicant into the organisms that leave the system and the flux egested by the organisms as assimilation and maintenance products. The diffusion transport fluxes are proportional to the area of the surfaces summed over all organisms. We assume that the surface (*e.g.*, outer membrane) of the organisms is proportional to their volume. The same holds at the population level. For organisms that propagate by division this is justified. This means that the surface area to volume ratio is included in the uptake and elimination rate constants. Furthermore, the toxicant is absorbed into the assimilation and maintenance products and egested into the system as dissolved toxicant.

The exchange of the toxicant between the water and the organisms is assumed to be much faster than the other biological processes, including dilution, assimilation, growth and maintenance. Due to the small size and large area to volume ratio for phyto- and zooplankton, it is assumed that the uptake and elimination of toxicants predominate the exchange between the organism and the water (Gobas, 1993). As in Hallam et al. (1993), for a *Daphnia* population it is assumed that the characteristic time for the internal distribution is short compared to the characteristic time for exchange with the water. We rewrite the system as a singular perturbation problem, where  $\kappa_a = \varepsilon k_{Ra}$  and  $\kappa_u = \varepsilon k_{Ru}$ , with  $\tau = t/\varepsilon$

$$\frac{dc_R R}{dt} = (\kappa_u c_W - \kappa_a c_R) R - \varepsilon \left( (I_{NR} - \mu_{NR}) \frac{N}{k_{NR} + N} + D + m_R(c_R) \right) c_R R, \quad (5.5a)$$

$$\frac{dc_W}{d\tau} = -(\kappa_u c_W - \kappa_a c_R) R + \varepsilon ((c_r - c_W) D + m_R(c_R) c_R R), \quad (5.5b)$$

where time scale separation occurs when  $\varepsilon \ll 1$ .

At the fast time scale we have the sub-model where  $\varepsilon \rightarrow 0$

$$\frac{dc_R R}{d\tau} = (\kappa_u c_W - \kappa_a c_R) R, \quad (5.6a)$$

$$\frac{dc_W}{d\tau} = -(\kappa_u c_W - \kappa_a c_R) R, \quad (5.6b)$$

where we used (5.2) and (5.4). In equilibrium we obtain

$$0 = \kappa_u c_W^* - \kappa_a c_R^*, \quad (5.7)$$

which gives in turn the quasi-steady state

$$\frac{k_{Ru}}{k_{Ra}} = \frac{\kappa_u}{\kappa_a} = \frac{c_R^*}{c_W^*} = \text{BCF}_{WR}, \quad (5.8)$$

where the Bio-Concentration Factor for the population ( $\text{BCF}_{WR}$ ) is the ratio of the internal toxicant concentration (with respect to the biomass density of the population) and the external toxicant concentration (with respect to the system volume). This relationship is now also used in non-equilibrium situations on the slow time scale.

We can now introduce the total toxicant concentration in the system  $c_T$ . The set of governing equations then becomes

$$\frac{dN}{dt} = (N_r - N) D - I_{NR} \frac{N}{k_{NR} + N} R, \quad (5.9a)$$

$$\frac{dR}{dt} = \left( \mu_{NR}(c_R) \frac{N}{k_{NR} + N} - (D - m_R(c_R)) \right) R, \quad (5.9b)$$

$$\frac{dc_T}{dt} = (c_r - c_T) D, \quad (5.9c)$$

where  $c_T = c_W + c_R R = c_W (1 + \text{BCF}_{WR} R)$ .

The effect of the toxicant on the physiology of the populations is modelled as a dependency of physiological parameters, such as growth rate and maintenance rate, on the toxicant concentration. In Kooijman and Bedaux (1996) the following expressions are proposed

$$m_R(c_R) = m_{R0} \left( 1 + \frac{(c_R - c_{RM0})_+}{c_{RM}} \right), \quad (5.10a)$$

$$\mu_{NR}(c_R) = \mu_{NR0} \left( 1 + \frac{(c_R - c_{RG0})_+}{c_{RG}} \right)^{-1}, \quad (5.10b)$$

where the subscript  $+$  operator is defined as  $x_+ = \max(0, x)$ , which is a non-smooth switch function. The parameter  $m_{R0}$  is the maintenance rate coefficient of the unstressed system ( $c_r = 0$ ). The toxicological parameters are the no-effect concentration (NEC), a threshold concentration for the onset of effects, and  $c_{RM}$ , the tolerance concentration for maintenance. Observe that Kooijman and Bedaux (1996) based these two parameters on the external concentrations (per volume of the system), and not the internal concentration (per biomass density), as is done here. Similarly, when the growth process is the mode of action, we have the equivalent parameters  $c_{RG0}$  and  $c_{RG}$ .

To calculate  $c_R(t)$ , we use

$$c_W = \frac{c_T}{1 + \text{BCF}_{WR} R}, \quad (5.11a)$$

$$c_R = \frac{\text{BCF}_{WR} c_T}{1 + \text{BCF}_{WR} R}, \quad (5.11b)$$

where  $t \geq 0$  depends on the two state variables  $c_T(t)$  and  $R(t)$ . The expression (5.11) is substituted into (5.10a) which, in turn, is substituted into (5.9b).

## 5.4 Analysis of the nutrient-prey system

To apply bifurcation analysis, we first need the system's equilibria. Equilibria of a system are fixed by the requirement that the time derivatives of the state variable are zero. Let equilibrium values  $N^*$  and  $R^*$  denote a possible solution. The equation for the dynamics of the toxicant concentration (5.11) gives in equilibrium situation  $c_T^* = c_R^* (1 + \text{BCF}_{WR} R^*) / \text{BCF}_{WR}$ . Depending on the environmental conditions, there will be one equilibrium  $E_1$ , or multiple positive equilibria  $E_1, E_2$ , where  $N^* < N_r$ ,  $R^* > 0$ ,  $c_W^* < c_r$ . Besides these equilibria there is a trivial solution  $E_0 = (N_r, 0, c_r)$ .

For the following analyses the relevant bifurcation types and their descriptions are characterised in Table 5.3.

Table 5.3: List of bifurcations, codim-one curves and codim-two points (for two-parameter bifurcation diagrams). The eigenvalues are of the Jacobian matrix evaluated at the equilibrium. The Floquet multipliers of the Monodromy matrix evaluated at a point on the limit cycle. See also Kuznetsov (2004) for theoretical consideration.

Bif.	Description
<b>Codim-one curves</b>	
$TC_{a,i}^{\pm}$	Transcritical bifurcation: – supercritical, + subcritical; $a = e$ or empty equilibrium : zero eigenvalue $a = c$ limit cycle: Floquet multiplier equal one $i = 1$ : invasion by population prey, $i = 2$ : invasion by predator
$H_i^{\pm}$	Hopf bifurcation: – supercritical, + subcritical ; zero real parts of pair of conjugate eigenvalues $i = 1$ : nutrient–prey system becomes unstable, $i = 2$ : nutrient–prey–predator system becomes unstable, origin of stable (supercritical) or unstable (subcritical) limit cycle
$T_1$	Tangent bifurcation for equilibrium: zero eigenvalue
$G^=$	Homoclinic bifurcation; global bifurcation for connection of equilibrium with itself of nutrient–prey system
$G^{\neq}$	Heteroclinic bifurcation; global bifurcation for connection between two saddle equilibria of nutrient–prey–predator system
<b>Codim-two points</b>	
$BT^{\pm}$	Bogdanov-Takens bifurcation point; global homoclinic cycle originates form this point
$B$	Bautin bifurcation point; transition from sub- to supercritical Hopf bifurcation origin of tangent limit cycle
$N$	Transition from sub- to supercritical transcritical bifurcation tangent bifurcation curve originates on boundary of region of bi-stability
$M$	Intersection of Hopf and transcritical bifurcation curves for equilibria origin transcritical bifurcation for limit cycle curve

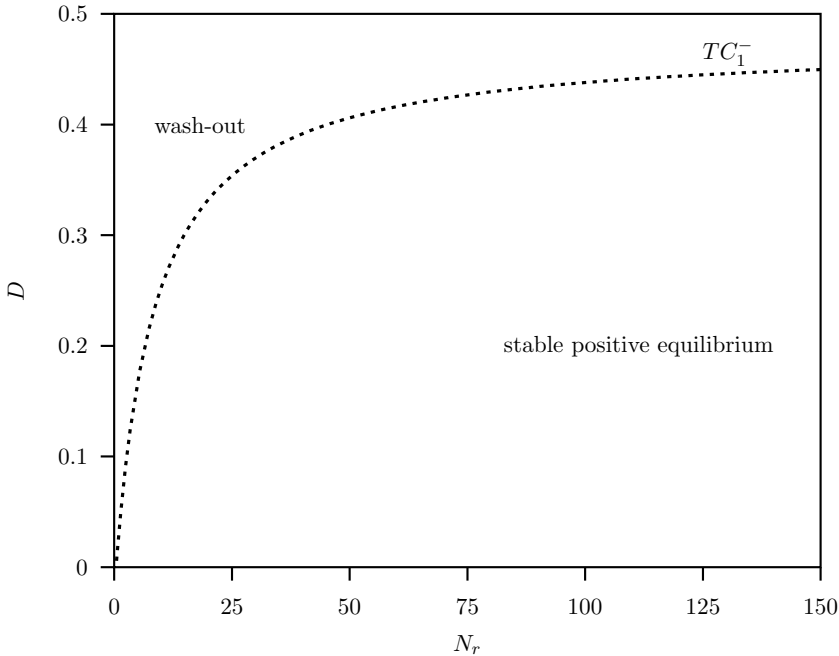


Figure 5.1: A two-parameter bifurcation diagram with nutrient inflow  $N_r$  and dilution rate  $D$  as free parameters for the population without toxicity stress ( $c_r = 0$ ) in the chemostat system, Eqn. (5.1). The dashed curve is the transcritical bifurcation curve  $TC_1^-$ . For dilution rates above this curve there is wash-out. Below the transcritical bifurcation curve the population can invade a nutrient system and establish at a stable positive equilibrium. A description of the parameters and their units is provided in Table 5.2.

#### 5.4.1 Unstressed nutrient-prey system

For the unstressed system (5.1) the two-parameter bifurcation diagram is shown in Fig. 5.1, where the environmental parameters  $N_r$  and  $D$  are the bifurcation parameters. Two regions can be distinguished in the bifurcation diagram, that are separated by a transcritical bifurcation  $TC_1^-$ . In the upper region the population cannot establish itself (equilibrium  $E_0$ , where  $R^* = 0$ ), for instance because the dilution rate is larger than the maximum growth rate of the population ( $D > \mu_{NR}$ ). In the lower region the population establishes itself (equilibrium  $E_1$ , where  $R^* > 0$ ).

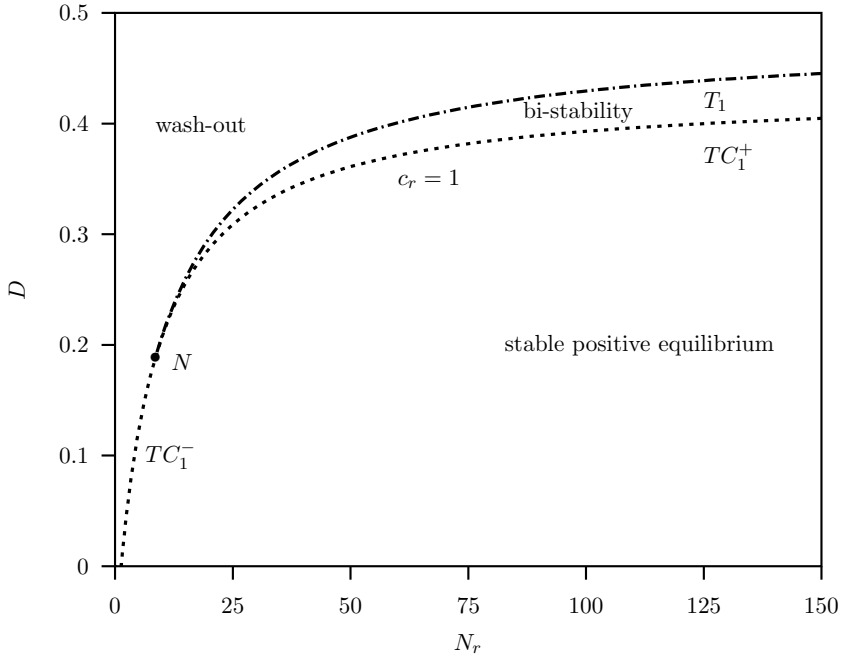


Figure 5.2: A two-parameter bifurcation diagram with nutrient inflow  $N_r$  and dilution rate  $D$  as free parameters for the population with toxicity stress in the chemostat system Eqn. (5.9), where  $c_r = 1$ . The thin curve labelled  $c_r = 1$  was already shown in Fig. 5.1 and is plotted here for reference. Dashed curves are transcritical bifurcation curves  $TC_1^\pm$ , and the dot-dashed curve is the tangent bifurcation  $T_1$ . At point  $N$  the tangent curve  $T_1$  originates, and the transcritical bifurcation changes from supercritical  $TC_1^-$  to subcritical  $TC_1^+$ . Wash-out occurs for dilution rates above the tangent curve  $T_1$ . Below the transcritical bifurcation curve the population can invade a virgin system and establish at a stable positive equilibrium. Between the two curves  $T_1$  and  $TC_1^-$  there is bi-stability (see text).

Local stability analysis of the positive equilibrium gives the long-term dynamics when the initial values for the state variables,  $N(0)$  and  $R(0)$ , are in the vicinity of the equilibrium. Calculations show that it is also globally stable (Smith and Waltman, 1994), that is, for all positive initial values,  $N(0) > 0$ ,  $R(0) > 0$ , there is convergence to the stable equilibrium. This property makes the chemostat a popular experimental apparatus for growth of populations of uni-cellular organisms.

### 5.4.2 Stressed nutrient-prey-toxicant system

The stressed case, where the toxicant concentrations are considered, is represented by Eqn. (5.9), with

$$c_T(t) = (c_T(0) - c_r) \exp(-Dt) + c_r, \quad (5.12)$$

which is the analytical solution of Equation (5.9c) with  $c_r > 0$ .

Substitution of this expression into the two-dimensional ecosystem with state variables  $N(t)$  (5.9a) and  $R(t)$  (5.9b) yields a non-autonomous system. For the asymptotic dynamics it suffices to study the autonomous system, where in Eqn. (5.9a)-(5.9b)  $c_T = c_r$  is substituted (see Smith and Waltman, 1994).

The bifurcation diagram for  $c_r = 1$  is shown in Fig. 5.2. In a toxicant stressed system there is a point  $N$  on the transcritical bifurcation curve, where a so-called tangent bifurcation curve  $T_1$  emanates from. Below point  $N$  at the curve  $TC_1^-$  the situation is the same as in the unstressed system. However, above point  $N$ , in the parameter region enclosed by  $T_1$  and  $TC_1^+$ , there is a different kind of behaviour, namely bistability. There are the trivial equilibrium  $E_0$  and equilibrium  $E_1$ , which are both stable and are both attractors, while the stable manifold of a third saddle equilibrium  $E_2$  functions as a separatrix of the two basins of attraction for the two equilibria, respectively. The initial values of the variables determine to which of the two attractors the system converges.

The bistability disappears at one side at the transcritical bifurcation  $TC_1^+$ , because one of the attracting equilibria disappears. The system then always converges to the positive attractor. At the other side, at the tangent bifurcation  $T_1$ , the bistability is lost together with the non-trivial attractor, since the positive equilibrium  $E_1$  collides with the saddle equilibrium  $E_2$ , and they both disappear. Only the trivial equilibrium  $E_0$  remains, which means that in the region of the diagram above the tangent curve the population always goes extinct. This is illustrated in Fig. 5.3, a one-parameter bifurcation diagram for  $N_r = 150$  and  $c_r = 1$ , with  $D$  the free parameter.

We conclude that the transcritical bifurcation curve in Fig. 5.2 changes character at point  $N$ , from supercritical ( $TC_1^-$ ) below  $N$  to subcritical ( $TC_1^+$ )

above  $N$ , while  $N$  is the origin for the tangent bifurcation  $T_1$ . Furthermore, the reduction of the dimension of the system by taking  $C_T = c_r$  holds for the analysis of the stability of the equilibria, but not when global aspects are involved, for instance, when one wants to determine to which equilibrium the system will converge when there are multiple equilibria.

Now we discuss the effect for higher toxicological loading ( $c_r > 1$ ). The region in the parameter space where bi-stability occurs grows with increasing  $c_r$ . For higher toxicant stress-levels more complex bifurcation patterns occur (see Fig. 5.4, where  $c_r = 9$ ). There is a supercritical Hopf bifurcation, denoted by  $H_1^-$ . We saw already that the system is essentially two-dimensional. With systems of dimension higher than one, oscillatory dynamics can occur, that is, the equilibrium is stable, but it can be a so-called spiral-node, where convergence to the equilibrium points is oscillatory instead of monotonous. More importantly, the equilibrium point can become unstable, where the orbit spirals away from the equilibrium point after a small perturbation. In this situation there can be a stable limit cycle, where the solution is periodic, and the orbit in the state-space converges to a closed orbit, called a limit cycle.

On the tangent bifurcation curve  $T_1$  there are two Bogdanov-Takens points, denoted by  $BT^+$  and  $BT^-$ . For a more detailed discussion of the Bogdanov-Takens bifurcation point in ecological models, we refer to Bazykin (1998) and Baer et al. (2006). Here we discuss only phenomena important for the understanding of the effects of toxic stress on the functioning of an ecosystem.

From the  $BT^+$  point, a subcritical Hopf bifurcation curve  $H_1^+$  emanates. This Hopf bifurcation becomes supercritical at the Bautin bifurcation curve  $B$ . In the two-parameter diagram Fig. 5.4 also a curve  $G^=$  originates from the point  $BT^+$ . HOMCONT (Doedel et al., 1997, Chapter 16), part of the computer package AUTO, can be used to continue this homoclinic cycle global bifurcation curve. The global bifurcation curve, which emanates from the  $BT^-$ -point, is shown in Fig. 5.4, bottom panel.

Figs. 5.5 and 5.6 are one-parameter diagrams for  $c_r = 9$  and  $N_r = 150$ . With higher dilution rates there is bi-stability, with two stable equilibria and one saddle equilibrium, similar to the situation in Fig. 5.3, where  $c_r = 1$ . For low dilution rates, below the Hopf bifurcation curve  $H_1^-$ , the equilibrium  $E_1$  is unstable, and a stable limit cycle exists, of which the extrema are depicted in Fig. 5.6. The amplitude of the limit cycle increases very fast when decreasing  $D$ . Simultaneously, the period of the stable limit cycle increases, while the orbit stays close to the saddle equilibrium  $E_2$  for long episodes. At the critical point  $G^=$  the cycle, now called a homoclinic cycle, touches the intermediate equilibrium  $E_2$ , breaks up, and disappears suddenly. For  $D$  values below this point the stable manifold of the saddle equilibrium  $E_2$  loses its separation function, and the stable trivial equilibrium  $E_0$  becomes the global attractor. Hence, below  $G^=$  there is always extinction.

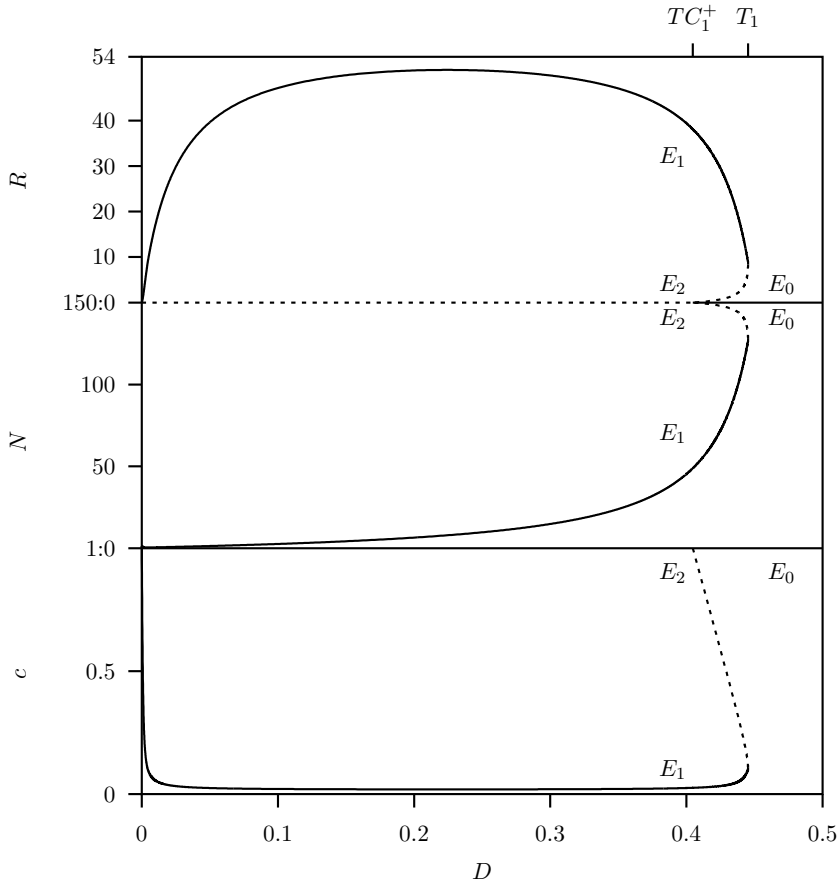


Figure 5.3: A one-parameter bifurcation diagram with dilution rate  $D$  as free parameter, for the population with toxicity stress in the chemostat system Eqn. (5.9), where  $N_r = 150$  and  $c_r = 1$ . Solid curves are stable equilibria  $E_0$ ,  $E_1$  and dashed curves  $E_2$ . Point  $T_1$  is the tangent bifurcation,  $TC_1^+$  the subcritical transcritical bifurcation. Between the two points  $T_1$  and  $TC_1^+$  there is bi-stability.

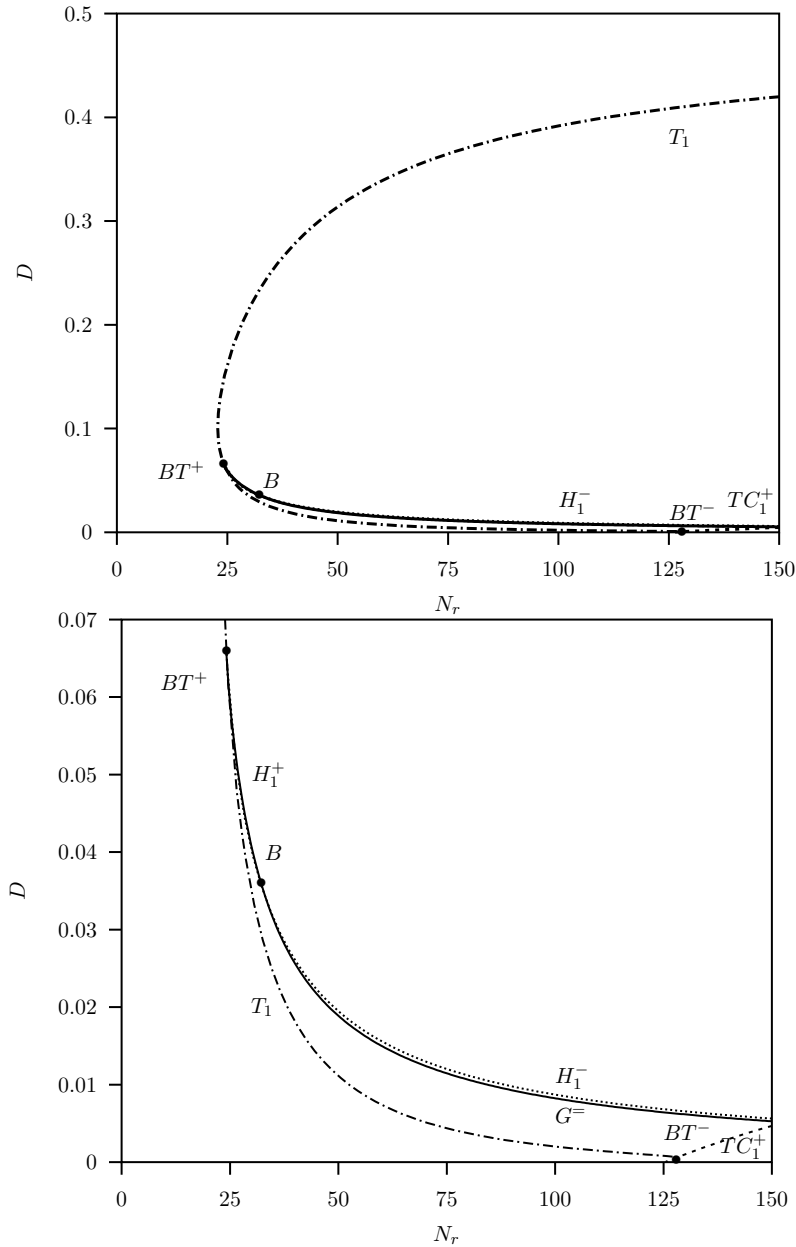


Figure 5.4: Top: a two-parameter bifurcation diagram with nutrient inflow  $N_r$  and dilution rate  $D$  as free parameters for the population with toxicity stress in the chemostat system Eqn. (5.9) where  $c_r = 9$ . Dashed lines indicate a transcritical bifurcation  $TC_1^+$  and dot-dashed lines indicate the tangent bifurcation  $T_1$ . Bottom: detail of top panel for low  $D$  values.

Decreasing the dilution rate further, the zero stable  $E_0$  and the saddle positive equilibrium  $E_2$  change stability at the subcritical transcritical bifurcation  $TC_1^+$ . For dilution rates in the range below  $G^=$  there is a stable limit cycle, associated with the Hopf bifurcation and the homoclinic point-to-point bifurcation, both emanating from the  $BT^-$ -point. A detailed discussion of this long-term behaviour is given by Baer et al. (2006).

## 5.5 Model for nutrient-prey-predator system

We formulate two models for the stressed nutrient-prey-predator system, where toxicant uptake by prey and predator is from water (bio-concentration), and for the predator from water and food (bio-accumulation). The state variables are again the nutrient density  $N(t)$ , the biomass density of the prey  $R(t)$ , the total toxicant content  $c_T(t)$ , and additionally the biomass density of the predator  $P(t)$ , which consumes the prey population. In one scenario the toxicant affects both populations, while in the other scenario it affects the prey population, but is has no effect on the predator population.

The motivation to study these two cases comes from the experimental results obtained by Liebig et al. (2008) . In a closed system, single species tests with the mixotrophic phytoflagellate *Cryptomonas* sp. and the planktonic ciliate *Urotricha furcata* and multi-species, where ciliates consume flagellates, were performed. Two toxicants were used: methyl parathion (an insecticide) and prometryn (a herbicide). Methyl parathion had an effect on both the flagellate and the ciliate population at the low  $mg/L$  concentration range, independently whether the organisms were exposed in the single-species or multi-species test system (first scenario). Prometryn had an effect on the flagellate population in the single- and multi-species test at the low  $mg/L$  concentration range. Ciliates were affected only in the single-species test at the  $mg/L$  range (second scenario).

### 5.5.1 Stressed system: both populations affected by toxicant

The maintenance processes of the prey and predator populations are both affected by the toxicant. The maintenance rate now depends on the toxicant concentration  $c_P$  as

$$m_P(c_P) = m_{P0} \left( 1 + \frac{(c_P - c_{PM0})_+}{c_{PM}} \right), \quad (5.13)$$

while for the prey population it is given by Eqn. (5.10a).

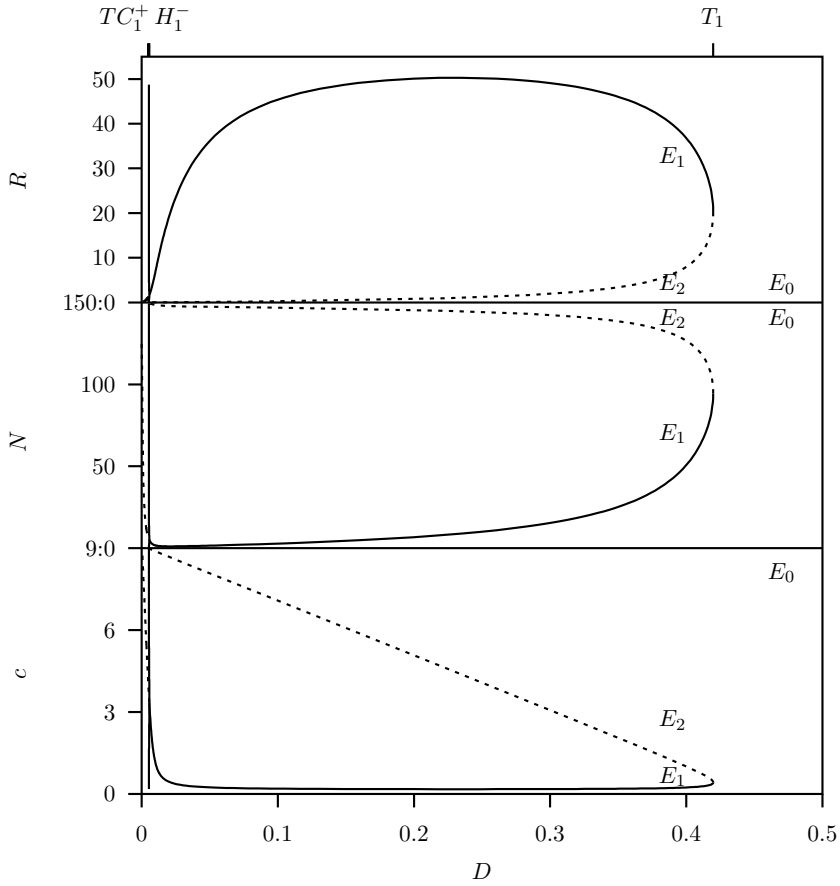


Figure 5.5: A one-parameter bifurcation diagram with dilution rate  $D$  as free parameter, for the population with toxicity stress in the chemostat system Eqn. (5.9), where  $N_r = 150$  and  $c_r = 9$ . Solid curves are stable equilibria  $E_0$ ,  $E_1$  or extreme values of the limit cycles, and dashed curves are unstable equilibria  $E_2$ . Point  $T_1$  is the tangent bifurcation,  $TC_1^+$  the subcritical transcritical bifurcation and  $H_1^-$  the supercritical Hopf bifurcation. A detail for small dilution rates  $D$  is given in Fig.5.6.

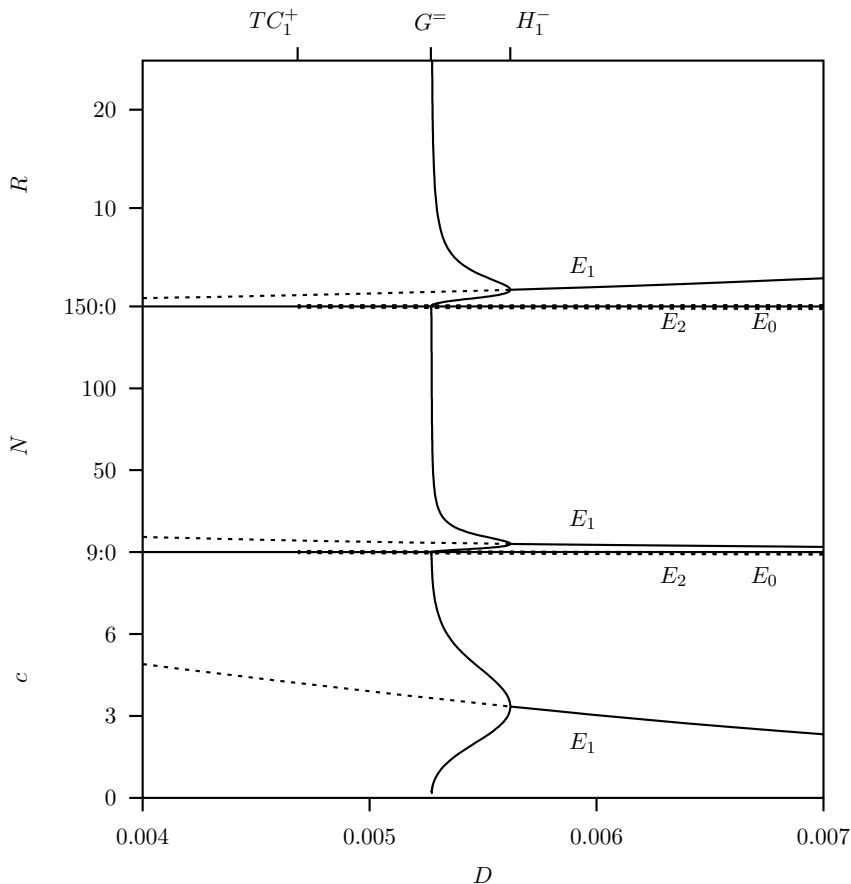


Figure 5.6: Detail of Fig. 5.5 in the neighbourhood of the global bifurcation  $G^=$ , a homoclinic cycle. Solid curves are stable equilibria  $E_0$ ,  $E_1$  or extreme values of limit cycles, and dashed curves are unstable equilibria  $E_1$ ,  $E_2$  (thick dashed curve is  $E_2$  which is hardly distinguishable from  $E_0$ ). A stable limit cycle originates at the Hopf bifurcation  $H_1^-$ , of which the extrema are shown. The period of this limit cycle goes to infinity when  $D$  approached  $G^=$ . Below  $G^=$  the trivial equilibrium  $E_0$  is the unique global attractor.

The governing set of equations with state variables  $N$ ,  $R$ ,  $P$  and  $c_P$ , becomes

$$\frac{dN}{dt} = (N_r - N)D - I_{NR} \frac{N}{k_{NR} + N} R, \quad (5.14a)$$

$$\frac{dR}{dt} = \left( \mu_{NR} \frac{N}{k_{NR} + N} - (D + m_R(c_R)) \right) R - I_{RP} \frac{R}{k_{RP} + R} P, \quad (5.14b)$$

$$\frac{dP}{dt} = \left( \mu_{RP} \frac{R}{k_{RP} + R} - (D + m_P(c_P)) \right) P, \quad (5.14c)$$

$$\begin{aligned} \frac{dc_P P}{dt} &= (k_{Pu} c_W - k_{Pa} c_P) P + c_R \mu_{RP} \frac{R}{k_{RP} + R} P \\ &\quad - \left( (I_{RP} - \mu_{RP}) \frac{R}{k_{RP} + R} + D + m_P(c_P) \right) c_P P, \end{aligned} \quad (5.14d)$$

$$\frac{dc_T}{dt} = (c_r - c_T)D, \quad (5.14e)$$

where  $c_T = c_W + c_R R + c_P P$ . The ODE (5.14c) describes the dynamics of the predator population. Compared to the model for the nutrient-prey system (5.9) there is an additional predation term in (5.14b). Uptake of toxicants by the predator is from the water and the consumed contaminated prey.

Equation (5.14d) has three terms. The first term on the right-hand side models the exchange rate of the toxicant from the water. The second term models the uptake rate from the contaminated prey. It is the product of the internal toxicant concentration in the prey  $c_R$  and the assimilated prey per unit of time. Here we assume that the efficiency for intake of the toxicant equals the assimilation efficiency for the prey ( $\mu_{RP}/I_{NR}$ ), and that no biotransformation takes place. The third term is the internal toxicant concentration in the predator  $c_P$  times the removal rate of the toxicant, absorbed in the washed-out predator biomass, plus the egested rate of assimilation and by-products into the system.

The one-compartment model for the internal toxicant concentration for the prey and predator populations are, using (5.3) and (5.14)

$$\begin{aligned} \frac{dc_R}{dt} &= k_{Ru} c_W - k_{Ra} c_R \\ &\quad - \left( (I_{NR} - \mu_{NR}) \frac{N}{k_{NR} + N} + D + m_R(c_R) + I_{RP} \frac{P}{k_{RP} + R} + \frac{1}{R} \frac{dR}{dt} \right) c_R, \end{aligned} \quad (5.15a)$$

$$\begin{aligned} \frac{dc_P}{dt} = & k_{Pu}c_W - k_{Pa}c_P + \mu_{RP} \frac{R}{k_{RP} + R} c_R - \\ & \left( (I_{RP} - \mu_{RP}) \frac{R}{k_{RP} + R} + D + m_P(c_P) + \frac{1}{P} \frac{dP}{dt} \right) c_P . \end{aligned} \quad (5.15b)$$

At equilibrium and using (5.14b) and (5.14c) we get

$$\begin{aligned} k_{Ru}c_W^* = & k_{Ra}c_R^* + \\ & \left( (I_{NR} - \mu_{NR}) \frac{N^*}{k_{NR} + N^*} + D + m_R(c_R) + I_{RP} \frac{P^*}{k_{RP} + R^*} \right) c_R^* , \end{aligned} \quad (5.16a)$$

$$\begin{aligned} k_{Pu}c_W^* + \mu_{RP} \frac{R^*}{k_{RP} + R^*} c_R^* = & k_{Pa}c_P^* + \\ & \left( (I_{RP} - \mu_{RP}) \frac{R^*}{k_{RP} + R^*} + D + m_P(c_P) \right) c_P^* . \end{aligned} \quad (5.16b)$$

We define the following BioConcentration and BioMagnification Factors for both populations

$$BCF_{WR} = \frac{k_{Ru}}{k_{Ra} + I_{NR}N^*/(k_{NR} + N^*)} , \quad (5.17a)$$

$$BCF_{WP} = \frac{k_{Pu}}{k_{Pa} + I_{RP}R^*/(k_{RP} + R^*)} , \quad (5.17b)$$

$$BMF_{RP} = \frac{\mu_{RP}R^*/(k_{RP} + R^*)}{k_{Pa} + I_{RP}R^*/(k_{RP} + R^*)} . \quad (5.17c)$$

The bio-accumulation factor for the predator population is defined as

$$BAF_{WP} = BCF_{WP} + BCF_{WR}BMF_{RP} , \quad (5.18)$$

which yields

$$c_R^* = BCF_{WR}c_W^* , \quad (5.19a)$$

$$c_P^* = BAF_{WP}c_W^* , \quad (5.19b)$$

where we also assume for the predator population that the uptake and elimination rates are much faster than other conversion rates. Then the bio-concentration factor (BCF), as given in (5.8),  $BCF_{WR} = k_{Ru}/k_{Ra}$ , and a similar expression for the predator,  $BCF_{WP} = k_{Pu}/k_{Pa}$ , apply. The total toxicant concentration  $c_T(t)$  becomes

$$c_T(t) = c_W(t)(1 + BCF_{WR}R(t) + BCF_{WP}P(t)). \quad (5.20)$$

In summary, the food chain model where both prey and predator populations are affected by the toxicant consists of Eqn. (5.14a), (5.14b), (5.14c), and (5.20).

### 5.5.2 Stressed system: predator unaffected by toxicant

We assume now that the toxicant in the prey population is not taken up by the predator population. Then the mass-balance equations read

$$\frac{dN}{dt} = (N_r - N)D - I_{NR} \frac{N}{k_{NR} + N} R, \quad (5.21a)$$

$$\frac{dR}{dt} = \left( \mu_{NR} \frac{N}{k_{NR} + N} - (D + m_R(c_R)) \right) R - I_{RP} \frac{R}{k_{RP} + R} P, \quad (5.21b)$$

$$\frac{dP}{dt} = \left( \mu_{RP} \frac{R}{k_{RP} + R} - (D + m_{P0}) \right) P, \quad (5.21c)$$

$$\frac{dc_T}{dt} = (c_r - c_T)D, \quad (5.21d)$$

where  $c_T = c_W(1 + BCF_{WR}R)$ .

This set of ODEs reduces to the unstressed system, without the ODE that describes the dynamics of the total toxicant concentration in the system  $c_T$ , and the toxicant does not affect the maintenance rate of the prey population,  $m_R(c_R) = m_{R0}$ . Note that for the predator population we have always  $m_P(c_P) = m_{P0}$ , which is a species-specific parameter. When  $P = 0$ , it reduces to the stressed nutrient-prey system (5.9).

## 5.6 Analysis of nutrient-prey-predator system

First we analyse the unstressed predator-prey system. Thereafter, the two stressed systems are analysed. In the first system both prey (via water) and predator (via water and food) populations are affected by the toxicant (herbicide or pesticide). In the second system, the toxicant (bactericide or algicide) only affects the prey population.

### 5.6.1 Unstressed nutrient-prey-predator system

For the unstressed nutrient-prey-predator system, Eqn. (5.21) but without toxicant and substituting  $m_R(c_R) = m_{R0}$ , the bifurcation diagram has been

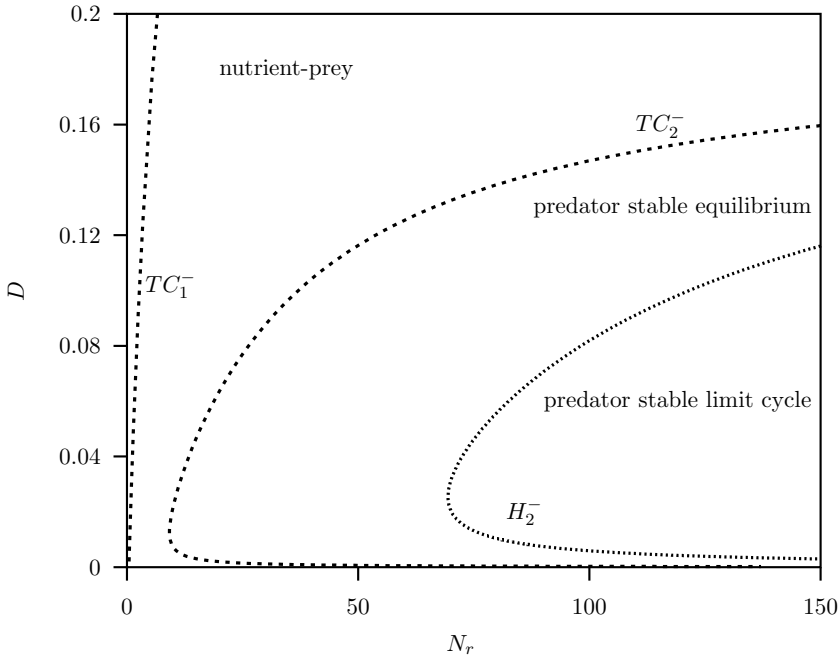


Figure 5.7: A two-parameter bifurcation diagram with nutrient inflow  $N_r$  and dilution rate  $D$  as free parameters for the unstressed ecosystem Eqn. (5.21a, 5.21b, 5.21c), with  $m_R(c_R) = m_{R0}$ , consisting of nutrient, prey and predator. Dashed curves  $TC_1^-$  and  $TC_2^-$  are transcritical bifurcations, the dotted curve is the Hopf bifurcation curve  $H_2^-$ .

discussed in an earlier paper by Kooi et al. (1998) as part of a food chain with a top-predator. Figure 5.7 shows the bifurcation diagram with  $N_r$  and  $D$  as bifurcation parameters.

The transcritical bifurcation curve  $TC_1^-$  is the same curve shown in diagram Fig. 5.1 for the nutrient-prey system. Bifurcation curves of the nutrient-prey system are also relevant for the nutrient-prey-predator ecosystem, when after a predator population is inoculated in the nutrient-prey system, the predator is not able to invade. On the other hand, when the predator can invade, the nutrient-prey bifurcation curve loses its relevance. This is the case for the region on the right-hand side of the transcritical bifurcation curve  $TC_2^-$  in Fig. 5.7, where the subscript 2 indicates that the predator population is involved. At this curve both the biomass and the growth rate of the predator population equal zero, that is, both factors on the right-hand side of (5.21c) are zero, resulting in a zero eigenvalue of the Jacobian matrix evaluated at that equilibrium point. Fig. 5.8 shows the one-parameter diagram where the

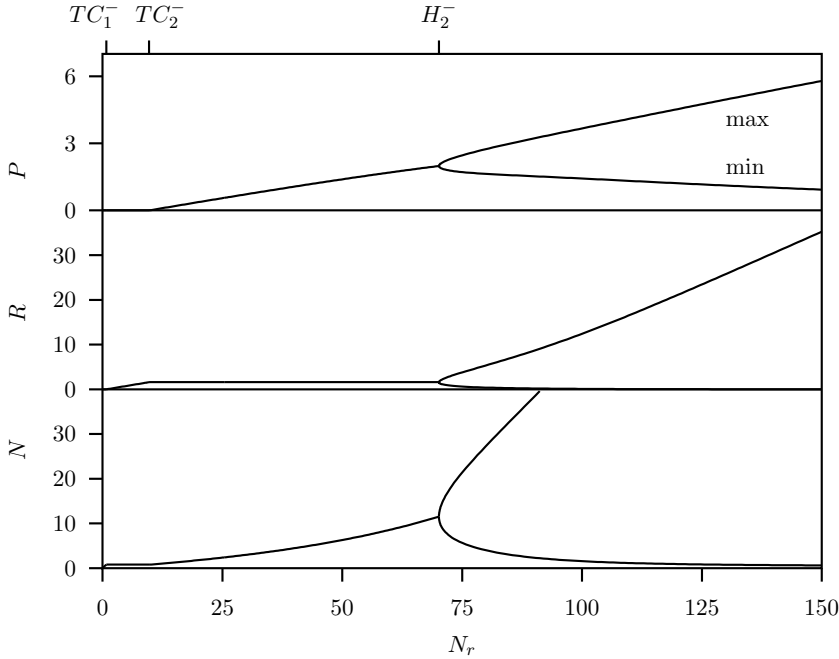


Figure 5.8: A one-parameter bifurcation diagram with nutrient level  $N_r$  as free parameter, for a predator-prey system Eqn. (5.21a, 5.21b, 5.21c), consisting of nutrient, prey and predator. The stationary biomasses of the nutrient  $N$ , prey  $R$  and predator  $P$  are depicted as a function of the nutrient level  $N_r$ . For high nutrient levels above  $H_2^-$  the system oscillates with extrema indicated. Only stable stationary states are shown.

equilibrium values for the four state variables  $c_W$ ,  $N$ ,  $C$  and  $P$  are depicted with bifurcation parameter  $N_r$ , where  $D$  is kept constant at  $D = 0.02$ . For low values of the nutrient input  $N_r$  only the nutrient is present. Between the points  $TC_1^-$  and  $TC_2^-$  the prey population can persist,  $R^* > 0$ , but the predator cannot invade and its equilibrium biomass is zero. For  $N_r$ -values above  $TC_2^-$  an interior equilibrium with  $P^* > 0$  exists.

When  $N_r$  is increased further (an event often referred to as nutrient enrichment) the system becomes unstable at a Hopf bifurcation, denoted by  $H_2^-$ . Above the  $H_2^-$  there is a stable limit cycle, and in Fig. 5.8 the extreme values during such a cycle are depicted. The phenomenon that under nutrient enrichment a system starts to oscillate is known as the “paradox of enrichment” (Rosenzweig, 1971, Chapters 3 and see Voorn and Stiefs et al. 2008).

### 5.6.2 Stressed system: both populations affected by toxicant

In this subsection the toxicant affects the prey and predator maintenance processes. The dynamics are described by ODE system (5.14). The calculated two-parameter bifurcation diagram, with  $N_r$  and  $D$  as bifurcation parameters, is shown in Fig. 5.9, where  $c_r = 9$ . Compared to the unstressed system, the transcritical bifurcation  $TC_1^-$  of Fig. 5.1 is replaced by the tangent bifurcation curve  $T$  and those bifurcation curves emanating from the Bogdanov-Takens bifurcation point  $BT^+$ , for instance the Hopf bifurcation curve  $H_1^-$  (Fig. 5.4 for the stressed nutrient-prey system).

The pattern of the bifurcations associated with stationary solutions with positive predator biomasses resembles that of the unstressed system Fig. 5.7. With enrichment, first the predator can invade, and for higher nutrient input concentrations above the Hopf bifurcation curve  $H_2^-$  the system oscillates.

### 5.6.3 Stressed system: predator unaffected by toxicant

The Hopf bifurcation curve  $H_2^-$  now intersects the Hopf bifurcation curve  $H_1^-$  and the transcritical bifurcation  $TC_{e,2}^-$  in a codim-two point  $M$ . The extra subscript  $e$  indicates that it is related to an equilibrium. On the right-hand side of the Hopf bifurcation curve  $H_2^-$  the nutrient-prey-predator system oscillates. Below curve  $H_1^-$  also the nutrient-prey system oscillates. Therefore invasion of the predator occurs via a limit cycle, which is stable considered as part of a nutrient-prey system, but unstable when a predator can invade. The point where the invadability changes is a transcritical bifurcation, but now for a cycle, and is indicated in Fig. 5.10 by  $TC_{c,2}^-$ . Below this curve the nutrient-prey-predator system cannot exist, and in that region of the diagram the curves and points shown in Fig. 5.4 for the nutrient-prey system apply.

In Fig. 5.10, a global bifurcation curve  $G^\neq$ , continued with HOMCONT (Doedel et al., 1997, one can also use the techniques developed in Van Voorn et al., 2007, forms the boundary of the region where the system possesses a stable limit cycle. This is a so-called heteroclinic cycle, which connects two saddle equilibria where the predator is absent.

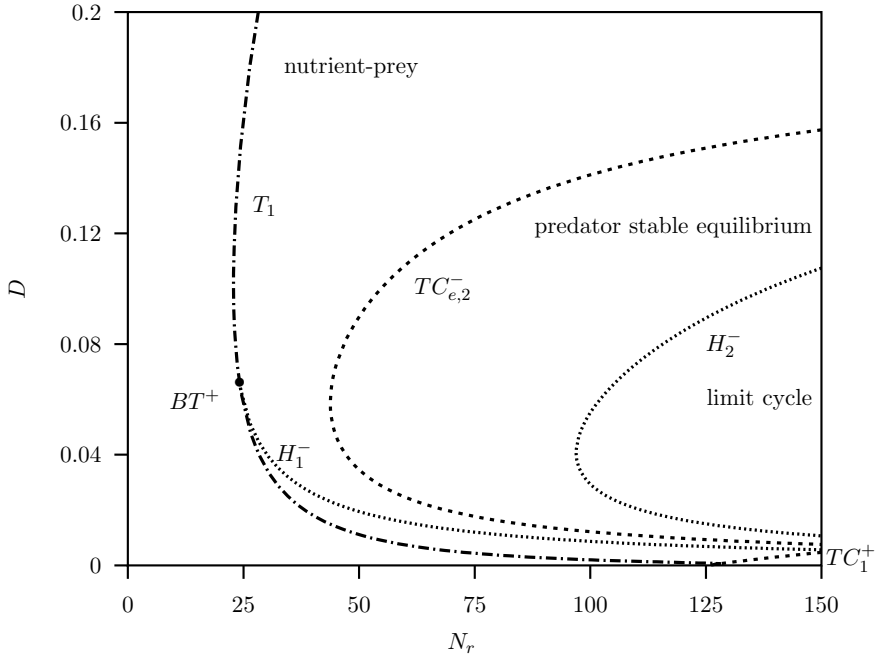


Figure 5.9: A two-parameter bifurcation diagram with nutrient inflow  $N_r$  and dilution rate  $D$  as free parameters for the ecosystem Eqn. (5.14) with  $c_r = 9$  where both population suffer from the toxicant. Dashed lines are transcritical bifurcations and dotted-dashed lines the tangent bifurcation. The predator is involved in bifurcation points on the following curves: Hopf bifurcation curve  $H_2^-$  and transcritical bifurcation  $TC_{e,2}^-$ . The bifurcation diagram for the nutrient-prey system are shown in Fig. 5.4.

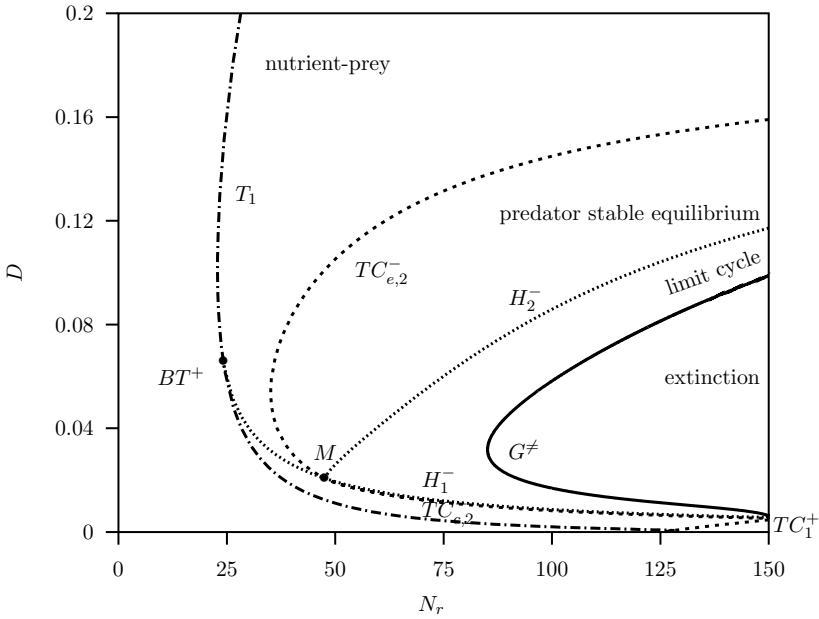


Figure 5.10: A two-parameter bifurcation diagram with nutrient inflow  $N_r$  and dilution rate  $D$  as free parameters for the stressed ecosystem Eqn. (5.21), with  $c_r = 9$ , where only the prey population suffers from the toxicant. Dashed curves are transcritical bifurcations, and dotted-dashed curves are the tangent bifurcations. The predator is involved in bifurcation points on the following curves: Hopf bifurcation curve  $H_2^-$ , transcritical bifurcation for invasion via equilibrium  $TC_{e,2}^-$ , transcritical bifurcation for invasion via a limit cycle  $TC_{c,2}^-$ , and heteroclinic connection: global bifurcation curve  $G^\neq$ . The bifurcation diagram for the nutrient-prey system is shown in Fig. 5.4.

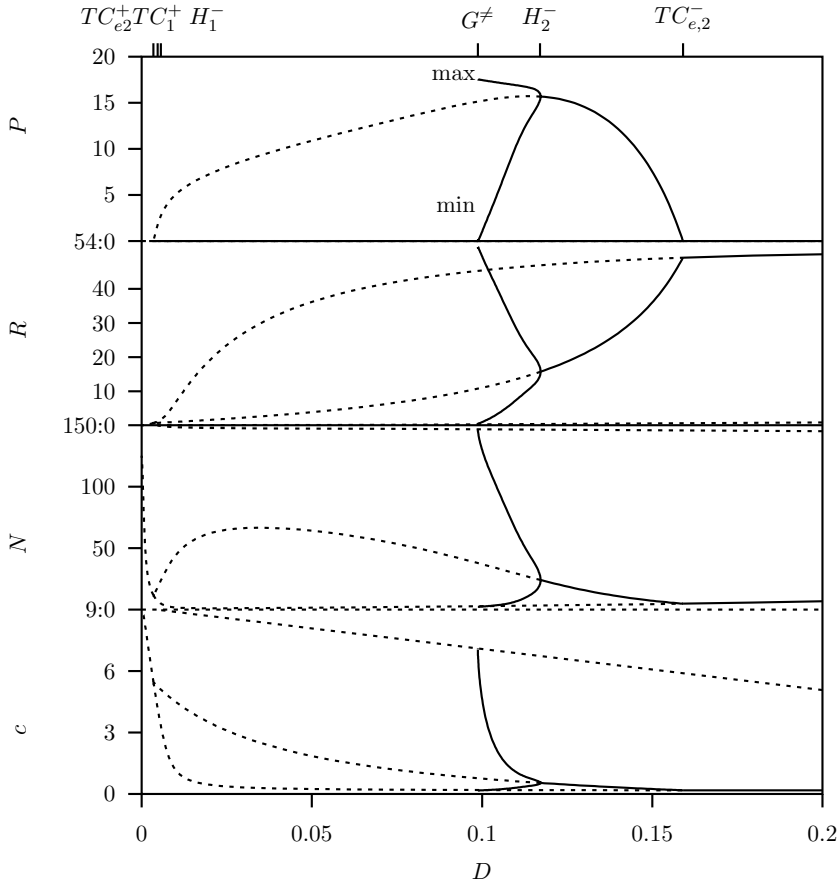


Figure 5.11: A one-parameter bifurcation diagram with dilution rate  $D$  as free parameter for the stressed system Eqn. (5.21), where  $N_r = 150$  and  $c_r = 9$ , and where only the prey population is affected by the toxicant. Solid curves are stable equilibria or extreme values of stable limit cycles, and dashed curves unstable ones. Observe that  $TC_{e2}^+$  is irrelevant, since just below  $H_1^-$  the prey population goes extinct and no invasion of the predator is possible.

With  $N_r = 150$ , and starting from the Hopf bifurcation curve  $H_2^-$  and lowering the dilution rate  $D$ , the period of the stable limit cycle goes to infinity, and the cycle tends to the heteroclinic cycle. This is illustrated in Fig. 5.11. At this global bifurcation point the limit cycle breaks. As a result, it becomes possible that a stable nutrient-prey system becomes unstable by invasion of a predator, and eventually the predator goes extinct together with the prey population, that is, the complete ecosystem is destroyed. This is a form of over over-exploitation as discussed in Van Voorn et al. (2007). This holds for the parameter range between  $G^\neq$  and the transcritical bifurcation  $TC_{2,e}^-$ .

## 5.7 Discussion

For an overview of different mathematical model formulations of unstressed ecosystems and their analyses, the reader may consult Kooi (2003), and references therein. In this Chapter we focus on the sublethal effects of a toxicant on the ecosystem structure and functioning. Important effects are extinction of species, invadability by a species from a neighbourhood, the different population abundances, and the long-term dynamics (stable equilibrium, oscillatory or chaotic behaviour).

We can compare the BCF, BMF and BAF formulations (5.17) and (5.18) with formulations in the literature, used for bio-accumulation in food web studies (Thomann, 1989; Gobas, 1993; Campfens and MacKay, 1997; Traas et al., 2004b). In most classical approaches, ecological and toxicological stressors are treated separately. The expression for the  $BCF_{WR}$  in 5.17a resembles Eq. (11) in Thomann (1989) or Eq. (4) in Gobas (1993), the derived expression for  $BAF_{WP}$  in (5.18) resembles Eq. (15a) in Thomann (1989), and the expression for the equilibrium of the internal toxicant concentrations  $c_R^*$  and  $c_P^*$  in (5.19) resembles Eq. (8) in Traas et al. (2004b) in the case of a food chain. For the analysis of food webs, besides the BMF and BAF-values, the dietary preference matrix, that fixes the feeding relationships, is needed to model the transport of the toxicant in the contaminated food through the system (see for instance Campfens and MacKay, 1997; Traas et al., 2004b).

The formulation of the exchange of the toxicant with the water is equivalent to that in Hallam et al. (1993), Barber et al. (1988), and Barber (2003). In these papers, a mass-balance equation for the total amount of toxicant in an individual fish is the starting point. The model for the conductance of the toxicant through the exposed membrane is based on physiological processes, employing fluid flow characteristic parameters as well as diffusion. For the application of that model for *Daphnia* only diffusion through the carapace is assumed. Later, in Barber et al. (1988), the concentration-based equation is derived, whereby a dilution term appears naturally. Here the starting point

is diffusion, and toxicant concentrations are the state variables to model this process, including the dilution term (the last term of Eq. (5.3)). Then the mass-balanced equation is derived in (5.4).

The formulation of the dilution-by-growth term in Eq. (5.3) resembles that of Eq. (24) in Clark et al. (1990), but observe that their formulation is for the individual fish, while here it is formulated on the population level. In our unstructured population model formulation we cannot distinguish between the individuals, only entities of the total number of individuals that compose the population numbers. Individuals that propagate by binary fission never reach equilibrium, instead they grow and divide at a threshold size into two newborns, but the population can reach an equilibrium. On the other hand, the population parameters entail individual characteristics. In our formulation the population-based removal term from the system,  $D$ , appears together with the individual-based egestion rates for the products formed in physiological processes. In deriving Eqn. (5.17) from (5.15) the equilibrium conditions are used, and this results in an ingestion term in the denominator of the expressions besides the elimination rate. When food is abundant the functional response is almost 1, and bio-factors become independent of the equilibrium abundances. This often applies for single-species experiments, but generally not for populations. In many papers, for instance Gobas (1993), dilution by growth is taken as a positive constant. In Clark et al. (1990), the notion pseudo-steady state is introduced to describe that no true equilibrium can be achieved while growth occurs.

For the simple ecosystems studied here, we found that toxicants can have large consequences for the long-term dynamical behaviour. When the maintenance process is the mode of action, the per capita maintenance rate coefficient is not constant anymore, but increases with the internal toxicant concentration. The concentration of the internal toxicant depends on the toxicant concentration in the water, which is in turn linked to the dynamics of the biomass of the population, since removal of the toxicant is partly via the biomass that leaves the system with the dilution. This is a feedback mechanism, due to which the repertoire of the dynamical behaviour of the stressed system is much more diverse, for instance, bi-stability, cyclic behaviour and global bifurcations can occur.

Bi-stability of the nutrient-prey system can be the result of various mechanisms, for instance the Allee-effect (Allee, 1931; Van Voorn et al. 2007). When a population is subject to an Allee effect, an predator invasion can lead to the collapse of the complete system under certain circumstances (see for instance Bazykin, 1998; Kent et al., 2003). Here we show that mathematically a heteroclinic bifurcation is associated with this biological phenomenon. Similarly, we found this phenomenon for the stressed nutrient-prey-predator system when the toxicant affects only the population. When the toxicant affects both pop-

ulations, toxic effects on the predator retard its growth, and this prevents over-exploitation of the nutrient-prey system. As a result, the size of the region in the diagram 5.9 with a stable equilibrium is much larger than when only the prey population is affected (see Fig. 5.10).

When the toxicant is a reactant in a chemical reaction within the organism, the compartment model for the uptake and elimination of the toxicant has to be adapted. As an example we mention the possibility that the kinetics of the reaction itself have to be taken into account, or the concentration of an enzyme that controls the reaction has to be considered. This can occur in biotransformation, the processes by which chemicals are altered by the organism, usually with the intention to increase their elimination rate. As a side-effect bio-activation, the production of reactive metabolites that are more toxic than the parent compound, can occur.

In Hallam et al. (1993), the step from individual to a *Daphnia* population is formulated and analysed. For the age- and size-structured population the so-called McKendrick-Von Foerster model is used. This is a partial differential equation (PDE) where food is kept constant. The use of this model for populations at different trophic levels of an ecosystem is problematic due to trophic interactions. Also in Hallam et al. (1993), an alternative relationship and its effect on the growth rate is formulated, which is a hyperbolic function of the internal concentration with three parameters. For a *Daphnia* population these parameters are based on quantitative structure-activity relationships (QSAR's). Similar to (5.10b), there is a threshold concentration for the onset of effects, which is calculated from the *no-observed-effect-level* (NOEC). The remaining two parameters are computed from the  $EC_{50}$  for growth, and the mortality concentration  $LC_{50}$ . Thus, these parameter values are based on descriptive parameters. For estimation of the DEBtox toxic effect parameters (5.10), time series of experimental data for aquatic bioassays are used, where a range of toxic stress levels and food availability levels are applied. The toxic effect parameters are estimated simultaneously with the ecological model parameters.

Comparison of the calculated bifurcation diagrams for different toxic stress levels yield important information about the toxic effects on the functioning of the ecosystem. Consider the unstressed system, whereby the environmental conditions are given (fixed  $N_r$  and  $D$ ). Let us assume that this point in the parameter space belongs to a region where the equilibrium is stable and positive. Increasing the input toxicant level  $c_r$  will change the position of the bifurcation curves, including the transcritical and tangent bifurcation curves. When at a certain level of stress a transcritical or tangent bifurcation curve passes through the point we are evaluating, we have the level of stress at which at least one population goes extinct. Such a threshold value is called the population extinct threshold (PET; Hallam et al., 1993). In the case of a Hopf bifurcation passing through the given point the ecosystem be-

comes unstable, leading to oscillatory behaviour. Increasing the stress further generally leads to oscillations of enlarged amplitude, increasing the chance of demographic or stochastic extinction occurring. Hence, the crossing of a bifurcation marks a structural change of the ecosystem. Also, given a toxic stress level  $c_r$ , it is possible to identify environmental conditions  $N_r$  and  $D$ , under which the toxic stress has no effect on the population abundances. This threshold concentration value is determined by the requirement that it equals the NEC value related to a sensitive processes within the organism that form a population. (The modelled mode of action should potentially be able to affect the population.)

The above-mentioned results can be applied in a risk assessment analysis. Here all parameters, which describe the physiological processes, and the environmental status are determined. In a natural setting these parameters are in general stochastic or random, either naturally or anthropogenically induced (Lindenschmidt, 2006; Lindenschmidt et al., 2007). In the case that the input level of the toxicant is uncertain, this translates directly into uncertainties for the occurrence of the structural changes and functioning of the ecosystem.

For the sake of simplicity, we have studied a short food chain, representing only the lowest trophic levels of an aquatic ecosystem, where several important ecological and toxicological factors (e.g., nutrient recycling, varying environmental conditions, spatial mixing, assimilation efficiency of contaminants) have been left out. Furthermore, the population model is unstructured for the prey and the predator, simplifying the step from individual to population. The hypothesis, that the toxicant uptake and elimination predominate the exchange between the organisms and the water, is not valid for species of higher trophic levels, but only for those on the lowest trophic level here. Admitting that the analysed food chain is only a simplified representation of a real ecosystem, we point out that our analysis is a first step in understanding more realistic and more complex aquatic systems, such as rivers and estuaries. Also, although simplified models will not provide precise forecasts for real ecosystems, due to uncertainties in the parameter values and environmental fluctuations, as mentioned above, the simulation of extreme situations (bifurcation analysis) can lead to understanding a range of potential outcomes. Furthermore, the model can easily be extended in many directions, while the analysis method remains applicable.

## 5.8 Conclusions

Despite high toxicant concentrations in the influent, the ambient toxicant concentrations in the system needs not to be high. This is the result of the following. The supplied toxicant-free (uncontaminated) nutrient is converted in the

system into biomass. This new biomass absorbs the toxicant. Together with the removed individuals it is removed from the system. Because the ambient toxicant concentration is generally low, the concentration of dissolved toxicant in the effluent is low, even when the concentration is high in the influent. Observe that there is no contradiction with mass conservation, because there is also transport of the toxicant via the contaminated organisms. When these organisms are removed from the effluent, it is purified.

There three different levels of modelling detail for the toxicant dynamics in the organisms can be distinguished:

- (1) The exchange of the toxicant between the water and the organisms is assumed to be much faster than the biological processes.
- (2) The ecosystem model is in equilibrium and the equilibrium abundances are used in the bio-accumulation model (BCF, BMF and BAF).
- (3) The dynamics of the internal toxicant is modelled explicitly and forms and integrated model together with the ecosystem model.

In large regions of the bifurcation diagrams (great variety of environmental conditions) the ecosystem does not possess a stable equilibrium, but instead there is a stable limit cycle. Hence, the equilibrium assumption generally made in models for bio-accumulation in aquatic ecosystems (Thomann and Connolly, 1984; Thomann and Mueller, 1987; Thomann, 1989; Clark et al., 1990; Gobas, 1993; Campfens and MacKay, 1997; Traas et al., 2004b) are valid only under restricted environmental circumstances.

The feedback mechanism between toxicant uptake/consumption and removal from the system is an important phenomenon, possibly leading to bi-stability in the nutrient-prey-contaminant system and collapse of the nutrient-prey-predator-contaminant system. Hence, the effects of both types of stressors, the biotic (competition, predation) and the abiotic (chemical or physical), on the ecosystem have to be analysed together.

*Acknowledgements* - The authors would like to thank Bert van Hattum, Pim Leonards and Markus Liebig for valuable discussions and comments on a draft version of the manuscript. The research of BWK and DB has been funded by the European commission, FP6 Contract No. 511237-GOCE. The research of GAKvV has been funded by the Computational Life Sciences program of the Netherlands Organisation for Scientific Research (NWO), project number 635.100.013.

# References

- [1] W. Allee, *Animal aggregations, a study in general sociology*, The University of Chicago Press, Chicago, Ill, 1931.
- [2] S. M. Baer, B. W. Kooi, Y. A. Kuznetsov, H. R. Thieme, Multiparametric bifurcation analysis of a basic two stage population model, *SIAM Journal on Applied Mathematics*, 66:1339–1365, 2006.
- [3] M. C. Barber, A review and comparison of models for predicting dynamic chemical bioconcentration in fish, *Environmental Toxicology and Chemistry*, 22:1963–1992, 2003.
- [4] M. C. Barber, L. A. Suárez, R. R. Lassiter, Modeling bioconcentration of nonpolar organic pollutants by fish, *Environmental Toxicology and Chemistry*, 7:545–558, 1988.
- [5] A. D. Bazykin, *Nonlinear dynamics of interacting populations*, World Scientific, Singapore, 1998.
- [6] P. Calow, R. M. Silby, V. Forbes, Risk assessment on the basis of simplified life-history scenarios, *Environmental Toxicology and Chemistry*, 16:1983–1989, 1997.
- [7] J. Campfens, D. MacKay, Fugacity-based model of PCB bioaccumulation in complex aquatic food webs, *Environmental Science Technology*, 31:577–583, 1997.
- [8] K. E. Clark, F. A. P. C. Gobas, D. Mackay, Model of organic chemical uptake and clearance by fish from food and water, *Environmental Science Technology*, 24:1203–1213, 1990.
- [9] A. Cunningham, R. M. Nisbet, Transients and oscillations in continuous culture, in: M. J. Bazin (Ed.), *Mathematics in Microbiology*, Academic Press, London, 1983, pp. 77–103.
- [10] D. L. DeAngelis, *Dynamics of Nutrient Cycling and Food Webs*, Population and Community Biology Series, Chapman & Hall, 1992.

- [11] E. J. Doedel, A. R. Champneys, T. F. Fairgrieve, Y. A. Kuznetsov, B. Sandstede, X. Wang, *AUTO97: Continuation and bifurcation software for ordinary differential equations*, Tech. rep., Concordia University, Montreal, Canada, 1997.
- [12] F. A. P. C. Gobas, A model for predicting the bioaccumulation of hydrophobic organic chemicals in aquatic food-webs: application to Lake Ontario, *Ecological Modelling*, 69:1–17, 1993.
- [13] J. Guckenheimer, P. Holmes, *Nonlinear Oscillations, Dynamical Systems and Bifurcations of Vector Fields*, 2nd Edition, Vol. 42 of Applied Mathematical Sciences, Springer-Verlag, New York, 1985.
- [14] T. G. Hallam, G. A. Canziani, R. R. Lassiter, Sublethal narcosis and population persistence: a modelling study on growth effects, *Environmental Toxicology and Chemistry*, 12:947–954, 1993.
- [15] C. S. Holling, Some characteristics of simple types of predation and parasitism, *Canadian Entomologist*, 91:385–398, 1959.
- [16] A. Kent, C. P. Doncaster, T. Sluckin, Consequences for predators of rescue and allee effects on prey, *Ecological Modelling*, 162:233–245, 2003.
- [17] A. Koelmans, A. van der Heijde, L. Knijff, R. Aalderink, Integrated modelling of eutrophication and organic contaminant fate & effects in aquatic ecosystems. A review, *Water Research*, 35:3517–3536, 2001.
- [18] B. W. Kooi, Numerical bifurcation analysis of ecosystems in a spatially homogeneous environment, *Acta Biotheoretica*, 51:189–222, 2003.
- [19] B. W. Kooi, M. P. Boer, S. A. L. M. Kooijman, Consequences of population models on the dynamics of food chains, *Mathematical Biosciences*, 153:99–124, 1998.
- [20] B. W. Kooi, J. C. Poggiale, P. Auger, S. A. L. M. Kooijman, Aggregation methods in food chains with nutrient recycling, *Ecological Modelling*, 157:69–86, 2002.
- [21] S. A. L. M. Kooijman, J. J. M. Bedaux, *The analysis of aquatic toxicity data*, VU University Press, Amsterdam, 1996.
- [22] S. A. L. M. Kooijman, *Dynamic Energy and Mass Budgets in Biological Systems*, Cambridge University Press, Cambridge, 2000.
- [23] Yu. A. Kuznetsov, *Elements of Applied Bifurcation Theory*, 3rd Edition, Vol. 112 of Applied Mathematical Sciences, Springer-Verlag, New York, 2004.

- [24] Yu. A. Kuznetsov, V. V. Levitin, *CONTENT: Integrated environment for the analysis of dynamical systems*, Centrum voor Wiskunde en Informatica (CWI), Kruislaan 413, 1098 SJ Amsterdam, The Netherlands, 1st Edition, 1997.
- [25] M. Liebig, G. Schmidt, D. Bontje, B. W. Kooi, G. Streck, W. Traunspurger, and T. Knacker. Direct and indirect effects of pollutants on algae and algivorous ciliates in an aquatic indoor microcosm. *Aquatic Toxicology*, 88(2):102–110, 2008.
- [26] K.-E. Lindenschmidt, The effect of complexity on parameter sensitivity and model uncertainty in river water quality modelling, *Ecological Modelling*, 190:72–86, 2006.
- [27] K.-E. Lindenschmidt, K. Fleischbein, M. Baborowski, Structural uncertainty in a river water quality modelling system, *Ecological Modelling*, 204:289–300, 2007.
- [28] S. J. Pirt, The maintenance energy of bacteria in growing cultures, *Proceedings of the Royal Society London (B)*, 163:224–231, 1965.
- [29] M. L. Rosenzweig, Paradox of enrichment: destabilization of exploitation ecosystems in ecological time, *Science*, 171:385–387, 1971.
- [30] H. L. Smith, P. Waltman, *The Theory of the Chemostat*, Cambridge University Press, Cambridge, 1994.
- [31] R. V. Thomann, Bioaccumulation model of organic distribution in aquatic food chains, *Environmental Science Technology*, 23:699–707, 1989.
- [32] R. V. Thomann, J. Connolly, Model of PCB in the Lake Michigan Lake Trout food chain, *Environmental Science Technology*, 18:65–71, 1984.
- [33] R. V. Thomann, J. A. Mueller, *Principles of surface water quality modeling and control*, Harper & Row, Publ., New York, 1987.
- [34] T. P. Traas, J. H. Janse, P. J. van den Brink, T. C. M. Brock, T. Aldenberg, A freshwater food web model for the combined effects of nutrients and insecticide stress and subsequent recovery, *Environmental Toxicology and Chemistry*, 23:521–529, 2004a.
- [35] T. P. Traas, A. P. van Wezel, J. L. M. Hermens, M. Zorn, A. G. M. van Hattum, C. J. van Leeuwen, Environmental quality criteria for organic chemicals predicted from internal effect concentrations and a food web model, *Environmental Toxicology and Chemistry*, 23:2518–2527, 2004b.

- 
- [36] G. A. K. van Voorn, L. Hemerik, M. P. Boer, B. W. Kooi, Heteroclinic orbits indicate overexploitation in predator-prey systems with a strong Allee effect, *Mathematical Biosciences*, 209:451–469, 2007.
- [37] G. A. K. van Voorn, D. Stiefs, T. Gross, B. W. Kooi, U. Feudel and S. A. L. M. Kooijman, Stabilization due to predator interference: Comparison of different analysis approaches, *Mathematical Biosciences and Engineering*, 5:567–583, 2008.
- [38] S. Wiggins, *Introduction to Applied Nonlinear Dynamical Systems and Chaos*, Vol. 2 of Texts in Applied Mathematics, Springer-Verlag, New York, 1990.



## Chapter 6

# Sublethal toxicological effects in a generic aquatic ecosystem

D. Bontje, B.W. Kooi, B. van Hattum and P. Leonards

The dynamical behaviour of an aquatic ecosystem stressed by limiting nutrients and exposure to a toxicant is analysed. The ecosystem is a defined stretch of river consisting of nutrients, pelagic and a benthic communities, detritus pools in the water body and sediment. We analyse the downstream river reach adjacent to the point of emission of a toxicant. The toxicant is taken up by the organisms and can affect their biological functioning (assimilation, growth, maintenance, reproduction, survival). This induces effects on the functioning of the populations formed by the organisms, and further on the biological status of the ecosystem, that is their structure e.g. extinction or invasion of species, and functioning. Sublethal, long-term effects due to biological and toxicological stressors will be studied together. The dynamic behaviour of all biotic and abiotic components as well as the toxicant concentration therein is mathematically described by a set of ordinary differential equations (ODEs). The long-term dynamic behaviour of this system is analysed using bifurcation theory. A reference state is defined and our aim is to quantify the effects of toxicological (toxic exposure), ecological (feeding, predation, competition) and environmental stressors (nutrient supply, dilution rate). To that end we calculate the boundaries of the range of parameters that quantify these stressors where the long-term dynamics (equilibrium, oscillatory or chaotic behaviour) is qualitatively the same. In this way we obtain levels of toxicant loading where the abundances of all populations are the same as in the reference case, the no-effect region (NER). We will also calculate the minimum toxic exposure levels that do not lead to a change in the composition of the ecosystem and

therefore its structure with respect to the reference unexposed situation, but where population abundances and internal toxicant concentrations may have been changed quantitatively. The model predicts that due to indirect effects even low sublethal toxic exposure can lead to catastrophic changes in the functioning and structure of the ecosystem, and that the long-term sensitivities of oligotrophic and eutrophic systems to toxic stress differ.

## 6.1 Introduction

The importance of the extrapolation of the results of toxicity bioassays to potential effects on the ecosystem has already been recognized for many years [17]. Since then detailed models for aquatic ecosystems have been formulated and analysed to perform such an extrapolation by running simulations whereby the time evolution of the populations and toxicant was calculated under different levels of toxicant loading. Although this gives insight on the short-term effects, it is cumbersome to draw clear conclusions for long-term sublethal effects on the ecosystem functioning and structure.

Here we combine process based mathematical modelling and bifurcation analysis to assess the effects of both toxicological and ecological stress on the functioning and structure of a generic aquatic ecosystem. We consider a stretch of a river with two abiotic compartments, the water and sediment bodies, and a food web consisting of interacting pelagic and benthic organisms. This system is stressed by a limiting nutrient and by exposure to a toxicant. We analyse the downstream river stretch adjacent to the point of emission of a single toxicant.

With the theoretical assessment of effects the following steps can be distinguished:

1. *Ecological theory* Biological functioning of the ecosystem. For an ecosystem we need:
  - a model for the individual life-cycle,
  - a model of each population using models of individual behaviour,
  - a model for the ecosystem, using models of populations including their mutual interactions and interaction with the physical environment.
2. *Environmental chemical theory* Fate of the toxicant. Environmental chemistry and geochemistry related models to describe emission, transport and distribution. Further a model for the exposure of the individuals by bioaccumulation and biomagnification.

3. *Toxicological theory* Effect module on individual level. The relationship between the internal concentration of the toxicant and the behaviour of an individual.
4. *Ecotoxicological theory* Lethal and sublethal effects on the ecosystem level. The relationship between the toxicological effects on the individual level and their effects on population level and finally ecosystem behaviour.
5. *Risk assessment* Using the exposure and effect models to assess ecosystem consequences (e.g. probability of extinction of one or more populations).

A Predicted Environmental Concentration (PEC) is obtained by the evaluation of the emissions, distribution and bioavailability of the toxicant in the different compartments (water, sediment) or from actually measured environmental concentrations of the toxicant (points 1 and 2). Various toxicokinetic models describe the accumulation of toxicants from the environment (water, sediment) into organic material (detritus, biota) [38, 15, 35, 50, 21, 5, 49]. The models proposed in these papers are based on the *ecosystem equilibrium assumption* and the *equilibrium partitioning principle* [15] for the chemicals. This allows for a strictly independent modelling of the ecological and toxicological processes, whereby classical models from both disciplines are used: ecosystem models and toxicokinetic models. The calculation of the distribution of the toxicant over the biotic and abiotic components (BAFs and BSAFs) requires for each population the lipid fraction and body weight, and for the ecosystem the dietary preference matrix (see for instance [51]).

In lower-tier ecosystem risk assessment, effect parameters are converted to generic Predicted No-Effect Concentrations (PNECs) (points 3 and 4). In a controlled environment tests are performed with single species each representing one of the three trophic levels of a pelagic food chain consisting of: primary producers (algae species), primary consumers (daphnids) and a secondary consumer (fish). These standard tests on lethality and effects yield  $LC_{50}$  and no-observed effect concentration (NOEC) values depending on the toxicant and the organism. The use of population or even ecosystem testing is relatively scarce in ecotoxicological risk assessment. In practice, mostly a reductionist approach is taken. Then these results are extrapolated to predict effects on the higher levels: populations and ecosystems. So-called assessment or application factors account for the uncertainties in extrapolation from laboratory to field, from single laboratory species to multiple field species, or from acute (short-term) to chronic (long-term) exposures, or from mortality as endpoint to reproduction or growth as endpoint. Factors used for the risk assessment required by national and international regulatory bodies, are sum-

marized in [19, 20]. No ecotoxicological hazard or risk is anticipated when the ratio  $PEC/PNEC$  is less than one.

Here we study a higher-tier process-based and generic aquatic model whereby no equilibrium assumptions are made *a priori*. Toxicants affect the individual behaviour while consequences on the ecosystem level are required. Therefore in the integrated, holistic modelling approach, the model has to combine descriptions of chemical (fate of the toxicant including uptake by the individuals) and biological processes (feeding, predation, competition). Models of these processes at the individual level are lifted up to the population level and finally ecosystem level whereby besides interactions between populations also interactions with the environment are taken into account.

The populations that make-up the ecosystem are modelled by a simplified version of the DEB model [32]. By assuming that all individuals within one population are identical we can use a simple unstructured population model formulation, which allows us to model the population dynamics with ordinary differential equations (ODEs). Physiological processes such as assimilation, maintenance, growth, reproduction and mortality are possibly the targets of the toxic effects depending on the mode of actions of the toxicant. A one-compartment model formulation is used for the uptake and elimination of the toxicant by the organisms, the detritus pools and also the detritus. As in the critical body residue approach [40], toxicants consistently produce a defined toxic effect depending on a dynamic internal concentration, regardless of the actual environmental variables. The toxicological effects on the population level are described by the DEBtox [33] methodology. In this concentration–effect model below a toxicant concentration threshold, called the NEC (No Effect Concentration), there is no effect. Above this threshold the intensity of the effect is a linear dependence on the internal toxicant concentration.

We also introduce a model aggregation technique whereby the full dynamic ecological model component is retained but the bioaccumulation model is reduced to the classical model based on the *ecosystem equilibrium assumption* and the *equilibrium partitioning principle*. Instead of uptake and elimination rates, easily available literature bioconcentration factor values can be used.

We focus on sublethal effects of a single toxicant on the ecosystem in a river. The toxicant enters the river from upstream emissions, tributaries and run-off and is taken to be homogeneously distributed at the modelled river section. The spatial structure of the species distribution is taken to be uniform in both the water and/or the sediment. The system consists of the following biota: pelagic phytoplankton (producer: algae), pelagic zooplankton (consumer: ciliates, *Daphnia*), benthic invertebrate (consumer: small animals, such as clams, worms, and crustaceans) that live on or in the bottom substrate of a water body and the sediment and one territorial fish (predator). We take nutrient recycling into account. Important environmental parameters are the

nutrient inflow concentration (e.g. phosphate, ammonium, total nitrogen) and the dilution rate. The latter being the amount of water per unit of time flowing in divided by the overlying water volume of the stretch of river.

The river ecosystem is modelled using a chemostat environment. The influent containing nutrients and toxicants, enters the well-mixed system with constant volume. From this system all pelagic biota, detritus and the dissolved toxicant in the overlying water leave the system with the effluent. Pore water is not modelled explicitly. No transport of the sediment is assumed by the outlet or influent. The ecological status of the ecosystem, or qualitative composition, is expressed as its species composition which can be effected. For example extinction of a species can occur due to starvation or a predatory species can invade from upstream or downstream. Also, the quantity of each species presence, namely the species abundance of the various populations can change due to toxic stress. The long-term dynamics of the ecosystem, including stable equilibrium, oscillatory or chaotic behaviour, can also be affected.

The dynamic behaviour of each population is described by one ODE which describes the time-dependent population biomass. Via trophic interactions and/or competition each ODE is coupled to other ODEs forming an ODE-system.

Trophic interactions are feeding relationships among ecosystem populations and are described with functional responses in which the ingestion rate per predator as a function of the abundance of the resources (prey or nutrients) saturates as the resource density increases. Competition is here considered as an indirect interaction between two or more populations, all feeding on a common prey population. In food chains, populations may consume a single prey population by direct trophic interactions. On the other hand in food webs, populations may feed also on multiple resources and/or are consumed by multiple predators whereby also indirect interactions occur. In line with related studies [2, 12, 13] we model a food web with detritus and nutrient recycling. The models that describe the various interactions between the populations are based on those derived in [31, 32, 42].

Less complex ecosystem models, which were also build with coupled ODEs, were studied in [4, 29, 30, 37]. Here we show that this approach of coupled ODEs also works for studying more realistic ecosystems.

In a number of recent papers [7, 8, 9, 10, 45] similar models are proposed and analysed with simulations. In [44], analysing multiple scenarios, many simulations in time were performed yielding information on short-term and long-term toxic effects. With respect to the long-term effects, simulations are rather cumbersome and analysing the output to find effects on the ecosystem functioning and structure is difficult and time-consuming.

We perform a *bifurcation analysis*. A bifurcation analysis focuses on the dependency of the long-term dynamic behaviour on model parameters. This technique gives directly under which conditions, for instance toxic exposure

and/or nutrient enrichment, the structure of the ecosystem changes because of invasion or extension of a population. The model parameters that are changed during an analysis are called control parameters. In a bifurcation analysis first steady states for the complete systems are calculated followed by a stability analysis. Then parameters are varied whereby in each point this procedure is repeated. Parameter values where the stability of the equilibrium changes are called bifurcation points. These points mark regions where the long-term dynamics change and in an ecotoxicological setting that means the functioning or structure of the ecosystem has changed.

For an introduction to bifurcation analysis we refer the reader to [22, 53, 34], and for applications in ecology to [3, 28]. Recently this technique has also been used in [24, 23, 1, 54] for applications in ecotoxicology. The aim is to show the power of bifurcation analysis techniques for the study of long-term sublethal effects on aquatic ecosystems to ecotoxicologist.

The integrated approach taken in this paper permits the study of indirect effects of the toxicant. Varying the toxicant load gives insight into the effects whereby all indirect effects are taken into account. We call the dilution rate and nutrient supply concentration *control parameters* since in our model formulation they determine the environment of the unexposed ecosystem. For the exposed system the toxicant inflow concentration is also a control parameter. We can use these control parameters as bifurcation parameters and this implies that the biological and toxicological components of the ecosystem are unchanged while only environmental components are altered.

We present analysis results for the case where the growth of the producer is affected by a herbicide. Measured parameter values from [37, 4] are used for the parameterization of the toxicant-effect module. The ecological parameter values are obtained from [45, 8, 10, 7, 9].

Analysis results are presented in diagrams which can not be further summarized into a generally valid single risk characterization ratio value, such as PEC/PNEC. Instead, for an ecosystem *No Effect Regions* (NERS) are predicted. At these levels of toxicant loading, the abundances of all populations are the same as in the control case. We will also calculate the boundary of the *Resistance Regions* (RRs). In these regimes toxic exposure levels do not lead to a change in the composition or dynamic behaviour of the ecosystem and therefore its structure, but population abundances and internal toxicant concentrations may change quantitatively.

## 6.2 Formulation of the ecological model

The amount of overlying water,  $V_W$ , in the river stretch/system and the amount of sediment,  $V_S$ , are assumed to be constant. The densities of the

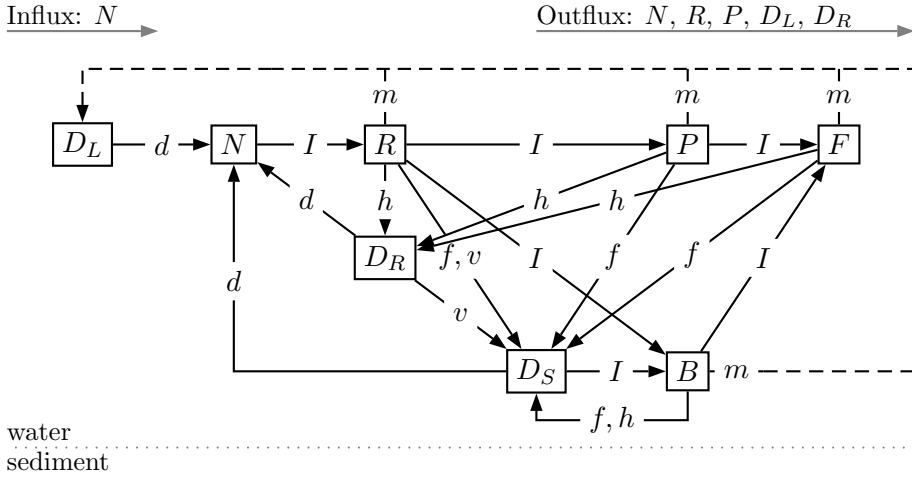


Figure 6.1: The positions of the biota in the generic aquatic ecosystem. The environmental parameters are the dilution rate  $D$  and the density of the nutrient in the incoming water  $N_r$ . Solid arrows denote trophic interactions between organisms and their respective food-source(s) and consequent ingestion ( $I$ ), faeces ( $f$ ), death ( $h$ ) or sinking ( $v$ ). Dashed lines denote the conversion of biomass into smaller compounds as a result of maintenance processes ( $m$ ). Bacterial degradation fluxes are annotated by ( $d$ ). For the explanation of the state variables, see Tables 6.1 and 6.2.

nutrient and pelagic biota are expressed in units of mass per volume of the overlying water and the density of the biota in the sediment is expressed in units of mass per volume of sediment. It is advantageous to introduce as a measure for the sediment mass  $S = V_S/V_W$ . The dilution rate  $D$  is defined as the amount of water flowing through the system per unit of time divided by the volume overlying water  $V_W$ .

In Fig. 6.1 the composition of the aquatic ecosystem is shown. The state variables of the system are listed in Table 6.1. The ecosystem consists of the water body, sediment bulk and the nutrient with density,  $N(t)$ , primary producer population with biomass density denoted by  $R(t)$ , the benthic consumer with biomass density denoted by  $B(t)$ , the pelagic consumer with biomass density denoted by  $P(t)$ , the predator with biomass density,  $F(t)$  and three variants of detritus with densities denoted by  $D_L(t)$  (labile),  $D_R(t)$  (refractory) and  $D_S(t)$  (sediment) which is as degradable as  $D_R$ . The pelagic system is a subset of the aquatic system without the benthic consumer  $B(t)$ . The benthic system is a subset of the aquatic system without the pelagic consumer  $P(t)$ . All abiotic and biotic densities are expressed, using  $S$ , with respect to the volume of the water body. This is possible since both the volume of the water body and the sediment body are kept constant.

Table 6.1: State variables for the ecological model:  $l$  length of environment [dm] ( $l^3$  is dimension of the volume of the overlying water in the system),  $m$  mass of organism [ $\text{mg}_{\text{dw}}$ ] or mass of nutrient (inorganic nitrogen) density [ $\text{mg N}$ ] and  $t$  time [d].

Variable	Description	Dimension	Unit
$N$	Nutrient mass density	$\text{m l}^{-3}$	$\text{kg N/L}$
$R$	Producer biomass density	$\text{m l}^{-3}$	$\text{kg}_{\text{dw}}/\text{L}$
$B$	Benthic consumer biomass density	$\text{m l}^{-3}$	$\text{kg}_{\text{dw}}/\text{dm}^3$
$P$	Consumer biomass density	$\text{m l}^{-3}$	$\text{kg}_{\text{dw}}/\text{L}$
$F$	Predator biomass density	$\text{m l}^{-3}$	$\text{kg}_{\text{dw}}/\text{L}$
$D_L$	Labile detritus biomass density	$\text{m l}^{-3}$	$\text{kg}_{\text{dw}}/\text{L}$
$D_R$	Refractory detritus biomass density	$\text{m l}^{-3}$	$\text{kg}_{\text{dw}}/\text{L}$
$D_S$	Detritus biomass density in sediment	$\text{m l}^{-3}$	$\text{kg}_{\text{dw}}/\text{dm}^3$
$S$	sediment-water volume ratio	$\text{l}^{-3} \text{l}^{-3}$	$\text{dm}^3/\text{L}$

Table 6.2: List of ecological parameters for the ecological model  $p \in \{R, B, P\}$  and  $q \in \{R, B, P, F, D_S\}$ :  $l$  length of environment [dm] ( $l^3$  is dimension of the volume of the overlying water in the system),  $m$  mass of organism in the water [ $\text{mg}_{\text{dw}}$ ] or mass of nutrient density [ $\text{mg N}$ ] and  $t$  time [d].

Parameter	Description	Dimension	Unit
$D$	Dilution rate	$\text{t}^{-1}$	$\text{d}^{-1}$
$N_r$	Nutrient mass density	$\text{m l}^{-3}$	$\text{kg N/L}$
$\alpha_R$	Labile detritus decay rate	$\text{t}^{-1}$	$\text{d}^{-1}$
$\alpha_L$	Refractory detritus decay rate	$\text{t}^{-1}$	$\text{d}^{-1}$
$v_s$	Sedimentation rate	$\text{t}^{-1}$	$\text{d}^{-1}$
$\mu_{pq}$	max. growth rate	$\text{t}^{-1}$	$\text{d}^{-1}$
$I_{pq}$	max. ingestion rate	$\text{t}^{-1}$	$\text{d}^{-1}$
$k_{NR}$	saturation constant	$\text{m l}^{-3}$	$\text{kg N/L}$
$k_{pq}$	saturation constant	$\text{m l}^{-3}$	$\text{kg}_{\text{dw}}/\text{L}$
$k_{Bq}$	saturation constant	$\text{m l}^{-3}$	$\text{kg}_{\text{dw}}/\text{dm}^3$
$m_q$	maintenance rate coefficient	$\text{t}^{-1}$	$\text{d}^{-1}$
$h_q$	hazard rate	$\text{t}^{-1}$	$\text{d}^{-1}$

We assume that the growth rate of the primary producer is limited by the nutrient and is not light-limited. The functional responses, being the intake rate of a consumer as a function of the food density, that model the predator-prey trophic interactions for each population read:

$$\begin{aligned} f_{NR} &= \frac{N}{k_{NR} + N} \quad , \quad f_{RP} = \frac{R}{k_{RP} + R} \quad , \\ f_{RB} &= \frac{R/k_{RB}}{1 + R/k_{RB} + SD_S/k_{D_S B}} \quad , \quad f_{D_S B} = \frac{SD_S/k_{D_S B}}{1 + R/k_{RB} + SD_S/k_{D_S B}} \quad , \\ f_{PF} &= \frac{P/k_{PF}}{1 + SB/k_{BF} + P/k_{PF}} \quad , \quad f_{BF} = \frac{SB/k_{BF}}{1 + SB/k_{BF} + P/k_{PF}} \quad . \end{aligned} \quad (6.1)$$

When a population consumes a single other population, for instance the consumer population  $P$  feeds on the producer population  $R$  the Holling type II functional response is used to model the trophic interaction where  $k_{pq}$  is the saturation constant,  $p, q \in \{R, B, P, F\}$ . The predator  $F$  feeds on the pelagic consumer  $P$ , part of the pelagic subsystem, and also on the benthic consumer  $B$ , part of the benthic subsystem. These food sources are both non-essential and this trophic interaction is modelled as substitutable food sources (see [42]). In a similar way the benthic consumers  $B$  consume the sediment detritus  $D_S$  and the producer population  $R$  in the overlying water. Note that in these cases the factor  $S$  converts all benthic densities into densities based on the volume of the overlying water.

The mass-balance equations for the aquatic ecosystem read:

$$\frac{dN}{dt} = D(N_r - N) + \rho_{NO}(-I_{NR}f_{NR}R + \alpha_L D_L + \alpha_R D_R + S\alpha_R D_S) \quad (6.2a)$$

$$\frac{dR}{dt} = R(\mu_{NR}f_{NR} - m_R - h_R - D - v_s) - SI_{RB}f_{RB}B - I_{RP}f_{RP}P \quad (6.2b)$$

$$\frac{dB}{dt} = B(\mu_{D_S B}f_{D_S B} + \mu_{RB}f_{RB} - m_B - h_B) - S^{-1}I_{BF}f_{BF}F \quad (6.2c)$$

$$\frac{dP}{dt} = P(\mu_{RP}f_{RP} - m_P - h_P - D) - I_{PF}f_{PF}F \quad (6.2d)$$

$$\frac{dF}{dt} = F(\mu_{BF}f_{BF} + \mu_{PF}f_{PF} - m_F - h_F) \quad (6.2e)$$

$$\frac{dD_L}{dt} = m_R R + m_P P + m_F F + S m_B B - D D_L - \alpha_L D_L \quad (6.2f)$$

$$\frac{dD_R}{dt} = h_R R + h_P P + h_F F - D_R(D + \alpha_R + v_s) \quad (6.2g)$$

$$\begin{aligned} \frac{dD_S}{dt} &= (h_B - \mu_{D_S B}f_{D_S B} + (I_{RB} - \mu_{RB})f_{RB})B - \alpha_R D_S \\ &\quad + S^{-1}((I_{NR} - \mu_{NR})f_{NR}R + (I_{RP} - \mu_{RP})f_{RP}P \\ &\quad + ((I_{PF} - \mu_{PF})f_{PF} + (I_{BF} - \mu_{BF})f_{BF})F + v_s D_R + v_s R) \end{aligned} \quad (6.2h)$$

The left-hand side of each equation is the temporal change of the biomass density of the nutrient  $N$ , populations  $R, B, P, F$  and the detritus pools  $D_R, D_L$  and  $D_S$ . The first term on the right-hand side of Eqn. (6.2a) models the in-flowing ( $N_r D$ ) and out-flowing nutrient ( $ND$ ) into and from the system. The second term is the ingestion rate of the producer population  $R$ . The latter three terms are due to recycling of the labile and refractory detritus. The detritivores involved with the nutrient mineralisation are not modelled explicitly but are assumed to be abundant. Therefore the mineralisation rates are linear in the densities of the two detritus pools  $D_R$  and  $D_L$  in the overlying water and one  $D_S$  in the sediment.

For the populations  $p \in \{R, B, P, F\}$  the terms on the right-hand side are those for growth, maintenance with rate  $m_p p$  and natural mortality  $h_p p$  and finally, except for the predator, the consumption rate. The term  $Dp$ ,  $p \in \{R, B, P\}$  models removal from the system by the outflow. Observe that the fish population is territorial and stays in the system.

The right-hand side of the equations describing the detritus pools  $D_R, D_L$ , model the input of the excreted maintenance products and dead material, respectively, from the pelagic populations. Those terms for the sediment detritus pool  $D_S$  model input of assimilation products of all populations together with sinking material.

The producer population  $R$  sinks to the bottom of the water body into the sediment with rate  $v_s$ . The equations for the detritus pools model their formation by the assimilation, maintenance and mortality processes. For the sediment detritus we assume that the refractory detritus in the overlying water sinks to the bottom of the water body and settles on the sediment with rate  $v_s$ , similar to the producer population.

We assume that all parameter values are known in the reference state of the ecosystem which represents the unexposed (control) situation. Later some of these parameters will depend on the internal concentration when the system becomes exposed by a toxicant.

### 6.3 Analysis of the unexposed aquatic system

This section presents the model predictions for the unexposed aquatic ecosystem (see Fig. 6.1). In Table 6.3 the reference values of the ecosystem parameters are given. These values are based on [43, 8, 10]. In these articles the trophic interactions are modelled by the preferences matrix formulations given in [41] while here they are modelled using the formulations with a mechanistic underpinning given in [42]. Therefore the half-saturation constants from [8, 10] are multiplied by a factor two. This is because with the derivation of the preferences model the values of the half-saturation constants for prey can

differ and are only equal in the restricting equilibrium situations [41]. Following [8, 10] the preference of the predator for each prey population, the pelagic and benthic consumers, equals 0.5. To ensure co-existence of the pelagic and benthic consumer the fish ( $F$ ) has a lower consumption rate and growth rate on  $P$  (0.6) than on  $B$  (0.85). Values are after [8, 10].

The results are presented in so-called bifurcation or operating diagrams, that show how the long-term dynamics of the systems depend on changes in one or two parameters. The parameter space shown in these diagrams is divided in regions (and also regimes of the parameters) where the ecosystem possesses a specific long-term temporal behaviour, for instance: stable/unstable equilibrium, stable/unstable limit cycles or chaotic behaviour. Boundaries between these regions indicate changed ecosystem functionality but also the species composition can be changed. The boundaries of the regions are formed by bifurcation curves. Most parameter value combinations can have multiple solutions for the ecosystem's species composition, unless stated otherwise, we assume that if invasion can occur that it will occur.

In this paper we show the effects of a toxicant mainly on the ecosystem in equilibrium. The equilibrium values of the state variables are calculated by solving the set of non-linear equations formed by the right-hand side of the system (6.2) equal to zero. The stability of this equilibrium is found by calculating the eigenvalues of the Jacobian matrix evaluated at that point. These eigenvalues are often complex numbers. When all eigenvalues have negative real parts the equilibrium is stable, otherwise it is unstable. Different types of combinations of the complex eigenvalues signify different system behaviour.

A zero real part of the eigenvalues fixes the location of the bifurcation curves when more than one parameter is varied in a continuation process. Similar but more complex procedures are available to calculate bifurcation points of limit cycles. These curves are calculated using free available computer packages such as AUTO [16] and MATCONT [14] running under MATLAB [39].

The most important bifurcations are listed in Table 6.4 and are not further explained here. The interested reader is referred to [28, 30] and Chapter 5 for a mathematical description and the ecological significance of these curves.

### 6.3.1 Results for the unexposed aquatic system

Figure 6.2 shows for an oligotrophic aquatic system the stationary nutrient and biomass values as a function of the nutrient density in the inflow  $N_r$  where the dilution rate equals  $D = 0.02$ . With enrichment, i.e. increasing  $N_r$ , first the producer invades above  $TC_1$  giving a stable R-system. For a small range of  $N_r$  between  $T_{2,b}$  and  $TC_{2,b}$ , the presence or absence of the benthic consumer depends on the initial conditions of the system.

At the Hopf bifurcation  $H_{2,b}^-$  this RB-system starts to oscillate. For en-

Table 6.3: Reference parameter set for the generic ecosystem model after [8, 10, 43]. Other parameter values are:  $\alpha_R = 0.1 \text{ d}^{-1}$ ,  $\alpha_L = 0.01 \text{ d}^{-1}$ ,  $v_s = 0.015 \text{ d}^{-1}$ .

Par.	Dimension	Values						
		$p =$ $q =$	$N$ $R$	$R$ $B$	$D_S$ $B$	$R$ $P$	$B$ $F$	$P$ $F$
$\mu_{pq}$	$\text{t}^{-1}$		3.705	1.03	1.03	1.03	0.85	0.6
$I_{pq}$	$\text{t}^{-1}$		3.8	1.8	1.8	1.8	1.3	1.3
$k_{pq}$	$\text{ml}^{-3}$		0.05	1.0	1.0	1.0	$2 \times 5.0$	$2 \times 5.0$
$m_q$	$\text{t}^{-1}$		0.02	0.035	0.035	0.035	0.053	0.053
$h_q$	$\text{t}^{-1}$		0.06	0.04	0.04	0.04	0.0001	0.0001

Table 6.4: List of bifurcations, codim-one curves and codim-two points (for two-parameter bifurcation diagrams).  $i = 0$ : N-system with no population present,  $i = 1$ : R-system: producer,  $i = 2, b$ : RB-system: producer and benthic consumer,  $i = 3, b$ : RBF-system: producer, benthic and fish,  $i = 3, p$ : RPF-system: producer, pelagic and fish,  $i = 4$ : RBPF-system: producer, benthic and pelagic consumer and fish predator.

Symbol	Description of bifurcation
$TC_i$	Transcritical bifurcation: invasion by prey or predator
$H_i^\pm$	Hopf bifurcation: $-$ supercritical, $+$ subcritical; internal equilibrium of ecosystem becomes unstable, origin of stable (supercritical) or unstable (subcritical) limit cycle
$T_i$	Tangent bifurcation: collision of an unstable and stable equilibrium or limit cycle
$TR_4$	Torus bifurcation: only for RBPF-system; boundary of complex dynamics
$I_i$	NER-isocline: below this curve is the no-effect region

richment above  $TC_{3,b}$  the predator invades and the resulting RBF-system still oscillates. When increasing  $N_r$  further, the RBF-system is stabilized and a stable equilibrium exists.

Figure 6.3 gives the diagram also for higher enrichment levels, including eutrophic conditions. The complete RBPF-system only exists in an intermediate range of  $N_r$  between the transcritical bifurcations  $TC_{4,b}$  and  $TC_{4,p}$ . At lower nutrient loads the benthic RBF-system occurs (see Figure 6.2) while for high nutrient the pelagic RPF-system exist. When the nutrient input is high the pelagic system starts to oscillate above the Hopf bifurcation  $H_{3,p}^-$ . This effect is related to the paradox of enrichment [47, 46]. For higher  $N_r$  values the oscillations become more and more severe and the system likely goes extinct when the biomass density of one population becomes extremely low during these heavy oscillations.

These results are taken as the reference states of the unexposed aquatic ecosystem which are later compared with the results of the exposed system to assess the effects of the toxicant on its functioning and structure.

## 6.4 Formulation of the ecotoxicological model

In this section we formulate the model for the exposure and fate of the toxicant and the concentration-effect model.

### 6.4.1 Model for the fate of the toxicant

In the next section the transport, distribution and exposure of the toxicant is modelled. A mass-balance formulation for the toxicant amounts in the different abiotic (water and sediment) and biotic (populations) compartments is used.

The toxicant concentration in the water is denoted by  $c_W(t)$ , sediment  $c_S(t)$ , and the internal toxicant concentrations by respectively  $c_R(t)$ ,  $c_B(t)$ ,  $c_P(t)$  and  $c_F(t)$ . Toxicant concentrations in detritus are denoted by  $c_{D_R}(t)$  and  $c_{D_S}(t)$  and because we assume that the amount of toxicant adsorbed to  $D_L$  is negligible we have  $c_{D_L} = 0$ . In the final formulation  $c_S(t)$  is normalized to the sediments organic carbon denoted by  $c_{S,oc}(t)$ .

In [30] a mass-balance model formulation is given for the transport, distribution and exposure of toxicant for the pelagic food chain. Here we derive the equation for toxicant concentration  $c_P(t)$  in the pelagic consumer  $P$  of which the dynamics is described by Eqn. (6.2d). The equation for the total amount

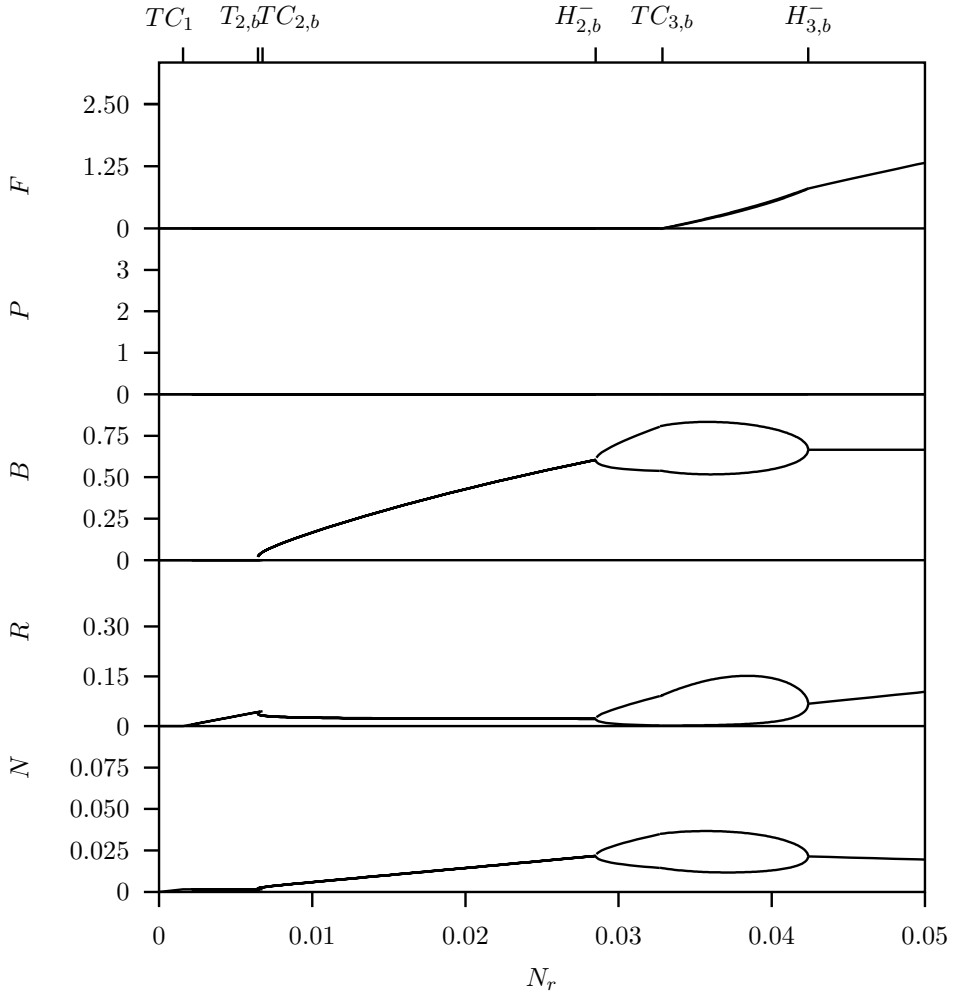


Figure 6.2: A one-parameter bifurcation diagram for the generic ecosystem at low nutrient input levels (oligotrophic). The bifurcation points are described in Table 6.4. There were cyclic behaviour (oscillations) occurs in the system each value of  $N_r$  has for each species an associated minimum and a maximum biomass density. See Figure 6.3 for biomass densities when  $N_r$  is higher than 0.05.

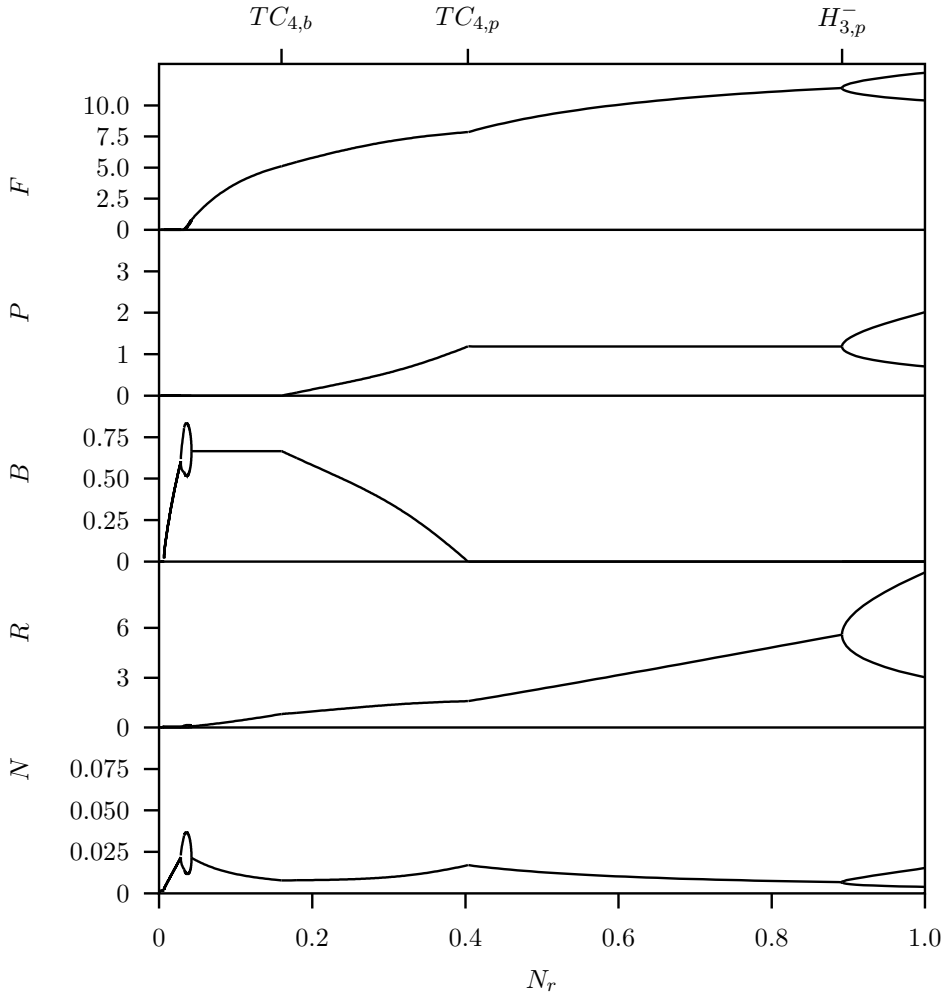


Figure 6.3: A one-parameter bifurcation diagram for the generic ecosystem in a chemostat with dilution rate  $D = 0.02$ . The stationary biomass of the nutrient  $N$ , producer  $C$ , benthic consumer  $B$ , pelagic consumer  $P$  and predator  $F$  is depicted as a function of the nutrient level  $N_r$ .  $N_r$  ranges from oligotrophic, via mesotrophic to eutrophic. For high nutrient levels ( $N_r > 0.87$ ) the pelagic system oscillates with extrema indicated. The bifurcation points are described in Table 6.4. Under oligotrophic conditions the benthic subsystem,  $P = 0$ , oscillates, see Figure 6.2.

of toxicant in the pelagic consumer  $c_P P$  reads

$$\begin{aligned} \frac{dc_P P}{dt} = & (k_{P_u} c_W - k_{P_a} c_P) P + c_R I_{RP} f_{RP} P - c_P I_{PF} f_{PF} F \\ & - c_P P ((I_{RP} - \mu_{RP}) f_{RP} + m_P + h_P + D) \end{aligned}$$

The left-hand side of each equation is the density (that is per volume of the overlying water) of the toxicant absorbed in each population (that is all constituent individuals). The first term on the right-hand side models the toxicant exchange by passive diffusion from the water. The uptake rate is denoted by  $k_{P_u}$  and the elimination rate by  $k_{P_a}$ . The  $c_R I_{RP} f_{RP} P$  term models consumption of contaminated prey and the  $c_P I_{PF} f_{PF} F$  term the predation by the predator population. These two terms described the transport of the toxicant by trophic interactions between the populations. The latter term models a number of excretion transport mechanisms for the whole population in the system. These terms are similar to those well-known from the classical bioaccumulation models that are formulated at the individual level. Here the formulation is at the population level. We assume that the toxicant is distributed evenly over the excreted products due to assimilation, maintenance and mortality. The first negative term,  $c_P P (I_{RP} - \mu_{RP}) f_{RP}$ , models the excretion of toxicant bound to products formed by the assimilation process (faeces). For the sake of simplicity we assume that the toxicant assimilation efficiencies are all 1. Excreted maintenance products loose their toxicant to the water when leaving the organism. Dead pelagic biomass adds to  $D_r$  and the toxicant within that biomass affect  $c_{D_r}$ . Dead benthic biomass adds to  $D_S$  and the toxicant within that biomass affect  $c_{D_S}$ . Other negative terms are due to maintenance  $c_P P m_P$  and mortality  $c_P P h_P$ . The  $c_P P D$  term is for instance the amount of toxicant that is transported from the system by the outflow (there is no inflow of organisms and therefore no inflow of toxicant by this mechanism). Note that these exchange terms also occur in the mass balance model for the population system (6.2).

Similar, but more complex, expressions for the dynamics of toxicant concentrations in the other biota and detritus compartments can be derived. Using the product-rule and Eqn. (6.2d) we obtain after some algebraic manipulations

$$\frac{dc_P}{dt} = k_{P_u} c_W - k_{P_a} c_P + I_{RP} f_{RP} (c_R - c_P)$$

Figure 6.4 shows an overview of the modelled toxicant fluxes for each compartment. The state variables of the system are listed in Table 6.5. Below the

equations are given:

$$\frac{dc_R}{dt} = k_{Ru}c_W - k_{Ra}c_R - I_{NR}f_{NR}c_R \quad (6.3a)$$

$$\frac{dc_B}{dt} = k_{Bu}c_W - k_{Ba}c_B + I_{D_S B}f_{D_S B}(c_{D_S} - c_B) + I_{RB}f_{RB}(c_R - c_B), \quad (6.3b)$$

$$\frac{dc_P}{dt} = k_{Pu}c_W - k_{Pa}c_P + I_{RP}f_{RP}(c_R - c_P) \quad (6.3c)$$

$$\frac{dc_F}{dt} = k_{Fu}c_W - k_{Fa}c_F + I_{PF}f_{PF}(c_P - c_F) + I_{BF}f_{BF}(c_B - c_F), \quad (6.3d)$$

$$\begin{aligned} \frac{dc_{D_R}}{dt} &= k_{D_Ru}c_W - k_{D_Ra}c_{D_R} \\ &+ D_R^{-1} \left( (c_R - c_{D_R})h_R R + (c_P - c_{D_R})h_P P + (c_F - c_{D_R})h_F F \right), \end{aligned} \quad (6.3e)$$

$$\begin{aligned} \frac{dc_{D_S}}{dt} &= k_{D_Su}c_W - k_{D_Sa}c_{D_S} \\ &+ (D_S S)^{-1} (v_s ((c_R - c_{D_S})R + (c_{D_R} - c_{D_S})D_R)) + \\ &D_S^{-1} \left( ((h_B - (I_{RB} - \mu_{RB})f_{RB} - (I_{D_S B} - \mu_{D_S B})f_{D_S B})(c_B - c_{D_S})B \right. \\ &+ S^{-1} \left( (c_R - c_{D_S})(I_{NR} - \mu_{NR})f_{NR}R + (c_P - c_{D_S})(I_{RP} - \mu_{RP})f_{RP}P \right. \\ &\left. \left. + (c_F - c_{D_S})(I_{PF} - \mu_{PF})f_{PF}F + (c_F - c_{D_S})(I_{BF} - \mu_{BF})f_{BF}F \right) \right). \end{aligned} \quad (6.3f)$$

The transport equations for the toxicant concentrations in the water  $c_W$  and the sediment  $c_S$  read respectively for the water and sediment compartments:

$$\begin{aligned} \frac{dc_W}{dt} &= (c_r - c_W)D + (k_{Ra}c_R - k_{Ru}c_W)R + (k_{Ba}c_B - k_{Bu}c_W)SB \\ &+ (k_{Pa}c_P - k_{Pu}c_W)P + (k_{Fa}c_F - k_{Fu}c_W)F \\ &+ (k_{D_Ra}c_{D_R} - k_{D_Ru}c_W)D_R + (k_{D_Sa}c_{D_S} - k_{D_Su}c_W)SD_S \\ &+ \alpha_R(c_{D_R}D_R + S c_{D_S}D_S) + (k_{Sa}c_S - k_{Su}c_W)S, \end{aligned} \quad (6.4a)$$

$$\frac{dc_S S}{dt} = (k_{Su}c_W - k_{Sa}c_S)S. \quad (6.4b)$$

The sediment  $S$ , biotic benthic organism  $B$  and sediment-detritus  $D_S$  stay in the system and therefore there is no transport of toxicant associated with the flow into or from the system by these three substances, see Eqns. (6.3b), (6.3f) and (6.4b).

Table 6.5: State variables for the toxicological model:  $\mu$  mass of toxicant [ $\mu\text{g}$ ],  $l$  length of environment [ $\text{dm}$ ] ( $l^3$  is dimension of the volume of the overlying water in the system), and  $t$  time [ $\text{d}$ ]. The unit of the uptake rate  $k_{pu}$  is  $\text{L}/(\text{kg}_{\text{dw}} \text{d})$  and of the elimination rate  $k_{pa}$  is  $1/\text{d}$  where  $p \in \{R, B, P, F, D_R, D_S\}$  and  $k_{Su}$  is  $\text{L}/(\text{dm}^{-3} \text{d})$ .

Variable	Description	Unit
$c_r$	Toxicant concentration in the inflow	$\mu\text{g L}^{-1}$
$c_W$	Toxicant concentration in the water	$\mu\text{g L}^{-1}$
$c_S$	Toxicant concentration in the sediment	$\mu\text{g dm}^{-3}$
$c_T$	Total toxicant concentration in the system	$\mu\text{g L}^{-1}$
$c_R$	Producer internal toxicant concentration	$\mu\text{g kg}_{\text{dw}}^{-1}$
$c_B$	Benthic consumer internal toxicant concentration	$\mu\text{g kg}_{\text{dw}}^{-1}$
$c_P$	Pelagic consumer internal toxicant concentration	$\mu\text{g kg}_{\text{dw}}^{-1}$
$c_F$	Predator internal toxicant concentration	$\mu\text{g kg}_{\text{dw}}^{-1}$
$c_{D_R}$	Refractory detritus internal toxicant concentration	$\mu\text{g kg}_{\text{dw}}^{-1}$
$c_{D_S}$	Sediment detritus internal toxicant concentration	$\mu\text{g kg}_{\text{dw}}^{-1}$

We define state variable  $c_T$  as the total toxicant concentration in all compartments together, including biota, detritus, sediment and water. In order to get this concentration one can multiply the concentration in each compartment with its volume and sum the results.

$$c_T = c_W + S c_S + \sum_p c_p p + S \sum_q c_q q. \quad (6.5)$$

with  $p \in \{R, P, D_R\}$  and  $q \in \{B, D_S\}$ . The toxicant transport equation for the total toxicant concentration reads

$$\frac{dc_T}{dt} = D(c_r - c_W - (c_R R + c_P P + c_{D_R} D_R)), \quad (6.6)$$

where we use the fact that the toxicant enters the system via the inflow and leaves the system dissolved in the water and also absorbed by the pelagic populations and adsorbed to the refractory detritus.

In Appendix A we reduce the model complexity by assuming that biological and toxicological processes run at time scales which differ in orders of magnitude. For all populations the aqueous toxicant exchange route from the water or pore water, as well as the exchange between water and sediment compartments is faster than the ecological and physiological processes, such as assimilation, maintenance and excretion. It is the behaviour of this model with reduced complexity which we will analyse.

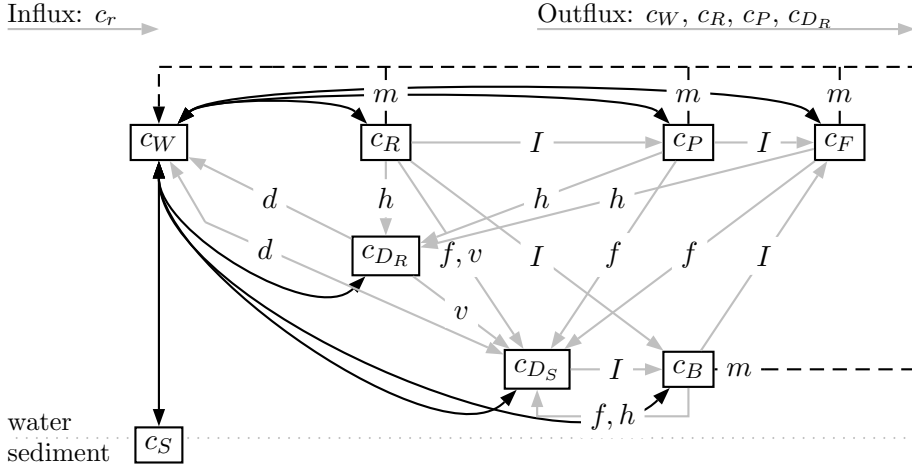


Figure 6.4: Toxicant fluxes from water to biota, to sediment and abiotic compartments. Black arrows denote toxicant fluxes related to processing of biomass such as predation, assimilation and degradation. Grey arrows denote toxicant fluxes associated with surface transport, gills/membrane uptake and passive diffusion. Labile detritus is assumed to have adsorbed negligible amounts of the toxicant. For the explanation of the labels see Tables 6.5 and 6.6.

### 6.4.2 Simplified bioaccumulation model

As in [25, 21, 30, 29] we assume here that the uptake and elimination rates are much faster than other physiological population rates. That is, the toxicant uptake from water (aqueous exposure) dominates that from toxic food (dietary exposure). For the lowest trophic levels this assumption is reasonable, but not always for higher trophic levels where the internal concentration can vary in time. The bioconcentration factors for all pelagic and benthic populations with  $p \in \{R, B, P, F\}$  are defined as follows

$$\text{BCF}_{Wp} = \frac{c_p}{c_W}, \quad (6.7a)$$

Similarly we have the partitioning coefficients for the detritus pools

$$K_q = \frac{c_q}{c_W}, \quad (6.7b)$$

where  $q \in \{D_R, D_S\}$ .

We derive in Appendix A an expression for the total toxicant concentration  $c_T$  absorbed in the populations and adsorbed by the detritus pools given by Eqn. (6.5).

$$\frac{dc_T}{dt} = D(c_r - c_W(1 + \text{BCF}_R R + \text{BCF}_P P + K_{D_R} D_R)). \quad (6.8)$$

This equation together with the ecological model Eqns. (6.2) whereby  $I_{NR}(c_R)$  and  $\mu_{NR}(c_R)$  are given by Eqn. (6.10), forms the set of ODEs that describes the dynamics of the exposed ecosystem. In the next section we analyse its long-term dynamics.

### 6.4.3 The effect module

Direct adverse toxic effects generally reduce population abundances by increasing mortality, increasing costs for growth or maintenance and decreasing assimilation efficiency. In the process-based DEBtox approach the populations are affected by a parameter alteration depending on the internal toxicant concentration: the *concentration-effect relationship*. In principle all physiological processes can be affected: assimilation, maintenance, mortality, growth, reproduction and in ecosystems the processes affected may differ for each population.

In previous papers [30, 29] the maintenance rate and the hazard rate depended on the toxicant concentrations for the producer  $c_R$ , benthic consumers  $c_B$ , pelagic consumer  $c_P$  and predator  $c_F$ , their dependencies are given by

$$\begin{aligned} m_p(c_p) &= m_p(0) \left( 1 + \frac{\max(0, c_p - c_{pM0})}{c_{pM}} \right), \\ h_p(c_p) &= h_p(0) \left( 1 + \frac{\max(0, c_p - c_{pH0})}{c_{pH}} \right), \quad p \in \{R, B, P, F\}. \end{aligned}$$

As in [4] we will give the results for the case where the toxicant affects only the maximum growth rate of the producer  $R$ ,  $\mu_{NR}(c_R)$ :

$$\mu_{NR}(c_R) = \mu_{NR}(0) \left( 1 + \frac{\max(0, c_R - c_{RG0})}{c_{RG}} \right)^{-1}. \quad (6.10)$$

The toxicant (Prometryn) is a herbicide and therefore we assume that for the producer the ingestion rate of nutrients and its growth rate are affected such that the yield or assimilation efficiency remains unaffected. This means that in system (6.2) and (6.3) the maximum ingestion rate  $I_{NR}$  and the maximum growth rate  $\mu_{NR}$  are not constant, but depend on the internal toxicant concentration  $c_R$ :  $\mu_{NR} = \mu_{NR}(c_R)$ . The relationship  $I_{NR}(c_R) = \mu_{NR}(c_R)/y_{NR}$  still holds true with the yield  $y_{NR}$  being constant.

The NEC parameter  $c_{RG0}$  is the threshold concentration value. Below this internal concentration threshold the parameter value equals the control value and there is no effect. Above the threshold value the change in the affected parameter value is proportional to the surplus internal toxicant concentration. Similar expressions hold for other possibly affected physiological process rates, depending on the mode of action.

## 6.5 Analysis of the exposed generic aquatic system

Above we showed how the species diversity and each species biomass depend on  $N_r$  for the unexposed system. In this section we give the model predictions for the same aquatic ecosystem exposed to a herbicide. The simulated herbicide only affects the growth of the producer (algae). The toxicological parameters and values are given in Table 6.6. Now, in addition the bifurcation parameter  $N_r$ , also the toxicant influx concentration ( $c_r$ ) is varied. The effect of the simultaneous continuation of  $N_r$  and  $c_r$  on the structure and composition of the system can now be studied. For  $c_r = 0$  the results are the same as for the control case. We assume that all organisms have fast toxicant uptake and elimination rates. The results will be presented in bifurcation diagrams for subsystems with increasing complexity starting with the producer-nutrient system (R-system).

The complete exposed system is described by Eqns. (6.2,6.8) where the maximum ingestion rate  $I_{NR}(c_R)$  and the maximum growth rate  $\mu_{NR}(c_R)$  are given by Eqn (6.10). Due to the switch in the concentration-effect relationship, the parameter  $\mu_{NR}(c_R)$  in its right-hand side, system 6.2 becomes a so-called piecewise-smooth continuous system, i.e. a set of differential equations with a piecewise-smooth continuous right-hand side [36]. The critical point where this switch occurs when a parameter is varied is called a discontinuity point. In [30, 29] a technique is proposed to calculate these points and curves when two parameters are varied simultaneously. In general, at discontinuity curves such as the NEC-isocline curves (denoted by  $I$ ), the eigenvalues of the Jacobian matrix evaluated at an equilibrium, are discontinuous. When crossing a discontinuity point, the leading eigenvalue can stay in the same half-plane of the complex plane, can pass the imaginary axis leading to a classical bifurcation or it can also jump from one side to the other side of the imaginary axis. In the latter case “new” phenomena can occur (see also [30, 29]).

In the next section we show this for the producer-nutrient system (R-system) in the water/sediment chemostat which forms the base of the aquatic ecosystem.

### 6.5.1 Analysis of the exposed R-system

The producer  $R$  grows on the nutrient  $N$  and forms labile detritus  $D_L$  (being instantaneously converted into nutrients) and refractory detritus  $D_R$ . Producer  $R$  and  $D_R$  sink to the bottom forming sediment detritus  $D_S$  (also being instantaneously converted into nutrients). The water transports  $N$ ,  $R$ ,  $D_L$  and  $D_R$  with the dilution rate  $D$  out of the system. In addition to nutrients with density  $N_r$  a toxicant with herbicidal properties enters this system, with concentration  $c_r$  in the inflow at dilution rate  $D$ . The toxicant will distribute itself

Table 6.6: Physiological and toxicant parameter values for the generic aquatic ecosystem.

Parameter	Description	Value	Units	Ref.
System				
$\rho_{NO}$	nitrogen content of biomass	0.06162	kg N kg <sub>dw</sub> <sup>-1</sup>	[7]
Sediment specific values				
$S$	sediment-water volume ratio: $V_S/V_W$	1	dm <sup>3</sup> soil <sub>dw</sub> L <sup>-1</sup>	
$\rho_S$	Soil density	2.6	kg <sub>dw</sub> dm <sup>-3</sup> soil <sub>dw</sub>	[26]
$f_{oc}$	Fraction organic carbon in the soil	0.003	kg <sub>oc</sub> kg <sub>dw</sub> <sup>-1</sup>	[55]
Prometryn, CAS Registry Number: 007287-19-6				
-----				
$c_p$	Toxicant concentration in inflow	varies	$\mu\text{g L}^{-1}$	
$c_{RG0}$	Producer internal no-effect concentration for growth: BCF <sub>dw</sub> $c_0$	9.57	mg tox kg <sub>dw</sub> <sup>-1</sup>	
$c_{RG}$	Producer internal tolerance concentration for growth: BCF <sub>dw</sub> $c_{Te}$	66.14	mg tox kg <sub>dw</sub> <sup>-1</sup>	
-----				
$c_0$	Algal ext. no-effect conc. for growth	4.57	$\mu\text{g L}^{-1}$	[4]
$c_{Te}$	Algal ext. tolerance conc. for growth	31.60	$\mu\text{g L}^{-1}$	[4]
$\rho_{AFDW}$	Wet biomass ash-free dry weight content	0.12	kg <sub>dw</sub> kg <sub>w</sub> <sup>-1</sup>	[52]
BCF <sub>w</sub> <sup>w</sup>	Toxicant bioconcentration factor	251.2	L kg <sub>w</sub> <sup>-1</sup>	
BCF <sub>dw</sub>	Toxicant bioconcentration factor:	2093	L kg <sub>dw</sub> <sup>-1</sup>	
$K_{dw}$	Partition coefficient: $\frac{\text{BCF}_{wkw}}{\rho_{AFDW}}$	2093	L kg <sub>dw</sub> <sup>-1</sup>	
log $K_{oc}$	Organic carbon-water part. coef.	2.4	$10 \log(\text{L kg}_{oc}^{-1})$	[55]

over the producer biomass, causing adverse effects on the producer's growth, carbon containing pools, i.e. detritus, and organic carbon in the sediment matrix. The producer species and these pools together form the R-system.

A two-parameter diagram is shown in Fig. 6.5 where both  $c_r$  and  $N_r$  are varied. For nutrient input below the transcritical bifurcation  $TC_1$  value these levels are too low to support the existence of the producer. Above the  $TC_1$  value and below the NEC-isocline  $I_1$  the producer is unaffected in the no-effect region (NER). Above this curve  $I_1$  and below the tangent bifurcation curve  $T_1$  is the resistance region (RR) where the equilibrium biomasses are affected but the producer still exists. This tangent bifurcation curve  $T_1$  originates at the indicated so-called codim-two point. Above the curve  $T_1$  the producer goes extinct due to the adverse effects of the toxicants.

In Figure 6.6 the equilibrium values for  $R$  and  $c_W$  as function of  $c_r$  are depicted for two different nutrient input conditions panel A:  $N_r = 0.0017$  and panel B:  $N_r = 0.002$ . So, Figure 6.6A applies for  $N_r$  values below this point and Figure 6.6B above a so-called codim-two point in Fig. 6.5.

In Figure 6.6A, increasing  $c_r$  starting in the unstressed situation, the toxicant concentration in the water  $c_W$  and consequently also the internal toxicant concentration in the producer  $c_R$  increases but is still below the NEC,  $c_{RG0}$  and therefore the equilibrium biomass of  $R$  remains unchanged. When  $c_R = c_{RG0}$  holds at the point  $I_{2,b}$  in Figure 6.6A, the R-system collapses and the extinction equilibrium becomes globally stable. Point  $I_{2,b}$  is a discontinuity point. Crossing this point the leading eigenvalue jumps from a negative value to a positive value. At that point the continuation analysis continues with decreasing  $c_r$  to locate the unstable equilibrium. This unstable branch terminates with decreasing  $c_r$  at a subcritical transcritical bifurcation  $TC_1$  where an exchange of stability occurs between an unstable positive equilibrium ( $R > 0$ ) and a stable producer extinction equilibrium ( $R = 0$ ).

In the region of interest with  $R > 0$  the water concentration  $c_W$  increases almost linearly with the inflow concentration  $c_r$  but is remarkably lower. This fact is related to the rather large BCF value. Much of the toxicant is in the biomasses and sediment and this reduces the water concentration.

In Figure 6.6B for  $N_r = 0.002$  with increasing  $c_r$  when  $c_R = c_{RG0}$  at the point  $I_{2,b}$  the equilibrium  $R$  value decreases due to the adverse effects of the toxicant. Increasing  $c_r$  further a tangent bifurcation denoted by  $T_1$  is reached where the equilibrium becomes unstable. For a higher  $c_r$  value the extinction equilibrium is globally stable. The unstable branch terminates again at a subcritical transcritical bifurcation  $TC_1$ .

This bifurcation pattern is characteristic for a hysteresis-loop. After the R-system is exposed to increasingly higher toxicant inflow values of  $c_r$  the system crashes catastrophically at  $I_1$  or  $T_1$ . By lowering  $c_r$ , the producer  $R$  can only invade again when the subcritical branching point  $TC_1$  is crossed. In

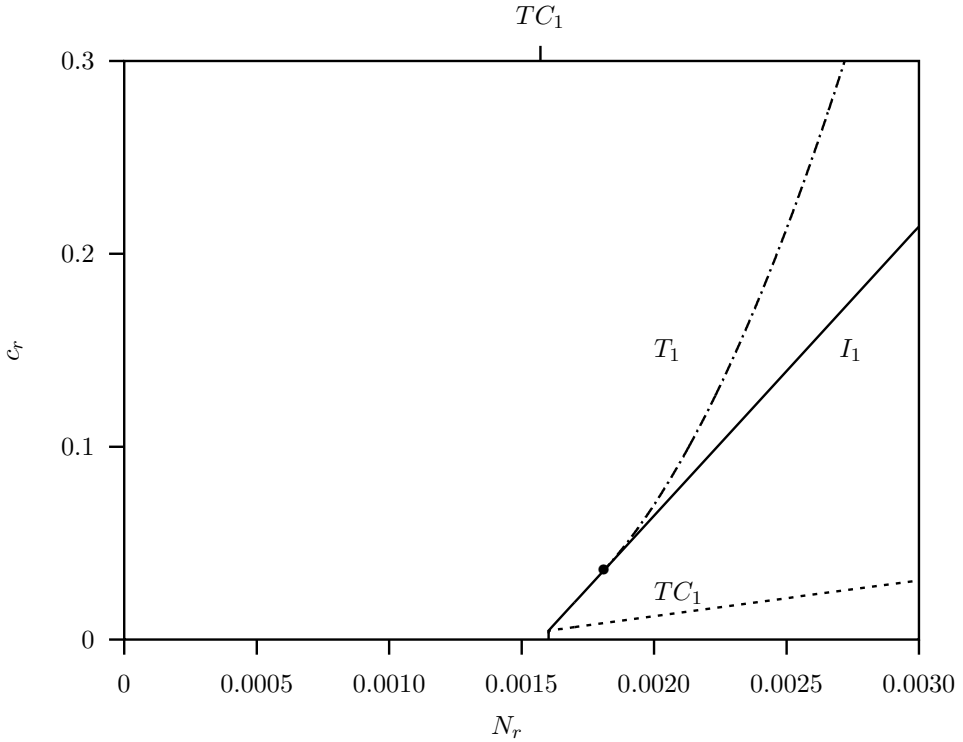


Figure 6.5: Two-parameter bifurcation diagram for the R-system, with nutrient inflow  $N_r$  and toxicant inflow concentration  $c_r$  as bifurcation parameters with dilution rate  $D = 0.02$ . The dot at the intersection of  $T_1$  and  $I_1$  is the codim-two point mentioned in Fig. 6.6. See Table 6.4 for a description of the bifurcation curves and Tables 6.3 and 6.6 for the parameter values.

this system bi-stability occurs between these critical points where the stable manifold of the unstable equilibrium acts as a separatrix for the two basins of attraction.

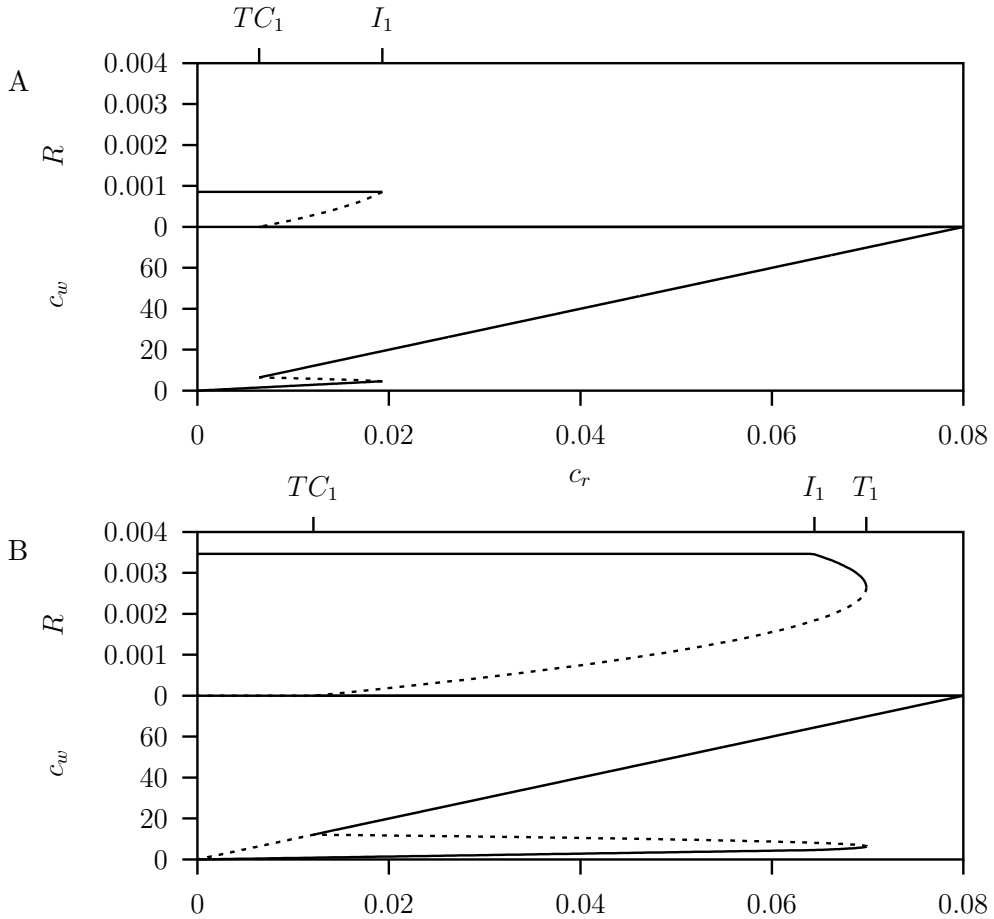


Figure 6.6: One-parameter bifurcation diagram for the nutrient-producer-system (R-system), with nutrient inflow  $N_r$  held constant at either A: 0.0017 or B: 0.002 while the toxicant inflow concentration  $c_r$  is continued. See Table 6.3 and 6.6 for other parameter values. In each panel is producer density  $R$  and the water concentration  $c_w$  are shown as a function of the toxicant inflow concentration  $c_r$ . Solid lines depict stable equilibria and dashed lines unstable equilibria. In panel A the nutrient inflow rate is taken such that the system is on the left of the codim-two point in Fig. 6.5 and in B on the right side.

## 6.5.2 Results for the exposed aquatic system

In this section we present the results for the exposed complete aquatic system. The bifurcation analysis is described in Appendix B where the technical details are given.

Fig. 6.7 is a compilation of the analysis results for the RBF, RPF and RBPF-systems, in this figure the regions with the same long-term dynamics are indicated. In each NER-region (darkest grey) the internal toxicant concentration of the producer population  $R$  is below the NEC, that is  $c_R < c_{RG0}$ . The upper boundary of each NER-region increases with increasing nutrient input concentration  $N_r$ . Thus at higher nutrient levels the system can withstand more toxicant influx  $c_r$  without being affected. The boundaries of each RR are affected in a similar manner. For the RPF-system the upper boundary is formed by the Hopf bifurcation  $H_{3,p}$  curve. For nutrient-levels below  $TC_{4,b}$  the pelagic consumer goes extinct (the RBF-system) while above  $TC_{4,p}$  the benthic consumer goes extinct (the RPF-system). The Hopf bifurcation  $H_{3,p}$  curve marks where with nutrient enrichment the RPF-system starts to oscillate. The top of the grey RR for the RPF-system is formed by a Hopf bifurcation curve  $H_{3,p}$  which also forms the righter boundary. Notice that there is for the RPF-system another  $TC_{3,p}$  bifurcation curve. The RR where a positive equilibrium exists (left-light grey region for the RBF-system, grey region for the RBPF-system and right-light grey region for the RPF-system) also increases in size with nutrient enrichment.

The one parameter diagram Fig. 6.8 has a variable toxicant inflow density  $c_r$  and a fixed  $N_r = 0.3$ . The biomasses remain stable up to a rather large toxicant input loading where the equilibrium becomes unstable at a Hopf bifurcation point  $H_4^-$ . Between this curve and the tangent bifurcation curve for limit cycles  $T_4$  the system oscillates. At the curve  $T_4$  the system collapses when  $c_r$  is increased beyond this point.

The lowest panel in Fig. 6.8A shows that the equilibrium nutrient density  $N$  increases with increased toxicant inflow concentration. The producer biomass  $R$  and also that of the other biota, remain fairly constant up-to the Hopf bifurcation point  $H_4^-$ . From Fig. 6.8B we conclude that the toxicant concentration in the water  $c_W$  also increases with increased toxicant inflow concentration, just as the nutrient density  $N$ . We recall that the toxicant reduces the producer ingestion and growth rate given by Eqn. (6.10) with  $c_R = BCF_{WR}c_W$  given by Eqn. (6.16). So, apparently, the increased nutrient density compensates the reduced maximum ingestion rate. This phenomenon occurs until the system crashes around  $c_r = 600$ .

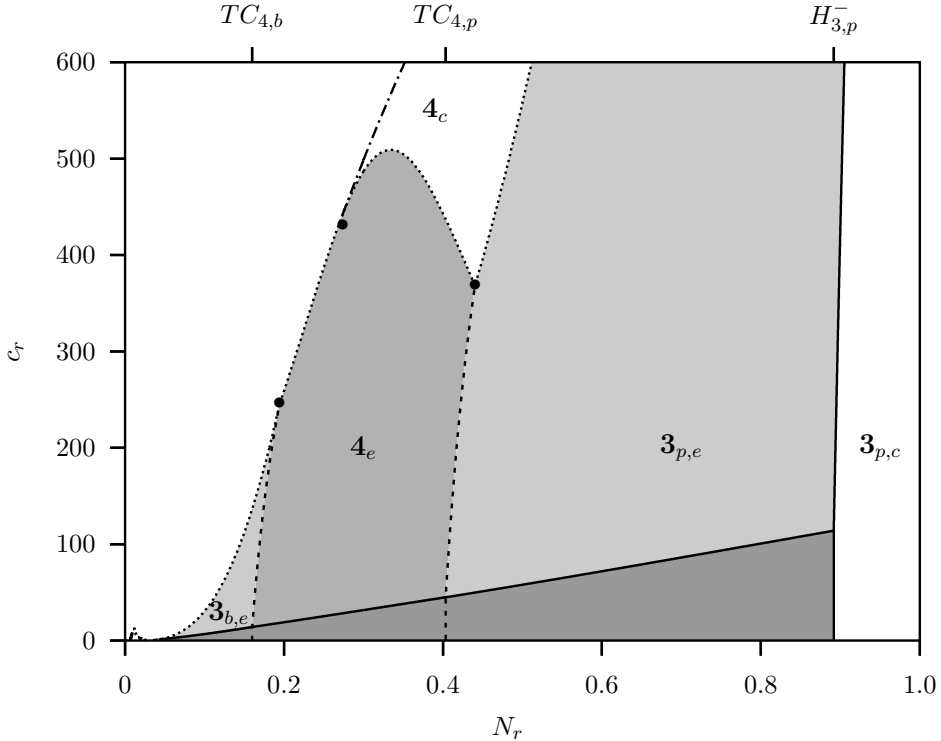


Figure 6.7: Two-parameter bifurcation diagram for the RBPF-system, with nutrient inflow  $N_r$  and toxicant inflow concentration  $c_r$  as bifurcation parameters. The parameters are the same as in Fig. 6.10. The dark grey region is the *No Effect Regime* (NER). The grey region is the *Resistance Region* (RR) for the RBPF-system in equilibrium denoted by  $4_e$ . The light grey region on the left is the RR for the RBF-system ( $3_{b,e}$ ) and on the right side the RR for the RPF-system ( $3_{p,e}$ ). The subscript  $c$  indicates oscillatory behaviour. Each NER and RR are separated by a NER-isocline (solid black line).

## 6.6 Discussion

Models taking indirect effects into account are described in the literature [27, 18, 45] and references therein. An implementation of the model described in [45] is available in a computer package AQUATOX [44]. The AQUATOX model is basically a mechanistic model but for the parametrisation many descriptive models are used with calibrated parameters based on literature data and (laboratory and field) experiments. In [44] the trophic interactions are modelled after the static approach developed in [41]. In this paper the model formulations for the trophic interactions are based on a dynamic approach and have a mechanistic underpinning given in [42, 32].

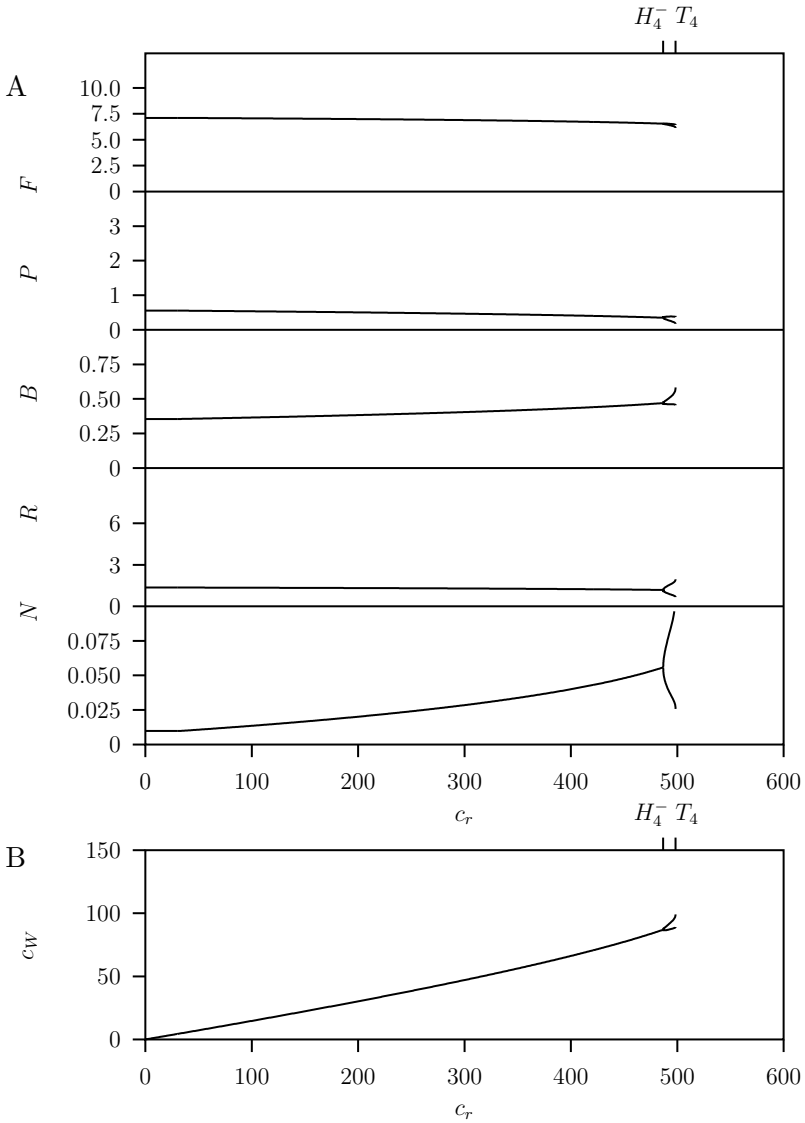


Figure 6.8: One-parameter bifurcation diagrams for the RBPF-system with the toxicant concentration in the inflow  $c_r$  as free parameter with dilution rate  $D = 0.02$  and input nutrient concentration  $N_r = 0.3$ . A: The stationary biomass of the nutrient  $N$ , producer  $C$ , benthic consumer  $B$ , pelagic consumer  $P$  and predator  $F$  is depicted as a function of the toxicant level  $c_r$ . B: The stationary ambient water concentration  $c_w$  is depicted as a function of the toxicant level  $c_r$ . For high toxicant inflow concentrations the system oscillates with indicated extrema. The bifurcation points are described in Table 6.4.

The dynamics of the pelagic and the benthic community are directly coupled with the fate and transport dynamics of the toxicant. The resulting model is, however, parameter rich. Therefore reduction techniques are used to derive a simplified model formulation. The resulting parameters are the same as those described in the literature where generally the ecosystem is assumed to be in equilibrium (see for instance [38, 15, 35, 50, 21, 5, 49]). In the reduced model the bioconcentration factors BCF, BAF, BSAF can easily be used as literature values can be found from standard toxicity bioassay studies. Because the ecosystem equilibrium assumption is not explicitly made for the ecological model and a time-scale separation argument is applied, the dynamic behaviour of the ecosystem is retained and therefore indirect effects can still be studied.

Assuming a time scale separation argument, the expressions for the bioconcentration factors that link the internal concentrations to the environmental toxicant concentration in the water and the sediment, are derived from our modelling approach. In this way the classical models become special cases of the generic model formulation. This time scale separation argument holds when the uptake of the toxicant by the water and sediment are much faster than the food intake rates and ecological physiological processes such as assimilation rate and maintenance rate. This is often true for highly hydrophobic toxicants. As a result the toxicant aqueous uptake route becomes dominant.

In the DEBtox concentration-effect relationship, the rates of the affected physiological population processes depend on the internal toxicant concentration: here the maximum ingestion and maximum growth rate of the producer. Which parameters are affected by the toxicant depends on the mode of action of the toxicant for the particular species. The parameters in the concentration-effect model: the no-effect concentration (NEC) and the tolerance concentration (TC), are unfortunately not measured in standard toxicity testing. These two parameters are specific for the DEBtox approach and therefore they have still to be estimated for instance using test-procedures developed in [37, 4]. Although toxic effects are studied using the DEBtox effect module, the integrated approach and the analysis technique based on non-linear dynamical theory can also be used when other effect modules are implemented.

When the uptake route from the water (aqueous exposure) for the pelagic and the pore water for the benthic organism dominates the food uptake route (dietary exposure), the effects caused by the interaction of the biological and toxicological processes can still be studied simultaneous in our approach. This is a direct consequence of the fact that the ecological model remains essentially unchanged, as well as the effect module. The calculation of the distribution of the toxicant over the various compartments is simplified, yielding fixed partitioning factors such as the BCFs and water-sediment partition coefficient ( $K$ ). The time dependence of the toxicant concentration in the water and sediment

compartments is then described by the transport equations Eqn. (6.4) together with Eqn. (6.6). This couples the dynamics of the populations to their internal toxicant concentrations using the constant bioconcentration factors.

Alternatively a model reduction is obtained when only the uptake rate is large and the elimination rate is of the same order as the physiological population rates. Then the dietary exposure route and the excretion routes matter. In this case the equilibrium values for the biomasses  $\{R, B, P, F\}$ , the solution of the equilibrium equations (6.2) are substituted into system (6.3). When the equilibrium condition for this system (6.14) is met this leads to alternative definitions of BCF, BAF and BSAF [30]. These expressions are similar to those in [6, 21, 51] where they were formulated at the individual level but here they are formulated on the level of the population. We do not elaborate on this specific model reduction approach, since the assumption of equilibrium biomasses in system (6.3) and non-equilibrium ecological model system (6.2) is inconsistent when these systems operate at the same time scale.

From the results presented in Figs. 6.5, 6.9 and 6.10 the interaction of the toxicant loading and nutrient enrichment is very important. Co-existence of the pelagic and benthic communities in the intermediate nutrient input can be classified as a predator mediated co-existence where the fish population is the predator.

Generally the no-effect region increases with nutrient enrichment. More available nutrients support more biomass in the system. More biomass means more mass over which the toxicant can partition, leading to overall lower internal concentrations for all species and thus making the whole system less vulnerable to the adverse effects of the toxicant.

Fig. 6.10 shows that in addition to a rather large no-effect region that on top of that the resistance region can also be larger. There is almost no effect up to high toxicant load at which point the system collapses. That phenomenon is discussed in [48]. In the case of the tangent bifurcation there are early-warning signals, as exemplified with Fig. 6.8 which is a cross-section of Fig. 6.10 at  $N_r = 0.3$ . However, when making a cross-section at  $N_r = 0.2$  in Fig. 6.10 just below point  $M_b$  the system collapses at a subcritical Hopf bifurcation instead of a tangent bifurcation with warning signals. When the Hopf bifurcation is approached, the equilibrium values do not change dramatically only the return time to the equilibrium (often related to resilience) goes to zero. Passing the Hopf bifurcation means that suddenly the equilibrium becomes unstable leading to the collapse, this is shown in Fig. 6.6.

For lower nutrient levels for the R-system the producer population goes extinct without any warning signals when the internal toxicant concentration exceeds the no-effect concentration, see Figure 6.6A.

In the process based approach it is crucial to have a “validated” model for the ecosystem in the “reference state”. One issue is the choice of an adequate

mathematical formulation. Here we use ordinary differential equations, ODEs, but sometimes better alternatives are partial differential equations PDE (see for instance [11]). The choice of the model formulation is directly related to the life-history of the species. Ordinary differential equations are most appropriate for species that possess a simple life-cycle such as microorganisms that propagate by binary fission, e.g. algae and ciliates. For species with multiple life-stages (egg, larvae, juvenile, adult) the use of partial or delay differential equations may be more appropriate.

## 6.7 Conclusions

We started with the process based approach where ecological and toxicological processes are modelled together. The resulting model, although already quite simplistic, requires knowledge about a lot of parameters of which many are not directly related to toxicity. Thereafter we derived expressions for the bioconcentration factors assuming time-scale arguments or dominance of one specific uptake route for the toxicant. This reduces the number of model parameters drastically.

Our approach is holistic in the sense that models for the ecosystem and the fate of the toxicant are fully integrated. This makes the evaluation of potential risks of long-term sublethal toxic stress on ecosystems functioning and structure possible. The expressions for the classical bioconcentration factors in the bioaccumulation models have been derived from our process-based ecosystem model using the time-scale separation techniques yielding toxicological equilibrium partitioning. However, no equilibrium assumption regarding the ecosystem was made and this allows for the study of direct as well as indirect effects of toxicological, ecological and environmental stresses simultaneously. Due to indirect effects toxic stress effects can be amplified or diminished.

Although we took the step from individual to population level model formulation as simple as possible, the integrated bioaccumulation model formulation showed emergence properties. As an example we mention “dilution by growth”. Individuals grow when there is a sufficient amount of food to support the existence of the population (as part of the ecosystem). However, at the population level the population biomass is constant when the ecosystem is in equilibrium, even when the individuals are born, grow and die.

The results indicate that the dynamic behaviour of the aquatic ecosystem is already complicated, due to the nonlinear interaction between the populations and between the populations and their environment. As a consequence, no single index can be given that would be equivalent with some kind of risk index. The effect depends very much on the abiotic environmental conditions fixed by the toxic exposure, but also the nutrient availability and the throughput

rate of the water. Here we analysed the effects of the toxic stress solely for the producer (algae) by a herbicide but the same approach can be used for other modes of stressing.

Bifurcation analysis deals with the dependency of the long-term dynamic behaviour of dynamics systems on parameters. Therefore this technique can be used for the assessment of toxic-effects related to a sensitivity analysis whereby parameters related to the exposure of the toxicant are altered focusing on the long-term sublethal effects. When the exposure concentration of the toxicant is taken as a continuation parameter, these plots show directly at which toxic level the structure, and hence the biodiversity, of the ecosystem changes.

The bifurcation analysis performed in this paper and the results obtained show the power of this technique for the study of long-term sublethal effects to ecotoxicologist. Short-term lethal effects can be analysed by simulation as is done for instance in [45].

One notable result is that, up to a high toxicant load, the equilibrium biomasses of all biota remain close to that of the control case but the ambient nutrient density increases with increasing toxicant load. Above this toxic stress the system collapses catastrophically. This shows that indirect population-dynamic phenomena can diminish toxicological effects.

In [17] it is stated that there is a general agreement on the need to extend toxicological assessments from the individual level of biological organization to higher levels (populations, communities and ecosystems), but no agreement on how to accomplish this task. Here we showed that for sublethal long-term effects the combination of process-based modelling and bifurcation analysis is a next step to the assessment of long-term toxic effects on aquatic ecosystems. The quality of the ecological reference model is crucial. It is well-known that the validation of ecosystem models for field predictions is problematic because of many uncertainties. Nevertheless this approach gives the relative effects of toxic and other environmental stresses simultaneously and reveals the mechanisms that cause indirect effects observed in the laboratory [37] and predicted for the field. Hence, nutrient enrichment allows for longer food chains and gives more resistance of the ecosystem against toxic exposure.

## 6.8 Appendix A

### Model reduction approaches

In this Appendix we derive the classical bioaccumulation models. The starting point is the dynamic model for the whole stressed ecosystem consisting of the ecological community including the nutrients and the toxicant.

Assuming equilibrium of all ODEs of the set of governing equations Eqns. (6.2), (6.3) and (6.4) leads to a large system of nonlinear equations and no simplification nor reduction of the system is obtained. Therefore additional assumptions are necessary. Compound parameters associated with these assumptions are given in Table 6.6. In this Appendix a time-scale separation technique is applied to obtain a reduced model. This approach is similar to the classical *equilibrium partitioning approach*.

We assume that the toxicant concentration in the pore water equals the concentration in the overlying water  $c_W$ . The toxicant concentration in the sediment organic carbon will be used as the reference toxicant concentration for the sediment compartment (see also [15]). The sediment toxicant concentration  $c_{S,oc}$  is expressed as mass toxicant per mass of organic carbon in the sediment bulk whereby

$$c_S = \rho_S f_{oc} c_{S,oc} .$$

The organic carbon is assumed to be well mixed with the sediment matrix and does not increase or decrease in quantity and is not affected by organisms. We take sediment organic carbon to be only in contact with pore water which is instantaneously in equilibrium with the surface water.

We introduce for the diffusion transfer rates in Eqns. (6.4a) and (6.4b):

$$\begin{aligned} k_{W,oc} &= k_{Su} , \\ K_{oc} &= \frac{k_{Su}}{\rho_S f_{oc} k_{Sa}} , \end{aligned}$$

Then Eqn. (6.4b) reads

$$\frac{dc_{S,oc}}{dt} = \frac{k_{W,oc}}{\rho_S f_{oc}} \left( c_W - \frac{c_{S,oc}}{K_{oc}} \right) . \quad (6.11a)$$

Eqn. (6.4a) becomes

$$\begin{aligned} \frac{dc_W}{dt} = & (c_r - c_W)D + (k_{Ra}c_R - k_{Ru}c_W)R + (k_{Ba}c_B - k_{Bu}c_W)SB \\ & + (k_{Fa}c_F - k_{Fu}c_W)F + (k_{Pa}c_P - k_{Pu}c_W)P \\ & + (k_{D_{Ra}}c_{D_R} - k_{D_{Ru}}c_W)D_R + (k_{D_{Sa}}c_{D_S} - k_{D_{Su}}c_W)SD_S \\ & + \frac{k_{W,oc}}{V_W} \left( \frac{c_{S,oc}}{K_{oc}} - c_W \right) \end{aligned} \quad (6.12a)$$

$$\frac{dc_{S,oc}}{dt} = \frac{k_{W,oc}}{\rho_S f_{oc}} \left( c_W - \frac{c_{S,oc}}{K_{oc}} \right) \quad (6.12b)$$

In our model the sediment detritus  $D_S$  is formed due to settling of both refractory detritus and algae from the overlying water and from faeces from the biota. We assume that this settled material only affects the top layer of the sediment and can be modelled as a separate chemical absorbing compartment in parallel to the organic carbon. The sediment detritus is organic material which is still degradable. In this model formulation, the sediment detritus does not increase or decrease the organic carbon density in the sediment bulk, these two absorbing compartments do not mix but interact indirectly via the surface water.

We assume that biological and toxicological processes run at time scales which differ in orders of magnitude. For all populations the toxicant exchange route from the water for the aquatic organisms, and from pore water for the benthic organisms, as well as the exchange between water and sediment compartments is faster than the ecological and physiological processes, such as assimilation, maintenance and excretion.

Then Eqns. (6.3e) and (6.3f) become

$$\begin{aligned} \frac{dc_{D_R}}{dt} &= k_{D_{Ru}}c_W - k_{D_{Ra}}c_{D_R} \\ \frac{dc_{D_S}}{dt} &= k_{D_{Su}}c_W - k_{D_{Sa}}c_{D_S}, \end{aligned}$$

and for the populations Eqns. (6.3a,6.3b, 6.3c,6.3d) into:

$$\frac{dc_R}{dt} = k_{Ru}c_W - k_{Ra}c_R \quad (6.14a)$$

$$\frac{dc_B}{dt} = k_{Bu}c_W - k_{Ba}c_B \quad (6.14b)$$

$$\frac{dc_P}{dt} = k_{Pu}c_W - k_{Pa}c_P \quad (6.14c)$$

$$\frac{dc_F}{dt} = k_{Fu}c_W - k_{Fa}c_F \quad (6.14d)$$

Equation (6.14b) shows that the dominant toxicant uptake route from the water for the benthic organisms living in the sediment is in agreement with the equilibrium partitioning principle [15].

A further reduction can be obtained when the dynamics of the toxicant is assumed to be in equilibrium, as is generally done in the classical bioaccumulation models. As in the equilibrium partitioning approach [15] it is assumed that sediment organic carbon can readily adsorb toxicants. Here we assume that the transfer rate  $k_{W,oc}$  in Eqn. (6.11a) is large with respect to the dilution rate  $D$  in Eqn. (6.4a) and physiological population rates in ODE-system (6.3). Then the quasi-steady state assumption is that we set  $dc_{S,oc}/dt = 0$  in Eqn. (6.4b) and this yields

$$K_{oc} = \frac{c_{S,oc}}{c_W} . \quad (6.15)$$

That is the toxicant concentration in the sediment  $c_{Soc}$  is proportional to the overlying water toxicant concentration  $c_W$  and the partition coefficient equals  $K_{oc}$  equivalent to the equilibrium partitioning assumption [15].

As in [25, 21, 30, 29] we assume here that the uptake and elimination rates are much faster than other physiological population rates. That is, the toxicant uptake from water (aqueous exposure) dominates that from toxic food (dietary exposure). For the lowest trophic levels this assumption is reasonable, but not always for higher trophic levels where the internal concentration can vary in time. The bioconcentration factors for all populations  $p \in \{R, B, P, F\}$  and the partitioning coefficients for the abiotic pools  $q \in \{D_R, D_S\}$  are defined as follows

$$\text{BCF}_{Wp} = \frac{c_p}{c_W} , \quad K_q = \frac{c_q}{c_W}$$

Then assuming a dominant toxicant uptake from the water and sediment we get by using the equilibria values of Eqns. (6.3) where ( $dc_p/dt = 0$ ) for the populations and the two detritus pools  $o \in \{R, B, P, F, D_R, D_S\}$

$$k_{ou}c_W = k_{oa}c_o ,$$

This implies that for the populations  $p \in \{R, B, P, F\}$

$$\text{BCF}_{Wp} = \frac{c_p}{c_W} = \frac{k_{pu}}{k_{pa}} , \quad (6.16)$$

that is each bioconcentration factor equals the ratio between the uptake rate and elimination rate. Similarly we have the partitioning coefficients for the abiotic pools

$$K_q = \frac{c_q}{c_W} = \frac{k_{qu}}{k_{qa}} ,$$

where  $q \in \{D_R, D_S\}$ .

For the total toxicant concentration absorbed in the populations and adsorbed in the abiota  $c_T$  given by Eqn. (6.5) we obtain directly the following equation

$$c_T = c_W(1 + S\rho_S f_{oc} K_{oc} + \sum_p \text{BCF}_p p + \text{BCF}_B S B + K_{D_R} D_R + K_{D_S} S D_S), \quad (6.17)$$

with for the pelagic biota  $p \in \{R, P, F\}$ .

We recall that using these bioaccumulation expressions do not imply that it is assumed that the biomasses in the ecological model system (6.2) are in equilibrium. The dynamics of the internal toxicant concentrations in all biotic and abiotic compartments is fully fixed by the single ODE Eqn. (6.8) and the algebraic Eqn. (6.17) for both  $c_T(t)$  and  $c_W(t)$ . Together with the ecological model system (6.2), the resulting system is a set of differential algebraic equations (DAEs) where the biomasses are the differential variables  $p$ , algebraic variables are used for the internal toxicant (effects) concentrations  $c_p(t)$ ,  $p \in \{R, B, P, F\}$ . This shows that using the equilibrium partitioning principle [15], the expression for the internal toxicant concentrations in the benthic compartments and also the expression for the toxicant adsorbed to the sediment organic carbon are used in Eqn. (6.17) but they do not occur in the mass balance equation (6.8). Hence the the internal toxicant concentrations  $c_B(t)$  is possibly effected directly, and  $c_S(t)$  causes only indirect effects.

## 6.9 Appendix B

### Analysis of the exposed aquatic ecosystem

In this Appendix a bifurcation analysis is described for the complete exposed aquatic ecosystem. We continue the analysis performed for the R-system in Section 6.5.1.

#### Analysis of the RB- and RBF-system

We continue with the results for higher nutrient levels where the nutrient-producer system is invaded by the benthic consumer  $B$  and the fish  $F$ . The diagram is shown in Fig. 6.9. Above the point  $T_{2,b}$  the nutrient input is sufficiently high to support the consumer  $B$ , i.e., the producer density exceeds the minimal requirements of the consumers. For a fixed  $N_r$  value just below point  $H_{2,b}^-$ , there is no effect when increasing the toxicant input concentration  $c_r$  up-to curve  $I_{2,b}$  where the internal toxicant concentration equals the NEC

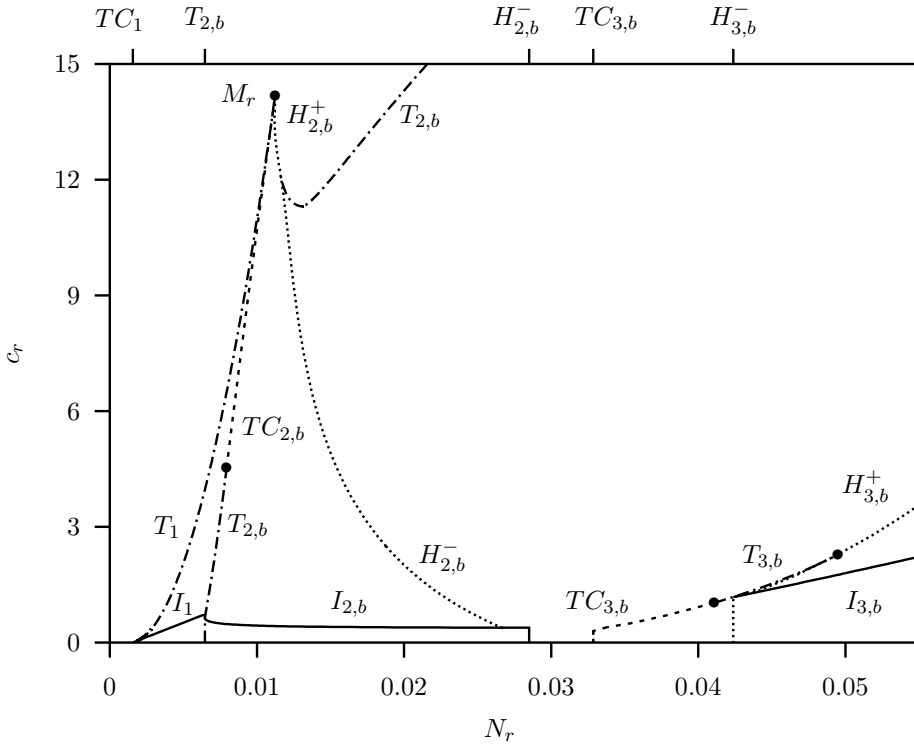


Figure 6.9: Two-parameter bifurcation diagram for the RBF-system, with nutrient inflow  $N_r$  and toxicant inflow concentration  $c_r$  as bifurcation parameters with dilution rate  $D = 0.02$ . See Table 6.4 for a description of the bifurcation curves and Tables 6.3 and 6.6 for the parameter values.

value. But when this value is passed the system starts to oscillate without passing a Hopf bifurcation point. This phenomenon is again due to the non-smoothness of the concentration-effect relationship at the NEC.

In the region between  $H_{2,b}^-$  and  $TC_{3,b}$  the unstressed system oscillates and this remains the case after toxicant loading. The limit cycle stays stable up-to the curve  $T_{2,b}$  which is a tangent bifurcation of the limit cycle. Increasing the toxicant load further leads to a catastrophic collapse of the RB-system. In the region between  $TC_{3,b}$  and  $H_{3,b}^-$  enrichment is high enough to support co-existence with the fish but the system still oscillates. However when the toxicant load is increased for this RBF-system, the fish goes extinct at rather low toxicant loading when crossing the  $TC_{3,b}$  curve as shown in Fig. 6.10. This curve transforms into a tangent bifurcation curve  $T_{3,b}$  which becomes a Hopf bifurcation curve  $H_{3,b}^+$ . For larger nutrient input levels this curve marks the point where the fish population goes extinct when the toxicant load increases. The curve  $I_{3,b}$  is also increasing with  $N_r$  and this means that the NER region

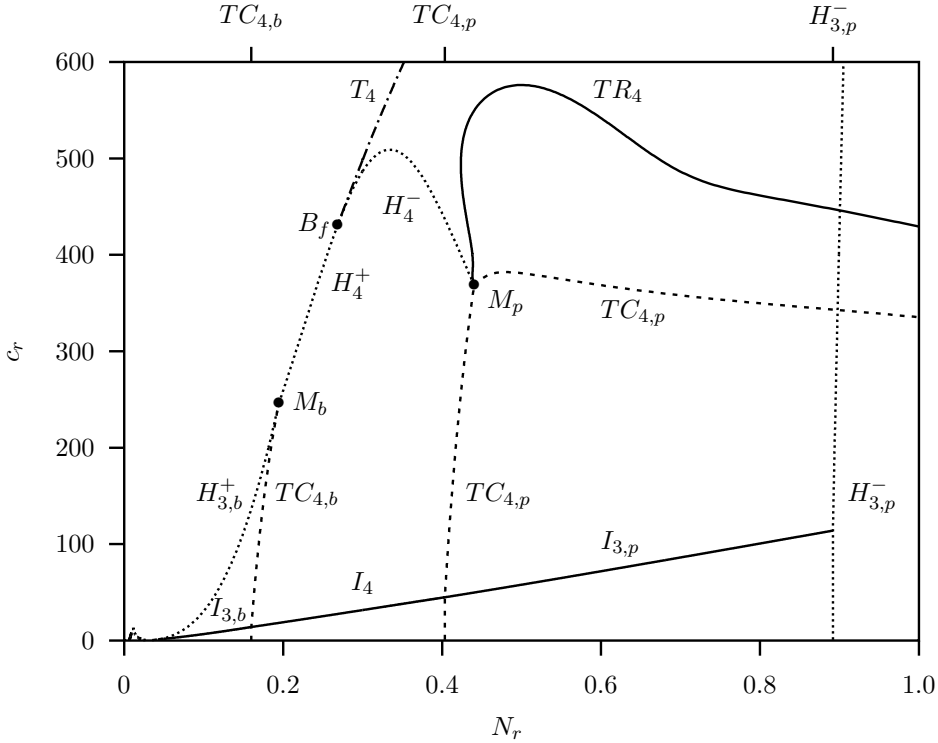


Figure 6.10: Two-parameter bifurcation diagram for the RBPF-system, with nutrient inflow  $N_r$  and toxicant inflow concentration  $c_r$  as bifurcation parameters with dilution rate  $D = 0.02$ . See Table 6.4 for a description of the bifurcation curves and Tables 6.3 and 6.6 for the parameter values.

also increases.

## Analysis of the RBPF-system

In Fig. 6.10 the two parameter bifurcation diagram is shown for the RBPF-system. Again  $N_r$  and  $c_r$  are the free parameters. The region of co-existence of all biota is between the curves  $TC_{4,p}$  and  $TC_{4,b}$ . The curve labelled  $I_4$  is the NEC-isocline curve now for the RBPF-system. Below this curve there is the no-effect region (NER).

The transcritical bifurcation curves  $TC_{4,b}$  and  $TC_{4,p}$  terminate in codim-two points denoted by  $M_b$  and  $M_p$  respectively. These two points are also connected by the supercritical Hopf bifurcation curve  $H_4^-$  and supercritical Hopf bifurcation curve  $H_4^+$ . The region between these two curves and the NEC-isocline curve  $I_4$  is the resistance region (RR).

Above the curve  $H_4^-$  the equilibrium is unstable and a stable limit cycle exists. In the so-called Bautin point  $B_f$  the Hopf bifurcation curve changes

from subcritical into supercritical and vice versa. From this point a tangent bifurcation curve for the limit cycle denoted by  $T_4$  emerges. At  $T_4$  the stable limit cycle collides with an unstable limit cycle.

From point  $M_p$  a so called torus or Neimark-Sacker bifurcation curve  $TR_4$  originates. At this bifurcation a limit cycle becomes unstable with two conjugated complex multipliers cross the unit circle. It is similar to the Hopf bifurcation of an equilibrium where the eigenvalues cross the imaginary axis. Between this torus bifurcation curve  $TR_4$  and the transcritical curve for the limit cycle of the full system  $TC_{4,p}$  the dynamics can be chaotic.

The one parameter diagram Fig. 6.8 has variable toxicant inflow density  $c_r$  and a fixed  $N_r = 0.3$ . The biomasses remain stable up to a rather large toxicant input loading where the equilibrium becomes unstable at a Hopf bifurcation point  $H_4^-$ . Between this curve and the tangent bifurcation curve for limit cycles  $T_4$  the system oscillates. At the curve  $T_4$  the system collapses when  $c_r$  is increased beyond this point.

The lowest panel in Fig. 6.8A shows that the equilibrium nutrient density  $N$  increases with increased toxicant inflow concentration. The producer biomass  $R$  and also that of the other biota, remain fairly constant up-to the Hopf bifurcation point  $H_4^-$ . From Fig. 6.8B we conclude that the toxicant concentration in the water  $c_W$  also increase with increased toxicant inflow concentration, just as the nutrient density  $N$ . We recall that the toxicant reduces the producer ingestion and growth rate given by Eqn. (6.10) with  $c_R = BCF_{WR}c_W$  given by Eqn. (6.16). So, apparently, the increased nutrient density compensates the reduced maximum ingestion rate. This phenomenon occurs until the system crashes around  $c_r = 600$ .

For nutrient-levels below  $TC_{4,b}$  the pelagic consumer goes extinct (the RBF-system) while above  $TC_{4,p}$  the benthic consumer goes extinct (the RPF-system). The Hopf bifurcation  $H_{3,p}$  curve marks where with nutrient enrichment the RPF-system starts to oscillate. The curve  $I_{3,p}$  is an extension of the  $I_4$  curve. It terminates at the Hopf bifurcation  $H_{3,p}$  where it loses meaning. Notice that there is for the RPF-system another  $TC_{3,p}$  bifurcation curve and also a Hopf bifurcation  $H_{3,p}$  curve, which are not shown in the figure because they play no essential role in the dynamics of the complete system.

In Fig. 6.7 the regions with the same long-term dynamics are indicated. In the NER-region the internal toxicant concentration of the producer population  $R$  is below the NEC, that is  $c_R < c_{RG0}$ . The maximum toxicant influx  $c_r$  value for this regions as function of the nutrient input concentration  $N_r$  is increasing. This means that the NER increases. Also the RR increases. For the RPF-system the upper boundary is formed by the Hopf bifurcation  $H_{3,p}$  curve (not labelled).

# References

- [1] F. S. Bacelar, S. Dueri, E. Hernandez-Garcia, and J. M. Zaldívar. Joint effects of nutrients and contaminants on the dynamics of a food chain in marine ecosystems. *Mathematical Biosciences*, 218(1):24–32, 2009.
- [2] S. M. Bartell, G. Lefebvre, G. Kaminski, M. Carreau, and K. R. Campbell. An ecosystem model for assessing ecological risks in Quebec rivers, lakes, and reservoirs. *Ecological Modelling*, 124(1):43–67, 1999.
- [3] A. D. Bazykin. *Nonlinear dynamics of interacting populations (Ed. by A. I. Khibnik and B. Krauskopf)*. World Scientific, Singapore, 1998.
- [4] D. Bontje, B. W. Kooi, M. Liebig, and S. A. L. M. Kooijman. Modelling long-term ecotoxicological effects on an algal population under dynamic nutrient stress. *Water Research*, 43:3292–3300, 2009.
- [5] J. Campfens and D. MacKay. Fugacity-based model of PCB bioaccumulation in complex aquatic food webs. *Environmental Science Technology*, 31:577–583, 1997.
- [6] K. E. Clark, F. A. P. C. Gobas, and D. Mackay. Model of organic chemical uptake and clearance by fish from food and water. *Environmental Science Technology*, 24(8):1203–1213, 1990.
- [7] F. De Laender, K. A. C. De Schamphelaere, P. A. Vanrolleghem, and C. R. Janssen. Comparison of different toxic effect sub-models in ecosystem modelling used for ecological effect assessments and water quality standard setting. *Ecotoxicology and Environmental Safety*, 69:13–23, 2008.
- [8] F. De Laender, K. A. C. De Schamphelaere, P. A. Vanrolleghem, and C. R. Janssen. Do we have to incorporate ecological interactions in the sensitivity assessment of ecosystems? An examination of a theoretical assumption underlying species sensitivity distribution models. *Environment International*, 34(3):390–396, 2008.

- [9] F. De Laender, K. A. C. De Schamphelaere, P. A. Vanrolleghem, and C. R. Janssen. Is ecosystem structure the target of concern in ecological effect assessments? *Water Research*, 42:2395–2402, 2008.
- [10] F. De Laender, K. A. C. De Schamphelaere, P. A. Vanrolleghem, and C. R. Janssen. Validation of an ecosystem modelling approach as a tool for ecological effect assessments. *Chemosphere*, 71:529–545, 2008.
- [11] A. M. De Roos, T. Schellekens, T. Van Kooten, and L. Persson. Stage-specific predator species help each other to persist while competing for a single prey. *Proc. Nat. Acad. Sci. U. S. A.*, 105:13930–13935, 2008.
- [12] D. L. DeAngelis. *Dynamics of Nutrient Cycling and Food Webs*. Number 9 in Population and Community Biology series. Chapman & Hall, London, 1992.
- [13] D. L. DeAngelis, S. M. Bartell, and A. L. Brenkert. Effects of nutrient recycling at food-chain length on resilience. *The American Naturalist*, 134:778–805, 1989.
- [14] A. Dhooge, W. Govaerts, and Yu. A. Kuznetsov. Matcont: A MATLAB package for numerical bifurcation analysis of ODEs. *ACM Transactions on Mathematical Software*, 29:141–164, 2003.
- [15] D. M. Di Toro, S. C. Zarb, D. J. Hansen, W. J. Berry, R. C. Swartz, C. E. Cowan, S. P. Pavlou, H. E. Allen, N. A. Thomas, and P. R. Paquin. Technical basis for establishing sediment quality criteria for nonionic organic chemicals using equilibrium partitioning. *Environmental Toxicology and Chemistry*, 10:1541–1583, 1991.
- [16] E. J. Doedel and B. Oldeman. Auto07p: Continuation and bifurcation software for ordinary differential equations. Technical report, Concordia University, Montreal, Canada, 2009.
- [17] S. Ferson, L. R. Ginzburg, and R. A. Goldstein. Inferring ecological risk from toxicity bioassays. *Water, Air, & Soil Pollution*, 90(1/2):71–82, 1996.
- [18] J. W. Fleeger, K. R. Carman, and R. M. Nisbet. Indirect effects of contaminants in aquatic ecosystems. *The Science of the Total Environment*, 317:207–233, 2003.
- [19] V. Forbes and P. Calow. Extrapolation in Ecological Risk Assessment: Balancing pragmatism and precaution in chemical control legislation. *BioScience*, 52(3):249–257, 2002.

- [20] V. Forbes, P. Calow, and R. M. Silby. The extrapolation problem and how population modeling can help. *Environmental Toxicology and Chemistry*, 27(10):1987–1994, 2008.
- [21] F. A. P. C. Gobas. A model for predicting the bioaccumulation of hydrophobic organic chemicals in aquatic food-webs: application to Lake Ontario. *Ecological Modelling*, 69:1–17, 1993.
- [22] J. Guckenheimer and P. Holmes. *Nonlinear Oscillations, Dynamical Systems and Bifurcations of Vector Fields*, volume 42 of *Applied Mathematical Sciences*. Springer-Verlag, New York, 2 edition, 1985.
- [23] C. R. Gwaltney, W. Luo, and M. A. Stadtherr. Computation of equilibrium states and bifurcations using interval analysis: Application to food chain models. *Ecological Modelling*, 203:495–510, 2007.
- [24] C. R. Gwaltney and M. A. Stadtherr. Reliable computation of equilibrium states and bifurcations in ecological systems analysis. *Computers & Chemical Engineering*, 31(8):993–1005, 2007.
- [25] T. G. Hallam, G. A. Canziani, and R. R. Lassiter. Sublethal narcosis and population persistence: A modelling study on growth effects. *Environmental Toxicology and Chemistry*, 12:947–954, 1993.
- [26] R. Jepsen, J. Roberts, and W. Lick. Effects of bulk density on sediment erosion rates. *Water, Air and Soil Pollution*, 99:21–31, 1997.
- [27] A.A. Koelmans, A. Van der Heijde, L.M. Knijff, and R.H. Aalderink. Integrated modelling of eutrophication and organic contaminant fate & effects in aquatic ecosystems. A review. *Water Research*, 35(15):3517–3536, 2001.
- [28] B. W. Kooi. Numerical bifurcation analysis of ecosystems in a spatially homogeneous environment. *Acta Biotheoretica*, 51:189–222, 2003.
- [29] B. W. Kooi, D. Bontje, and M. Liebig. Model analysis of a simple aquatic ecosystems with sublethal toxic effects. *Mathematical Biosciences and Engineering*, 5(4):771–787, 2008.
- [30] B. W. Kooi, D. Bontje, G. A. K. van Voorn, and S. A. L. M. Kooijman. Sublethal toxic effects in a simple aquatic food chain. *Ecological Modelling*, 212(3/4):304–318, 2008.
- [31] B. W. Kooi, L. D. J. Kuijper, and S. A. L. M. Kooijman. Consequence of symbiosis for food web dynamics. *Journal of Mathematical Biology*, 49(3):227–271, 2004.

- [32] S. A. L. M. Kooijman. *Dynamic Energy Budget theory for metabolic organisation*. Cambridge University Press, Cambridge, 2010.
- [33] S. A. L. M. Kooijman and J. J. M. Bedaux. *The analysis of aquatic toxicity data*. VU University Press, Amsterdam, 1996.
- [34] Yu. A. Kuznetsov. *Elements of Applied Bifurcation Theory*, volume 112 of *Applied Mathematical Sciences*. Springer-Verlag, New York, 3 edition, 2004.
- [35] P. F. Landrum, H. Lee, and M. J. Lydy. Toxicokinetics in aquatic systems: model comparisons and use in hazard assessment. *Environmental Toxicology and Chemistry*, 11:1709–1725, 1992.
- [36] R. I. Leine. Bifurcations of equilibria in non-smooth continuous systems. *Physica D*, 223:121–137, 2006.
- [37] M. Liebig, G. Schmidt, D. Bontje, B. W. Kooi, G. Streck, W. Traunspurger, and T. Knacker. Direct and indirect effects of pollutants on algae and algivorous ciliates in an aquatic indoor microcosm. *Aquatic Toxicology*, 88:102–110, 2008.
- [38] R. D. Markwell, D. W. Connell, and A. J. Gabric. Bioaccumulation of lipophilic compounds from sediments by oligochaetes. *Water Research*, 23:1443–1450, 1989.
- [39] Matlab. *Matlab package*. The MathWorks, Natick, Massachusetts, USA, 2008.
- [40] L. S. McCarty and D. MacKay. Enhancing ecotoxicological modeling and assessment. Body residues and modes of toxic action. *Environmental Science & Technology*, 27:1719–1728, 1993.
- [41] R.V. O’Neill. Indirect estimation of energy fluxes in animal food webs. *Journal of Theoretical Biology*, 22:284–290, 1969.
- [42] R.V. O’Neill, D.L. DeAngelis, J.J. Pastor, B.J. Jackson, and W.M. Post. Multiple nutrient limitations in ecological models. *Ecological Modelling*, 46:495–510, 1989.
- [43] R. A. Park and J. S. Clough. Aquatox for windows: A modular fate and effects model for aquatic ecosystems. Technical Report 2, EPA, 2004.
- [44] R. A. Park and J. S. Clough. Aquatox for windows: A modular fate and effects model for aquatic ecosystems. Technical Report 3, EPA, 2009.

- [45] R.A. Park, J. S. Clough, and M. C. Wellman. Aquatox: Modeling environmental fate and ecological effects in aquatic ecosystems. *Ecological Modelling*, 213:1–15, 2008.
- [46] M. L. Rosenzweig. Paradox of enrichment: destabilization of exploitation ecosystems in ecological time. *Science*, 171:385–387, 1971.
- [47] M. L. Rosenzweig and R. H. MacArthur. Graphical representation and stability conditions of predator-prey interactions. *The American Naturalist*, 97:209–223, 1963.
- [48] M. Scheffer, J. Bascompte, W. A. Brock, V. Brovkin, S. R. Carpenter, V. Dakos, H. Held, E. H. van Nes, M. Rietkerk, and G. Sugihara. Early-warning signals for critical transitions. *Nature*, 461:53–59, 2009.
- [49] S. Sharpe and D. Mackay. A framework for evaluating bioaccumulation in food webs. *Environmental Science Technology*, 34:1203–1213, 2000.
- [50] R. V. Thomann, J. Connolly, and T. F. Parkerton. An equilibrium model of organic chemical accumulation in aquatic food webs with sediment interaction. *Environmental Toxicology and Chemistry*, 11:615–629, 1992.
- [51] T. P. Traas, A. P. van Wezel, J. L. M. Hermens, M. Zorn, A. G. M. van Hattum, and C. J. van Leeuwen. Environmental quality criteria for organic chemicals predicted from internal effect concentrations and a food web model. *Environmental Toxicology and Chemistry*, 23(10):2518–2527, 2004.
- [52] H. W. van der Veer, J. F. M. F. Cardoso, and J. van der Meer. The estimation of deb parameters for various northeast Atlantic bivalve species. *Journal of Sea Research*, 56:107–124, 2006.
- [53] S. Wiggins. *Introduction to Applied Nonlinear Dynamical Systems and Chaos*, volume 2 of *Texts in Applied Mathematics*. Springer-Verlag, New York, 1990.
- [54] J. M. Zaldívar, F. S. Bacelar, S. Dueri, D. Marinov, P. Viaroli, and E. Hernández-García. Modeling approach to regime shifts of primary production in shallow coastal ecosystems. 2009.
- [55] C. G. Zambonin, F. Catucci, and F. Palmisano. Solid phase microextraction coupled to gas chromatography mass spectrometry for the determination of the adsorption coefficients of triazines in soil. *Analyst*, 123:2825–2828, 1998.

# Chapter 7

## Discussion

We want a comfortable life style which includes housing, transport, healthcare and food and if possible some entertainment. This all requires building materials, energy, medicines, consumer goods and much more. For this we require resources such as arable land, mining for metals and salts, fresh water and mineral oils such as petroleum for energy. These resources are then processed on an industrial scale leading to the wanted products. In every step from extracting the resource from the environment, via production and transport, to usage and burning or burying the waste products chemicals enter the environment. This eventually leads to pollution of fresh water and the marine environment, air, arable land and contamination of food products. In the long run this adversely affects human health, food production and the re-usability of resources, including fresh water, agricultural land and air.

In order to protect human health and resources and to simultaneously minimize the impact of chemical emissions to the environment rules and regulations have been issued by governments. Regulations which are too strict will make products and goods too expensive, regulations which are too lenient will not protect human health and resources on the long run. The perception of what is strict and what is lenient depends to which stake holder group you would ask this.

The rules and regulations have grown, or evolved, as insight changed and protection aims expanded. Now, in the European Union, governments have largely harmonised their guidelines and same risk assessment procedures. These guidelines have evolved by listening to the industry, scientists, environmental protection agencies, and other interest groups such as nature conservationists. The resulting guidelines are a mix of common sense, science, worst-case assumptions and compromises. A major side effect of all these compromises is that although the European Union legislation for existing chemicals has been in place for a few decades, risk assessment has been performed for

137 compounds [3] of the 143,000 chemicals [2] that are registered to be used by the industry. Not all chemicals need to be assessed due to low production volumes or expected absence of toxicological properties.

Even if scientific insight changes or other guidelines would be more pragmatic, changing the rules of the game would inconvenience the players and would affect the continuity of the whole system. Therefore to prevent arbitrariness, existing legislation can and will only change slowly. On the one hand continuity and predictability are good. On the other hand, this makes the system of guidelines slow to absorb new insights and even adverse to new ways of looking at risk assessment and its procedures.

More specifically, classical descriptive statistics (NOECs, LC50s, EC5, etc.) form the heart of current risk assessment approach as they are used to predict at what environmental concentrations a chemical might affect organisms. A Predicted Environmental Concentration (PEC) is obtained by the evaluation of the emissions, distribution and bioavailability of the toxicant in the different compartments (water, sediment) or from actually measured environmental concentrations of the toxicant. In ecosystem risk assessment, descriptive statistics are converted to generic Predicted No-Effect Concentrations (PNEC). If an environmental toxicant concentration is at this value then no organism should be at risk. Thus no ecotoxicological hazard or risk is anticipated when the ratio PEC/PNEC is less than one. Therefore highly standardized toxicity laboratory tests are performed to obtain descriptive statistics as input for the risk assessment leading to the PEC/PNEC ratio. At the same time the guidelines have evolved to only use this type of input. As a result, laboratory tests which do not produce data to derive descriptive statistics are worthless from a risk assessment point of view. This discourages the development and execution of more complex and dynamic toxicological experiments. With no complex data to learn from the growth of knowledge on how to describe and analyse this complex data is stunted. This is a deadlock from which it is hard to escape and progress.

It is more and more realized that humans depend on the ecosystem around them for what nowadays is called ecosystem goods and services. Also protection of biodiversity is now a goal on itself. This requires methods to predict the effect of toxicants on ecosystems. Unfortunately ecosystems are complex and dynamic, thus classical descriptive statistics are a dead end, while the whole system of risk assessment is build around those statistics.

Mechanistic modelling can handle complex and dynamic data but does not produce output to which the risk assessment is accustomed and can work with. A mechanistic model (or biology based model) uses equations to model biological processes in an organism and the used parameters have a meaning full interpretation, such as growth rate, death rate, nutrient assimilation rate, etc. Fortunately, the use of mechanistic modelling (including the

DEBtox-approach) instead of descriptive statistics has slowly gained acceptance. Mechanistic modelling is now even acknowledged as a standard method by the OECD in the section on biology-based methods in [8]. This indicates that authorities do absorb new insights and approaches as they become available, albeit slowly as the DEBtox approach has been around since 1996 [7]. In [5] and [6] the differences between mechanistic ecotoxicology modelling and the statistical approach are discussed in more detail.

Downstream river stretches suffer from upstream chemical emissions. When looking at the Rhine for example one sees that pollution ignores and crosses borders on its way to the sea. The EU acknowledge this problem and implemented the Water Framework Directive (WFD) in which a legal framework was established that protects and restores clean water across Europe and ensures its long-term, sustainable use. The WFD forces EU Member States to work together to improve the ecological status of water bodies that are shared with other Member states.

By taking a clean surface water body as a benchmark, one can identify which species are missing, are reduced in density or are opportunistically present in a polluted or stressed water body that is otherwise similar in all characteristics to the clean reference water body. The ecological status of the unaffected water body is defined as high status and the more affected the body is the lower the status is defined to be, with good status being an acceptable status.

The WFD sets the goal of achieving a good status for all of Europe's surface waters and groundwater by 2015. This is a major challenge, as recent assessments estimate that at least 40 percent of the EU's surface water bodies are at risk of not meeting the 2015 objective. In the Netherlands, over 95 percent of surface water bodies are considered at to be at risk of not having a good ecological status [4].

To date severe gaps of knowledge impede the evaluation and mitigation of the causes for an insufficient ecological status in many aquatic ecosystems. The EU Modelkey project is designed to bridge these knowledge gaps. Two goals, amongst many, of the Modelkey project are, one: to develop predictive modelling tools and methods for effect-assessment, and two: to provide a better understanding of cause-effect-relationships between environmental pollution and changes in biodiversity, as biodiversity affects the the ecological status of the water bodies.

The work presented in this dissertation allows to take a few steps closer to understand the cause-effect-relationships between environmental pollution and changes in biodiversity and to use this understanding to make a new tool for in the tool kit of the risk assessor.

Roughly stated, to model the effects of toxicants on the ecosystems one needs a model for the unexposed system, or reference system, and a toxicant-

effect module to describe the effect of the toxicant on the organisms within the reference system. As an indication on how extensive the literature is on ecological modelling: since 1975, 4,500 articles on ecological modelling with roughly a fifth related to chemical stress or toxicants have been published in only just the journal *Ecological Modelling*. Thus there is ample literature to learn how to build a reference model. However, most articles on modelling chemical stress or toxicant effects have effect-modules based on descriptive statistics, making them less useful.

We showed how a biology based model can be used to quantify the effect of toxicants on algae which simultaneously suffer from nutrient stress. Note that this experimental setup is as simple as current standardized toxicity laboratory tests for deriving descriptive statistics. As we have a biology based model for the reference system and a quantification of the effects of the toxicants on the algae, now we can do extrapolations between measured concentrations and between time-points and between nutrient conditions. These extrapolations would not have been possible with the descriptive approach.

Modelling the ecology of algae and ciliates on a laboratory scale, led to an ecological reference model in which feeding behaviour differences between ciliates were incorporated. Bifurcation analysis was used to investigate the long-term behaviour of the different laboratory scale ecosystems.

A biology based model for the reference system together with an effect module for the toxicant effect can be used to analyse dynamic and complex multi-trophic toxicity data, which lead to parameter values for biological rates and a quantification of the toxicant effect. Again, analysis of dynamic data is not been possible with descriptive statistics.

Often in ecological models the toxicant water concentration is not affected by the presence of biota, detritus and sediment. We retained dynamic toxicant concentration in the modelled environmental compartments of water and sediment, while feedback remained possible with the dynamic internal concentration for the organism and dynamic concentrations in detritus.

We analysed and presented the effects of toxicant on a simplified multi-trophic aquatic ecosystem. This was an opportunity to develop approaches for finding no-effect regions (NERs) and resistance regions (RRs) as a manner to graphically represent the toxicant effects on species densities and ecosystem composition. In parallel with our efforts, recently other groups have performed bifurcation analysis in relation to aquatic ecotoxicology [1].

Increasing the complexity of the aquatic ecosystem model led to a now not-so-simple generic multi-trophic aquatic reference model. We found the NERs and RRs when exposing the modelled organisms to an ab- and adsorbing herbicide. The 2D-bifurcation graph of toxicant influx versus nutrient loading revealed that eutrophic systems are more toxicant resistant than oligotrophic systems.

The results presented in this dissertation might persuade experimentalists to create more datasets with dynamic multi-trophic interactions under exposed conditions and, importantly, publish the complete datasets without summarizing the results into descriptive statistics. The resulting datasets could then provide modellers with input to produce more ecological reference models. This all should lead to more parameter values for biological rates and parametrized effects of toxicants.

These parameter values are needed to run generic multi-trophic aquatic reference models, which are needed to find the NERs and RRs as exemplified in Chapter 6. Eventually, it should be possible to supplement the current approach of using a PEC/NEC-ratio for ecological risk assessment with ecological risk bifurcation diagrams. Thereby adding a new tool into the tool box of ecological risk assessors.

## References

1. F. S. Bacelar, S. Dueri, E. Hernandez-Garcia, J. M. Zaldívar, Joint effects of nutrients and contaminants on the dynamics of a food chain in marine ecosystems, *Mathematical Biosciences*, 1(218):24–32, 2009.
2. European Chemicals Agency, <http://apps.echa.europa.eu/preregistered/>
3. European Commission Joint Research Centre, Full list of priority compounds, <http://ecb.jrc.ec.europa.eu/esis/index.php?PGM=ora>
4. European Commission (DG Environment), Cleaning up Europe's Waters: Identifying and assessing surface water bodies at risk, *Water Notes on the Implementation of the Water Framework Directive*, Water Note 2, ISBN 978-92-79-09298-5, March 2008.
5. T. Jager, E. H. W. Heugens, and S. A. L. M. Kooijman. Making sense of ecotoxicological test results: towards application of process-based models. *Ecotoxicology*, 15:305–314, 2006.
6. T. Jager, T. Vandenbrouck, J. Baas, W. M. De Coen, and S. A. L. M. Kooijman. A biology-based approach for mixture toxicity of multiple endpoints over the life cycle. *Ecotoxicology*, 19(2):351–361, 2010.
7. S. A. L. M. Kooijman, A. O. Hanstveit, and N. Nyholm. No-effect concentrations in algal growth inhibition tests. *Water Research*, 30(7):1625–1632, July 1996.
8. Organisation for Economic Co-operation and Development (OECD), Current approaches in the statistical analysis of ecotoxicity data: a guidance to application, *Environment Health and Safety Publications Series on Testing and Assessment*, No. 54, 2006, ENV/JM/MONO(2006)18.



# Chapter 8

## English summary

### Toxicant effects on algae

Practically all life on earth indirectly depends on energy from sunlight. This energy is harvested with photosynthesis by ‘green’ organisms. Beside macrophytes, in the aquatic environment algae play the role of being the primary producers of stored energy. All other organism depend directly or indirectly on them. If the primary producers are hampered in their activities, effects will cascade down the whole ecosystem. To be able to predict the long-term effects of toxicants on ecosystems, the first puzzle is to solve how the primary producer responds to toxicant stress.

The very short-term effects of toxicants on algae are already known and are well documented using classical descriptive statistics. However, for ecosystem modelling there are additional requirements that are not covered by these short-term statistical procedures. First, the classical approach gives results that are difficult to extrapolate to other time points or other exposure concentrations. Furthermore, the effects are often measured and described on the population level and not on the level of the individual. Therefore its is not possible see which process within an individual was affected, e.g. nutrient assimilation, growth, reproduction or death.

When one models an ecosystem these processes have to be considered separately and included separately. Also the modelled toxicant effect should preferably affect only the correct biological processes. Thus, the classical descriptive statistics based on OECD guidelines [13, 14] are of limited use for long-term effect modelling, see for explanation [7, 8].

To obtain useful long-term dose-effect relationships for algae we designed, in collaboration with ECT Oekotoxikologie GmbH, an experiment in which there would be long-term exposure (as in multiple algal generations), nutrient limitation and toxicant stress.

The model for the algal growth should be able to extrapolate between

time points, between toxicant doses and should incorporate mass-balance and explicitly describe nutrient uptake, growth and death of the algae.

We made a conceptual model with all relevant biological processes and derived a mathematical model for the algal growth, similarly as done in Section 1.2 of the General introduction. In short, the mathematical model consist of coupled ODEs, resulting in a Marr-Pirt model for the algae and book keeping of the limiting nutrient. The DEBtox module [1, 10] was used to approximate the effect of the toxicant on the biological processes, yielding a time-independent continuous dose-response model. The mathematical model was coded into a computer model.

The experimental setup was designed with the conceptual model in mind, thus the output of the experiments was usable as input for the computer model. As the mass-balance of a closed system is easier to model than that of an open system, the experiments were done in a closed glass flask: an Erlenmeyer. The experiment generated two data sets: one in which the toxicant was a herbicide and a second in which the toxic stressor was an insecticide. The results were analysed using the classical descriptive statistical approach of the OECD [13, 14] and published in *Aquatic Toxicology* [12].

The computer model was also applied on the two data sets. The data fit produced a quantification of rates that determine the growth and death of the algae under reference conditions and a quantified dose-effect relation for each toxicant and its affected process. To describe the normal growth of the algae only three parameters were needed and two for each toxicant effect-relation. Without using *a priori* knowledge the data fits reveal that the herbicide affected the growth-process of the algae and the insecticide the death-process.

Hallam et al. discussed in 1993 [6] the concept of a minimal toxicant concentration at at which a population will go extinct given a specific food availability. Using the fitted parameter values and the equations we calculate the toxicant concentration at which the algal population will go extinct given known nutrient loads. This yields a deterministic continuous function of extinction concentrations depending on the nutrient load, in other words, a deterministic population extinction threshold. Using standard data fitting techniques we obtained the co-variance matrix which contains the interdependency of the parameters values. Combining this covariance matrix with a second order Taylor approximation leads to a confidence interval around this deterministic population extinction threshold.

This would not have been possible with the OECD approach of descriptive statistics. With the deterministic mechanistic modelling approach, it is possible to do predictions between concentrations, between time points and even outside the original experimental conditions. The above mechanistic analysis and discussion were published in *Water Research* [2] and form Chapter 2.

## Effects of toxicants on algal-predator system

Now that we could model and determine long-term effects on a small single species system, could we do the same for a real but very simple multi-trophic ecosystem? This would help extend the conceptual framework and resulting mathematical model should help us to answer the ultimate question on how toxicants affect ‘natural’ and therefore big and complex ecosystems.

An algal-predator-toxicant system was designed, again together with ECT, consisting of the same algal species and the predator was taken to be an algivorous ciliate. This data and the statistical analysis are also published in [12].

In this model the default Marr-Pirt building block, as used to describe the algal growth, could not also be used to satisfactorily reproduce the growth dynamics of the ciliates. The more sophisticated dynamic energy budget model (DEB) with reserves [11] did improve the data fit to the measurements of the ciliate population size but not enough.

A key factor in the ciliate population dynamics, that is not covered in both the default Marr-Pirt and DEB models, is the existence of a feeding threshold for ciliates [16]. The feeding threshold is implemented in the standard Holling type II functional response as an additional term which lowers the perceived prey density for the predator.

The analysis of the small multi-trophic ecosystem in by Weisse et al. in [16] resulted in an article in which we model the observed, but still unexplained, effect of a feeding threshold in the Holling type-II functional response on the time evolutions of ciliate and algae densities inside a confined volume. Also, the long-term effects of the feeding thresholds on the dynamics of these algal-ciliate ecosystems were analysed with bifurcation theory. Above findings are published in *Mathematical Modelling of Natural Phenomena* [3] and form Chapter 3.

The above work helped us to realize that the ciliate species used by ECT could also have a feeding threshold and that this property should be included in the conceptual framework.

## Effects of toxicants on an algal-predator system with feeding threshold

The analysis continued, but now the idea of a ‘feeding threshold’ was added to the conceptual framework. So far, this conceptual framework contains: mass-balancing, ODEs (identical individuals), Marr-Pirt model for algal growth, DEB reserve-model for the ciliates, feeding threshold for predation on the algae by ciliates and DEBtox concentration-effect relationships. Even with the inclusion of the feeding threshold the dynamics from the model did not match the

dynamics in the experimental data.

Work published by Eichinger in 2009 [5] put us on the way to include starvation in the DEB growth model for the ciliates. Starvation leads to structure mobilization which again gives shrinkage and leads to less rapid predator population decline. Therefore, we added ‘shrinkage’ to our conceptual framework and the data fits improved. The model captures most but not all of the behaviour of the affected system. Results are presented in Chapter 4.

Incorporation into the conceptual framework of a reserve, shrinkage and a feeding threshold leads to more dynamics in the computed time evolution of the ciliate biomass. However, each new addition to the conceptual framework leads to an increase in the number of equations and parameters in the mathematical model. Still the predicted dynamics do not match the experimentally observed dynamics to full satisfaction. Likely, not all the relevant behaviour of the ciliates is captured in enough detail but adding more detail to the conceptual framework is not warranted given the size of the data sets. Independent of the above modelling efforts, it can be concluded that the data sets do show that it is experimentally possible to demonstrate indirect toxicant effects (occurring as reduced densities) on the trophic level directly above the affected producer.

## Toxicant effects on a simple riverine ecosystem

Parallel to the above mentioned work, we investigated whether it was feasible at all to analyse a mathematical high dimensional ODE-system that represents a more complex but still simplified riverine ecosystem which is under nutrient and toxicant stress. We found it is feasible to analyse such an exposed high dimensional ecological systems, thus in theory an up scaling from Erlenmeyer to river is possible.

To be more specific, the aquatic ecosystem consists of a limiting nutrient, primary producers, consumer and a predator. Other components are two types of detritus and bacterial degradation of the detritus for the closure of the food circle. This work has been published in *Ecological Modelling* [9]. There we describe how species biomass densities responded to gradual changes in the rate of water flow, toxicant inflow concentration and nutrient inflow concentration.

The species together form the ecosystem, presence or absence of species determine the ecosystem structure. The activities of the species determine the ecosystem processes. We devised a method to find areas in the parameter-space where the ecosystem is quantitatively not affected. These areas we defined to be no-effect regions. These areas are formed by combinations of values for nutrient loading and toxicant loading where the biomass densities are not affected. The bifurcation analysis also resulted in areas where the quantities are changed but not the ecosystem structure. Finally we determined where

quantitative changes in biomasses occurred and simultaneously the behaviour of the ecosystem was changed. Thus in this system toxicant stress was just one stress besides nutrient stress and removal from the system due to flow rate. Results are presented in Chapter 5.

### **Toxicant effects on a simple riverine ecosystem with sediment**

Organisms within an aquatic ecosystem suffer simultaneously from multiple stresses from abiotic factors, trophic interactions and from anthropogenic sources such as habitat changes and chemical stress. Natural systems are complex. We summarize the processes, attributes and composition into one simplification. This simplification still has many behavioural characteristics of the natural system but is vastly reduced in complexity. The resulting model is still high in dimensions. The resulting system consists of a limiting nutrient, a primary producer, a benthic consumer, pelagic consumer, predator, three pools of detritus and sediment. We call this system the reference system as it is not affected by toxicants. This system is a simplification of a natural aquatic ecosystem but the major relevant processes that occur within a natural system are present. These processes being photosynthesis, nutrient limitation, competition for food, predation, detritus formation from death, faeces and algal sinking and finally degradation of detritus into the limiting nutrient. Note that this system is a food circle not a food web or chain. All biota can absorb and release the toxicant and the toxicant can adsorb to the sediment.

As a representative for the primary producer we took one algal species, with species property values from [2] to parameterize the algae and their response to the toxicant. Benthic invertebrates such as clams and worms were modelled with only one species which is to summarize all the characteristics of these species. The predator is taken to be an aquatic vertebrate such as a fish, its parameters are from [4]. The predator fish is stationary, which is more appropriate for large aquatic vertebrates. Other parameter values are from e.g. Aquatox [15], which is an ecotoxicological model that predicts short and middle long-term effects of toxicant on fresh water ecosystems.

The behaviour of our simplified ecosystem was analysed with bifurcation theory. We found in the case that we modelled the direct effects of a herbicide on the algae that the biomasses of the other species responds rather gradually to the increased concentration of the toxicant. However, often the gradually changed biomasses remained at an intermediate density and then suddenly all species went extinct, a catastrophic collapse occurred. Recovery of the system would only occur if the toxicant influx was severely reduced.

We also found that eutrophic systems can postpone their collapse due to higher initial biomasses and therefore higher toxicant binding capacity, consequently reducing bioavailability of the toxicant for the algae.

In general we found that before a system-collapse or loss of species occurs, the system is not behaving much differently than at a slightly lower toxicant influx rate. Therefore, there are no or difficult to see warnings before the system collapses due to one drop of toxicant too many. This means, that potentially devastating effects can result from a slight increase in the toxicant influx rate, without any type of warning.

An additional effect is that the recovery of the system is potentially also very difficult. The existence of a tangent bifurcation should be interpreted as a threshold for species to successfully re-invade the system, making it more difficult to restore the ecosystem. Results are presented in Chapter 6.

We like to stress that although long-term predictions are made, the predicted short-term dynamics could still be validated using multi-species models as proposed in [12], Chapter 2, 3 and 4.

# References

- [1] J. J. M. Bedaux and S. A. L. M. Kooijman. Statistical analysis of bioassays based on hazard modelling. *Environmental and Ecological Statistics*, 1:303–314, 1994.
- [2] D. Bontje, B. W. Kooi, M. Liebig, and S. A. L. M. Kooijman. Modelling long-term ecotoxicological effects on an algal population under dynamic nutrient stress. *Water Research*, 43:3292–3300, 2009.
- [3] D. Bontje, B. W. Kooi, G. A. K van Voorn, and S. A. L. M. Kooijman. Feeding threshold for predators stabilises predator-prey systems. *Mathematical Modelling of Natural Phenomena*, 4(6):91–108, 2009.
- [4] F. De Laender, K. A. C. De Schamphelaere, P. A. Vanrolleghem, and C. R. Janssen. Validation of an ecosystem modelling approach as a tool for ecological effect assessments. *Chemosphere*, 71:529–545, 2008.
- [5] M. Eichinger, S. A. L. M. Kooijman, R. Sempéré, and J. -C. Poggiale. Consumption and release of dissolved organic carbon by marine bacteria in pulsed-substrate environment: from experiments to modelling. *Aquatic Microbial Ecology*, 56:41–54, 2009.
- [6] T. G. Hallam, G. A. Canziani, and R. R. Lassiter. Sublethal narcosis and population persistence: a modeling study on growth effects. *Environmental Toxicology and Chemistry*, 12:947–954, 1993.
- [7] T. Jager, E. H. W. Heugens, and S. A. L. M. Kooijman. Making sense of ecotoxicological test results: towards application of process-based models. *Ecotoxicology*, 15:305–314, 2006.
- [8] T. Jager, T. Vandenbrouck, J. Baas, W. M. De Coen, and S. A. L. M. Kooijman. A biology-based approach for mixture toxicity of multiple endpoints over the life cycle. *Ecotoxicology*, 19(2):351–361, 2010.
- [9] B. W. Kooi, D. Bontje, G. A. K van Voorn, and S. A. L. M. Kooijman. Sublethal contaminants effects in a simple aquatic food chain. *Ecological Modelling*, 212:304–318, 2008.

- 
- [10] S. A. L. M. Kooijman, A. O. Hanstveit, and N. Nyholm. No-effect concentrations in algal growth inhibition tests. *Water Research*, 30(7):1625–1632, July 1996.
- [11] S. A. L. M. Kooijman. *Dynamic Energy Budget theory for metabolic organisation*. Cambridge University Press, Great Britain, Cambridge, 2010.
- [12] M. Liebig, G. Schmidt, D. Bontje, B. W. Kooi, G. Streck, W. Traunspurger, and T. Knacker. Direct and indirect effects of pollutants on algae and algivorous ciliates in an aquatic indoor microcosm. *Aquatic Toxicology*, 88:102–110, 2008.
- [13] OECD. OECD guidelines for the testing of chemicals. Proposal for updating guideline 201: Freshwater alga and cyanobacteria, growth inhibition test. *ENV/JM/TG*, 5:8–31, 2004.
- [14] OECD. OECD guideline for testing of chemicals - 201 Freshwater alga and cyanobacteria, growth inhibition test. <http://www.oecd.org>, March 23:1–25, 2006.
- [15] R.A. Park, J. S. Clough, and M. C. Wellman. Aquatox: Modeling environmental fate and ecological effects in aquatic ecosystems. *Ecological Modelling*, 213:1–15, 2008.
- [16] T. Weisse, N. Karstens, V.C.L. Meyer, L. Janke, S. Lettner, and K. Teichgräber. Niche separation in common prostome freshwater ciliates: the effect of food and temperature. *Aquatic Microbial Ecology*, 26:167–179, 2001.

# Nederlandse samenvatting

## Een analyse van de gevolgen van gif- en nutriëntstress in aquatische ecosystemen

Aquatische organismen van verschillende soorten leven in een complexe samenleving, aangeduid met het begrip aquatisch ecosysteem. Wanneer gifstoffen in het milieu komen, leidt dit tot minder goed functionerende aquatische ecosystemen. Individuen in dit systeem worden direct beïnvloed door gifstoffen, wat kan leiden tot een verlaagde biodiversiteit en verlaagde primaire productie. Gifstoffen kunnen echter ook indirecte effecten veroorzaken. In mijn onderzoek wil ik de directe en indirecte gevolgen van gifstoffen op grote aquatische ecosystemen voorspellen.

Traditioneel wordt beschrijvende statistiek gebruikt om het effect van gif op kleine kunstmatige ecosystemen samen te vatten door middel van een aantal kengetallen. De extrapolatie van dit soort kengetallen van een klein naar een groter en ingewikkelder systeem is onmogelijk omdat kennis van de onderliggende processen ontbreekt. Verder blijkt de beschrijvende statistiek niet in staat bruikbare kengetallen af te leiden uit resultaten van complexere proefopzetten waarin de dichtheiden van meerdere soorten variëren in de tijd.

Het is ook mogelijk voorspellingen te doen op basis van computersimulaties. Deze simulaties zijn gebaseerd op wiskundige modellen: versimpelde weergaven van de werkelijkheid, die nog wel de essentie moeten vangen van de processen in een ecosysteem. Ecosystemen zijn complex, waardoor een wiskundig model voor een dergelijk systeem al snel veel vergelijkingen kan hebben waardoor analyse tijdrovend en moeilijk wordt.

In veel bestaande ecosysteemmodellen worden de korte termijn gevolgen van gifstoffen bestudeerd en minder vaak de lange termijn gevolgen. Indien de lange termijn gevolgen bestudeerd worden, dan wordt vaak aangenomen dat het ecosysteem in een constante toestand of evenwicht is. Onze eigen modellen zijn voor zowel de korte als de lange termijn bruikbaar en de aanname van ecosysteem evenwicht is niet toegepast. Dit zorgt er ook voor dat kleine verandering in het systeem over de tijd kunnen culmineren tot grote effecten.

De interacties van de componenten van een ecosysteem kan men beschrijven met een wiskundig model. Samen met collega's uit Frankfurt in Duitsland ontwikkelden ik en collega's een serie van experimenten om te testen of de door ons gehanteerde vergelijkingen wel gebruikt kunnen worden om deze interacties te benaderen.

Eerst stelden we onder laboratoriumcondities een algenpopulatie langdurig bloot aan gifstof- en nutriëntstress. Ons wiskundig model simuleerde de dynamische groei van deze algen goed, en kon de interacties van het gif en nutriënten goed verklaren. Dat zou niet mogelijk zijn op basis van extrapolatie met klassieke beschrijvende statistiek.

Vervolgens breidden we het wiskundige model uit met een consument waarna we onze modelaanpak hebben getest met literatuurdata van prooi-predator experimenten. Vervolgens testten we onze aanpak met data van experimenten met prooi, predator en gifstof. Uiteindelijk formuleerden we een generiek riviermodel op basis van onze modelaanpak aangevuld met literatuurwaardes.

In veel bestaande ecosysteemmodellen wordt aangenomen dat de interne gifstof concentratie in een gemodelleerd organisme synchroon fluctueert met de externe waterconcentratie. In andere woorden: de verhouding van de interne en externe concentratie wordt constant genomen. Dit principe staat bekend als evenwichtspartitie. In de door ons ontworpen modellen hoeft dit principe niet toegepast te worden, maar als compensatie zijn dan veel aanvullende parameterwaardes nodig.

We lieten zien hoe onze modellen versimpeld kunnen worden tot een vorm waarin evenwichtspartitie is toegepast, en dus minder parameters nodig zijn, zonder dat we het doorwerken van kleine veranderingen tot grote gevolgen verliezen tijdens deze versimpeling. Vanwege deze voordelen hebben we dit principe toegepast voor een generiek riviermodel. Wat we niet uit het oog verloren was de massabalans van het gif en het feit dat de gifconcentraties kunnen fluctueren in de tijd.

We besloten om geen complex model voor een specifiek gestresst ecosysteem te bouwen en te bestuderen, maar om een generiek aquatisch ecosysteem te nemen en te bestuderen. In dat generieke riviermodel wordt elk trofisch niveau vertegenwoordigd door één soort. Dit generieke riviermodel bestaat uit één limiterende nutriënt, een producent, een vrij zwemmende consument, een op de bodem levende consument, een vrij zwemmende predator, dood organisch materiaal, sediment en water. Het resulterende model analyseerden we met een techniek genaamd bifurcatie analyse.

Met deze techniek analyseerden we de indirecte gevolgen van simultaan optredende gifstofstress en nutriëntenstress op het gemodelleerde ecosysteem, terwijl de stressoren direct inwerken op het niveau van het individu. We keken hoe het generieke aquatische systeem reageert op een gifinstroom variërend

van afwezig tot veel, terwijl de nutriëntbeperking varieerde van oligotroof tot eutroof. De waarden van de stressparameters varieerden langs een continue schaal. Elke combinatie van gifstofinstroom en nutriëntbeperking leidde tot andere dichtheden van de aanwezige soorten, inclusief dichtheid nul oftewel uitsterving. Ook waren er situaties aan te geven waarin de soortsaanstelling en het gedrag van het ecosysteem identiek zijn terwijl de dichtheden variëren.

Voor een generiek riviersysteem, met evenwichtspartitie toegepast, bestudeerden we de directe en indirecte lange termijn gevolgen van een herbicide dat zich ophoopt in organisch materiaal. We wisten al dat eutrofiëring een systeem kan destabiliseren, ook bekend als de paradox van verrijking. Wij concluderen dat verrijking de gevolgen van een toenemende gifinstroom kan vertragen, maar uiteindelijk zal het systeem zonder waarschuwing in elkaar storten. Voordat de soorten zich weer kunnen vestigen en herstellen, zal zowel de nutriënteninstroom als de gifstofinstroom drastisch omlaag moeten.

De benodigde parameterwaardes zijn verkregen door gegevens van kleine experimentele ecosystemen te analyseren met ecosysteemmodellen. Door de verkregen parameterwaardes (aangevuld met literatuurwaardes) te combineren met een model voor een generiek aquatisch ecosysteem, kunnen we voorspellingen doen voor gecombineerde gif- en nutriëntstress. Dit alles zonder beschrijvende statistiek of de aanname van ecosysteem evenwicht toe te passen.

De gedane stappen die leidden tot de voorspellingen van dichtheden van soorten en uitsterving kunnen herhaald worden voor andere gifstoffen. De resulterende voorspelde gevolgen kunnen dus dienen om de gevolgen van gifstofemissies in te kunnen schatten. Dit laatste is in potentie nuttig voor mensen die milieunormen afleiden voor gifstoffen of moeten beslissen of een nieuwe stof op de markt mag komen.



# List of publications

S. A. L. M. Kooijman, J. Baas, D. Bontje, M. Broerse, C. A. M. van Gestel, and T. Jager. Ecotoxicological applications of Dynamic Energy Budget theory, Chapter in *Ecotoxicology Modeling* edited by J. Devillers, Springer, 2009.

D. Bontje, B. W. Kooi, G. A. K van Voorn, and S. A. L. M. Kooijman. Feeding threshold for predators stabilises predator-prey systems. *Mathematical Modelling Natural Phenomena*, 4(6):91-108, 2009.

D. Bontje, B. W. Kooi, M. Liebig, and S. A. L. M. Kooijman. Modelling long-term ecotoxicological effects on an algal population under dynamic nutrient stress. *Water Research*, 43:3292-3300, 2009.

B. W. Kooi, D. Bontje, G. A. K van Voorn, and S. A. L. M. Kooijman. Sublethal contaminants effects in a simple aquatic food chain. *Ecological Modelling*, 212:304-318, 2008.

B. W. Kooi, D. Bontje, and M. Liebig. Model analysis of a simple aquatic ecosystems with sublethal toxic effects. *Mathematical Biosciences and Engineering*, 5:771-787, 2008.

M. Liebig, G. Schmidt, D. Bontje, B. W. Kooi, G. Streck, W. Traunspurger, and T. Knacker. Direct and indirect effects of pollutants on algae and algivorous ciliates in an aquatic indoor microcosm. *Aquatic Toxicology*, 88:102-110, 2008.

S. A. L. M. Kooijman, J. Baas, D. Bontje, M. Broerse, T. Jager, C. A. M. van Gestel, and B. van Hattum. Scaling relationships based on partition coefficients and body sizes have similarities and interactions. *SAR and QSAR in Environmental Research*, 18:315-330, 2007.

D. Bontje, T. P. Traas, and W. C. Mennes. A human exposure model to calculate harmonized risk limits – model description and analysis. Report 601501022, National Institute for Public Health and the Environment (RIVM), 2005.

T. P. Traas and D. Bontje. Environmental risk limits for alcohols, glycols, and other relatively soluble and/or volatile compounds. 2. integration of human and ecotoxicological risk limits. Report 601501027, National Institute for Public Health and the Environment (RIVM), 2005.

D. Bontje, J. Hermens, T. Vermeire, and T. Damstra. Integrated risk assessment: Nonylphenol case study. Report WHO/IPCS/IRA/12/04, International Programme on Chemical Safety (IPCS), Geneva, Switzerland, 2004.

# Dankwoord

Nog voor het project begon was er de sollicitatie. Een goed gesprek, maar ik was toch bang - was ik niet een beetje licht wat betreft programmeren en wiskundevaardigheid? Nog geen tien minuten na afloop, ik was met George aan het bijpraten, kwam het verlossende woord. Aangenomen als promovendus..... Dat had ik niet verwacht - wel gehoopt! - maar zeker niet zo snel. Bas, dit bleek typisch iets voor jou. Noem het intuïtie of ervaring, maar je besloot in één oogopslag dat het goed was. Gelukkig voor mij.

Daarna volgden meer positieve ervaringen. Veel van mijn vrienden en kennissen zijn AIO geworden. Af en toe klaagden ze over langzame reacties op manuscripten, over gebrek aan visie en richting, of dat ze als AIO het minst belangrijke waren van alle projecten van hun prof. Ik leefde in een andere wereld. Je bekeek mijn schrijfsels snel, stutte of renoveerde ze op inhoudelijke gronden en tijdens de koffiepauzes maakten we informele updates van de planning. Dat werkte prima voor ons.

Er was meer te leren over de wetenschap van Bas. Tijdens de koffie vertelde je ons regelmatig over universiteitspolitiek, NWO-subsidieperikelen, EU-projectaanvragen en bijbehorende administratie. Het raakte me op dat moment niet direct, maar het was wel ontzettend educatief voor mogelijke beursaanvragen. Ik realiseer me goed hoe luxe het is om amper vergaderingen te hebben.

Bas, ik heb het theoretisch raamwerk van DEB niet vooruitgeholpen. Ik modelleerde de effecten van gif op een ecosysteem, was daardoor meer gericht op een correcte massabalans van zowel de nutriënten als het gif, en op een variabelenarm model voor de beestjes i.v.m. bifurcatie-analyses. Een compleet DEB-model was voor mij nog een brug te ver. Misschien de volgende AIO?

Een AIO-project van meerdere jaren heeft zo zijn eigen dynamiek van voor- en tegenspoed. Het heeft wat voeten in aarde voordat je eindelijk een geaccepteerd & gepubliceerd artikel hebt. Buiten dat het review-process erg lang kan duren, moet je eerst goed onder woorden brengen wat het probleem is, uitzoeken wat je voorgangers al gedaan hebben, modelontwikkeling, data vinden/verkrijgen en fitten, resultaten verwerken en documenteren en indien het resultaat goed, is eindelijk een artikel schrijven. Bij de acceptatie van je eerste

artikel voel je jezelf toch groeien: je hoort dan echt bij de club der wetenschappers, tot die tijd ben je eigenlijk een amateur. Dat vier je met taart en een paar dagen lang ben je heel blij. Daarna van je roze wolk af en weer hard aan de slag want één artikel is slechts één hoofdstuk.

Omdat onderzoek zijn momenten van zwaar weer en tegenslag kent is er soms een vleugje tegenzin. De leuke momenten zijn fijn om te delen, tijdens de wat mindere momenten wilde ik niet teveel over werk praten. Afleiding was dan erg gewenst. De beruchte AIO-dip heb ik gelukkig naar mijn gevoel ontweken, maar zonder de steun van familie en vrienden was dat zeker niet gelukt.

Maar eerst dank natuurlijk aan al mijn collega's. In alfabetische volgorde: Jan, Jorn, Laure, Matthijs, Omta-pedia (Anne-Willem), Tineke en Tjalling (de Bastogne-koekjes zijn nu echt op). Dank dat ik gebruik mocht maken van al jullie eigen specialiteiten om een programmeerprobleem, Engelschrijven-probleem, achtergrondkennisprobleem of sociaal-netwerk-probleem op te lossen.

Marian, dank voor de blijvende warme belangstelling naar de stand van mijn proefschrift en zeker voor het willen proeflezen.

Theo, Theo en Joop, jullie hebben mijn eerste schreden op het ecotoxicologie pad gezien en al in een vroeg stadium gesteund. Ik had toen niet verwacht dat er een boekje uit voort zou komen.

Sinds mijn eerste jaar als student zie ik op een vaste avond in de week dezelfde vrienden. Ik geloof dat ons 10-jarig lustrum ons is ontschoten. Zonder Robert, Gieljan, Wouter en Hans waren de afgelopen jaren een stuk minder leuk geweest. Dan had ik nooit kennisgemaakt met Roberts collectie *musica obscura*, met de *flat earth society* of met Lxor van B. Dan had ik al helemaal nooit vier mensen tegelijk een goudvis met geheugenverlies na zien doen of iemand semi-wekelijks koffie uit zijn *neus* zien proesten tijdens een lachstuip. Mijn grootste vergissing was om, de dag nadat mijn verstandkiezen waren getrokken en ik niet meer heerlijk onder de pijnstillers zat, toch hun gezelschap op te zoeken en te zeggen dat lachen pijn doet. Even serieus, verstopt onder het geinen stonden we wel voor elkaar klaar met raad en daad of een luisterend oor. Dank voor deze goede jaren.

Mirte, ook bij jou kan ik met mijn verhalen terecht en vice versa. Dankzij jou kijk ik nog eens verder dan mij eigen 'denkraam' en beslommingen.

Soms wilde ik juist wel over het werk praten, bij voorkeur natuurlijk wanneer ik daar niet was. George, dat ging bij jou thuis, met onze eega's erbij, altijd prima. Voor jou is één paragraaf te kort om je recht te doen. Dus dan maar incompleet. Mijn voorkeur voor heldere en primaire kleuren heb ik met jou boven water en onder woorden gekregen: we zijn bij de benaming Nijntjekleuren blijven hangen. Je was nooit te beroerd om in een discussie zeer stellig aan een kant te beginnen en na alle argumenten over te stappen naar een com-

pleet andere mening. Dat kunnen niet veel mensen, hun ingesleten mening of vooroordeel na één discussie bijstellen zonder te acclimatiseren.

Ben ik als een ‘onbeschreven blad’ ter wereld gekomen en heeft mijn opvoeding mij gebracht waar ik ben? Als dat zo is dan zouden mijn broer Sander en zus Eveline ook biologie zijn gaan studeren. Echter, die zijn ieder 120 graden een andere kant op gegaan. En ja ha het boekje is nu echt af. Als het aanleg is, en dus genetisch, dan was dat, denk ik, niet genoeg geweest zonder het goede voorbeeld van mijn vader en zijn praktische houding van “als je ergens aan begint dan maak je het af” en het voorbeeld van mijn moeder: “als je iets doet, doe het dan ook goed”. Het is een combinatie van halsstarigheid en hard werken, doorspekt met zorgzaamheid die ik mee heb gekregen van mijn ouders via hetzij genetisch materiaal hetzij opvoeding. Dankzij jullie goede voorbeeld van hoe om te gaan met de wereld is het met mij tot nu toe best goed gelopen. Aad, Gemma, dank voor de gave om zelf te denken, zelf te doen: de gave van zelfstandigheid.

Ja, Marije, hoe ver moest je deze tekst doorscannen tot je *eindelijk* jouw naam tegen komt, ... aagje. Ik heb veel van je gekregen, liefde, aandacht, geborgenheid, natuurlijk Marijn. Je viste zelfs fouten uit mijn manuscripten. Soms denk ik dat jij beter in mijn werk was geweest dan ik, maar dan had de wereld een bevlogen dierenarts minder gehad. Op een van Marijns T-shirts staat: Mama + Papa = 100% Me. Dat maakt mij nieuwsgierig naar de toekomst.

*Last but not least*, Bob Kooi. Waar te beginnen. Zonder jou was dit proefschrift van mindere kwantiteit en, veel erger, van mindere kwaliteit geweest. Wanneer ik weer eens op een detail zat te pielen, gaf jij me de spreekwoordelijke schop onder mijn achterwerk. Hak nou eens een knoop door en wees weer productief. Jouw geestelijke bagage van voorgaande projecten heeft mij heel wat doodlopende onderzoekssporen bespaard.

Ik ben een bioloog die wiskunde zowel nuttig als leuk vindt. Echter, soms schoot ik tekort in bagage. Sommige wiskundige concepten zijn voor mij net vlinders die je kunt vangen in je handen, waar je naar kan gluren om je te verwonderen over hun schoonheid, en die je dan maar los moet laten. In mijn handen gaan ze uiteindelijk toch dood. Bob, voor veel ‘vlinders’ heb jij mij eerst het eitje laten zien, daarna de rups, dan de ingewikkelde transformatie van rups naar ‘vlinder’. De ‘vlinders’ kan ik nu catalogiseren, de rupsen kan ik nu zelf opkweken, sommige zijn zich zelfs al aan het verpoppen.

# Acknowledgements – Project Modelkey

Dear Markus Liebig, you actively tried to think in a ‘modellers’ kind-of-way and asked questions until *I* was the one who finally understood what kind of experiment I *exactly* was asking you to perform. You and your team mates Nina Platenik, Gunnar Schmidt, Tineke Sloomweg and Roland Kuhl did excellent work. Thanks again.

I extend courtesy to Georg Streck for performing chemical analyses and to Anna Romani for counting bacteria.

I wish to thank Kees van Gestel, Pim Leonards and Bert van Hattum for providing feedback on manuscripts.

Helena Guasch, Sergi Sabater, and Anna Romani, you all brainstormed with me on how to construct a biofilm model that could handle your available data. Although multiple deliverables did not result in an article, I enjoyed the literal and figurative look outside my field of expertise, especially the field trip and the tour of the laboratory.

Mechthild Schmitt-Jansen and both Stephanie’s, you were pleasant company during congresses and meetings, but most of all, you are very constructive thinkers. You supplied me with multiple data sets - the last one seems to do it. Or maybe it’s just that I finally developed the knack of asking for the right type of data.

Werner Brack, Michaela Hein, Jos van Gils, Dick de Zwart and everyone else in the Modelkey project, thanks for all discussions and feedback during meetings and presentations.

And of course, dear taxpayer, thank you for EU-grant 511237-GOCE.



